Flood risk management in urban areas : added value of cellular automata and agent-based modelling

Hao-Ming Hsu

Gestion du Risque d'Inondation dans les Zones Urbaines

Valeur Ajoutée des Automates Cellulaires et de la Modélisation à Base d'Agents

Hao-Ming HSU

Polytech'Lab

Présentée en vue de l'obtention du grade de docteur en
Sciences pour l'Ingénieur
d'Université Côte d'Azur

Dirigée par :
Philippe GOURBESVILLE

Soutenue le :
29 Mars 2024

Devant le jury, composé de :

Ming-Che HU,
Professeur, Université Nationale de Taïwan

Morgan ABILY,
Maître de Conférences, Université Côte d'Azur

Philippe AUDRA,
Professeur, Université Côte d'Azur

Philippe GOURBESVILLE,
Professeur, Université Côte d'Azur

Reinhard HINKELMANN,
Professeur, Université Technique de Berlin

Tsun-Hua YANG,
Professeur Associé, Université Nationale Yang Ming Chiao Tung

POLYTECH NICE-SOPHIA
POLYTECH'LAB

MINISTRY OF EDUCATION 教育部

Flood Risk Management in Urban Areas:

Added Value of Cellular Automata and Agent-Based Modelling

Jury :

Président du jury
Philippe AUDRA, Professeur, Université Côte d'Azur, France

Rapporteurs
Reinhard HINKELMANN, Professeur, Université Technique de Berlin, Allemagne
Tsun-Hua YANG, Professeur Associé, Université Nationale Yang Ming Chiao Tung, Taïwan

Examinateurs
Ming-Che HU, Professeur, Université Nationale de Taïwan, Taïwan
Morgan ABILY, Maître de Conférences, Université Côte d'Azur, France
Philippe GOURBESVILLE, Professeur, Université Côte d'Azur, France

Acknowledgement

First and foremost, I would like to express my sincere gratitude to my supervisor, Professor Philippe Gourbesville, for his invaluable tutelage, helpful advice and suggestions, continuous support and great patience. His knowledge and experience inspired my academic research and helped me overcome many obstacles throughout my doctoral study.

Furthermore, I would like to extend my deepest appreciation to my jury members for their patience, support, comments and suggestions during the whole defence process. Doctor Philippe Audra from Université Côte d'Azur (France) had been providing his helpful comments as my thesis monitoring committee member for three years and also helped me deal with many administrative process within the doctoral school and the university. Doctor Tsun-Hua Yang from National Yang Ming Chiao Tung University (Taiwan) had been providing his insights and useful suggestions as my thesis monitoring committee member for three years and always being kindly supporting and encouraging my doctoral study and academic life. Doctor Reinhard Hinkelmann, from Technische Universität Berlin (Germany), Doctor Ming-Che Hu from National Taiwan University (Taiwan) and Doctor Morgan Abily from Université Côte d'Azur (France), they all generously provided their knowledge and expertise during the doctoral thesis defence, helping me improve my work.

Additionally, this endeavour would not have been possible without the generous financial support from the Ministry of Education of Taiwan who provided 3-year scholarship for my doctoral study and research. I also want to extend my appreciation to the Taipei Representative Office in France for their great passion and heart-warming service.

I also appreciate all the support I received from my classmates: Charlene Monaco, Mingyan Wang, Paguédame Game; from my lab mates: Hézouwé Amaou Tallé, Lian Guey Ler, Masoud Ghulami; from personnel of Polytech Nice-Sophia: Ali Beikbaghban, Christine Lestrez, Laure Vallet, Na Yin; from the master students of EuroAquae. Thanks should also go to all the personnel from Polytech'Lab, the Doctoral School for Fundamental and Applied Sciences, Polytech Nice-Sophia and the University of Côte d'Azur. Without their sufficient mental and technical support, my doctoral study could not be successfully achieved and my life in France could not be so wonderful.

I would like to further express my special thanks to my family, especially my parents, Kung-Hui Hsu and Chih-Hui Chou. Without their tremendous understanding and unwavering support all through my study and my life abroad, I would never have completed my PhD journey. I am deeply indebted to them.

Lastly, thanks for everyone who has spent time and who will spend time on my doctoral thesis.

Résumé

Gestion du Risque d'Inondation dans les Zones Urbaines :
Valeur Ajoutée des Automates Cellulaires et de la Modélisation à Base d'Agents

Les inondations sont les catastrophes naturelles les plus courantes dans le monde, pouvant causer de graves dégâts humains et matériels, en particulier dans les zones urbaines. Par conséquent, la gestion du risque d'inondation est essentielle pour prévenir et réduire leur impact et gérer le risque d'inondation résiduel.

Cette étude a d'abord examiné plusieurs événements d'inondation historiques dans le monde, et en particulier dans les zones d'étude en France et à Taïwan. L'efficacité et les problèmes sur les cas d'applications ont également été analysés et résumés.

Ensuite, puisque les modèles à base d'agents (ABMs) sont des outils idéaux pour simuler les actions, les réactions et les interactions d'individus autonomes et de l'environnement dans un système complexe, afin d'évaluer l'efficacité et les résultats des stratégies de réduction des risques d'inondation, cette étude a utilisé un ABM, NetLogo, pour analyser les interactions possibles du comportement humain et de l'environnement avec différentes stratégies. Un ABM couplé a été développé, combinant (i) un modèle d'évacuation, pour les simulations d'agents afin d'étudier un éventuel processus d'évacuation pendant une inondation, et (ii) un modèle d'écoulement de surface 2D d'automates cellulaires (CA), pour les simulations d'inondation. Plusieurs études de cas et tests de référence ont été sélectionnés pour vérifier les modèles et évaluer leurs performances. Le modèle d'évacuation pourrait générer des résultats plausibles du processus d'évacuation, et les résultats ont montré l'importance des cartes de risque/inondation et du timing des alarmes d'avertissement. Le modèle d'écoulement de surface CA 2D pourrait produire des résultats de modèle prometteurs, et les résultats ont montré un grand accord entre les prédictions du modèle et les observations en termes d'étendue de l'inondation, de niveaux d'eau et de vitesses d'écoulement calculées.

Ensuite, l'ABM couplé a été appliqué pour analyser la gestion communautaire des risques d'inondation dans la zone d'étude. Les résultats de l'ABM couplé ont révélé sa capacité à réaliser des simulations d'inondations et le potentiel de générer des résultats plausibles de l'interaction entre les crues, les stratégies d'intervention et le comportement humain pendant une inondation.

Enfin, l'étude a proposé des applications possibles de l'ABM couplé et la faisabilité de l'intégration de l'ABM couplés et un Système d'Aide à la Décision (DSS). Malgré les avantages possibles dans divers domaines, il y a encore de nombreuses lacunes à

combler à l'intérieur d'un point de vue structurel sur ce type d'approche et de modèles. Les questions les plus importantes concernant le fonctionnement du DSS étaient la manière de normaliser le format, la communication et l'interopérabilité entre les différents composants existants.

Les perspectives de cette étude visent à étudier et à améliorer la gestion existante des risques d'inondation, à sensibiliser le public aux crises et à améliorer la gestion communautaire des risques d'inondation.

Mots Clés :

Automates Cellulaires, Gestion des Risques d'Inondation, Modèle à Base d'Agents, NetLogo, Simulation Hydraulique

Abstract

Flood Risk Management in Urban Areas:
Added Value of Cellular Automata and Agent-Based Modelling

Floods are the most common natural disasters worldwide, which can cause serious damage to property and fatality, especially in urban areas. Hence, flood risk management is essential to avoid new flood risk, to prevent and to reduce existing impact of floods and to manage residual flood risk.

This study first briefly reviewed several historical flood events worldwide, and especially the applications of flood risk treatment of the study areas in France and in Taiwan. The effectiveness and problems of the applications were also analysed and summarised.

Then, since Agent-Based Models (ABMs) are ideal tools for simulating the actions, reactions and interactions of autonomous individuals and the environment in a complex system, in order to evaluate the effectiveness and outcomes of flood risk reduction strategies, this study employed an ABM, NetLogo, to analyse the possible interactions of human behaviour and the environment with different strategies. A coupled ABM was developed, combining (i) an evacuation model, for the agent simulations to investigate possible evacuation processes during flood, and (ii) a cellular automata (CA) 2D overland flow model, for inundation simulations. Several case studies and benchmark tests were selected for verifying the models and evaluating the model performances. The evacuation model could generate plausible outcomes of the evacuation process, and the results showed the importance of the risk/flood maps and the warning alarm timing. The CA 2D overland flow model could produce promising model outputs, and the results showed great agreement between model predictions and observations in terms of inundation extent, water levels, and flow velocities.

Next, the coupled ABM was applied to analyse the community-based flood risk management of the study area. The results of the coupled ABM revealed its capability of conducting inundation simulation and the potential for generating plausible outcomes of the interaction between flood water, response strategies and human behaviour during a flood event.

Finally, the study proposed possible applications of the coupled ABM and feasibility of integration of the coupled ABM and a Decision Support System (DSS). Despite the possible advantages in various fields, there were still many gaps inside the structure to be filled. The most important issue about the operation of the DSS was the way of

format standardisation, communication and interoperability between the various existing components.

The study aims to investigate and to improve existing flood risk management, to raise public crisis awareness and to enhance community-based flood risk management.

Keywords:
Agent-Based Model, Cellular Automata, Flood Risk Management, Hydraulic Simulation, NetLogo

Table of Contents

Table of Figures

Table of Tables

Chapter 1.
Introduction

Chapter 1 Introduction

1.1 Background

Floods are the most common natural disasters worldwide. In the past two decades between 2000 and 2019, an average of 367 natural disaster events occurred every year, of which floods were the majority, accounting for 44% of the total disasters, as shown in Figure 1-1. (Centre for Research on the Epidemiology of Disasters, 2020)

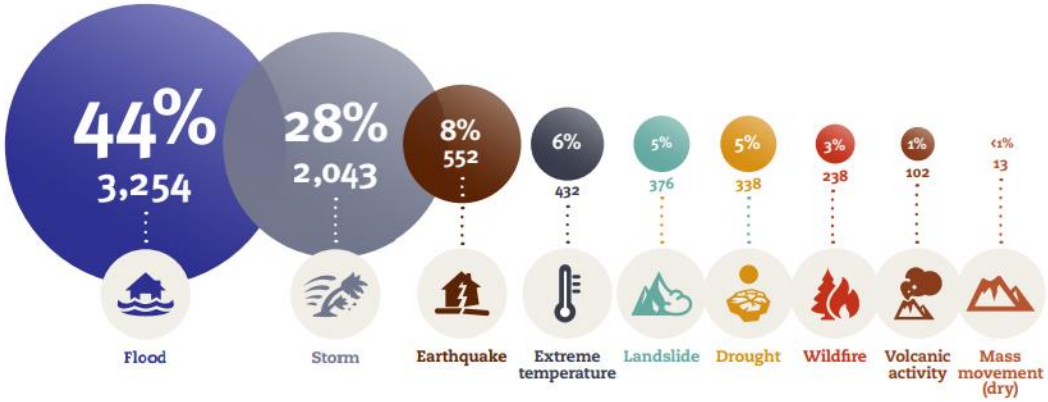

Figure 1-1. The percentage of occurrences of disasters. (source: Centre for Research on the Epidemiology of Disasters (2020))

According to the study (Rentschler et al., 2022), around 1.81 billion people, 23% of world population, are at risk of 1-in-100 year floods, facing water depth exceeding 0.15 metres. More than two-third of the world's flood-exposed people is located in South Asia, East Asia and Pacific region. The regional exposure estimates are shown in Figure 1-2.

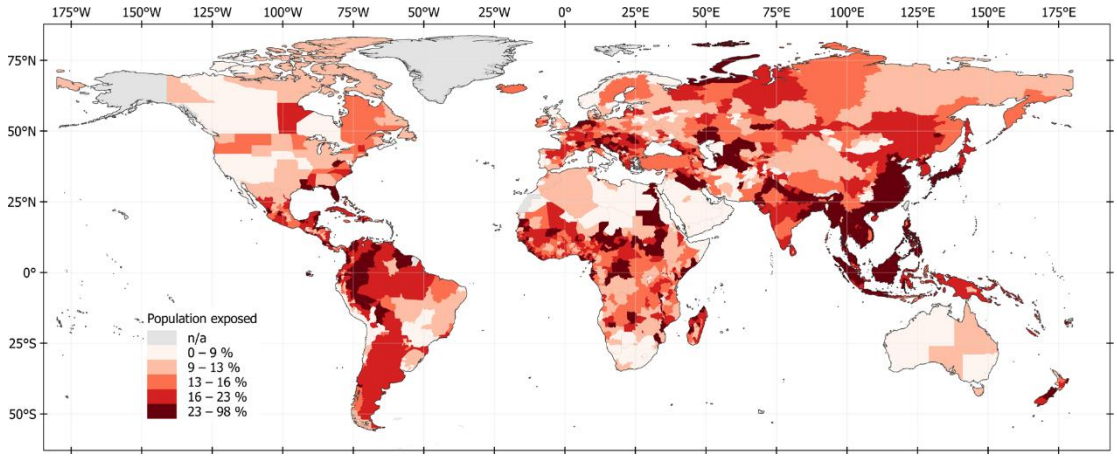

Figure 1-2. The percentage of population exposed to flood risk at the subnational level. (source: Rentschler et al. (2022))

Flood can cause fatalities and serious damage to property. Floods led to tremendous economic damage of approximately 651 billion USD, caused more than 100,000

deaths and affected around 1.65 billion people across the two decades. (Centre for Research on the Epidemiology of Disasters, 2020) Thus, flood risk management is essential to lower the risk, to prevent and to mitigate the crisis. Several different strategies and measures have been developed in response to flood disasters risk, and from flood disasters people also learned lessons to improve existing flood risk management. Some examples are described in the following sections, from Europe to Africa, South America, North America and to Asia. Those measures, both structural and non-structural, include: dams, detention/retention systems, sewer systems, diversion channels, pumps, floodwalls, floodgates, dykes, levees, barriers, relocation plans, flood/risk/disaster prevention maps, forecasting systems, early warning systems, monitoring systems, decision support systems, evacuation plans, smart water systems, civil security and volunteers, community-based flood risk management, flood insurance.

Asturias, Spain

Due to 8-day uninterrupted rain together with the thunderstorms in June 2010, the water levels of Sella River and Nalón River were tripled and overflowed, causing floods in Asturias. 20 roads were closed and rail services were interrupted; hundreds of evacuation processes were called, including a hospital, and 11 education centres were suspended. (La Nueva España, 2010; Basterra, 2017) After the event, a risk map was published by the national government as part as its civil security plan (Ministerio de Agricultura Alimentación y Medio Ambiente: Confederación Hidrográfica del Cantábrico, 2014), and the thresholds and the warning levels of different weather phenomena were also established. (Agencia Estatal de Meteorología, 2022)

Jeddah, Saudi Arabia

Two catastrophic flash flood events happened in Jeddah in 2009 and 2011, with a rainfall of 70 mm and 111 m in 3 hours for each event respectively. More than a hundred people died and around 10,000 houses and 17,000 vehicles were damaged. (Youssef et al., 2016) The average damages caused by the flash floods in the city cost nearly 2.6 billion USD. (Dano, 2020) After the events, dams, retention basins and drainage channels were built to protect the city. (Ali, 2018)

Nigeria

Since the mid-September 2022, Nigeria had been experiencing heavy rainfall and river overflows resulting in extreme flooding across the country. As of October 2022, more than 1.3 million people had been displaced and more than 2.8 million people had been affected. (European Commission's Directorate-General for European Civil

Protection and Humanitarian Aid Operations, 2022) Continuous rains and river bursts into October further increased the number of casualties, with 4.4 million people affected, 2.4 million displaced and 662 deaths recorded in December. (United Nations International Children's Emergency Fund, 2022) The United Nations released 10.5 million USD on 18 November 2022 for providing clean water, sanitation, emergency shelters and health care assistance (United Nations Office for the Coordination of Humanitarian Affairs, 2022). Flood level alerts from hydrological monitoring stations could also help the rapid interventions in the flooded areas along river Niger (International Federation of Red Cross and Red Crescent Societies, 2022).

Vargas, Venezuela

In 1999, an unprecedented record for accumulative precipitation of 1,207 mm in nine days, from 10 to 18 December, caused flash floods and debris flows. (Pan American Health Organization, 1999) The number of victims was estimated at between 15,000 and 50,000 (Grases et al., 2000), whereas another research work assessed at no more than 800 (Altez, 2010). After the event, sediment control dams, rain gauge stations and hydrometric stations were installed, and many rivers in the urban areas were channelled. (Lopez et al., 2010) Furthermore, early warning systems (Courtel et al., 2010) and programmes for strengthening community-based flood risk management were established. (Rodríguez et al. 2010)

Itajaí Valley, Brazil

A record-breaking rainfall fell on Blumenau in 2008 with total rainfall of 1000 mm in November, which was seven times more than the average rainfall, causing floods and landslides and thus 135 deaths. (Severo et al., 2011) After the event, historical flood maps were generated and published online. (Município de Itajaí, n.d.) A study project for disaster prevention and mitigation in Itajaí Valley was launched (Agência de Cooperação Internacional do Japão, 2011), and many telemetric stations were installed to monitor meteorological, climatological or hydrological information and to issue warnings and alerts to the publics. (Alertablu, n.d.)

Rio de Janeiro, Brazil

Due to torrential rainfall, two floods and mudslides events hit Rio de Janeiro in 2010, causing more than 70 deaths and over 4,000 homeless in January and more than 180 deaths and over 3,000 homeless in April. (BBC News, 2010; Folha de S.Paulo, 2010) After the events, four underground reservoirs and a diversion tunnel were designed to improve the resilience in Tijuca area. (C40 Cities Climate Leadership Group, 2015) An operational centre was also established for monitoring, forecasting, issuing

warning to the publics and coordinating different agencies. (Kitchin, 2014; Pinto & de Castro, 2022)

La Plata, Argentina

Torrential rains fell on La Plata between the afternoon of 2 April and the early morning of 3 April with accumulated rainfall of 392 mm, causing the death of more than 80 people and 350,000 hectares under water, affecting 190,000 residents. (Santiago Filipuzzi, 2021) After the event, the causes of the flood were investigated, and the flood maps and risk maps were generated. (Facultad de Ingenieria, 2013; Universidad Nacional de La Plata, 2017) Some sections of a stream were enlarged to increase the transport capacity. (Redacción Clarín, 2019) Flood diversion channels and monitoring systems were also built to protect the city. (La Política Online, 2018)

Córdoba, Argentina

On 15 February 2015, Córdoba was hit by intense rainfall of 200 to 250 mm, 320 mm in 12 hours in some areas, causing flooding that killed eight people and caused millions of dollars in damage. 250 homes had to be rebuilt and 1,780 homes needed to be repaired. 400 people were forced to evacuate and power was cut in Córdoba. (Davies, 2015; Pérez, 2020) After the event, during the reconstruction process, rivers were widened and deepen; floodwalls and multiple retention lagoons were also built to store water during heavy rains. Monitoring systems were also built to estimate potential floods in the region. Municipal civil defences work in a more coordinated manner and volunteer fire stations are becoming more networked. (Cuellar, 2020)

New York, the US

In late October 2012, Hurricane Sandy struck the coast of New York resulting in flooding due to storm surges and high tides and caused 43 deaths and 19 billion USD in damage. The flooded area was greater than the city's projection for 1-in-100 year flood due to sea level rise and the Federal Emergency Management Agency 1983 projection of the 100-year floodplain. (Rosenzweig & Solecki, 2014) After the event, some areas were redesigned to be lifted based on the projected sea level rise and storm surge. Some structures were included in the resiliency projects, such as floodwalls, floodgates, levees, barriers, and new parallel conveyance sewer lines to increase capacity and convey excess flow pump stations (City of New York, n.d.-a; n.d.-b). Furthermore, the flood insurance rate maps were also updated to reflect the current flood risk. (City of New York Mayor's Office of Recovery and Resiliency, 2015)

Flood in Seoul, South Korea

Torrential rains, with accumulated rainfall exceeding 500 mm, fell on Seoul in August 2022, resulting in a flood and caused power cuts, at least 9 deaths, around 2,800 homes damaged and more than 160 homeless. Some roads and underground services were also interrupted. (BBC News, 2022; Roh, 2022) After the event, underground rainwater storage tunnels along with the existing rainwater storage facility were planned to be built. (Yoo, 2022) Free installation of floodwalls provided by the government could also prevent floods, especially for semi-basement houses and buildings in low-lying areas. (Lee, 2018)

Incheon, South Korean

Heavy rain fell on 23 July, 2017 in Incheon with intensity higher than 100 mm/hour, causing an underground railway construction site, commercial buildings and numerous houses flooded with at least one death. Some roads and train services were also interrupted. (Yoon, 2017; Kang, 2017) After the event, a rainwater retention facility was designed to be built beneath a children's park. (Lim, 2021) The designed return period standard for the sewer systems were also raised from 20 years to 50 years. Furthermore, an information and communications technology based (ICT-based) system was designed to monitor water levels and flows in the sewer systems. When flood risk areas are identified, pump stations and sluice gates will operate automatically. (Kim, 2021)

1.2 Objectives of the Research

Floods are the most common natural disasters worldwide, which can cause serious damage to property and fatality, especially in urban areas. Hence, flood risk management is essential to avoid new flood risk, to prevent and to reduce existing impact of floods and to manage residual flood risk. In order to evaluate the effectiveness and outcomes of flood risk reduction strategies, this study employs an Agent-Based Model (ABM) to analyse the possible interaction between human behaviour and the environment with different strategies. The main objectives of the research are:

- to review the flood risk management, risk reduction strategies and to review the applications of flood risk treatment of the study areas in Nice (France) and in Taipei (Taiwan)
- to develop a coupled ABM combining an evacuation model and a cellular automata (CA) 2D overland flow model to analyse the interaction between human behaviours and the environment during flood events
- to evaluate the effectiveness and outcomes of flood risk reduction strategies
- to propose possible applications of the coupled ABM and to evaluate the feasibility of integration of the coupled ABM and a decision support systems (DSS)
- to investigate and to improve existing flood risk management, to raise public crisis awareness and to enhance community-based flood risk management

1.3 Thesis Structure

This doctoral thesis consists of 7 chapters. A brief description of rest chapters is as follows:

- Chapter 2 describes the concept of flood risk management and risk reduction strategies against flood risk, then reviews the applications of flood risk treatment of the study areas during historical events in the study sites, and finally analyses and summarises the effectiveness and problems of the applications.
- Chapter 3 introduces agent-based models (ABMs) and elaborates the methodologies of the study: agent modelling, cellular automata (CA) inundation modelling and inundation-agent coupled modelling.
- Chapter 4 introduces the case studies and the benchmark tests for model verification and then describes the results and the performance of the models.
- Chapter 5 introduces the flood risk management of the study area and the applications of the coupled ABM to evaluate the performance of the risk management.
- Chapter 6 introduces possible applications of the coupled ABM and feasibility of integration of the coupled ABM and DSSs.
- Chapter 7 concludes the study and provides future perspectives.

Chapter 2.
Flood Risk Management

Part of this chapter has been published:

Hsu, H. M., & Gourbesville, P. (2022). Applications of non-structural measures and self-protection against flood in urban areas in Taiwan and in France. In *Proc. 39th IAHR World Congress* (pp. 19-24). https://doi.org/10.3850/IAHR-39WC2521711920221389

Chapter 2 Flood Risk Management

Floods are the most common natural disasters worldwide, which can cause serious damage to property and fatality, especially in urban areas. Hence, flood risk management is essential to avoid new flood risk, to prevent and to reduce existing impact of floods and to manage residual flood risk. In this chapter, the concept of flood risk management and risk reduction strategies (structural measures and non-structural measures) against flood risk are introduced. Then the applications of flood risk treatment of the study areas, Alpes-Maritimes (France) and Taipei (Taiwan), during historical events are described, and the effectiveness and problems of the applications are also analysed and summarised. Finally, numerical modelling for flood risk management is introduced.

2.1 Introduction of Flood Risk Management

According to United National Office for Disaster Risk Reduction (2017), the definition of disaster risk is:

> The potential loss of life, injury, or destroyed or damaged assets which could occur to a system, society or a community in a specific period of time, determined probabilistically as a function of hazard, exposure, vulnerability and capacity.
>
> (United National Office for Disaster Risk Reduction, 2017, p. 75)

There are four main components which can determine the risk: hazard, exposure, vulnerability and capacity. In terms of flood risk, hazard is then the potential of occurrence of floods, which may cause loss of life, damage to properties and negative impact on the environment, and hazard increases with probability, flood depth, flow velocity and duration of flood. Exposure to flood hazard relates to the potential of danger to human and property damage in hazard-prone areas, and thus flood risk only exists in an area where people or assets may be damaged during flood. Vulnerability of people or properties refers to the susceptibility to flood hazard. Capacity refers to capability of managing and reducing flood risks and strengthening resilience, including drainage systems, crisis awareness, emergency responses and post flood support and so on. Thus the flood risk management aims to avoid new flood risk, to prevent and to reduce existing impact of floods and to manage residual risk, by means of reducing the flood hazard (by lowering flood occurrence, water depth, flow velocity, duration of flood, etc.), reducing exposure to flood hazard (by relocating, applying building codes, zoning laws, etc.) and diminishing vulnerability to flood hazard by increasing capacity (by improving drainage systems, applying flood monitoring and early warning systems, increasing public crisis awareness and preparedness, etc.).

The flood risk management follows the process outlined in the international standards on risk management, ISO 31000 (International Organization for Standardization, 2018) as shown in Figure 2-1.

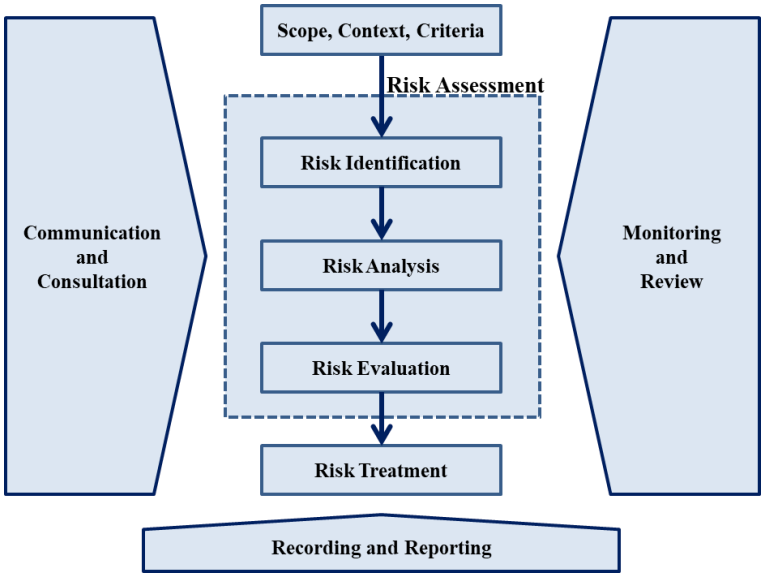

Figure 2-1. The flowchart of risk management process. (redrawn from: International Organization for Standardization (2018))

The first step, "Scope, Context, Criteria", is to understand the context of flood risk management to determine the objectives and influence of the flood risk management process and to define the purpose and scope of the flood risk assessment. The second step, "Risk Assessment", consists of three components: "Risk Identification", "Risk Analysis" and "Risk Evaluation". "Risk Identification" is to find, to recognise and to describe flood risk with the process of collecting the related knowledge and experience, data and information about historical events to draw initial conclusions about the importance of specific flood hazard, exposure, vulnerability and capacity to help the stakeholders understand the direction of "Risk Analysis" and "Risk Evaluation" and then design corresponding plans for the potential risks. "Risk Analysis" is to understand the details of flood hazard, exposure, vulnerability and capacity and their interactions to assess the potential impact and frequency of occurrence of flood. This step analyses flood hazard with the exposure, all dimensions of vulnerabilities (including physical, economic and environmental) and effectiveness of the existing capacities (including all structural and non-structural measures) to manage the risk. "Risk Evaluation" is to compare the severity of flood risk against the level of the risk to determine the relative priority for the purpose of managing the risk, and thus the tolerability of the risk leading to corresponding decisions in "Risk Treatment" step. The tolerability of flood risk can be categorised into three types: acceptable risk, tolerable risk and intolerable risk, based on the probability of

occurrence and extent of consequences, and the illustration is shown as Figure 2-2.

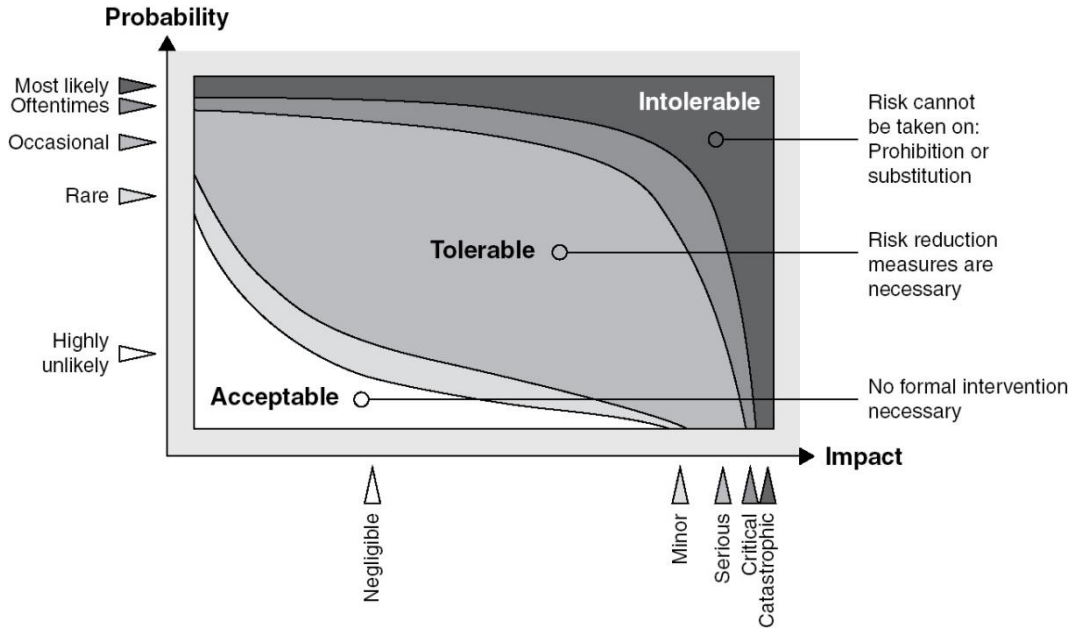

Figure 2-2. The illustration of acceptable, tolerable and intolerable risks. (source: Renn (2013))

The third step, "Risk Treatment", is the process of selecting and employing measures against flood in response to Risk Evaluation to reduce the flood risk. Generic risk treatment strategies to cope with flood risk can be categorised into four different types: risk avoidance, risk reduction, risk transfer and risk acceptance. Risk avoidance is to avoid any involvement in activities leading to flood risk or to fully eliminate the risk, and the strategy is usually applied to deal with the intolerable risk associated with high probability of occurrence and with high impact. Risk reduction is to reduce the impact of flood and probability of flood risk to an acceptable level, and it can be categorised into structural measures and non-structural measures. Further information about both structural and non-structural measures will be elaborated in section 2.2. The strategy of risk reduction is usually applied to deal with the tolerable risk associated with mid to high probability of occurrence but with mid to low impact. Risk transfer is to pass or share the risk to other parties through contracts or flood insurance, and the strategy is usually applied to deal with the tolerable risk associated with low probability of occurrence but with mid to high impact. Risk acceptance is to retain the possible impact of flood risk, and the strategy is usually applied to deal with the acceptable risk associated with low probability of occurrence and with low impact. The illustration of the concept of the above-mentioned risk treatment strategy selection is shown as Figure 2-3. A combination of multiple risk treatment strategies with different measures can be adopted together to deal with flood risk.

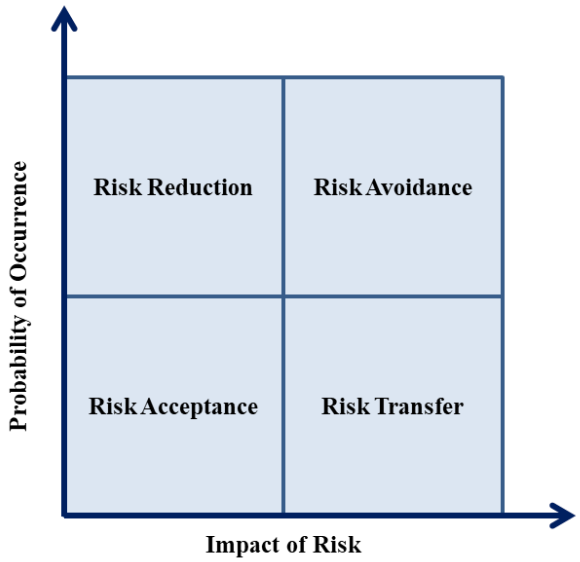

Figure 2-3. The illustration of risk treatment strategy selection.

"Recording and Reporting" is to ensure stakeholders share the same understanding about risks and risk management and to enhance the quality of interaction with each other by means of documenting the relevant information about the flood risk management process and the outcomes in formal reports for publishing, sharing, communicating, planning, decision-making and further improving the existing flood risk management. The step of "Communication and Consultation" should take place in all stages of the flood risk management process to help relevant stakeholders in understand flood risk, to raise crisis awareness and to exchange information and opinions for supporting decision-making. "Monitoring and Review" is to assure and improve the quality and effectiveness of process design, implementation and outcomes by detecting changes and identifying new risks. This step is required within each stage of the flood risk management to assure the effectiveness of the risk treatment due to changing flood risk.

2.2 Structural and Non-structural Measures

According to United Nations Office for Disaster Risk Reduction (n.d.), the definition of structural measures is:

> Structural measures are any physical construction to reduce or avoid possible impacts of hazards, or the application of engineering techniques or technology to achieve hazard resistance and resilience in structures or systems.

Common structural measures for flood disaster risk reduction include dams, dykes, levees, seawalls and floodwalls, flood diversion channels, river channel improvements, sewer systems, pump stations, retention ponds and detention ponds, resistant construction, shelters and so on. The majority of these structural measures are implemented to directly lower the flood hazard, and thus flood risk. Despite various implements of structural measure, flooding may be still inevitable in extreme weather condition. Conventional structural measures may not be sufficient to eliminate flood risk and tend to create a false sense of security to the public. Accordingly, non-structural measures and self-protection are essential to flood disaster management, enhancing community resilience to flood. (Andjelkovic, 2001)
Different from structural measures, the definition of non-structural measures from United Nations Office for Disaster Risk Reduction (n.d.) is:

> Non-structural measures are measures not involving physical construction which use knowledge, practice or agreement to reduce disaster risks and impacts, in particular through policies and laws, public awareness raising, training and education.

Common non-structural measures for flood disaster risk reduction include flood monitoring and forecasting systems, flood early warning systems, risk assessment, disaster preparedness, crisis response plans, post-flood recovery and reconstruction, flood plain regulation, building codes, zoning laws, relocation, flood insurance, resilient plans, business continuity plans, research, disaster education, public awareness, evacuation and rescue, volunteers and so on. Different from structural measures aiming physical intervention against flood, non-structural measures focus on modifying human behaviours. Most of those non-structural measures are employed to lower the vulnerability and exposure to flood risk and to increase capacity.
A combination of different available options amongst structural and non-structural measures can be implemented together, which can make flood risk management more flexible to deal with flood risk at different levels. An antecedent research (Petry, 2002) presents the importance of integration of both structural and non-structural measures and provides an overview of advantages and weakness as shown in Table 2-1.

Table 2-1. An overview of advantages, disadvantages and improvement priorities of structural and non-structural measures. (source: Petry (2002)).

MEASURES TO COPE WITH FLOODS	STRUCTURAL	NON-STRUCTURAL
CLASSIFICATION	*EXTENSIVE* • reshaping of land surface • protection from erosion • delay of runoff processes • increase of infiltration • urban works *INTENSIVE* • levees, dikes, floodwalls • dams and reservoirs • floodways and diversion works • polders and fills • drainage works	*REGULATION* • zoning • coding *FLOOD DEFENCE* • forecasting • warning • floodproofing • evacuation • relocation *INSURANCE* • governmental • private • mixed
ADVANTAGES	• runoff delay and increase of infiltration • flood attenuation • downstream discharge control • groundwater control	• no significant environmental changes • improved organizational relations in the area • effectivity in dealing with flood impacts and damages
DISADVANTAGES	• reduction of floodplain fertility • high potential of ecological impacts • morphological changes • land subsidence	• raise of property value and invasion of floodplains • higher level of insurance coverage needed
IMPROVEMENT PRIORITIES	• reforestation • erosion control • soil conservation • retention ponds • impact mitigation of reservoirs • construction of platforms and polders in floodplains	• institutional and legal frameworks • implementation of insurance systems and coverages • forecasting/warning systems

Several historical events and applications of structural and non-structural measures against flood disaster in the study areas in France and in Taiwan will be described in the section 2.3. The actions of the applications during historical events are chronicled, from preparedness to response, and the pros and cons of the actions are analysed and summarised in the study.

2.3. Applications of Flood Disaster Risk Reduction of the Study Areas

Applications of risk reduction, structural and non-structural measures, against flood during the historical events since 2015 are compared in two study areas of this study: the department of Alpes-Maritimes, France and Taipei City, Taiwan.

The department of Alpes-Maritimes is located in the south part of France, in the Mediterranean area, as shown in Figure 2-4 (a). According to Météo-France (2020a), recent extreme weather events showed intensification and an increase in frequency of extreme rainfall, especially those exceeding 200 mm in 24 hours. Taipei City is in the north part of Taiwan, in Southeast Asia, as shown in Figure 2-4 (b), facing monsoon and convective rain in the period of May-September and 3 to 4 typhoons on average every year in summer and early autumn. These heavy rainfall events may cause severe flood and inundation. Furthermore, because of climate change, frequency of flood may even increase. (Hirabayashi et al., 2013; Tabari, 2020)

(a)  (b) 

Figure 2-4. (a) The department of Alpes-Maritimes, France (source: TUBS, 2015), and (b) Taipei City, Taiwan. (source: TUBS, 2011)

2.3.1 Historical Events

Alpes-Maritimes, France

A storm struck the department of Alpes-Maritimes on 3 October 2015 with maximum rainfall intensity 78 mm/hour in Nice, and 152 mm in 2 hours in Mandelieu-la-Napoule. Nice received the equivalent in rain of an average October, about 10% of its average yearly precipitation in two days. The storm caused 20 casualties and insured damage ranging from 550 to 650 million euros. (Libération, 2015, Météo-France, 2015; Ministère de l'Intérieur, 2015; Préfet des Alpes-Maritimes, 2016; Salvan, 2017; Binacchi, 2019) In 2020, catastrophic Storm Alex struck the department on 2 October with accumulated rainfall of 150 mm to 500 mm in 24 hours and locally more than 300 mm in 12 hours (450mm to 500 mm in the hinterland). The accumulative rainfall set a record with the equivalent of one to three months of average October rainfall. (Météo-France 2020a, 2020b) The storm caused 10 casualties, 8 missing, 13,000

victims and estimated damage at one billion euros. 420 houses were affected (180 totally destroyed and 240 at risk) and 20 bridges were destroyed; around 100 kilometres of roads and more than thousand kilometres of hiking trails were damaged. (Binacchi, 2021a, 2021b; Département des Alpes-Maritimes, 2021; Jocteur Monrozier, 2021) On 20 October 2023, Storm Aline brought heavy rains for several hours, reaching up to 200 mm in Vésubie, 175 mm in Roya and 130 mm in Tinée. Landslides and mudslides partially destroyed roads and villages causing the damage up to tens of millions of euros. (Le Figaro, 2023) On 2 November 2023, another storm, Ciaran, hit Alpes-Maritimes and caused at least 2 casualties and 16 injuries, and 820,000 houses were out of power during the storm. (Damien Allemand, 2023a)

Taipei, Taiwan

Typhoon Soudelor struck the city of Taipei on 8 August morning in 2015 with maximum accumulative rainfall 582 mm in 24 hours and maximum rainfall intensity 24 mm in 10 minutes and 103.5 mm in 1 hour. The typhoon caused 128 injuries and 137 flooding cases, and failure of power and water supply. (Taipei City Fire Department, 2015a) In the same year, another Typhoon, Dujuan, hit the city on 28 September evening with maximum accumulative rainfall 506 mm in 24 hours and maximum rainfall intensity 89.5 mm/hour. Dujuan caused 110 injuries, 1 death and 79 flooding cases, and failure of power and water supply. (Taipei City Fire Department, 2015b) One year after, Typhoon Megi hit Taipei on 27 September morning in 2016 with maximum accumulative rainfall 527.5 mm in 24 hours and maximum rainfall intensity 133.5 mm/hour, causing 46 flooding cases. (Taipei City Fire Department, 2016b)

Due to a stationary front, a 6-hour plum rain fell on 2 June morning in 2017 with maximum rainfall intensity of 33.5 mm in 10 minutes and more than 90 mm in 1 hour. It resulted in 4 injuries and 433 flooding cases. (Taipei City Fire Department, 2017a) Moreover, a convective rain poured down on 8 September evening in 2018 with maximum rainfall intensity 27.5 mm in 10 minutes, 138 mm in an hour and 223 mm in 3 hours, causing 126 flooding cases. (Taipei City Fire Department, 2018c) Another convective rain came down on 22 July afternoon in 2019 with maximum rainfall intensity more than 28 mm in 10 minutes, 136.5 mm in an hour, causing 244 flooding cases. (Taipei City Fire Department, 2019a)

In addition, there were other 6 different typhoons and tropical depression hitting Taipei with heavy rain since 2015. Some of them brought about more than 200 mm to 400 mm in 24 hours, with maximum rainfall intensity around 35 mm to 90 mm per hour. Fortunately the rainfall intensity in urban areas was much lower than those in the other places and rain was not concentrated, and thus no flooding cases were

generated. (Taipei City Fire Department, 2016a, 2017b, 2018a, 2018b, 2019b, 2019c)

2.3.2 Applications of Flood Risk Management

Drainage Systems

In Nice, there were 2 reservoirs with total capacity of 40,000 m^3 and 30 pump stations; the total length of sewer pipelines was around 320 km, and the urban drainage networks in Nice city are shown in Figure 2-5. (Salvan, 2017) In Taipei, there were 4 retention ponds, 88 pump stations and 517 portable pumps (including the pumps which can be mobilised through open contracts) (Taipei City Fire Department, 2017a); the total length of sewer pipelines was around 716 km (Hydraulic Engineering Office, 2022), and the urban drainage networks in Taipei city are shown in Figure 2-6. (Wang et al., 2021) The structures operated normally during the historical events in both study areas, the chief cause of which was intense rainfall exceeding the designed return period. The only exception of the events happened in Taipei on 2 June in 2017 due to failure of inlets which were covered by fallen leaves. (Taipei City Fire Department, 2017)

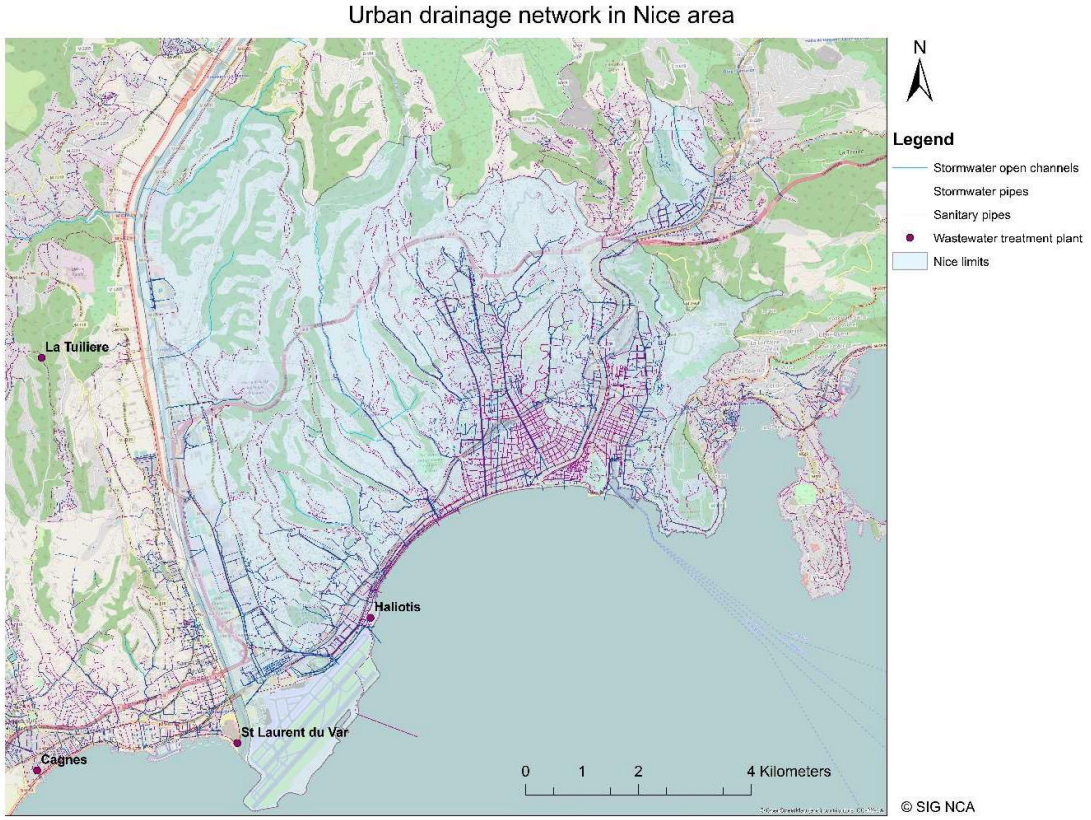

Figure 2-5. The urban drainage networks in Nice. (source: Salvan (2017))

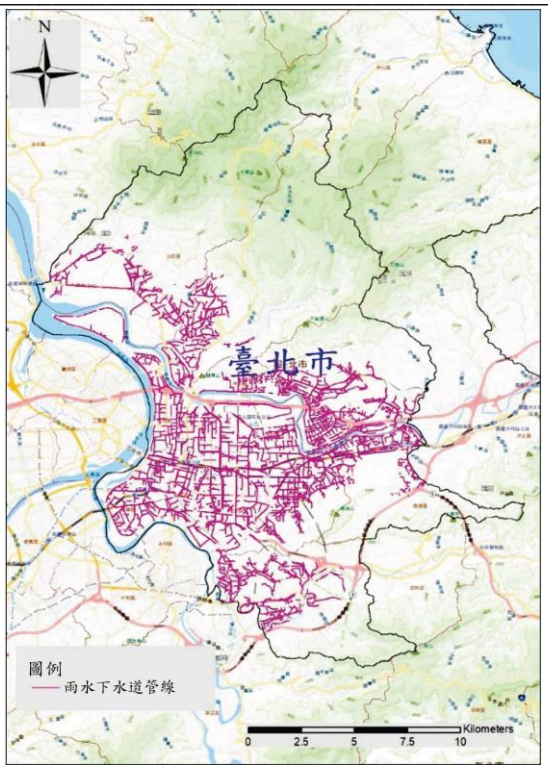

Figure 2-6. The urban drainage networks in Taipei. (source: Wang et al. (2021)) The red purple lines are the stormwater pipelines.

Risk Maps and Flood Maps

Vulnerability maps, flood maps and risk maps of Nice (Batica, 2015) and of Taipei (National Taiwan University, 2012) had been generated before the crises. All the maps were also published online, and everyone could access and download. These maps were utilised as reference for crisis management. Examples of flood map and risk maps are as shown in Figure 2-7 (France) and Figure 2-8 (Taiwan).

(a)

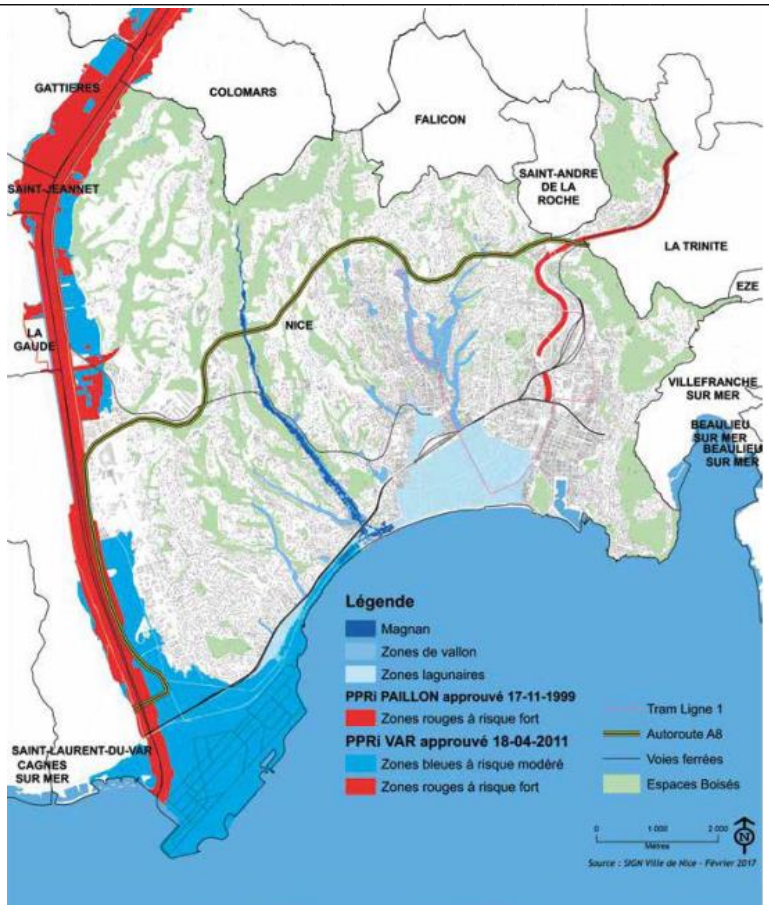

(b)

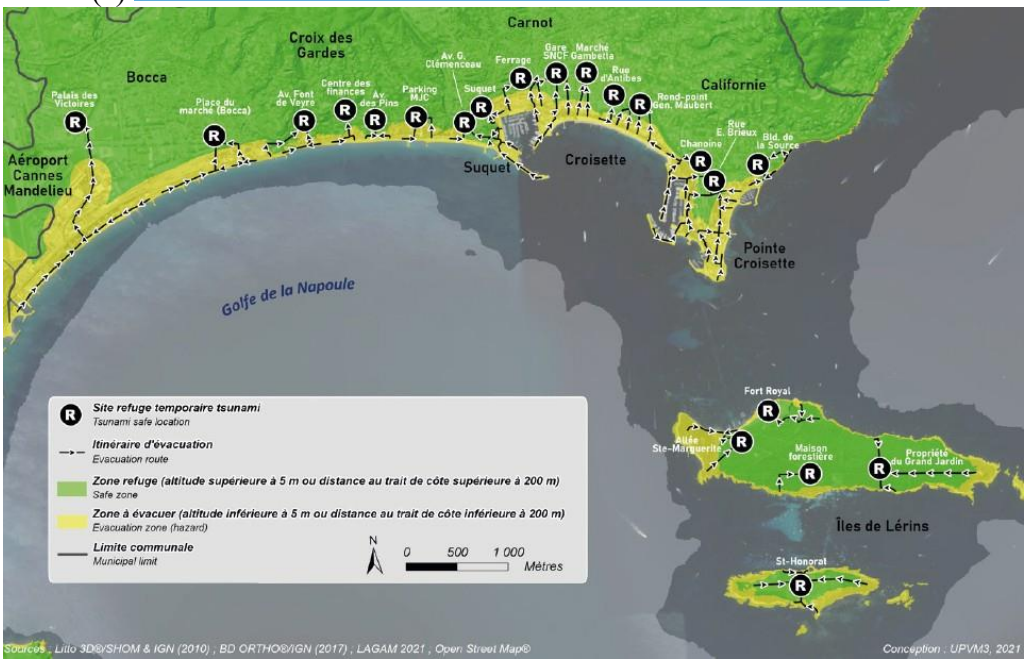

Figure 2-7. (a) The flood risk map of Nice, France. (source: Direction de la Prévention et de la Gestion des Risques (2017)). The red areas are high-risk areas, and the blue areas are moderate-risk areas. (b) The tsunami risk map of Cannes, France. (source: Ville de Cannes (n.d.)) The green areas are the safe zones with altitudes above 5 metres and more than 200 metres from the coast; the yellow areas are the evacuation zones with altitudes below 5 metres and within 200 metres from the coast; the dot-dash lines are evacuation routes.

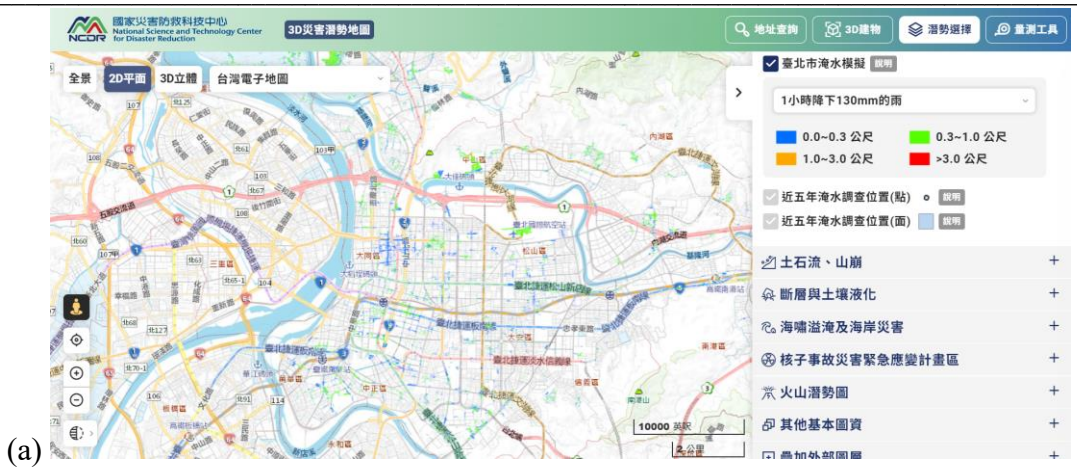

(a)

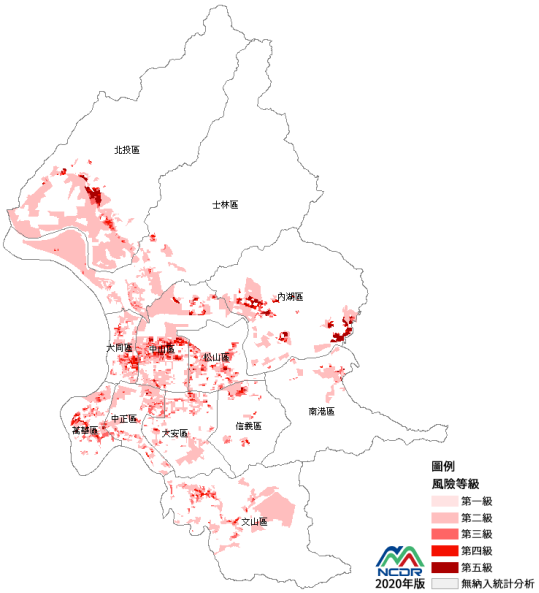

(b)

Figure 2-8. (a) An example of the online flood maps of Taipei, Taiwan, under different scenarios. (source: National Science and Technology Center for Disaster Reduction (n.d.)). The figure shows the output of inundation simulation of 130 mm rainfall in 1 hour. (b) An example of the flood risk maps of Taipei, Taiwan. (source: National Science and Technology Center for Disaster Reduction (2021)) The darker the colours are, the higher the risk is.

Warning and Alert Systems

In Alpes-Maritimes, during the storm event in 2015, Météo-France announced an orange warning on 3 October at 11:00 for the storm risk from 14:00. The warning was relayed by the Prefecture at 12:44, and then a yellow alert of flood was announced in the afternoon for the Var River. The information was posted on press media and social networks. (Préfet des Alpes-Maritimes, 2016) These warnings and alerts were broadcast about 6 hours ahead before the rain event. For Storm Alex in 2020, a red warning was announced on 2 October at 06:07 for the department, indicating high probability of exceptional rainfall intensity between 250 mm and 500 mm of rain

locally in 12 hours, about 14 hours ahead before the peak of rainfall, and then red alert of flooding was announced at 18:30. (20 minutes, 2020; French Government, 2020; Mérou, 2020; Groupe URD, 2021a) An example of river stages monitoring information and flood alert is shown as Figure 2-9, and the weather warnings for Storm Alex is shown as Figure 2-10. After the events, the Nice City Government provided SMS service for sending disaster information, as shown in Figure 2-11.

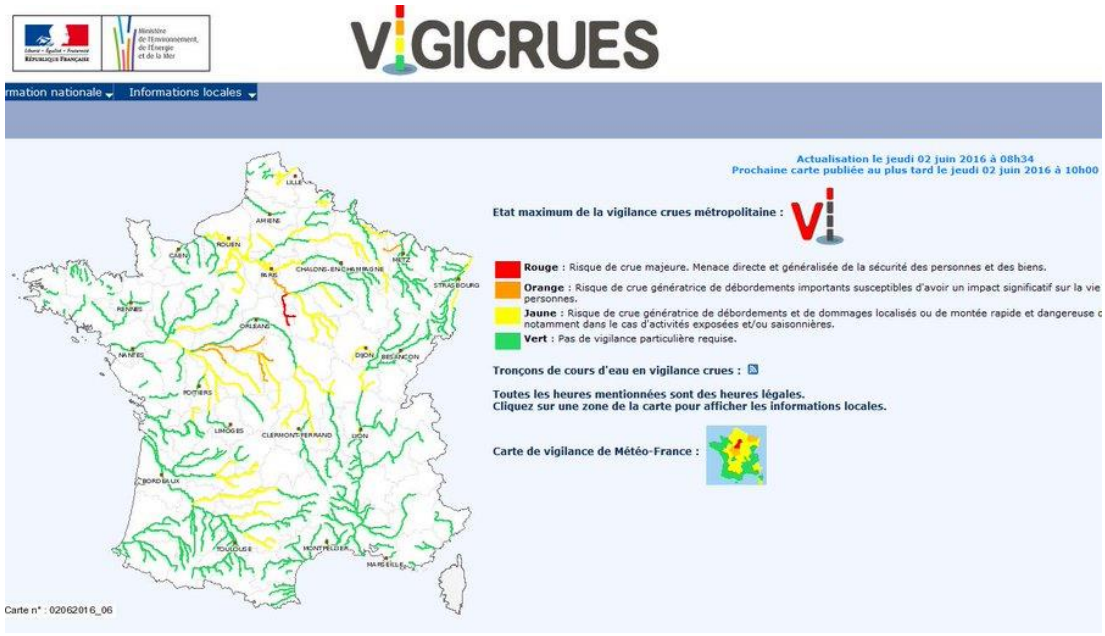

Figure 2-9. Example of river stages monitoring information and flood alert provided on Vigicrues website. (source: Gouvernement (2016)) The red, orange, yellow and green colours show different levels of risk of the rivers: red is the highest and green is the lowest.

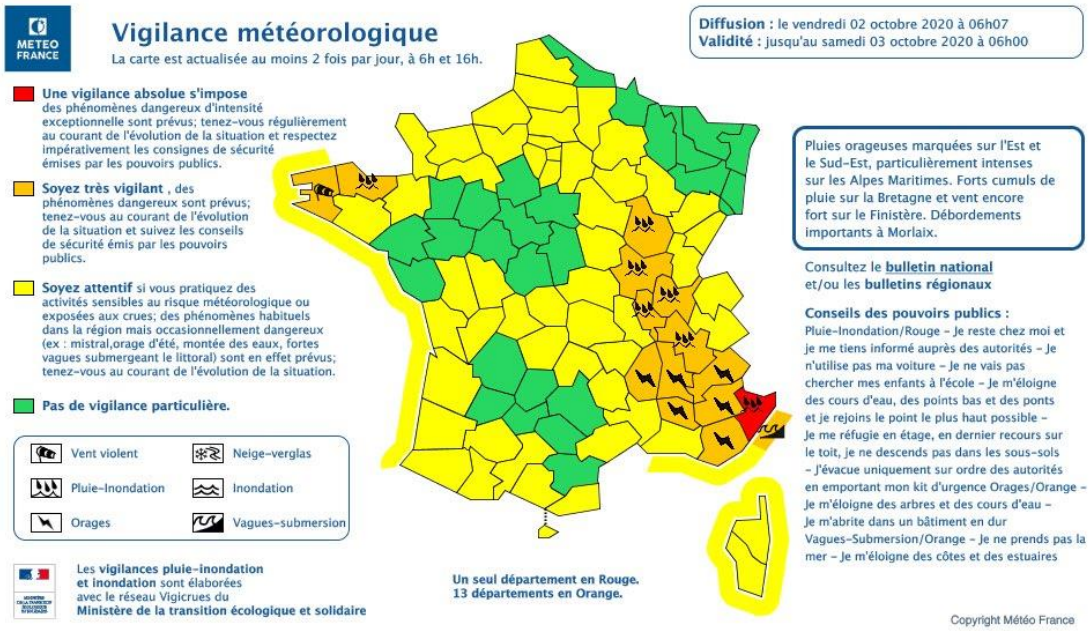

Figure 2-10. The weather warnings announced by Météo-France for Storm Alex. (source: Météo-Paris (2020)) The red, orange, yellow and green colours show different levels of vigilance: red is the highest and green is the lowest. Six icons at the low left corners means: violent wind, rain-flood, thunderstorms (on the left), snow-ice, inundation, waves-submersion (on the right). The text on the low right corner shows some advice from the authorities under different weather warnings in French.

Figure 2-11. The poster from Nice city government for advertising the SMS service for sending disaster information. (source: Ville de Nice (n.d.)) The text on the left means "SMS alert. Major risk." in French; the text on the right means "storms, earthquakes, attacks.... will be alerted by SMS in real time" in French.

In Taiwan, by definition, official typhoon warnings were issued just 18 hours before typhoon radii were expected to hit on land. In Taipei, emergency operation centre (EOC) started operating 1 to 2 days before landfall of the typhoons Soudelor, Dujuan and Megi, dealing with the incoming crises. (Taipei City Fire Department, 2015a, 2015b, 2016b) In contrast, for plum rain and convective rain, people had shorter time to respond. For the plum rain event on 2 June in 2017 (the peak of rainfall was about

between 10:00 to 14:00), Taipei city was informed about a possible heavy rain on 26 May and received warnings at 08:00 on 1 June and 08:00 on 2 June. At last, EOC was asked to operate at 10:50. For the convective rain event on 8 September in 2018 (the peak of rainfall was about between 16:30 to 18:30), Central Weather Bureau informed Taipei city about a possible heavy rain 3 days before the event. EOC sent warnings at 14:46 to the government and at 16:45 to the public on 8 September through social messaging application by the official account of Taipei city government. For the convective rain event on 22 July in 2019 (the peak of rainfall was about between 15:10 to 15:40), EOC in Taipei issued a rain warning at 08:33 in the weather forecast report and sent warnings at 12:22, 15:14, 15:22, 15:35 through social messaging application and at 15:34 through SMS to the public on 22 July. (Taipei City Fire Department, 2017a, 2018c, 2019a) By virtue of the 200-years return period design of the dykes around Taipei, only 1st to 3rd level of alert of river level had been announced during the events, without any alert of flooding, albeit the high water. (Taipei City Fire Department, 2015a, 2015b, 2016b, 2017a, 2018c, 2019a) Examples of the online information about the weather warnings and the flood alerts are shown in Figure 2-12. A screenshot of the map information display system of Taipei for displaying real-time hydrological information and disaster prevention information is shown as Figure 2-13.

(a)

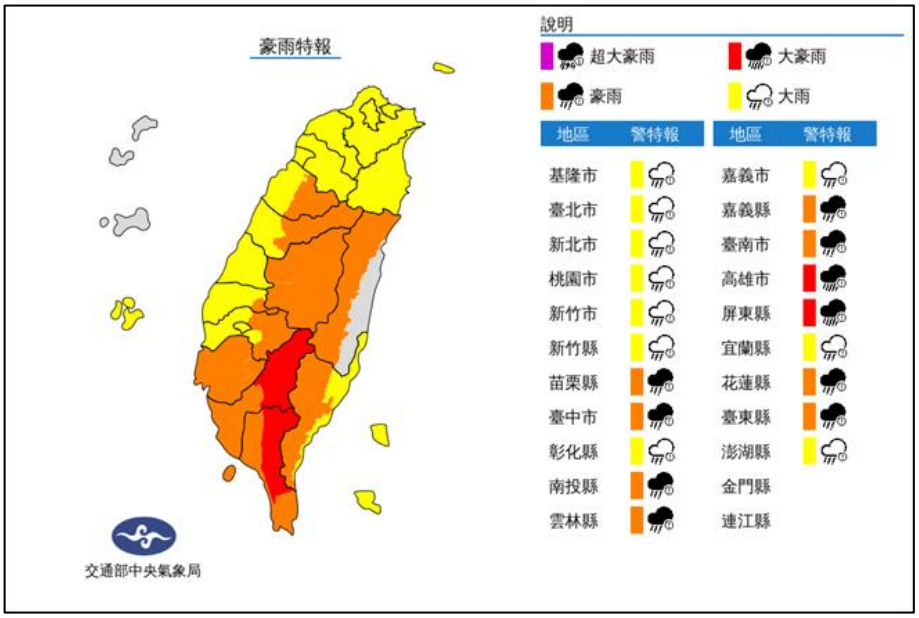

(b)

Figure 2-12. Examples of the online information about (a) the weather warnings (source: Central Weather Administration (n.d.)). The purple, red, orange and yellow colours show different levels of torrential rain warning: the purple is the highest and the yellow is the lowest; grey areas mean no warnings. The text on the right are the names of different cities. (b) The flood alerts (source: Water Resources Agency (n.d.-b)) in Taiwan. The red areas are under first alert and the yellow areas are under seconds alert.

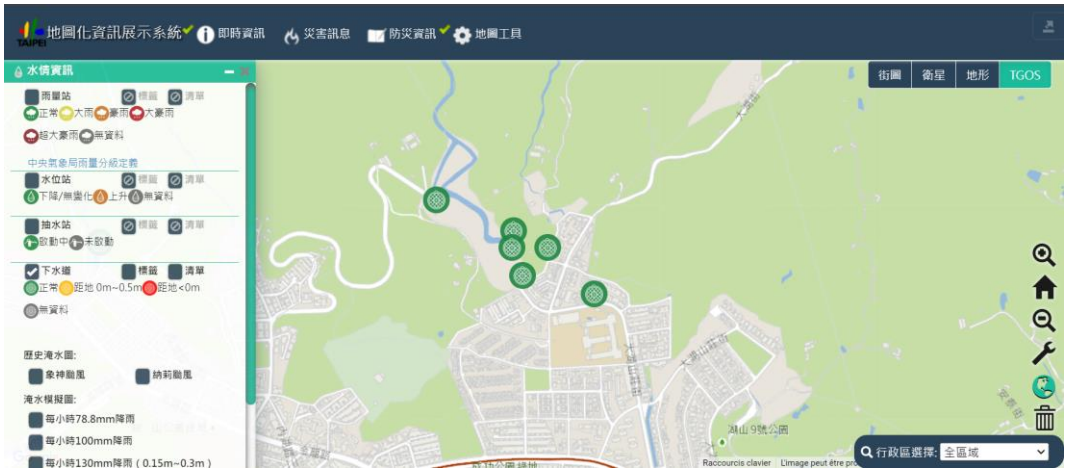

Figure 2-13. An example of map information display system for displaying real time hydrological information and disaster prevention information. (source: Taipei City Emergency Operations Center (n.d.)) The green dots on the map mean the manholes are under normal situation. If the water levels are 0 – 0.5 metres below the tops, the dots will turn into yellow dots; if the water levels are less than 0 metre below the tops (surcharge), the dots will turn into red dots.

Suspension and Evacuation

In Alpes-Maritimes, during the storm event in 2015, the people in Allianz-Riviera Stadium and in Palais Nikaïa concert hall were evacuated. Around 1,200 people in Alpes-Maritimes had to be accommodated, and some were proposed to stay in hotel. (Préfet des Alpes-Maritimes, 2016) During Storm Alex in 2020, schools were suspended whole day on 2 October, and preventive evacuation was underway for residents in the valley before the storm. Two gymnasiums in Carros and Saint-Martin-du-Var, and Palais Nikaïa concert hall in Nice were opened as shelter in the evening. 1,490 people were evacuated by helicopter and 700 people were received in emergency accommodation centres. (French Government, 2020; Mérou, 2020) During Storm Aline, residents in the valleys and a campsite in Antibes were evacuated. All schools were closed. Shopping centres and buses only opened in the afternoon. (Mathilde Frénois, 2023)

In Taipei, before Typhoon Soudelor in 2015, Taipei city government appealed people to stay home and called off schools and works on 7 August evening (announced at 10:30 on 7 August) and 08 August whole day (announced at 20:00 on 7 August). 61 people were evacuated, 29 in schools and the rest in their relatives' or friends' houses. Similarly, before Typhoon Dujuan in 2015, people were asked to stay indoors, and the government called off schools and works on 28 and 29 September whole day (announced at 22:00 on 27 and 22:00 on 28 respectively). 283 people were evacuated preventively, 2 in a school, 2 in a district office and the rest in their relatives' or friends' houses. In the plum rain event in 2017, a preschool was flooded at 11:26, and

then EOC received the call at 11:32. 49 people (40 children and 9 teachers) were evacuated with the help of rescue team to a temple, an upper and safe area, at 12:00.

Traffic and Deployment

In Alpes-Maritimes, roads, railways, and airlines were affected in the storm event in 2015. (Préfet des Alpes-Maritimes, 2016) During Storm Alex in 2020, bus lines and trains were cancelled, and many roads were closed in the afternoon on 2 October. Then, the exits of motorway in Nice were closed at night, and the valleys were inaccessible due to road cut off, as shown in Figure 2-14. During Storm Aline in 2023, bridges and roads were swept away. Parks, gardens and beaches were closed to the public. (Mathilde Frénois, 2023) In the same year, during Storm Ciaran, trains were cancelled, and many roads and tunnels were closed. (Emilie Moulin, 2023; Nice Matin, 2023a; 2023b; 2023c) The Figure 2-15 is the announcement about the interruption of train service from National Society of the French Railways. (Société Nationale des Chemins de Fer Français, SNCF, 2023) In addition, the closure of the well-known beaches and the coastal promenade in Nice was also announced because of 5-metre-high wave. (Damien Allemand, 2023b)

Figure 2-14. The bridge destroyed during Storm Alex. (source: Météo-Paris (2020))

Figure 2-15. Train traffic was interrupted after a rock falls on the railway track. (source: SNCF (2023)) The texts in French mean: 1. When rockfalls are signalled visually or by sensors, the driver immediately stops the train; 2. The traffic will be interrupted in the concerned area. Then, maintenance teams will be called to the site to inspect the material damage. 3. If the train is blocked and cannot leave, passengers will be transferred by road transport. The evacuated train can reach a garage site or the maintenance workshops if it is damaged. If traffic remains interrupted, the maintenance teams are responsible for removing the rocks to free the track. 4. Once the track has been freed and after installation tests, the network manager authorises the resumption of traffic gradually and possibly at a reduced speed

Helicopters flew to the isolated areas in the upper Roya, Tinée and Vésubie valleys in the north part of Alpes-Maritimes, helping in evacuating and transporting medical equipment, bottled water and food. (Groupe URD, 2020) Flights via the Nice Côte d'Azur Airport were suspended since the evening, and the passengers in the airport were asked to stay indoors. (Mérou, 2020; Jocteur Monrozier, 2021) In Taipei, portable pumps and rescue equipment were deployed at high-risk areas, and sandbags and water gates were prepared before the heavy rain at high flood potential areas and

at every entrance of metro stations, according to the risk maps and the flood maps. Vehicles in high-risk areas were removed, and public transport was also adjusted (cancelled or making a detour). Evacuation gates were closed to ensure no passage between the inside and the outside of the dykes. (Taipei City Fire Department, 2015a, 2015b, 2016b, 2017a)

Telecommunication

In Alpes-Maritimes, the radio system could work properly during the storm in 2015, whereas the electrical networks and the telephone networks were cut off and thus the related communication services. (Préfet des Alpes-Maritimes, 2016) Similarly, during Storm Alex in 2020, many people in hinterland could not utilise electricity, telephone, and internet services. In order to ensure the conveyance of information to the isolated people in the valleys, satellite telephones and radio aerials were distributed to ensure the contact. (Dumain, 2020; Groupe URD, 2020, 2021a, 2021b; Juszczak, 2020) In Taipei, people experienced an internet slowdown due to the influence of strong wind of typhoon, and no internet in some suburban areas, including a reservoir administration. To maintain communication, 5 network hosts were designed for the administration. (Taipei City Fire Department, 2015a, 2015b) Additionally, other than radio, television and press media, the government also utilised social messaging application and short message service cell broadcast (SMS-CB) to the people inside high-risk areas, especially for short duration intense rainfall events. (Taipei City Fire Department, 2017a, 2018c, 2019a)

Power and Water Supply

In Alpes-Maritimes, a utility company provided generators to restore communication and to preserve food in refrigerators and freezers, after the failure of power supply during Storm Alex. Many water distribution networks had also been destroyed due to the flood. People were depending on bottled water at first before the installation of distribution pipes and small emergency water purification systems for drinking water. (Groupe URD, 2020) In Taipei, water supply was suspended during Typhoon Soudelor for about 2 days because of high turbidity. (Taipei City Fire Department, 2015a) In the same year, before Typhoon Dujuan, people were asked to store water for possible water cut-off due to water turbidity, considering the experience during Soudelor. Water supply was suspended during Dujuan for about 1 to 4 days, and meanwhile water tanks and nurse tanker were deployed before the restoration of water supply, as shown in Figure 2-16. (Taipei City Fire Department, 2015b) Power supply was cut off for about 1 to 2 days because of the strong wind of the typhoons, not the flood, and people were using generators before restoration. (Taipei City Fire

Department, 2015a, 2015b, 2016b)

Figure 2-16. Water tankers and nurse tankers. (source: Taipei City Fire Department (2017a))

Volunteers

Volunteers mostly helped in clearing and cleaning, providing and distributing materials, restoring, bringing relief to victims. In Alpes-Maritimes, during the storm in 2015, there were 120 volunteers from French Red Cross 06, 90 volunteers from other departments and 80 first aiders from the departmental civil security association. (Préfet des Alpes-Maritimes, 2016) Similarly during Storm Alex 2020, there were numerous volunteers from all over France, including 150 volunteers from the French Red Cross and Monégasque Red Cross. (Lagrange, 2020; Groupe URD, 2021b) In Taipei, during Typhoon Soudelor, about 400 volunteers and soldiers were helping every day, and at least 25 volunteers during the plum rain event in 2017. (Taipei City Fire Department, 2015a, 2017a)

Education and Awareness

In Alpes-Maritimes, before Storm Alex in 2020, Breil-sur-Roya had been involved in an exercise two weeks before the storm. This exercise was a commune plan of crisis management, connecting the actors for emergency responses to flood events. The exercise facilitated the organisation of municipal teams during the storm, and furthermore, following the exercise, preventive evacuations had been carried out before the arrival of Storm Alex. (Groupe URD, 2020) Furthermore, posters and brochures were also spread for disaster education. Some examples of the posters are shown in Figure 2-17 and the brochures for different target audiences are shown in Figure 2-18. In Taipei, before typhoons, people were taught to clean trenches and inlets of sewer systems, deploy floodgates and sandbags against flood, and prepare food and water in case of cut-off. In addition, people were taught to accept a concept that flood might still happen despite well-design flood protection structures, and therefore, people should learn self-protection and self-rescue. (Taipei City Fire Department, 2015b, 2018c, 2019a)

(a) 

(b) 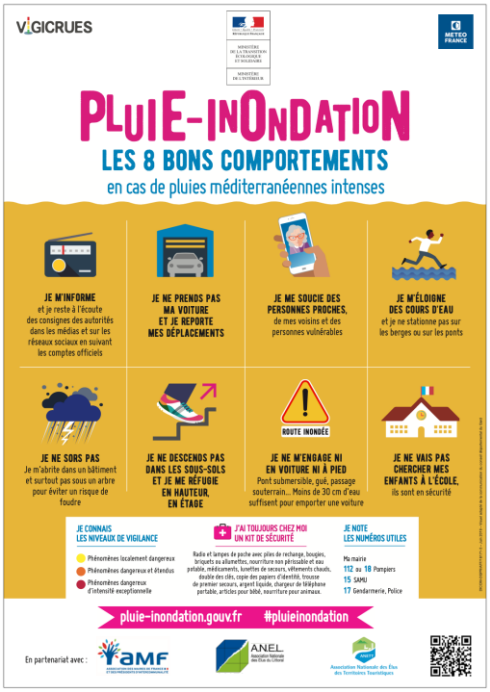

Figure 2-17. The posters for disaster education from (a) Nice city government (source: Ville de Nice (n.d.)) and from (b) Communauté de la Riviera Française. (source: Communauté de la Riviera Française (2019))

The poster (a) teaches the public how to face major risk. People should listen to the radio, not go to school to find their children, not make phone calls, not smoke and only bring essential items. When facing inundation, people should close doors and windows, cut off gas and eletricity, and climb to high place as quickly as possible in case of a torrential flood. Orange or red weather warnings mean that dangerous or exceptionally intense dangerous phenomena are expected. People should follow the safety instructions issued by the local authorities and the media.

The poster (b) introduces eight good behaviours during rain and inundation situation: (1) listening to the instructions from the authorities in the media and on social networks by following the official accounts, (2) not taking their cars and postponing their trips, (3) caring about the people around themselves, neighbours and vulnerable people, (4) staying away from waterways and not parking on river banks or on bridges, (5) not going out and sheltering in buildings, (6) not going down into the basement but going upstairs, (7) not travelling by car or on foot, and (8) not going to find their children at school.

(a)

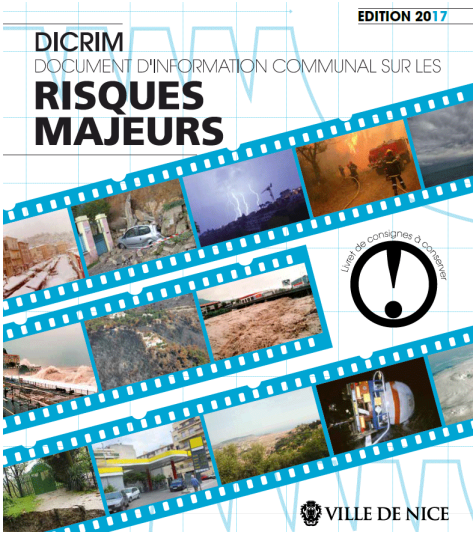

(b)

(c)

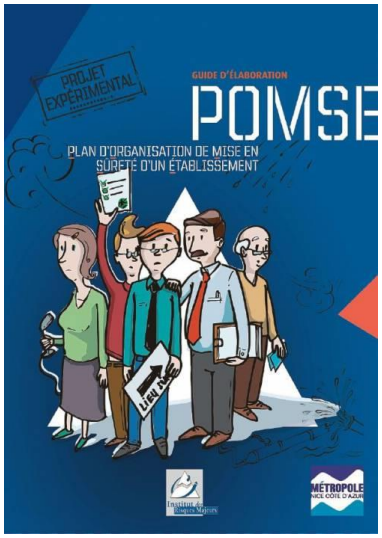

Figure 2-18. The municipal documents of major risks information for disaster education (a) for adults (source: Ville de Nice (2017)), (b) for families (source: Ville de Nice (2010), and (c) for organisations. (source: Ville de Nice (2012))

2.3.3 Problem Statement

All the flood maps, the risk maps and the flood simulation maps were utilised as references to prepare for and respond to crisis effectively, such as deployment of portable pumps and sandbags, preventive evacuation, etc. In Taipei, all the maps were generated and published online for everyone. The maps showed their value that all flooded cases of the event in 2019 were located inside the flood simulation maps. Equally important, found from flood maps, 24 different areas had been flooded for multiple times, implying that systemic problems might exist to be solved. In contrast, for the department of Alpes-Maritimes, though the maps were generated, with only briefly recorded information about historical flood events, it would not be sufficient to find the causes and the results of the events, and thus corresponding solutions to flood. Moreover, although preventive information and measures for disaster had been established, the contents were out-of-date, which should be updated regularly. (Préfet des Alpes-Maritimes, 2016) Although the maps are helpful for flood risk management planning, without street-scale detail information, the maps can hardly be used for crisis response.

Warning and alert systems offered important signals to the public to properly react to crisis. A problem rose in the historical events in Alpes-Maritimes about confusion. Without proper instruction, warning and alert may not be useful. The actors did not know how to respond without connection between the levels of warning and the corresponding actions. (Préfet des Alpes-Maritimes, 2016; Groupe URD, 2021a) Another form of problem could be found in Taipei. For the typhoons and the stationary front, the incoming possible crises could be anticipated and perceived 3 to 5 days earlier, but for the convective rains, sometimes just few hours due to the uncertainty in weather prediction. Although the typhoon warnings were issued 18 hours before the landfalls, people could have been preparing for possible difficult situation since the formation of the typhoons. On the contrary, for the short-duration intense rainfall events, people might not have such enough time.

Suspension and evacuation were good ways to lower exposure to crisis. If possible, people should have a whole-day suspension and be able to receive the announcement before leaving home. It had better not call half-day suspension, called once in Alpes-Maritimes in October 2021 (Rédaction Nice, 2021), which could cause problems with children pick-up, traffic congestion due to sudden enormous numbers of commuters and so on. (Taipei City Fire Department, 2015a, 2016b) For storms and typhoons, people could have adequate time to prepare for and could be evacuated and be sheltered in advance. Sheltered from crisis, people were usually arranged to stay in stadiums, concert halls, schools and so on. Instead, when the number of evacuees was small, hotels could be an option as shelter owing to the cost-benefit principle. (Préfet

des Alpes-Maritimes, 2016; Taipei City Fire Department, 2015b) Additionally, government can have open contracts with wholesale companies, supermarkets, convenient stores and so on. During crisis, the stores would be open to victims, providing basic commodities. Buses from the Nice Metropolis intended for evacuation were trapped and then washed away, as shown in Figure 2-19, which was a human error recognised by the transport company in charge. (Cyril Bottollier-Lemallaz, 2023; Damien Allemand, 2023)

Figure 2-19. Buses from the Nice Metropolis intended for evacuation were trapped and then washed away. (source: Damien Allemand (2023))

Cancellation and detour of public transport, closure of high-risk areas, and deployment of sandbags and water gates would lower exposure to crisis. Sandbags were delivered before crisis, and people who had been ever flooded or were inside high flood potential areas were subsided for installation of water gates. (Taipei City Fire Department, 2015b, 2017a, 2018c, 2019a) Preventive deployment of portable pumps, rescue equipment, first responders could lower flood vulnerability. People could quickly react during crisis. On the other hand, when inundation occurs in several different places at the same time, especially pluvial flood events, government may not have adequate personnel and equipment to deal with. To ensure adequate protection during crisis, governments can have open contracts with equipment companies and labour dispatching companies.

Telecommunication is import for transmitting and receiving information about crisis

and for coordinating operations for crisis. However, people may commonly have problem with information acquisition during crisis. Government provided several ways for sending and receiving information to avoid telephone congestion and internet congestion, such as using different phone numbers and multiple telecom companies' services. Government also utilised social messaging application, short message service, as shown in Figure 2-20, and specific APPs for disaster management, such as Taipei City Disaster Prevention APP. People could check relevant information such as weather, rainfall, water levels, evacuation routes, disaster prevention maps, traffic, and so on. In contrast, sometimes people would not report disaster information through government channels or on government platforms but on social networks or social media. Government should also collect disaster information on these media and analyse public opinion. (Taipei City Fire Department, 2015b)

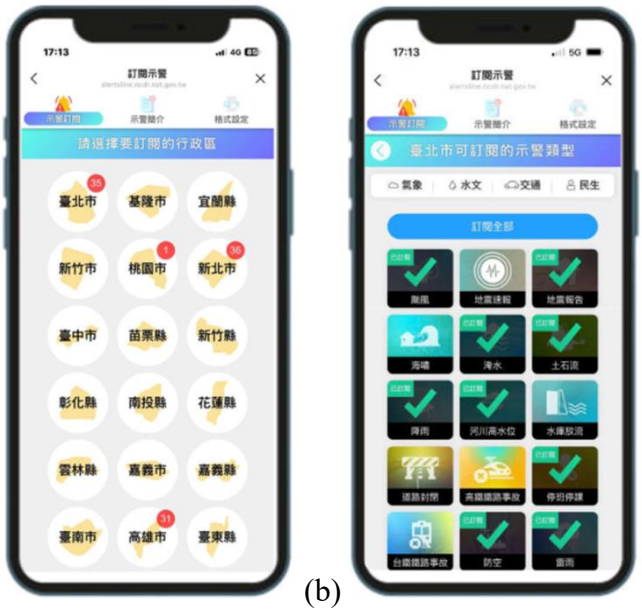

(a) (b)

Figure 2-20. The information about disaster management which can be automatically and manually received on social message application in Taiwan. (source: National Science and Technology Center for Disaster Reduction (n.d.)) (a) the cities of interest people can subscribe. (b) the information of interest people can select: typhoon, inundation, flood, rainfall, etc.

People faced water cut-off due to disruption of supply network or turbidity and encounter power cut-off and thus communication. The cut-off of the basic necessity commonly happens during crisis. These necessities as well as telecommunication should be ensured, and key structures, such as hospitals, shelters, EOC, should have their own systems or back-up systems.

The donation and the actions of volunteers during severe situation represented great solidarity and generosity. The volunteers mostly help with cleaning and clearing,

restoring, finding accommodation, rescuing and so on. They were helpful and useful but difficult to be managed, such as work schedules, mission distribution, storage of materials, and rationing mechanism of food and water, etc. Sometimes they could only improvise during crisis. The planning of the works was challenging when many volunteers working on the several different sites. This could be overcome through intensive communication and coordination between government, people in need and volunteers. (Groupe URD, 2020, 2021a) For this intention, volunteer firemen, volunteer policemen and civil defence can participate in government disaster prevention education and training and then can be mobilised and arranged by local authorities. Furthermore, volunteers can also be mobilised to provide inter-regional support. (Taipei City Fire Department, 2015a, 2015b)

Public crisis awareness needs to be raised and risk culture should be established. The citizens need to learn self-protection and self-rescue, such as the preventive evacuation in Breil-sur-Roya area before Storm Alex. Without crisis awareness and risk culture, even with proper alert transmission, there were several inappropriate behaviours, such as driving through flooded areas, rescuing cars in the basement during flood and so on. During the storm in 2015, the chief cause of fatality was linked to improper behaviour: 8 people in Mandelieu-la-Napoule drowned whilst trying to access to their car in underground parking areas to move their cars out of the garage; 3 people in Vallauris died when trying to pass through flooded underpasses. (Libération, 2015; Radio Télé Luxembourg, 2015; Préfet des Alpes-Maritimes, 2016); 3 people died in a retirement home in Biot, due to lack of personnel to shelter vulnerable people in time on the ground floor during the flood in 2015. (Préfet des Alpes-Maritimes, 2016); and a couple was carried away with their house despite several evacuation orders in Storm Alex. (Binacchi, 2021b) The above-mentioned tragedies could have been avoided. According to the report (Préfet des Alpes-Maritimes, 2016), during the disaster, the duty of citizen is to get information, to secure themselves and to respect the regulations and the suggestions in risk prevention plan. Government should provide the people sufficient education for disaster self-defence and reaction to warning and alert systems, especially for those living in high-risk areas.

2.4 Numerical Modelling for Flood risk management

Numerical modelling is essential to flood risk management, which can provide important information, and thus corresponding strategies against flood can be developed. Hydrological and hydraulic modelling can provide a comprehensive view of flood hazard, such as water depth, flow velocity, flood extent and duration of flood. Detail flood simulations under different scenarios can generate flood maps for designing flood prevention and protection structures, land use zoning, evacuation routes and flood insurance and so on. Examples of flood potential map of Nice and Taipei are shown in Figure 2-21 and Figure 2-22. The detailed flood simulations are conducted by solving physics equations for hydrodynamics, and those for urban flood are more complex due to several different structures and facilities. Besides, real-time modelling can help flood forecasting and early warning.

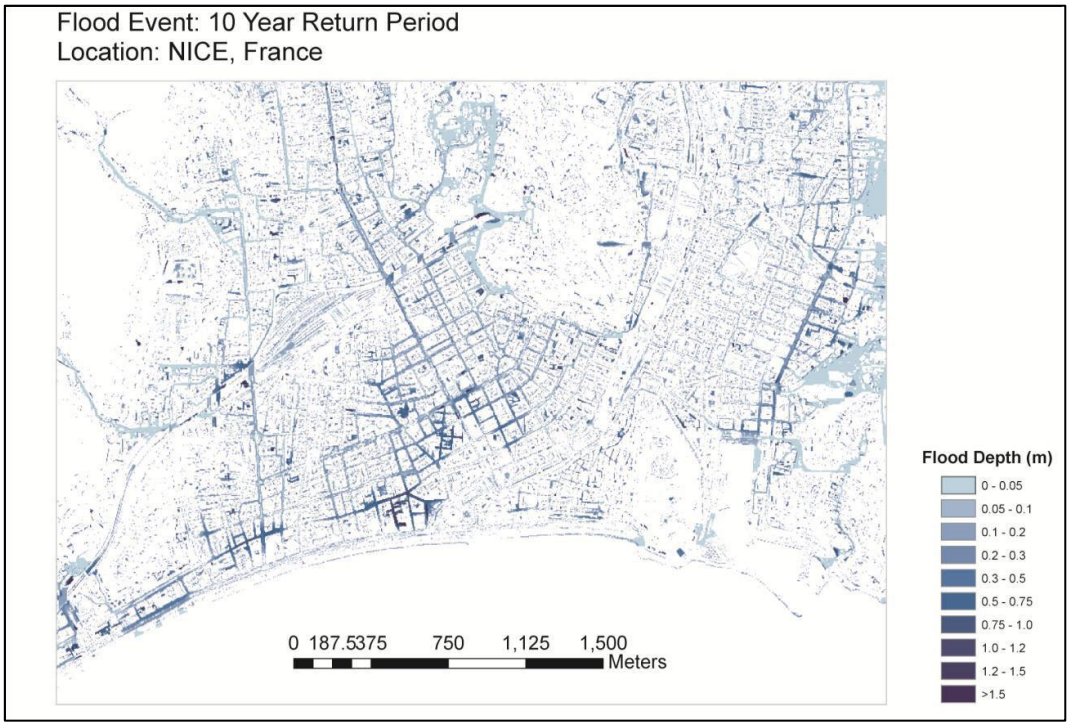

Figure 2-21. The flood potential map of Nice under the scenario of 10-year return period rainfall. (source: Batica (2015))

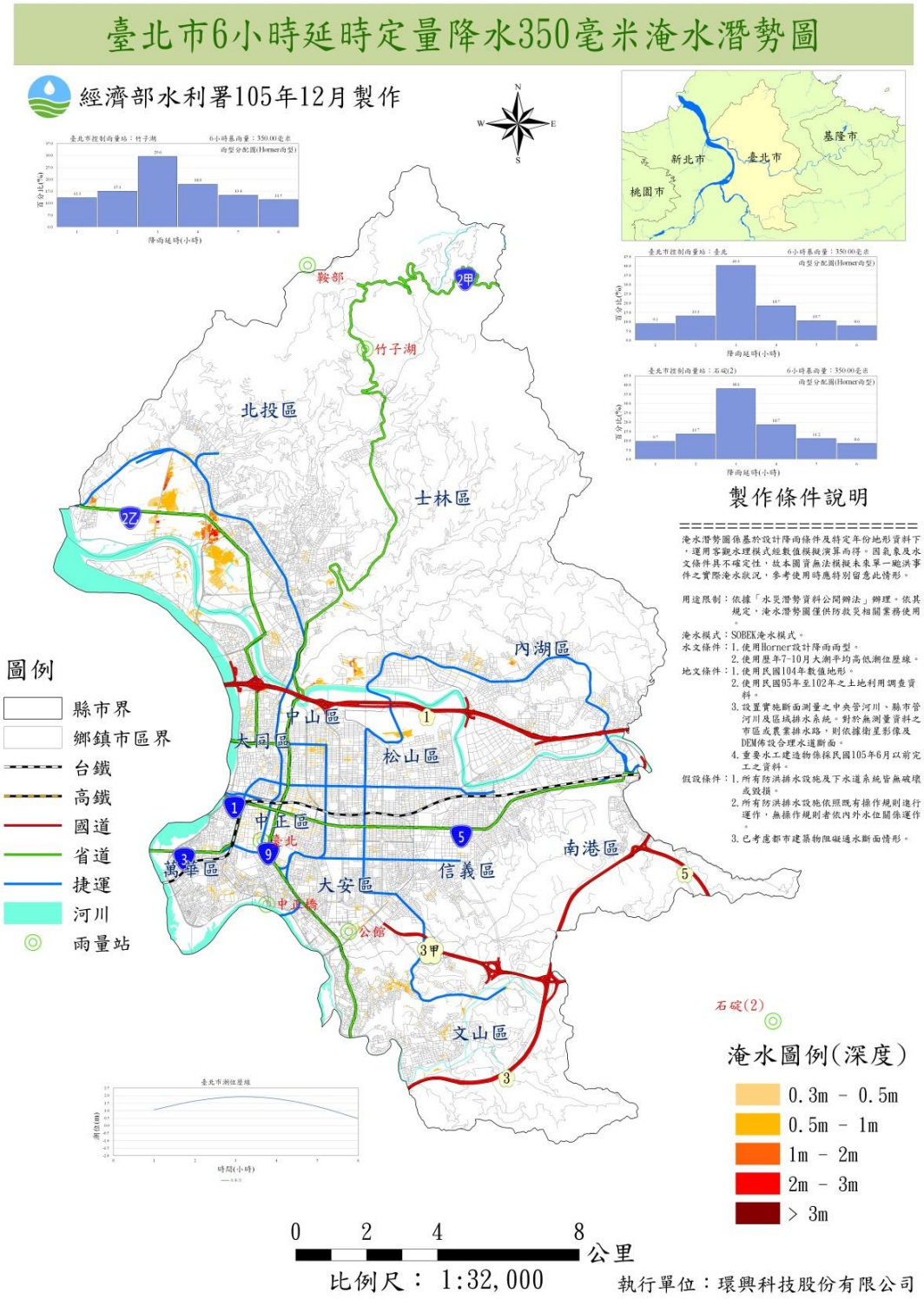

Figure 2-22. The flood potential map of Taipei under the scenario of 350 mm accumulated rainfall in 6 hours. (source: Water Resources Agency (n.d.-a)) The assumptions were: (1) all flood controlled facilities and sewer systems normally operated, (2) all flood controlled facilities operated with their own standard operating procedures (SOPs), and (3) buildings would block water flow.

In addition to hydrological and hydraulic modelling, agent-based modelling can also

be helpful to well understand human behaviour and interactions between human and environment, such as evacuation process during flood events (Dawson et al., 2011), as shown in Figure 2-23, and during tsunami (Mas et al., 2012; Wang & Jia, 2021), as shown in Figure 2-24, as well as analysis of manpower for disaster management (Dressler et al., 2016) and so on.

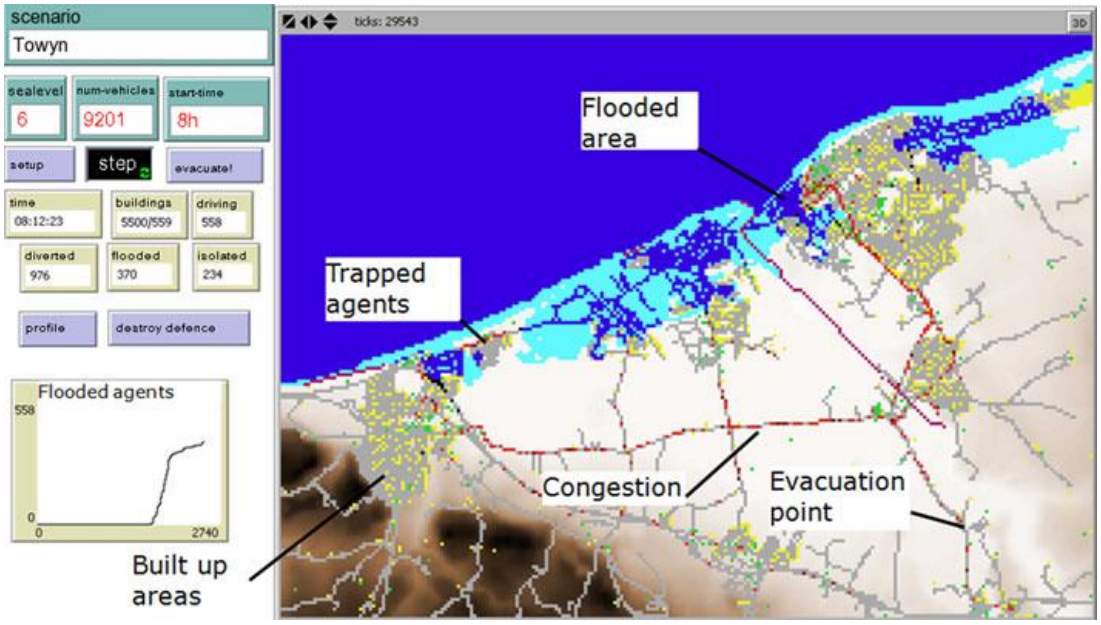

Figure 2-23. A screenshot of the agent-based model. (source: Dawson et al. (2011))

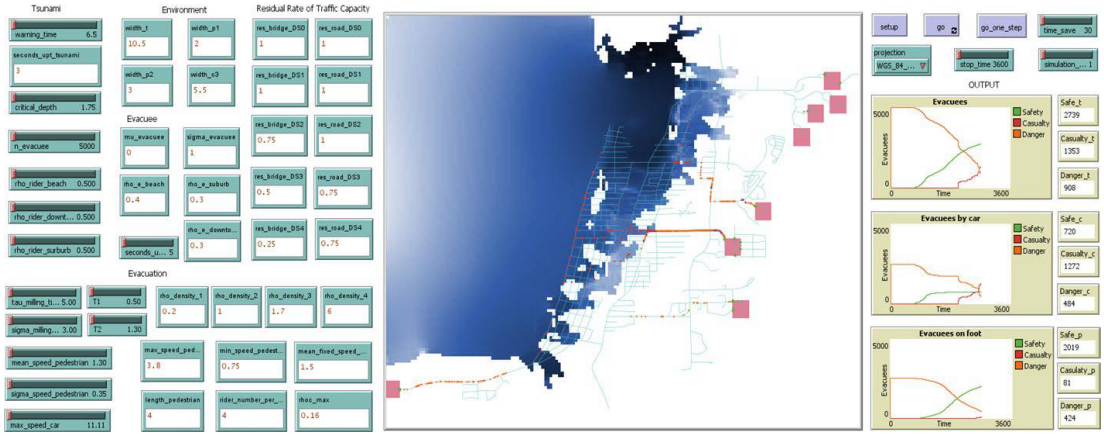

Figure 2-24. A screenshot of the agent-based tsunami evacuation model. (source: Wang & Jia (2021))

2.5 Summary

This chapter introduced the concept of flood risk management and reviewed the applications of structural and non-structural measures against flood disasters during the historical events in France and in Taiwan. Several problems within the applications are also pointed out. Before the crises, the risk maps and the flood maps could be useful for deployment and traffic management; the warning and the alert systems could deliver important signals for people to follow the instructions for the crises; suspension and evacuation were effective ways to lower exposure to crisis. During crisis, maintenance of telecommunication, water and power was essential, and volunteers could aid. However, people might not fully understand how to properly respond and thus the non-structural measures might not be able to perform smoothly. Government should provide sufficient education for disaster to raise crisis awareness and establish risk culture, and the public should learn self-protection and self-rescue.

Floods are the most common natural disasters worldwide. Flood can cause fatality and serious damage to property, and thus, flood risk management is essential to avoid new flood risk, to prevent and to reduce existing impact of floods and to manage residual flood risk.

Chapter 3.
Research Methodology

Part of this chapter has been submitted for publication.

Chapter 3 Research Methodology

Extreme rainfall events and floods can cause severe damage and fatality, and thus flood disaster management is essential to lower the risk. Structural measures such as dykes, sewer systems, pumps, etc., can efficiently mitigate flood risk but cannot eliminate the risk. Therefore, non-structural measures such as flood risk maps, warning alarms, evacuation and so on, are crucial to flood disaster management. (Andjelkovic, 2001; Hsu & Gourbesville, 2022) In order to evaluate the effectiveness and outcomes of structural and non-structural measures during a flood event, this study employs an Agent-Based Model (ABM) to analyses the possible interaction between human behaviour and the environment with different structural and non-structural measures. Two historical flood events in Magnan area in Nice (France) and in Dahu area in Taipei (Taiwan) were selected for case study. This chapter first introduces ABMs and elaborates the methodologies for: (1) agent simulations, (2) Cellular Automata (CA) inundation simulations and (3) inundation-agent coupled simulations.

3.1 Agent-Based Model

This study conducts inundation-agent coupled simulations to analyse the interaction between human behaviour and the environment with the help of agent-based models (ABMs). ABMs are ideal tools, which are designed for simulating the actions, reactions and interactions of autonomous individuals (agents) and the environment (cells) in a complex system. Each individual and computational cell will follow specific behaviour rules to act, react and interact with each other. ABMs have been used in several different regions, such as in biology, (An et al., 2009; Cogoni et al., 2023) in ecology, (Chichorro et al., 2022; Crouse et al., 2022) in social science, (Ahimbisibwe et al., 2021; de Oliveira Simoyama et al., 2022; Flache et al., 2022; Amadae & Watts, 2023) in epidemiology, (Akwafuo et al., 2020; Hinch et al., 2021; Kerr et al., 2021; Daghriri & Ozmen, 2021) etc. This research utilised an ABM, NetLogo (Wilensky, 1999), to run the inundation-agent coupled simulations. NetLogo is a free open-source multi-agent programming language and modelling environment, first created in 1999 and maintained by the Center for Connected Learning Computer-Based Modeling at Northwestern University, Evanston, Illinois, United States. NetLogo is a dialect of the Logo language, written in Scala and Java, and it is a freeware can be download at the official websites and used without restriction: https://ccl.northwestern.edu/NetLogo/ (software) and https://github.com/NetLogo/NetLogo (source code). (Tisue & Wilensky, 2004)

Two main models were built in the ABM: an evacuation model for agent simulations and a cellular automata (CA) 2D overland flow model for inundation simulations.

These two models can run separately. The detailed information about the agent simulations will be elaborated in Section 3.2 and the inundation simulation in Section 3.3. Furthermore, these two models can also be combined into an inundation-agent coupled mode, and the coupled model will be elaborated in Section 3.4. The aims of the ABM are to explore the influences of structural and non-structural measures under different scenarios, to analyse the interaction between human behaviour and the environment and to improve the existing response strategies and community-based flood risk management.

3.2 Agent Simulations

The ABM for agent simulations focuses on non-structural measures, connecting with hydraulic simulations. The study first used MIKE drainage-overland coupled hydraulic model (DHI, 2016a) to simulate an historical flood event in Magnan area, Nice, and then NetLogo was utilised to run agent simulations to represent possible human behaviours with non-structural measures. For evacuation simulation, antecedent relevant research utilised ABMs to analyse indoor evacuation, (Wirth & Szabó, 2018) evacuation behaviour during flood events (Dawson et al., 2011; Nakanishi et al.,2019) and during tsunami. (Mas et al., 2012; Wang et al., 2016; Wang & Jia, 2021) The evacuation simulations of this study mainly focused on non-structural measures in disaster management, without taking other factors, such as structural measures, psychological factors, etc., into consideration for keeping the simplicity to well understand the possible effects of the non-structural measures. Three non-structural measures were taken into account:

- risk maps and flood maps
- warning alarm
- evacuation

The flow chart of the study is shown as Figure 3-1. The agent-based simulations were conducted by NetLogo in which the autonomous individuals (agents) interacted with flood with several behaviour rules under different scenarios. Inundation simulations were conducted by a hydraulic model which provided time series information about flood events. The information of flood was extracted, converted into ASCII format and then stored in a database, and thus the information could be easily imported into the ABM directly. Behaviour rules defined the way agents act and react with each other and the environment. In the study, we focused on evacuation route selection and evacuation rules. In addition, alarm thresholds were used to determine when agents start to evacuate, and a relationship between walking speed and water depth was utilised to define how the agents were affected by the flood water. The detailed information will be elaborated in the following sections.

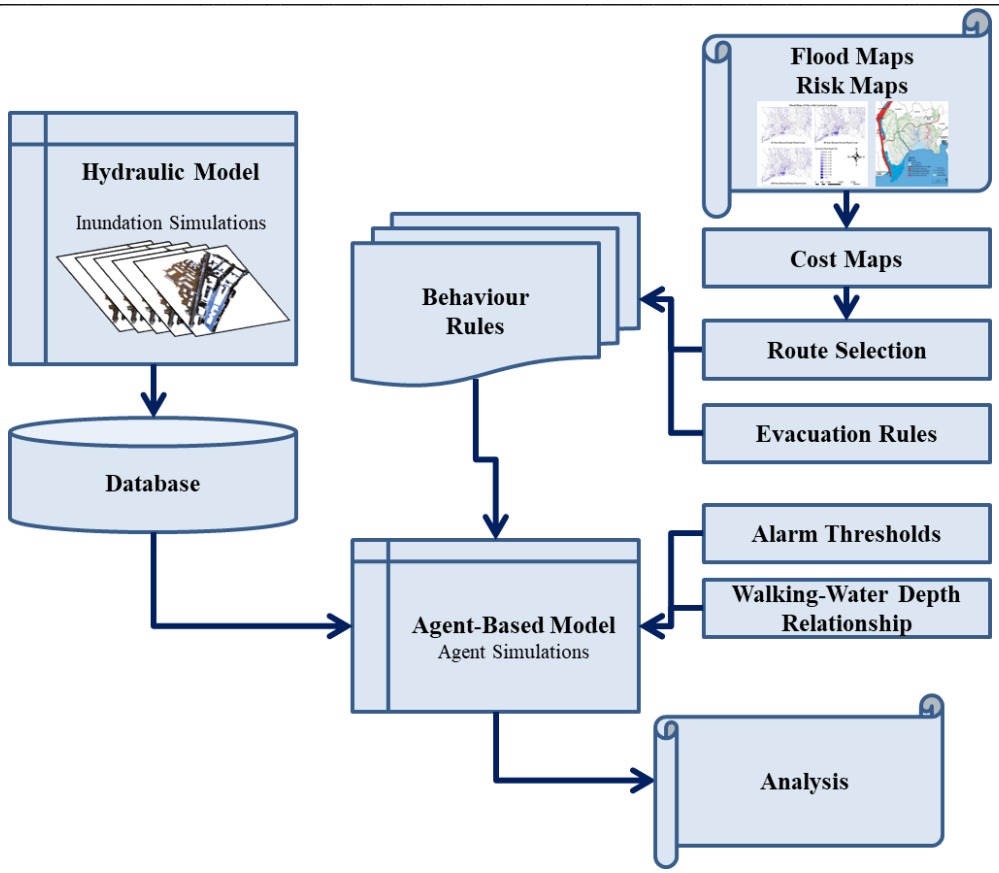

Figure 3-1. The flow chart of the agent simulation.

Evacuees in the ABM would move towards shelters according to their evacuation routes when the alarm was raised. The evacuees' walking speed would be affected by water during flood and the evacuation routes could also be altered in consideration of risk maps and flood maps. The interface of the ABM is shown in Figure 3-2. The pink matchstick figures represent the evacuees, and the red house figure at the upper right corner is the shelter in the study site; the blue shaded areas indicate the water depth: the darker the colour is, the deeper the water depth is. Some key parameters are shown and can be changed easily by clicking the switches or moving the sliders. In the ABM, the number of evacuated people, the number of trapped people, the number of moving people and the number of people passing through flooded areas, where the water depth was greater than 0.3 metres, were counted through time. The average evacuation time and the average evacuation distance of successfully evacuated people were calculated as well.

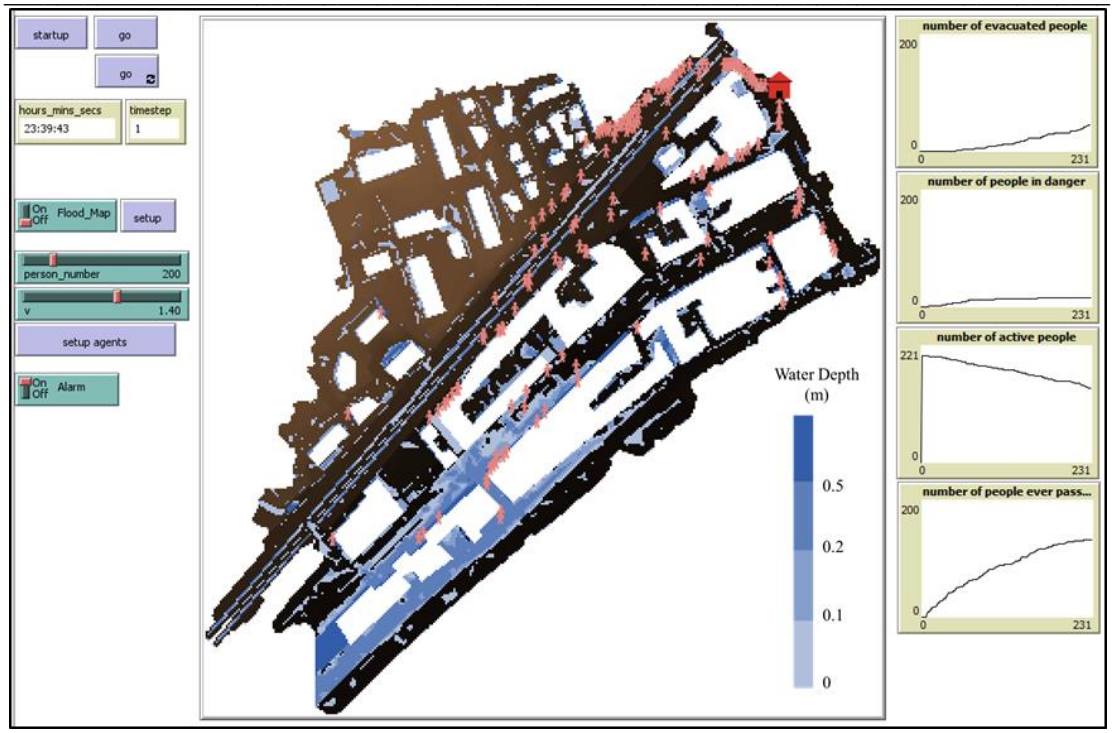

Figure 3-2. The interface of the agent-based model.

3.2.1 Evacuation Model

The descriptions of the ABM follow the ODD protocol (Grimm & Railsback 2005; Grimm et al. 2006; 2010; 2020) consisting of three categories: "Overview", "Design concepts" and "Details" (ODD), and seven elements: "purpose and patterns", "entities, state variables and scales", "process overview and scheduling", "design concepts", "initialisation", "input data" and "submodels". The ABM used in the study is described in the following sections.

Overview

Purpose and Patterns

The model is to predict the possible effects of the non-structural measures against flood in disaster management and to analyse how flood water affect human safety and walking speed during evacuation process in a flood event. The following three non-structural measures are taken into account: risk maps and flood maps, warning alarm and evacuation. The performance of the measures will be evaluated, and the outcomes will be discussed. The model is not designed to realistically represent the evacuation process in detail but simply attempt to explore the possible influences of these non-structural measures under different scenarios.

The people evacuating without the risk maps and flood maps may choose the shortest routes to the shelters neglecting potential flooded areas, whereas the people evacuating with the maps may spend more time making detours to move towards the

shelter safely. The evacuation timing is also important. If the warning alarm is not raised in time, the people may not be able to evacuate safely. In the model, the number of trapped people and the number of people passing through flooded areas (water depth ≥ 0.3 m) were counted through time for checking the performance of the evacuation process. Similarly, the average evacuation time and the average evacuation distance of successfully evacuated people were calculated as indexes to evaluate the evacuation process.

Entities, State Variables and Scales

The following four entities are included in the model: observer, agents, shelters and the patches. The observer controls the global variables. The agents represent the evacuees who will move towards the shelters when the alarm is raised. The shelters represent the destination for the evacuees. The patches represent the environment of the study area. The variables, the descriptions and the units of these entities are listed in the Table 3-1.

Table 3-1. The entities and the variables of the model.

Entity	Variable	Description	Unit
Observer	time	simulation time	s
	timestep	time step	s
	Alarm	whether the warning alarm is raised or not	True/False
	Maps	whether the risk maps and flood maps are considered or not	True/False
	person_number	the number of total evacuees	-
	v	the initial walking speed of each evacuee	m/s
	Passing_Flooded_Areas_People	the number of the evacuees passing through flooded areas	-
	Trapped_People	the number of the trapped people	-
	Evacuated_People	the number of the successfully evacuated people	-
	Avg_Evacuation_Dist	the average evacuation distance of the successfully evacuated people	m
	Avg_Evacuation_Time	the average evacuation time of the successfully evacuated people	s
Agent	Size	body size	m
	Step_Size	step size	m
	V_Agent	walking speed	m/s
	Evacuation_Dist	total evacuation distance	m
	Evacuation_Time	total evacuation time	s
	Status	status of the agent: ”normal”, “trapped” and “evacuated”	-
	Passing_Flooded_Areas	whether the agent ever passing through flooded areas or not	True/False
Shelter	Capacity	the capacity of the shelter	-
Patch	Cost	the accumulated cost at the patch from the shelter	m
	Water_Depth	the water depth at the patch	m

The spatial extent is divided into 334 × 342 square cells, with 75,931 invalid cells and 38,297 valid cells in these total 114,228 cells based on the study area. The spatial information is directly imported from ASCII files. The model sets the simulation time as 25 hours representing the duration of the case study and a tick in the model indicates 1 second. The detailed information about the spatial and temporal data about the case study is elaborated in Section 4.1.1.

Process Overview and Scheduling

The model covers the whole historical flood event and the evacuation process. The observer, the agents, the shelters and the patches update the variables every time step. The flow chart of the process is shown as Figure 3-3. The simulation starts at the beginning of the historical event and finishes at the end of the event, and the simulation time will update each time step. Each time step, the model checks the simulation time and imports the corresponding output of the inundation simulation for updating the water depth of each patch. The detailed information about the inundation simulation is elaborated in Section 3.2.2. Then the model checks whether the alarm is raised or not. The detailed information about the alarm thresholds is elaborated in Section 3.2.3. When the alarm is raised, all the agents start to move towards the shelters according to the cost map: the evacuees choose the routes with the lowest cost of the neighbour patches each time step. The detailed information about the cost maps is elaborated in Section 3.2.4. During the evacuation process, the evacuation time and the evacuation distance of each evacuee are calculated and update each time step. The flood water affects evacuees' walking speeds: the walking speeds decrease monotonically with increasing water depth. The relationship between evacuees' walking speed and flood water depth is elaborated in Section 3.2.5. When an evacuee is on a patch with the water depth higher than 1 metre, the evacuee is trapped. On the contrary, when an evacuee reaches the location of the shelters, the evacuee is regarded as successfully evacuated people and then vanishes from the computational domain. Finally, the model counts the number of trapped people and the number of people passing through flooded areas and calculates the average evacuation time and the average evacuation distance of successfully evacuated people, and the model starts the next time step until the end of the simulation time.

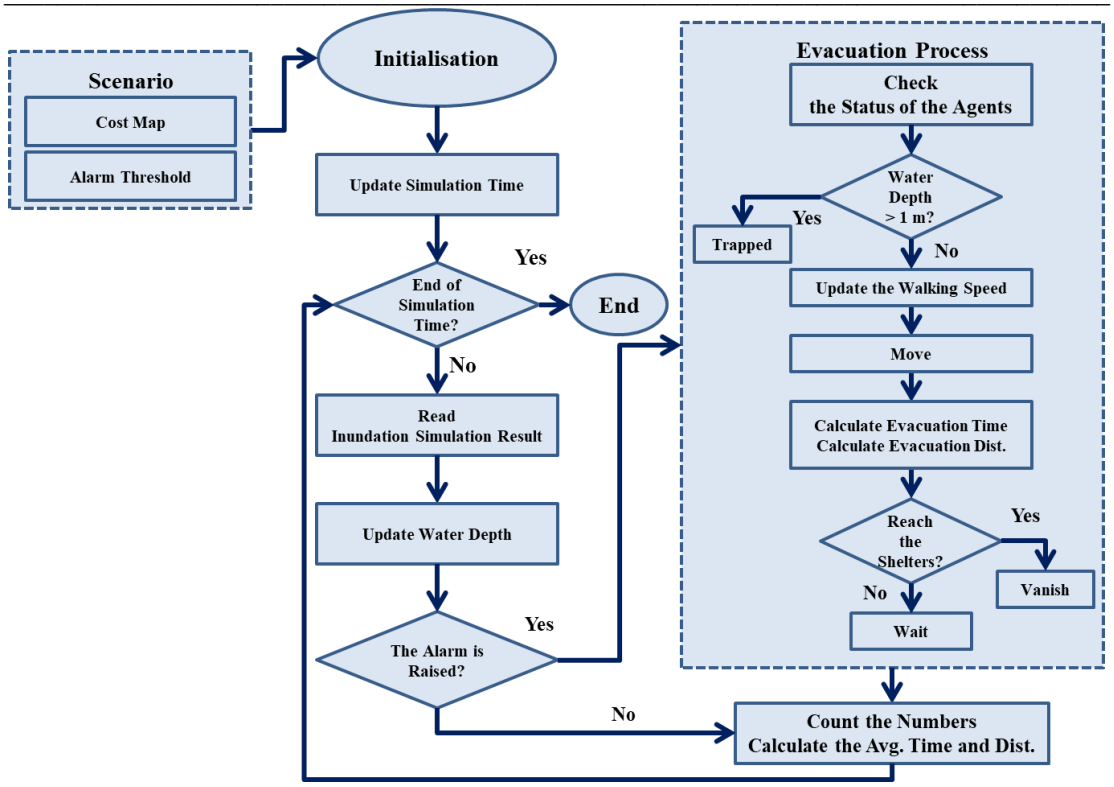

Figure 3-3. The flow chart of the ABM.

Design Concepts

Design Concepts

Basic Principles

This model is designed to predict possible outcomes of evacuation. In the study, evacuees are assumed to choose the evacuation routes with the lowest cost towards the shelters when the warning alarm is raised. The information about the costs is provided by a cost map. In this study, two cost maps and two alarm thresholds were used. The detailed information about the cost maps and the alarm thresholds is elaborated in Section 3.2.3 and 3.2.4. Flood influences human safety and affects walking speed. The higher the water depth is, the slower the people's walking speed will be, and the walking speed will even drop to 0 m/s (being trapped).

Emergence

Walking speed of each agent is affected by water depth of the patch the agent locates. The relationship between evacuees' walking speed and flood water depth is elaborated in Section 3.2.5. The status of each agent is determined by water depth and the patch the agent locates. If an agent locates in a patch where the water depth is higher than 1 metre, the agent's status will be "trapped". If an agent is in a patch where a shelter locates, the status of the agent will be "evacuated". Otherwise, the status will be "normal". In addition, if an agent ever passes through flooded areas

where the water depth is higher than 0.3 metre, the variable “Passing_Flooded_Areas” will be “True”. Agents’ evacuation time will increase by adding the time step through time when evacuation process starts. Correspondingly, agents’ evacuation distance will increase by adding the product of time step and walking speed.

Adaptation

In the study, evacuees are assumed to choose evacuation routes with the lowest cost towards the shelters when the warning alarm is raised. When evacuating, agents move according to the costs of patches each time step. The information of the cost is from an external input: cost maps.

Objectives

The average evacuation time and the average evacuation distance of all successfully evacuated agents are calculated, and the number of trapped agents and the number of agents subjected to flood who ever pass through flooded areas are counted as indexes for checking the performance of the evacuation process.

Many indexes can be used to evaluate the evacuation process, such as number of injuries and fatalities, number of safe evacuees in certain time, time needed to evacuate certain number of people, evacuation time, queuing time, evacuation distance and so on. (Drager et al., 1993; Lovas, 1994) Different from evacuation from buildings, the evacuees in the ABM were spread over comparatively larger wide-open areas, and thus evacuation time and distance varied considerably, depending on locations where each evacuee was located. In this study, only the average evacuation time and the average evacuation distance of all successfully evacuated people were calculated as indexes for each simulation for checking the performance of the evacuation process. Since the number of safe evacuees can be easily calculated as the total number of evacuees minus the number of trapped people, only one of these numbers was used in the study.

Sensing

In the model, whilst evacuating, agents move towards the shelters according to the costs of the adjacent patches each time step. The agents only check the eight neighbours first before moving.

Interaction

During evacuation, if a patch is occupied by other agents and no room for the others, the evacuees who are nearby the patch would stop and wait. Agents are assigned a body width and a step size. When the distance between an evacuee and the agents

who occupy the target patch is shorter than the value of the body width plus the step size, the evacuee would not move.

Stochasticity

There is no stochasticity in any variable but in locations of the agents. All the agents are generated randomly in the valid computational domain. The initial walking speed of all the agents can be randomly assigned, however, after sensitivity analysis (Section 3.2.5), only one value is used universally.

Observation

The key outputs monitored from the model are the number of trapped people, the number of people passing through flooded areas, the number of evacuated people, the average evacuation time and the average evacuation distance of the successfully evacuated people.

Details

Initialisation

The model is initialised by importing a cost map of the study area for building valid computational domain and locating the shelters. In this study, 200 evacuees were randomly generated in the whole computational domain in the ABM under daily estimation of active pedestrian in the study areas. More information about the number of total evacuees is elaborated in Section 3.2.6. The costs of each patch are initialised according to the imported cost map, and the water depths are all set at 0 metre at the beginning. The capacity of the shelters is set as infinite in this study, which will accommodate all the evacuees in the study. The simulation time is set as the beginning of the historical event at the initial time step and the time step is set as 1 second as a constant. The status of the alarm is off at the beginning. The number of trapped people, the number of people passing through flooded areas, the number of evacuated people, the average evacuation time and the average evacuation distance are all 0 at the initial time step. Body sizes and step sizes of each agent are simply set as 0.5 metres. Initial walking speeds of all the agents are set as 1.4 m/s and the determination of the initial walking speed is elaborated in Section 3.2.5. The initial status of the agents is “normal” and the variable “Passing_Flooded_Areas” is “False”.

Input Data

Two forms of external information are used in the study: cost maps and inundation simulations. The model imports a cost map of the study area for building valid computational domain and locating the shelters according to the scenario, providing

the costs of each patch. The cost maps were established by a GIS software for determining the evacuation routes of each agent. Inundation simulation results are imported into the model for updating the water depths of each patch through time. The inundation simulation results were provided by a hydraulic model, and the corresponding results are imported according to the simulation time in the ABM. The detailed information about the cost maps and the inundation simulations is elaborated in Section 3.2.2 and Section 3.2.4.

Submodels

Scenario

In the study, 4 different scenarios are used, based on two different alarm thresholds and two cost maps. The 4 simulation scenarios (S1 – S4) are listed in Table 3-2. The global variable "Maps" is "True" with the consideration of the maps and is "False" without the consideration of the maps. When a specific scenario is selected, the corresponding cost map will be imported and the trigger of the warning alarm will be set. The cost maps were established by a GIS software in ASCII format, and the files can be imported directly into the model and update the variable "cost" of the patches. The detailed information about the cost maps and the alarm thresholds is elaborated in Section 3.2.3 and Section 3.2.4. Since all the evacuees were randomly generated, 100 simulations were conducted for each scenario to lower the model uncertainty which arose from the distribution of the evacuees.

Table 3-2. The simulation scenarios.

	Scenario			
	S1	S2	S3	S4
Alarm Threshold	25 mm/hr	25 mm/hr	35 mm/hr	35 mm/hr
Risk Maps and Flood Maps	-	O	-	O

Update Simulation Time

The global variable "time" can be updated by adding the time step, and it can be calculated by the following equation:

$time^{t+1} = time^{t} + timestep$

Read Inundation Simulation Results and Update Water Depth

The model checks the simulation time and then imports the corresponding output of the inundation simulation. The inundation simulation results were generated by a hydraulic model in ASCII format, and the files can be imported directly into the model and update the variable "Water_Depth" of the patches. The detailed

information about the hydraulic simulation is elaborated in Section 3.2.2.

The Alarm Is Raised?

The model checks the simulation time and thus the corresponding rainfall intensity to check whether the rainfall intensity reaches the threshold or not. When the rainfall intensity reaches the threshold, the global variable "Alarm" will be "True" and then agents will start to evacuate. The detailed information about the alarm is elaborated in Section 3.2.2.

Check the Status of the Agents

If an agent locates in a patch where the water depth is higher than 1 metre, the variable "Status" of the agent's will be "trapped". If an agent is in a patch where a shelter locates, the "Status" will be "evacuated". Otherwise, the "Status" will be "normal". If an agent ever passes through flooded areas where the water depth is higher than 0.3 metre, the variable "Passing_Flooded_Areas" will be "True".

Update the Walking Speed

The initial walking speeds, "V_Agent", of all the agents are assigned as the global variable "v". The walking speed of each agent will be changed individually according to the water depth of the patch the agent locates. The relationship between evacuees' walking speed and flood water depth is elaborated in Section 3.2.5.

Move

If "Alarm" is "True", every agent moves. The agents check the "Cost" of the eight neighbour patches and then move towards the patch with the smallest value of "Cost" at their walking speed "V_Agent".

Calculate Evacuation Time and Evacuation Distance

Agents' evacuation time, "Evacuation_Time", will increase by adding the time step through time since the warning alarm is sounded. It can be calculated by the following equation:

$$Evacuation\_Time^{t+1} = Evacuation\_Time^{t} + timestep$$

Correspondingly, agents' evacuation distance, "Evacuation_Dist", will increase by adding the product of time step and walking speed, "V_Agent". It can be calculated by the following equation:

$$Evacuation\_Dist^{t+1} = Evacuation\_Dist^{t} + timestep \cdot V\_Agent$$

Reach the Shelters?

If an agent is in a patch where a shelter locates, the "Status" of the agent will be "evacuated" and then the agent will vanish from the computational domain.

Count the Numbers and Calculate the Average Evacuation Time and Distance

The model counts the number of the evacuees passing through flooded areas, the number of the trapped people and the number of the successfully evacuated people by simply checking the variables "Status" and "Passing_Flooded_Areas" of the agents, and then the model stores these numbers in the following three global variables respectively, "Passing_Flooded_Areas_People", "Trapped_People" and "Evacuated_People". The global variables, "Avg_Evacuation_Dist" and "Avg_Evacuation_Time", are the average evacuation distance and average evacuation time of the successfully evacuated people. The model can easily calculate the values of the variables by averaging the "Evacuation_Time" and "Evacuation_Dist" of all the agents with the "Status" which is "evacuated".

3.2.2 Hydraulic Simulation

Human safety and walking speed of evacuees will be influenced by the flood in the ABM. For providing detailed information about the historical flood of Magnan, this study utilised a coupled hydraulic model presented by Salvan (2017) to conduct the inundation simulation. The coupled model, MIKE FLOOD, was developed by Danish Hydraulic Institute (DHI) (2016a), combining a one-dimensional (1D) sewer network model, MIKE URBAN (DHI 2014) and a two-dimensional (2D) overland flow model, MIKE 21. (DHI, 2016b) The upstream rainfall-runoff model and the 1D sewer networks of the whole Magnan were built in MIKE URBAN, whilst the 2D overland flow model in the downstream part was built in MIKE 21 with 2-metre resolution and closed boundaries. Building areas in the MIKE 21 model were excluded from the computational domain and thus the total precipitation was proportionally increased by 27%. The above-mentioned subcatchment of the upstream rainfall-runoff model and the 1D sewer networks, the catchment of the urban 2D overland flow model and the 1D sewer networks of the MIKE model, and the coupled nodes of the MIKE FLOOD 1D-2D coupled model are shown in Figure 3-4.

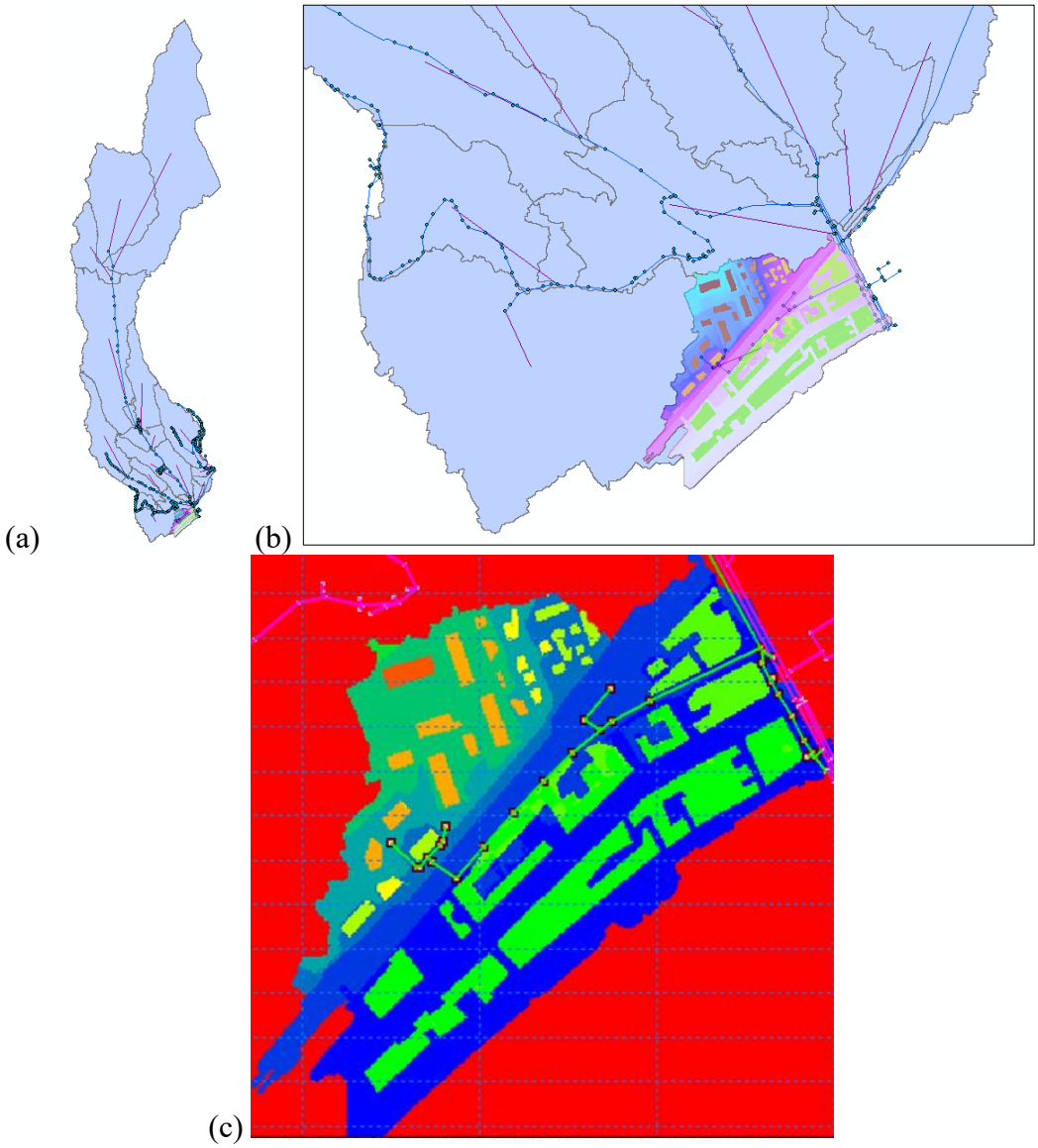

Figure 3-4. (a) The subcatchment of the upstream rainfall-runoff model and the 1D sewer networks and (b) the catchment of the urban 2D overland flow model and the 1D sewer networks of the MIKE model. (source: Salvan (2017)) The dots are manholes and the blue lines are pipelines. The sky blue areas are subcatchments and the purple lines indicates the pour points of each subcatchment. (c) The coupled nodes of the MIKE FLOOD 1D-2D coupled model. (source: Salvan (2017)) The red squares are the coupled manholes and the green lines are the pipelines between the coupled manholes; the white squares and the purple lines are the other manholes and the other pipelines.

Outputs of the coupled model provided time series information about the historical flood, and then the information was extracted and imported into the ABM to investigate the influence of the flood on evacuation. The flood information from the MIKE FLOOD coupled mode only provided flood water for agent simulations in the ABM, and it did not change agents' evacuation routes, whereas cost maps were used to determine agents' evacuation routes in the ABM. The results of inundation

simulation from the hydraulic model provided flood water by which the agents were affected. The agents evacuated according to cost maps, and meanwhile the agents' walking speed would be slowed by the flood water and even dropped to 0 m/s and trapped. Detailed information about the cost maps and the relationship between walking speed and water depth will be elaborated in Section 3.2.4 and Section 3.2.5. The numbers of trapped people and of people passing through flooded areas (water depth ≥ 0.3 m) were counted through time in the ABM for checking the performance of the evacuation process.

3.2.3 Warning Alarm

In the ABM, the warning alarm was off at the beginning of the simulation and only be raised when specific conditions were met. The conditions could be a specific threshold of accumulated rainfall, rainfall intensity, water level at certain locations and so on. According to the proposed thresholds for government interventions during extreme weather events in Nice city (Dorgigné et al., 2017), local authorities should start following the weather forecast from 25 mm accumulated precipitation in an hour and initiating sheltering process from 50 mm in an hour. However, the proposed thresholds are applied to the whole Nice city, not to any specific area, and therefore the thresholds may not be sufficiently appropriate in this study. In the historical event, inundation occurred in Magnan areas when rainfall did not exceed the proposed threshold. Thus, we conservatively selected two different rainfall intensities based on the two peaks on the hyetograph instead of the original proposed thresholds according to accumulative rainfalls for testing the effect of evacuation timing. We chose two different rainfall intensities, 25 mm/hr and 35 mm/hr, as the thresholds. When rainfall intensity exceeded the threshold, the warning alarm would go off, and everyone would start to evacuate.

3.2.4 Cost Maps, Risk Maps and Flood Maps

A fire station at the northeast corner of the study site was selected as the shelter, as shown in Figure 3-5. We assumed that every evacuee would choose the evacuation route with the lowest cost to the shelter. Provided that all the costs of moving between adjacent cells were the same, the total cost of the evacuation process for an evacuee was only determined by the distance between the evacuee's location and the goal. Thus, in order to determine the evacuation routes, we first calculated the accumulated distance, i.e., cost, from the shelter for each cell. The buildings were regarded as inaccessible areas, where evacuees would not be able to pass through or stay inside. Hence an accumulated cost map could be generated, as shown in Figure 3-5 (a). In the ABM, every evacuee would search the cell with the lowest accumulated cost amongst

its eight neighbour cells at each time step. Given that potential flooded areas and high-risk areas were the areas to avoid, the cost map could be further improved. According to the risk map presented by the Department of Risk Prevention and Management of Nice (Direction de la Prévention et de la Gestion des Risques, 2017) and the flood maps of Nice for different scenarios (Batica, 2015), an improved cost map was generated by making potential flooded areas inaccessible and increasing the costs at high-risk areas. The improved cost map is show as Figure 3-5 (b). We first regarded the high-risk areas as impassable areas and calculated accumulated distances from the shelter to each cell. Next, we calculated accumulated distances from the high-risk areas to the low-risk areas and then increased the costs to ensure the evacuees at the high-risk areas would move to the low-risk areas first and then to the shelter. In the study, we simply added the maximum cost to those at the high-risk areas, albeit the costs only needed to be higher than ones of the neighbours. The two cost maps were utilised for checking the effect of risk maps and flood maps on evacuation routes in the ABM.

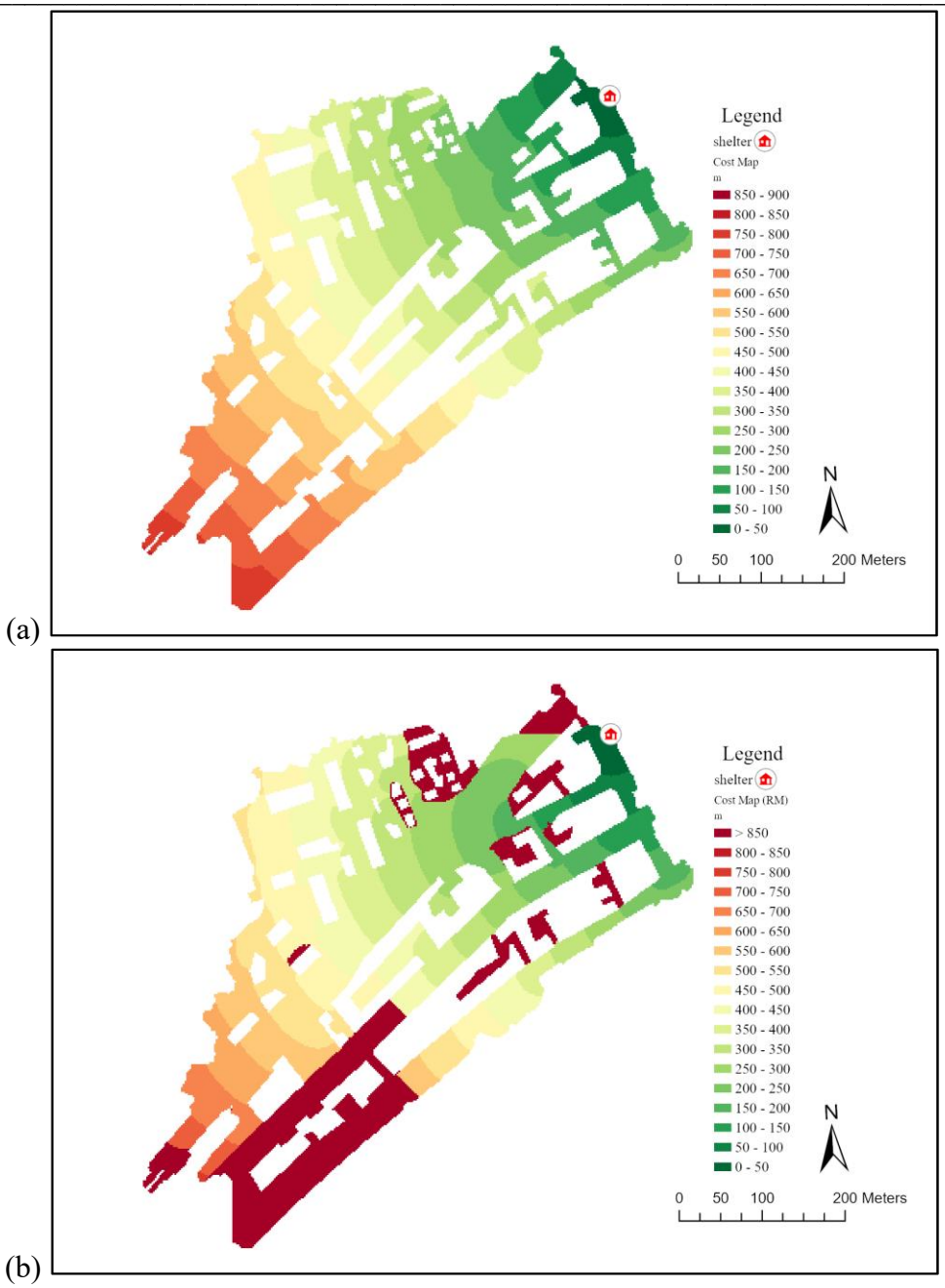

Figure 3-5. (a) The accumulated cost map and (b) the updated accumulated cost map.

3.2.5 Walking Speed

According to antecedent research on free walking speed variation across ages and gender (Ando et al., 1988), the speed ranges between around 0.8 m/s (children around 5 years old and female seniors over 70 years old) and 1.6 m/s (young male around 20 years old), as shown in Figure 3-6.

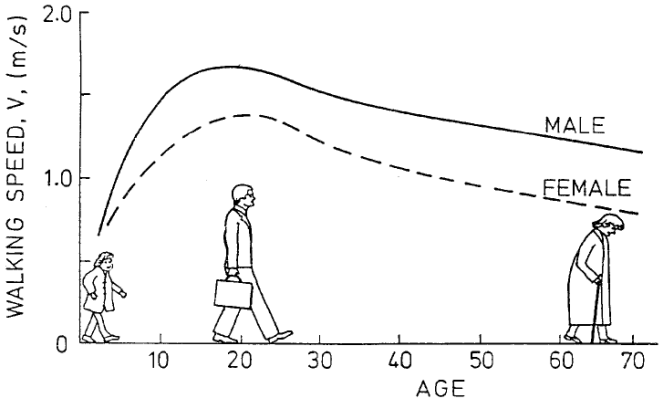

Figure 3-6. Walking speed variation across ages and gender. (Ando et al., 1988)

To check the uncertainty in input parameters, this study conducted sensitivity analysis to examine the model outputs under different initial walking speed settings. The study focused on the majority of outdoors active people, neglecting children (younger than 12) and elders (older than 65), and thus this study tried different initial walking speeds first to determine how the parameter affected the results. 7 different initial walking speeds were selected: 1.0 m/s, 1.1 m/s, 1.2 m/s, 1.3 m/s, 1.4 m/s, 1.5 m/s and 1.6 m/s, and this study ran 10 simulations for each initial walking speed under a scenario that the people started to evacuate when rainfall intensity $\geqq$ 25 mm/hr without the consideration of the risk maps and the flood maps. The boxplots of the average evacuation time, the average evacuation distances, the percentage of trapped people and percentage of people passing through flooded areas under different initial walking speed settings are shown as Figure 3-7. Figure 3-7 (a) and (b) indicate the fact that basically the average evacuation time decreased proportionally with the walking speed since the evacuation routes were not changed. The percentages of trapped people and people passing through flooded areas show no big difference except the one with initial walking speed of 1.0 m/s in Figure 3-7 (c) and (d). Due to the slower walking speed of 1.0 m/s, not all the evacuees could reach the shelter in time before the more serious inundation, and the percentages of trapped people and people passing through flooded areas were about one-eighth more than the others. Since only the young teenagers and the elders far away from the shelter would affect the results, to keep the simplicity, in the study, a single initial walking speed was set for all the evacuees in the ABM. Based on the antecedent research on free walking speed on flat areas (Ando et al., 1988; Thompson & Marchant 1995a; 1995b), as shown in Figure 3-8, the initial walking speed of all the evacuees was set at 1.4 m/s.

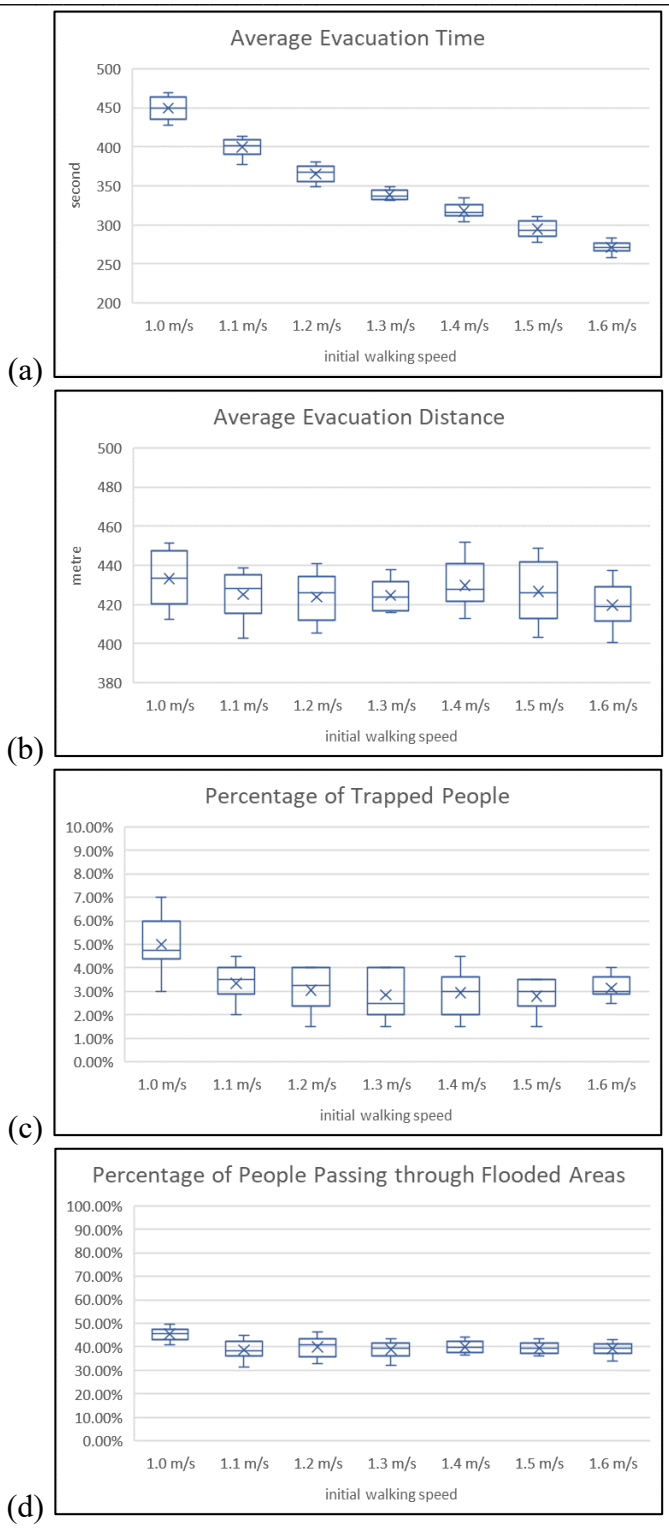

Figure 3-7. The boxplots of (a) the average evacuation times, (b) the average evacuation distances, (c) the percentage of people passing through flooded areas, and (d) the percentage of trapped people under different initial walking speed settings.

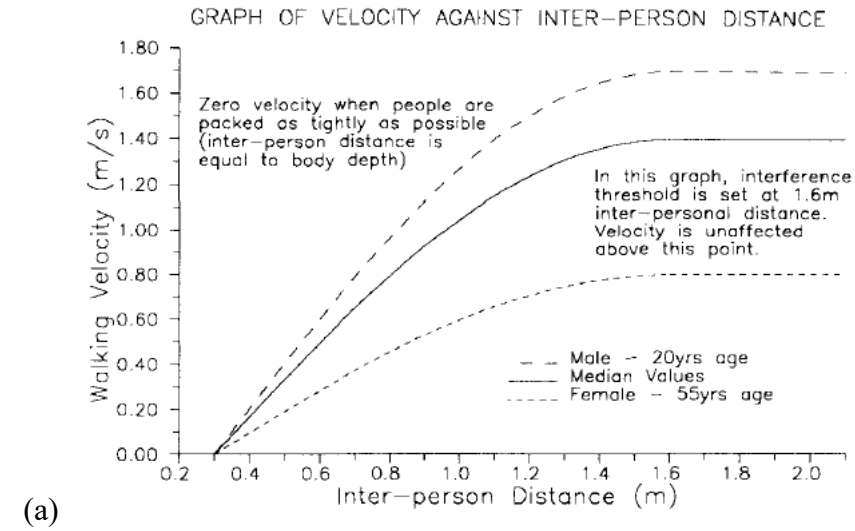

(a)

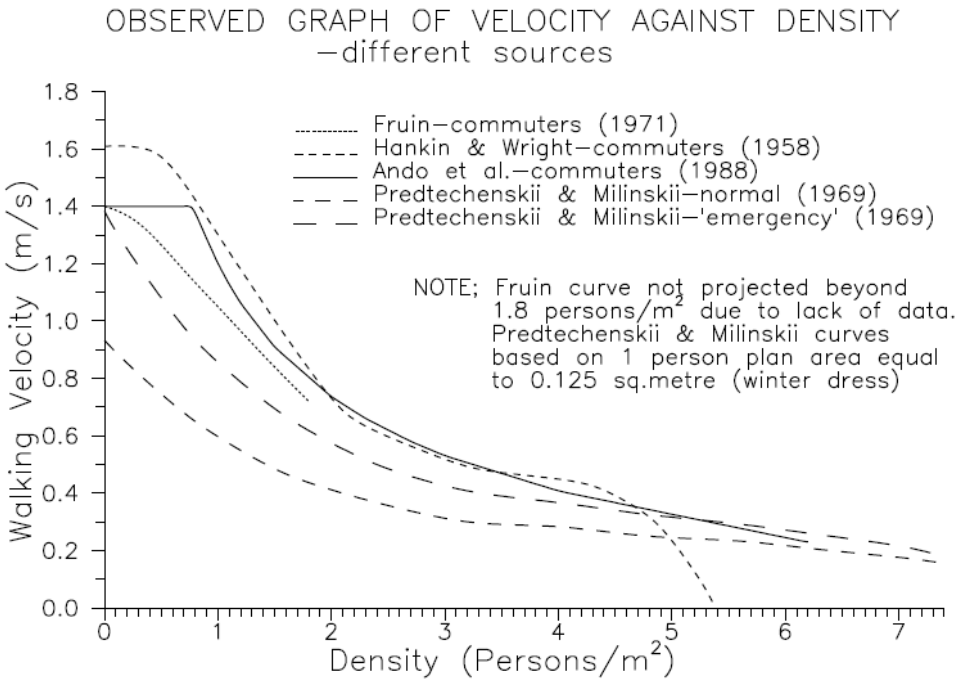

(b)

Figure 3-8. Walking velocity (a) against inter-person distance. (source: Thompson & Marchant (1995a)) and (b) walking velocity against density (persons/m^2). (source: Thompson & Marchant (1995b))

Since flood water would influence human safety and affect walking speed, an instability index and a relationship between people's walking speed and water depth were introduced into the ABM. Previous research investigated the relationship between human instability and flood. (Abt et al., 1989; Karvonen et al., 2000; Suetsugi, 1996; Jonkman & Penning-Rowsell, 2008) A critical depth-velocity product was proposed by many researchers as an instability index to check the human instability. In this study, an average critical depth-velocity product of 0.96 m^2/s was selected in a conservative way. In addition, several experiments examined the relationship between walking speed and flood. (Ishigaki et al., 2009; Chanson et al.,

2014; Lee et al., 2019; Bernardini et al., 2020; Dias et al., 2021) In this study, we integrated the antecedent research and determined the relationship between evacuees' walking speed and flood water depth in the ABM as shown in Figure 3-9. The walking speed was set at 1.4 m/s and decreased monotonically with increasing water depth, ignoring factors of gender, age, height, weight, etc. When water depth was higher than 1 metre, evacuees were trapped and unable to move. If evacuees reached the shelters, the evacuees would vanish.

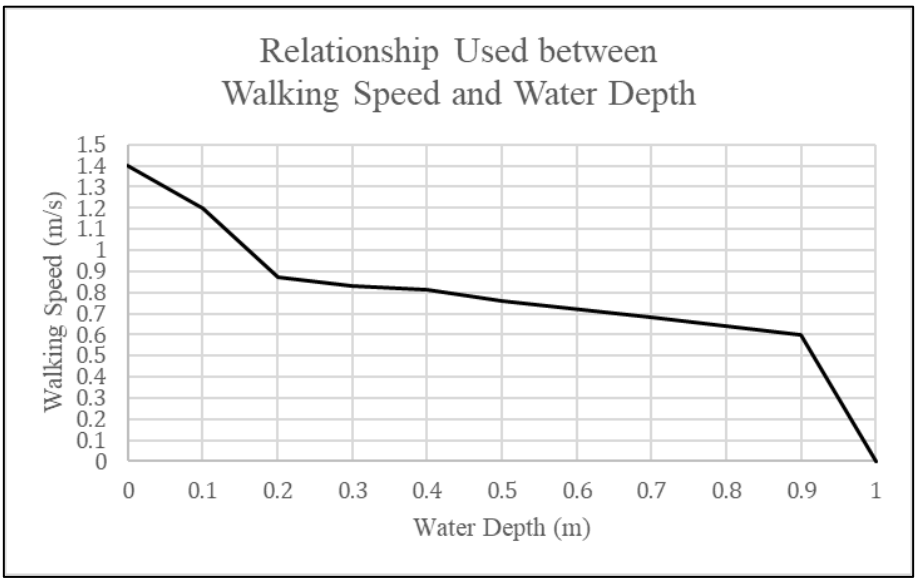

Figure 3-9. Relationship used between walking speed and flood water depth.

3.2.6 Number of Total Evacuees

According to rough estimation of daily active pedestrians in the study areas, the number of people active outdoors during the day is approximately 200. Before conducting the agent simulations, in order to check the uncertainty in the number of evacuees, a sensitivity analysis was conducted to examine the model outputs under different numbers of total evacuees: 20, 40, 60, 80, 100, 150, 200, 250 and 300. This study ran 10 simulations for each number of evacuees under a scenario that people started to evacuate at the initial walking speed of 1.4 m/s when rainfall intensity $\geqq$ 25 mm/hr without the consideration of the risk maps and the flood maps. The boxplots and the coefficients of variation of the average evacuation time, the average evacuation distances, the percentage of trapped people and percentage of people passing through flooded areas under different numbers of total evacuees are shown as Figure 3-10 and Figure 3-11. From the boxplots, it can be seen that when the number is smaller than 100, the variations of the indexes are obvious, showing larger ranges and even some outliers in Figure 3-10 (d). On the other hand, Figure 3-11 shows that the coefficients of variation of the indexes are acceptable, less than 0.3, except of

those of the percentage of trapped people when the numbers of evacuees are equal and less than 60. From the sensitivity analysis, it can be seen that increasing the number of total evacuees can reduce the variability of the indexes and obtain stable results, and the model can produce acceptable results with stability and consistency when the number is larger than 60. Therefore, randomly generating 200 evacuees in the whole computational domain in the ABM for the agent simulations is satisfactory from sensitivity analysis and general daily observation.

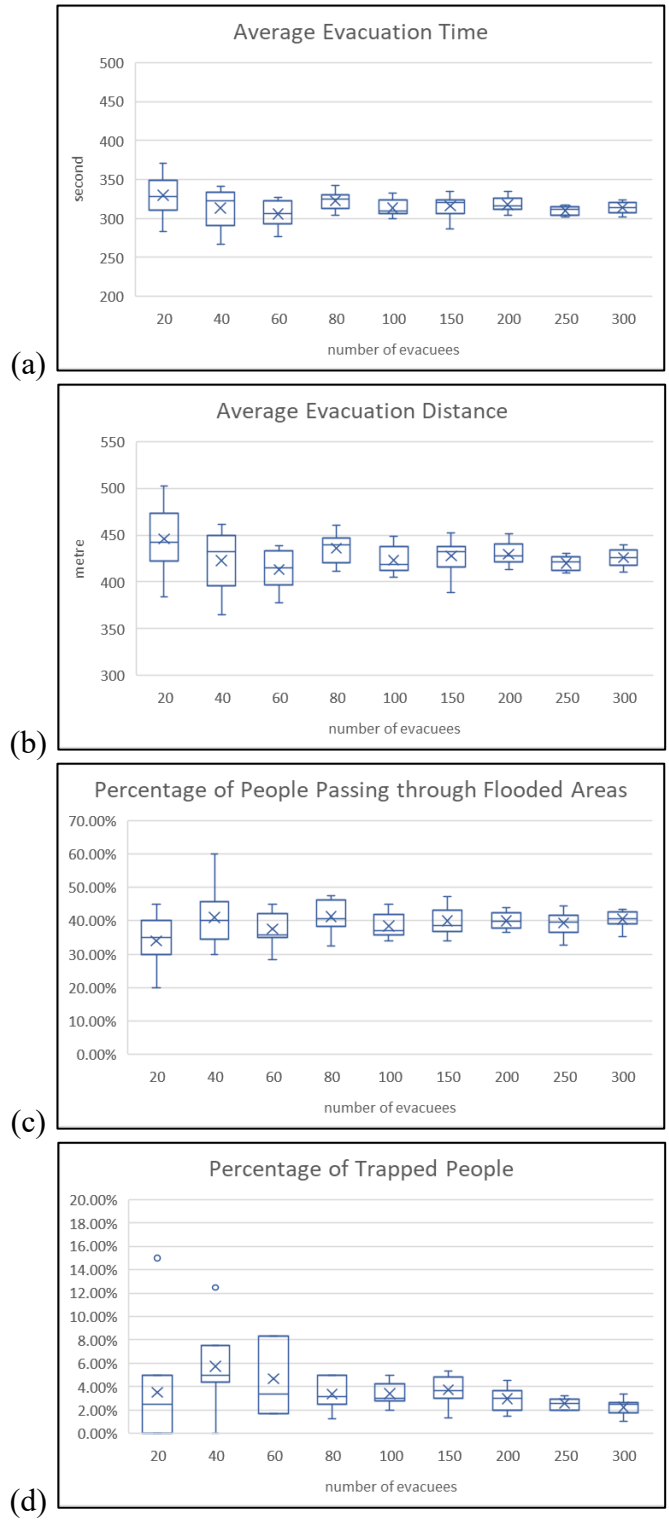

Figure 3-10. The boxplots of (a) the average evacuation times, (b) the average evacuation distances, (c) the percentage of people passing through flooded areas, and (d) the percentage of trapped people under different numbers of total evacuees.

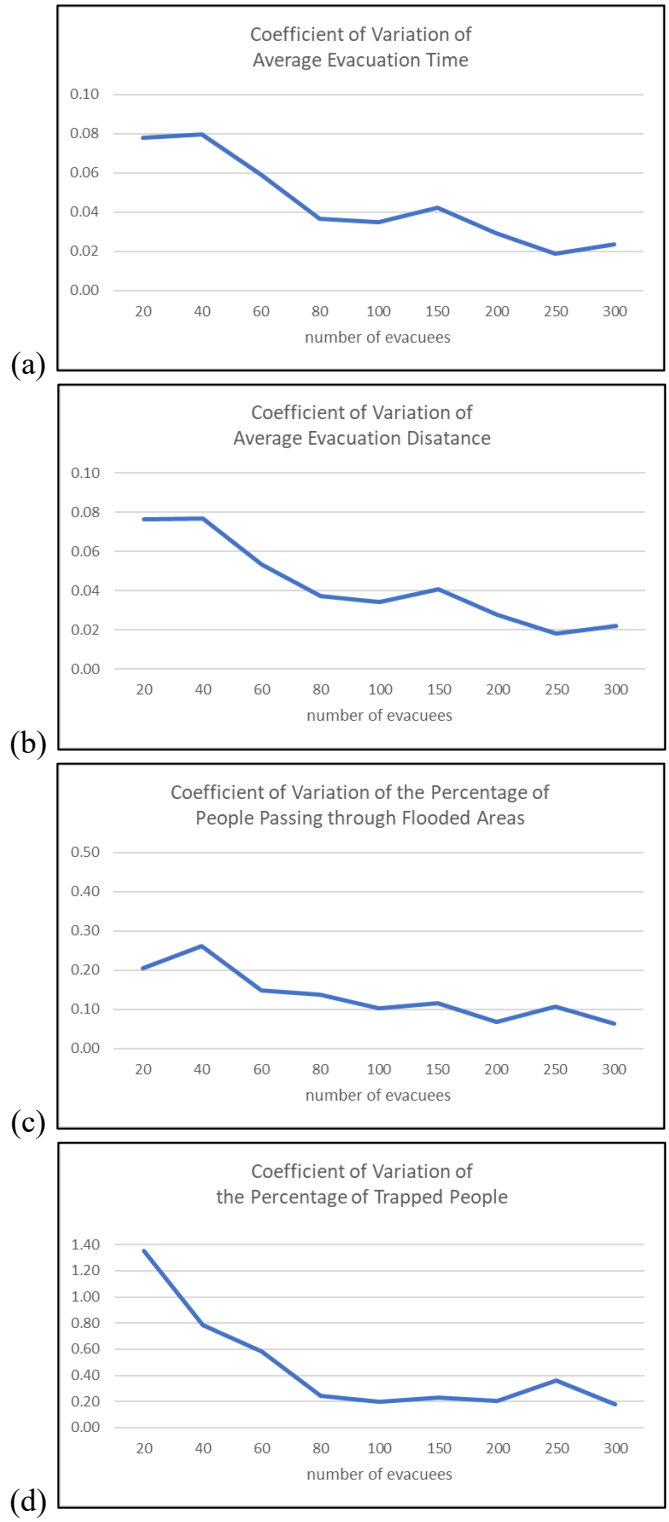

Figure 3-11. The coefficients of variation of (a) the average evacuation times, (b) the average evacuation distances, (c) the percentage of people passing through flooded areas, and (d) the percentage of trapped people under different numbers of total evacuees.

3.3 Inundation Simulations for 2D Overland Flow

Inundation simulation is essential to flood disaster management, providing important information about distribution of water and risk areas, and thus corresponding disaster management strategies against flood can be developed. To analyse the outcomes of disaster management strategies against flood, tools for simulating the interaction between flood water, response strategies, human behaviour and human safety during flood are essential. In flood disaster management region, antecedent research used ABMs to simulate evacuation process during flood events. (Dawson et al., 2011; Wang et al., 2016; O'Shea et al., 2020; Oh et al., 2021; Wang & Jia, 2021) If an ABM only imports outputs of hydraulic models as reference to conduct agent simulation, the water distribution cannot be changed, which is unable to represent the influences of some structural measures like floodwall, sandbags, pumps and so on. Therefore, the cellular automata (CA) inundation modelling of this study followed the antecedent research (Dawson et al., 2011) utilising an ABM, NetLogo, to develop an inundation model for 2D overland flow simulations. In this case, water distribution can be altered in the ABM, even during evacuation process. However, conducting complex hydrodynamic simulations in an ABM is time-consuming. To shorten the computational time for hydraulic simulation, there are various ways: reducing the complexity of terrain-sewer model to street-sewer model (Yang et al., 2018; 2020), running a 2D overland flow model and a 1D sewer model separately instead of a coupled model (Hsu et al., 2000), using cellular automata, (CA) for 2D modelling (Ghimire et al., 2013; Guidolin et al., 2016; Chang et al., 2021; Wijaya et al., 2023) etc. In consideration of applicability and suitability of the cell system of NetLogo, the CA concept was applied to develop a 2D overland flow model which uses simple rules to distribute the water between cells instead of solving complex physics equations. Although several CA hydraulic models have been used, verified and validated, the models have not been built in an ABM before. Therefore, the model performance of CA 2D inundation simulation of this study was evaluated by comparing the model outputs with three UK Environment Agency benchmark cases (Néelz & Pender, 2013) and two historical events, one in Nice, France and one in Taipei, Taiwan. The detailed information about the historical events is elaborated in Section 4.1 and Section 4.2. The aims of this model are to establish a simple 2D overland flow model in an ABM and to represent structural measures in urban areas.

3.3.1 Cellular Automata 2D Overland Flow Model

The descriptions of the CA 2D overland flow model in ABM follow the ODD protocol consisting of three categories: “Overview”, “Design concepts” and “Details” (ODD), and seven elements: “purpose and patterns”, “entities, state variables and

scales", "process overview and scheduling", "design concepts", "initialisation", "input data" and "submodels". The ABM used in the study is described in the following sections.

Overview

Purpose and Patterns

The model is to establish a simple 2D overland flow model for inundation simulations and to explore the possible influences of structural measures under different scenarios. The following structural measures were also taken into account: floodwalls, sandbags, inlets of sewer systems and pumps. The performance of the measures will be evaluated, and the outcomes will be discussed. The model redistributes water proportionally between cells according to the weights based on the difference in water levels between a cell and its neighbour cells. The model can provide key information about water depth, flow velocity and maximum water depth in an inundation simulation of each cell.

Entities, State Variables and Scales

The following two entities are included in the model: observer and patches. The observer controls the global variables and the patches represent cells of the whole computational domain of the study area. Since this CA model is only to conduct inundation simulations, no agents are introduced into the model. The variables, the descriptions and the units of these entities are listed in the Table 3-3.

The spatial extent is divided into several square cells, and the number of and the size of the cells are varied, depending on the cases. The spatial information is directly imported from ASCII files. The simulation time is also different, depending on the cases. The model uses adaptive time step, and therefore every tick in the model may refer to different length of time. The detailed information about the spatial and temporal data about the case study is elaborated in Section 4.2.

Table 3-3. The entities and the variables of the CA overland flow model.

Entity	Variable	Description	Unit
Observer	time	simulation time	s
	Simulation_Duration	the end time of the simulation	s
	timestep	time step	s
	Max_V	the maximum velocity over the whole domain	s
	cellsize	the grid size	m
	inflow	the list of the inflow discharge	m^3/s
	rainfall	the list of the rainfall	mm/hr
Patch	valid	check the grid is valid or not	m
	elevation	the elevation of the grid	m
	ManningN	the Manning's roughness coefficient of the grid	$s/m^{1/3}$
	water_depth	the water depth at the grid	m
	max_depth	the maximum water depth at the grid	m
	neighbour_N	the adjacent grid on the north side	-
	neighbour_E	the adjacent grid on the east side	-
	neighbour_S	the adjacent grid on the south side	-
	neighbour_W	the adjacent grid on the west side	-
	DeltaLevel_N	the difference in water level between the grid and the north neighbour grid	m
	DeltaLevel_E	the difference in water level between the grid and the east neighbour grid	m
	DeltaLevel_S	the difference in water level between the grid and the south neighbour grid	m
	DeltaLevel_W	the difference in water level between the grid and the west neighbour grid	m
	DeltaLevel_Max	the maximum difference in water level between the grid and the neighbours	m
	DeltaVolume_N	the available water storage volume between the grid and the north neighbour grid	m^3
	DeltaVolume_E	the available water storage volume between the grid and the east neighbour grid	m^3
	DeltaVolume_S	the available water storage volume between the grid and the south neighbour grid	m^3
	DeltaVolume_W	the available water storage volume between the grid and the west neighbour grid	m^3
	DeltaVolume_Max	the maximum available water storage volume between the grid and the neighbours	m^3
	DeltaVolume_Min	the minimum available water storage volume between the grid and the neighbours	m^3
	DeltaVolume_Total	the total available water storage volume between the grid and the neighbours	m^3
	weight_N	the weight of the north neighbour grid	-
	weight_E	the weight of the east neighbour grid	-
	weight_S	the weight of the south neighbour grid	-
	weight_W	the weight of the west neighbour grid	-
	weight_0	the weight of the grid	-
	weight_Max	the maximum weight of the grid and the neighbours	-
	V_critical	the critical velocity of the grid	m/s
	V_Manning	the average velocity of the grid	m/s
	V_Max	the local intercellular velocity determined by V_critical and V_Manning	m/s
	V_N	the flow velocity northwards	m/s
	V_E	the flow velocity eastwards	m/s
	V_S	the flow velocity southwards	m/s
	V_W	the flow velocity westwards	m/s
	V_mean	the mean flow velocity	m/s
	I_total	the total transferable water volume	m^3
	previous_I_total	the previous total transferable water volume	m^3
	I_N	the water volume to be transferred northwards	m^3
	I_E	the water volume to be transferred eastwards	m^3
	I_S	the water volume to be transferred southwards	m^3
	I_W	the water volume to be transferred westwards	m^3
	I_Max	the maximum water volume to be transferred	m^3
	floodwall_N	the height of the floodwall on the north side	m
	floodwall_E	the height of the floodwall on the east side	m
	floodwall_S	the height of the floodwall on the south side	m
	floodwall_W	the height of the floodwall on the west side	m
	outflow	the outflow discharge of pumps or manholes	m^3/s

Process Overview and Scheduling

The model covers the whole event, and the observer and the patches update the variables every time step. The simulation starts at the beginning of an event and finishes at the end of the event, and the simulation time is updated each time step. The beginning, the end and the simulation time varied according to the cases, which are elaborated in Section 4.2. Each time step, the model will check the simulation time first and then calculate and update all the variables in Table 3-3. Finally, the model updates the time step for the next computing process until the end of the simulation time. The detailed information about the inundation simulation is elaborated in Section 3.3.2.

Design Concepts

Design Concepts

Basic Principles

This model is designed to run inundation simulation. The model redistributes water proportionally between cells according to the weights based on the difference in water levels between a cell and its neighbour cells. The detailed information about the inundation simulation is elaborated in Section 3.3.2.

Emergence

No agents involve in the model, and all the variables of the cells will only be affected by equations of the CA model listed in Section 3.3.2.

Adaptation

No agents involve in the model, and all the variables of the cells will only be affected by equations of the CA model listed in Section 3.3.2.

Objectives

The model is to establish a simple 2D overland flow model for inundation simulations. Therefore, the model performance is determined by how close the model output is to the results of the benchmark test or the observation, in terms of water depth, flow velocity, flood extent and so on. The detailed information will be elaborated in Section 4.2.

Sensing

No agents involve in the model, and all the variables of the cells will only be affected by equations of the CA model listed in Section 3.3.2.

Interaction

No agents involve in the model, and the variables of a cell will only be affected according to the variables of the neighbour cells by equations of the CA model listed in Section 3.3.2.

Stochasticity

There is no stochasticity in any variable.

Observation

The key outputs from the model are water depth, flow velocity and maximum water depth in an inundation simulation of each cell.

Details

Initialisation

The model is initialised by importing geographic data listed in the section "Input Data" for building the computational domain. The water-related variables (such as water depth, velocity, water volume, etc.) of each cell are all set at 0 at the beginning. The simulation time is set as the beginning of the case at the initial time step and the time step is set as 1 second.

Input Data

The model imports information about elevation, Manning's roughness coefficient and height of floodwalls into each corresponding cell for building the computational domain. All the files are generated by a GIS software in ASCII format, which can be imported directly into the ABM.

Submodels

Update Simulation Time

The global variable "time" can be updated by adding the time step, and it can be calculated by the following equation:

$$time^{t+1} = time^{t} + timestep$$

Rainfall

This submodel is used to put rainfall into the model. The model first checks the simulation time and then introduces the corresponding amount of water into the computational domain. The detailed information about the inundation simulation is elaborated in Section 3.3.2.

Inflow

This submodel is used to put inflows into the model. The model first checks the simulation time and then introduces the corresponding amount of water into the computational domain at specific patches. The detailed information about the inundation simulation is elaborated in Section 3.3.2.

Weighted Cellular Automata 2D Inundation model

The model is the main core for inundation simulation. All the information and the equations are elaborated in Section 3.3.2.

3.3.2 The Weighted Cellular Automata 2D Inundation model

This study utilised NetLogo model to develop a 2D overland flow model through the adoption of the concept of CA from the Weighted Cellular Automata 2D model (WCA2D model) (Guidolin et al., 2016), using the Cartesian cells and von Neumann neighbourhood. Instead of solving complex physics equations, the model redistributed water proportionally between cells based on the weights. The WCA2D model is written by low-level programming language, C/C++ and OpenCL, and the computation can be executed on graphics processing units (GPUs), which can substantially improve the modelling efficiency. In contrast, this study only adopts the concept and rewrites the code by NetLogo software, which cannot do any parallel processing, and thus GPU computing.

The CA model first calculated the difference in water levels between a cell and its neighbour cells and then gave weights to the cells based on the available water storage volumes. Next, the CA model computed the local intercellular velocities and then distributed the water proportionally according to the weights. At last, the CA model updated the water depth, volume, velocity and so on, and then updated the simulation time to rerun the process. The flowchart of the CA 2D overland flow model is shown as Figure 3-12.

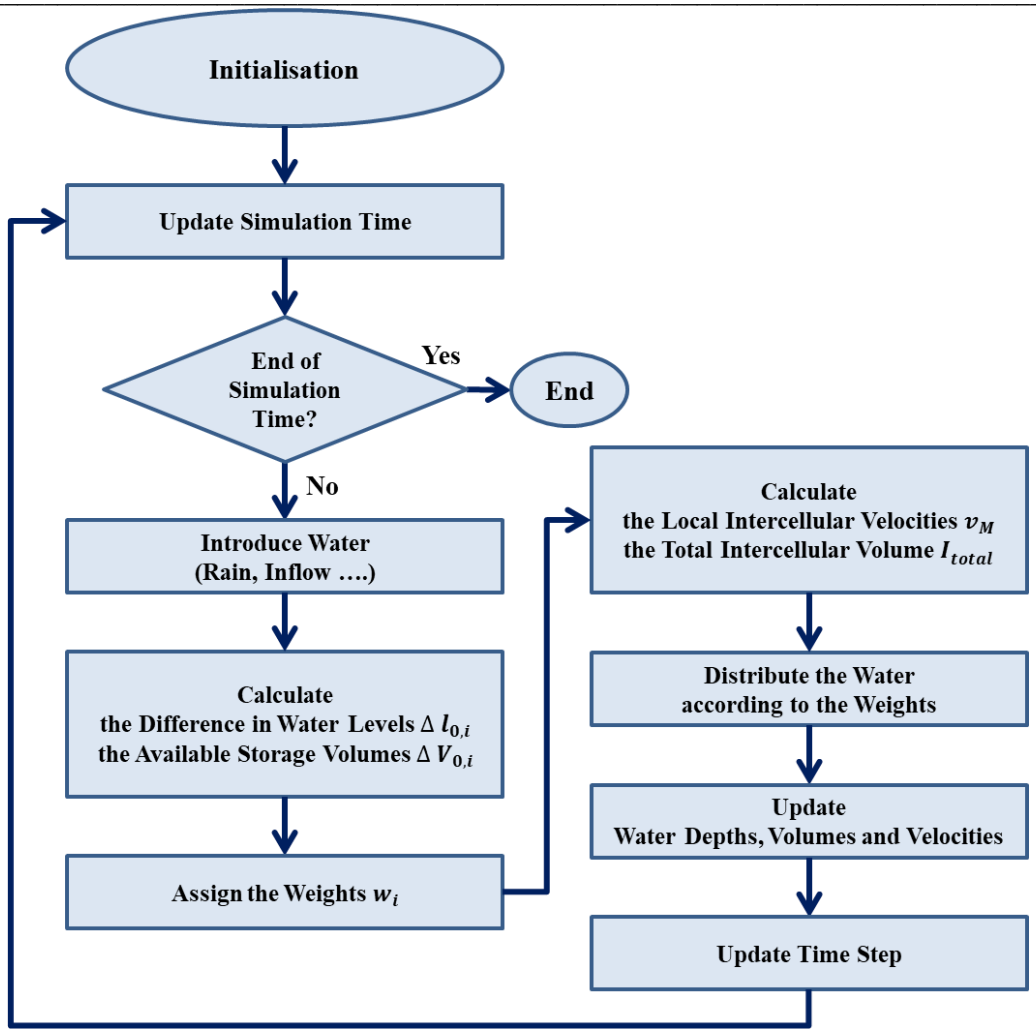

Figure 3-12. The flowchart of the CA 2D overland flow model.

If the water level at the central cell was greater than the water level of a neighbour, the water would go into the neighbour cell from the central. The available water storage volume could be defined as the product of the difference in water level and the cell area. Then the minimum, maximum, and the total volume differences could be calculated by the following Equations:

$$\Delta l_{0,i} = \max\{l_0 - l_i, 0\} \ \forall i \in \{1 \dots n\} \tag{3-1}$$

$$\Delta V_{0,i} = A \, \Delta l_{0,i} \ \forall i \in \{1 \dots n\} \tag{3-2}$$

$$\Delta V_{min} = \min\{\Delta V_{0,i} \big|_{i=1\dots n}^{\Delta l_{0,i} > \tau}\} \tag{3-3}$$

$$\Delta V_{max} = \max\{\Delta V_{0,i} \big|_{i=1\dots n}\} \tag{3-4}$$

$$\Delta V_{total} = \sum_{i=1}^{m} \Delta V_{0,i} \quad (3\text{-}5)$$

where n is the cell number of the neighbour cells, l_0 (m) is the water level at the central cell, l_i (m) is the water level of the i^{th} neighbour cell, $\Delta l_{0,i}$ (m) is the difference in water level between the central cell and the neighbours, A (m^2) is the cell area, $\Delta V_{0,i}$ (m^3) is the available water storage volume between the central cell and the neighbours, ΔV_{min} (m^3) is the minimum available water storage volume, ΔV_{max} (m^3) is the maximum available water storage volume, ΔV_{total} (m^3) is the total available water storage volume, τ is tolerance of the water level difference.

The water would be redistributed according to the weights of the central cell and the neighbour cells, and the weights were defined as Equation (3-6) and shown as Figure 3-13 (a):

$$w_i = \frac{\Delta V_{0,i}}{\Delta V_{total} + \Delta V_{min}}, w_0 = \frac{\Delta V_{min}}{\Delta V_{total} + \Delta V_{min}} \; \forall i \in \{1 \dots n\} \quad (3\text{-}6)$$

where w_i is the weight of the i^{th} neighbour cell, and w_0 is the weight of the central cell.

A limitation was placed to prevent the local velocity from becoming critical flow. The local intercellular velocity was determined based on critical flow condition and the Manning's equation as Equation (3-7) and (3-8):

$$v_{critical} = \sqrt{gd} \quad (3\text{-}7)$$

$$v_{manning} = \frac{1}{n} R^{\frac{2}{3}} S^{\frac{1}{2}} \quad (3\text{-}8)$$

where $v_{critical}$ (m/s) is the critical velocity, g (m/s^2) is the gravitation acceleration, d (m) is the water depth, $v_{manning}$ (m/s) is the average velocity, n ($s/m^{1/3}$) is the Manning's n roughness coefficient, R (m) is the hydraulic radius and S is the hydraulic gradient.

Therefore, the maximum intercellular velocity v_M (m/s) from the central cell to the neighbours could be determined by Equation (3-9):

$$v_M = min\left\{\sqrt{gd_0}, \frac{1}{n} {d_0}^{\frac{2}{3}} \sqrt{\frac{\Delta l_{0,M}}{\Delta x}}\right\} \quad (3\text{-}9)$$

where d_0 (m) is the water depth of the central cell, $\Delta l_{0,M}$ (m) is the difference of water level between the central cell and the neighbour cell with the largest weight, Δx (m) is the cell size.

The maximum volume I_M (m^3) to be transferred from the central cell to the neighbour with the largest weight M at time step Δt could be calculated as Equation (3-10):

$$I_M = v_M \, d_0 \, \Delta x \, \Delta t \tag{3-10}$$

The total transferable volume $I_{total}^{t+\Delta t}$ (m^3) could be calculated as Equation (3-11):

$$I_{total}^{t+\Delta t} = min\left(d_0 A \, , \frac{I_M}{w_M} \, , I_{lc} + I_{total}\right) \tag{3-11}$$

The first term of Equation (3-11) is the total water volume of the central cell, and the second term is the transferable water volume I_M (m^3) of the neighbour cell with the largest weight divided by the weight w_M. The third term is used to constrain the total transferrable volume; where the I_{lc} (m^3) is the transferable water volume which will not cause oscillation between cells, i.e., the water level of the central cell from being lower than the neighbours at the next time step; the I_{total} (m^3) is the total amount of transferable volume at the previous time step, used to prevent large difference between time steps. The I_{lc} (m^3) could be determined by Inequality (3-12) and Equation (3-13). As shown in Inequality (3-12), the left-hand-side is the water level of the central cell at the next time step $t + \Delta t$, and the right-hand-side is water level of a neighbour receiving water from the central cell at time $t + \Delta t$. When the water levels of the central cell and of the neighbour cell are the same, the equality of Inequality (3-12) holds and Equation (3-13) is satisfied.

$$l_0 - \frac{I_{lc}^{t+\Delta t}}{A} \geq l_c + \frac{1}{A} \left(I_{lc}^{t+\Delta t} w_c\right) \tag{3-12}$$

$$I_{lc} = \frac{A \, (l_0 - l_c)}{1 + w_c} \tag{3-13}$$

where A (m^2) is the cell area, l_c (m) is the water level of a neighbour cell which will first reach the same water level as the central cell whilst receiving water from the central cell, w_c is the weight of the neighbour cell with the water level l_c.

Total volume to be transferred from the central cell to each i^{th} neighbour cell with weight w_i at time $t + \Delta t$ would be:

$$I_i^{t+\Delta t} = w_i \, I_{total}^{t+\Delta t} \quad \forall i \in \{1 \dots n\} \tag{3-14}$$

The volumes to be transferred between cells are shown as Figure 3-13 (b).
Equation (3-15) and (3-16) were used to update the water depth and velocity:

$$d_0^{t+\Delta t} = d_0^t - \frac{\sum_{i=1}^{n} I_i^{t+\Delta t}}{A} + \frac{\Delta V_0^{in}}{A} - \frac{\Delta V_0^{out}}{A} \tag{3-15}$$

$$v_i^{t+\Delta t} = \frac{I_i^{t+\Delta t}}{d_{0,i}^{t+\Delta t} \, \Delta x \, \Delta t} \; \forall i \in \{1 \dots n\} \tag{3-16}$$

where n is the cell number of the neighbour cells, $I_i^{t+\Delta t}$ is the volume transferred to the i^{th} neighbour cell, ΔV_0^{in} (m^3) is the input volume such as inflow and rainfall into the central cell, ΔV_0^{out} (m^3) is the output volume from the central cell due to infiltration, pumps, manholes, etc., A (m^2) is the cell area, d_0^t and $d_0^{t+\Delta t}$ are the water depth of the central cell at time t and at time $t + \Delta t$.
The adaptive time step Δt was calculated simply by using Courant-Friedrichs-Lewy (CFL) condition:

$$\Delta t = min\left(\alpha \frac{\Delta x}{v_{max}} \, , \Delta t_{min}\right) , 0 > \alpha \geq 1 \tag{3-17}$$

where Δx (m) is the cell size, v_{max} (m/s) is the maximum velocity, α is a coefficient to maintain stability, Δt_{min} is the minimum time step determined by the users. The illustration of the CA hydraulic model is shown in the Figure 3-14.

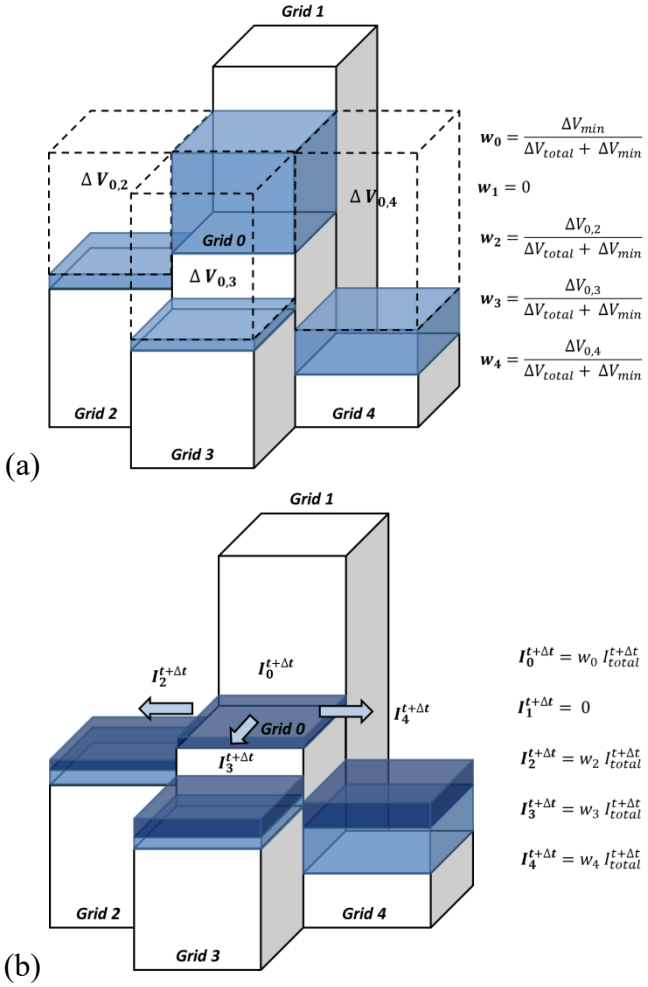

Figure 3-13. (a) The illustration of computing the weights and (b) the illustration of computing the volumes to be transferred.

For urban inundation simulation, relevant structures should be considered in the model. To represent floodwalls, sandbags, fences and so on, the height of these structures L_i was introduced into Equation (3-1):

$$\Delta l_{0,i} = \max\{l_0 - \max(l_i, L_i), 0\} \ \forall i \in \{1 \dots n\} \qquad (3\text{-}18)$$

Thus, the weights and the volumes to be transferred between cells with influence of structures are shown as Figure 3-14 (a) and (b). Different from simply lifted the elevation of the cells to represent the structures, the cells can still contain water as what they were before.

This study simply regarded manholes as inlets, and no surcharge flow will occur. The orifice equation was used to calculate the flow into manholes:

$$Q = C_o A_m \sqrt{2gd_0} \tag{3-19}$$

where Q (m^3/s) is the flow discharge into manhole, C_o is the orifice discharge coefficient; A_m is the net area of manholes, g (m/s^2) is the gravitation acceleration, d_0 (m) is the water depth. The ΔV_0^{out} (m^3) in the Equation (3-15) can be calculated by the product of the Q (m^3/s) and the time step Δt. The illustration of the presentation of inlets/pumps in the CA model is shown in the Figure 3-15.

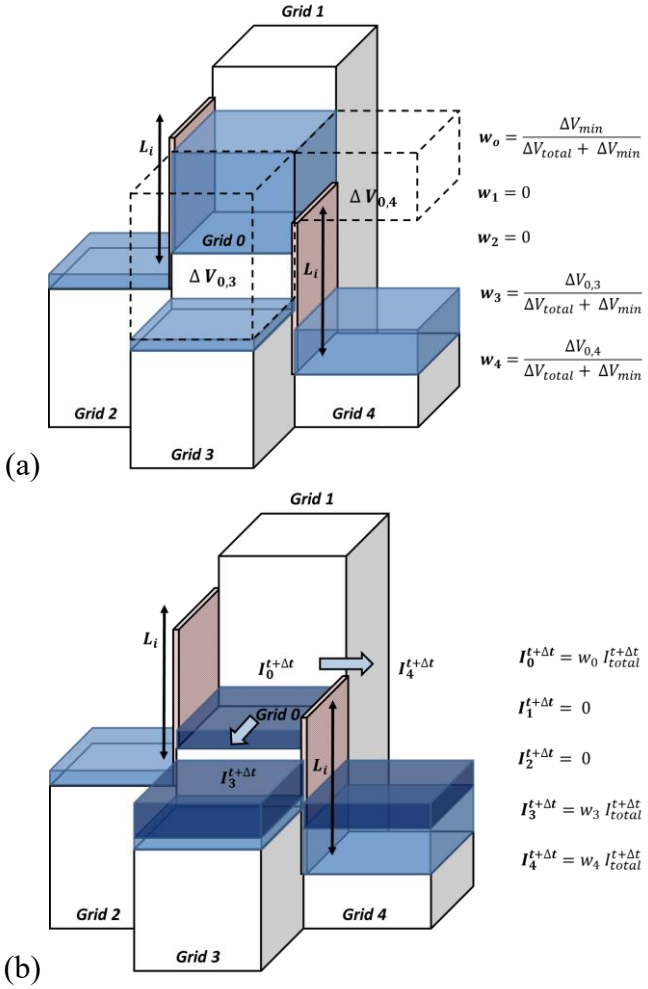

Figure 3-14. (a) The illustration of computing the weights with influence of structures and (b) the illustration of computing the volumes to be transferred with influence of structures.

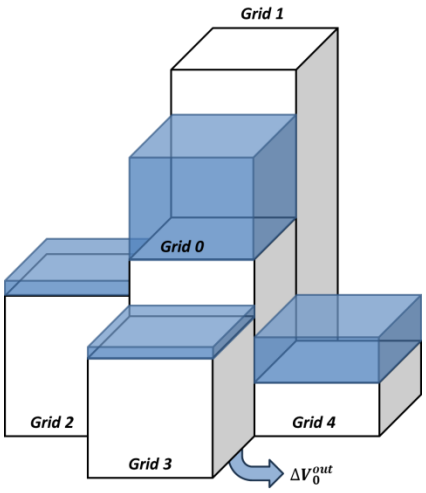

Figure 3-15. The illustration of the presentation of inlets/pumps in the CA model.

3.4 Inundation-Agent Coupled Simulations

At last, this study tries to run agent simulation coupled with inundation simulation. Two historical events, one in Nice and one in Taipei, are used to check the practicability of the inundation-agent coupled model. The inundation-agent coupled model combines above-mentioned agent simulation (in Section 3.2) and inundation simulation (in Section 3.3).

3.4.1 Inundation-Agent Coupled Model

The inundation-agent coupled model is used to analyse the interaction between human behaviour and the environment during a flood event. The inundation simulation can provide information about the flood to each cell, affecting the agents' behaviour during the agent simulation, and vice versa. The framework of the inundation-agent coupled model is shown in Figure 3-16.

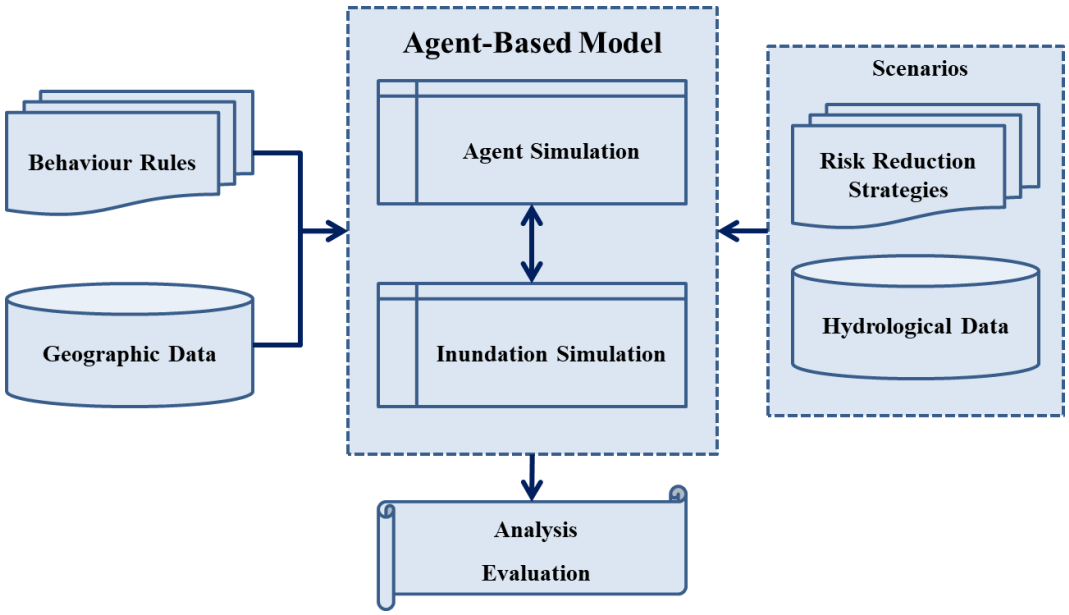

Figure 3-16. The framework of the inundation-agent coupled model.

Scenarios information is imported into the ABM, and thus the corresponding risk reduction strategies (including structural and non-structural measures) and hydrological data, together with geographic data to build and initialise the model. Behaviour rules are provided to the ABM to define the way agents and cells act and react with each other and the environment. Hydrological data are used to introduce water for the CA overland flow model for inundation simulations and to trigger some specific risk reduction strategies.

The ODD structure of the coupled model in ABM can simply combine the structures of the evacuation model (in Section 3.2) and CA overland flow model (in Section 3.3). Since one model is for the agents and the other one, for the environment, there is

no confliction within the coupled model, except for the information of flood which is only from the CA overland flow model in the ABM, not from the external files. The time step of the coupled model changes through time according to CFL condition in the CA overland flow model (check the adaptive time step in Section 3.3.2).

3.4.2 Cost Maps, Risk Maps and Flood Maps

The coupled model runs inundation-agent coupled simulation for two historical events, one in Nice and one in Taipei, and therefore, cost maps of the Dahu area in Taipei are also needed for the agent simulation. (The detailed information about the cost maps, the risk maps and the flood maps of Magnan area in Nice is introduced in Section 3.2.4.) The cost maps of the Dahu area were generated in the same way as the maps of Magnan area. The evacuation map of Dahu for inundation disaster (Hydraulic Engineering Office, 2021) is shown in Figure 3-17.

Figure 3-17. The evacuation map of Dahu for inundation disaster. (source: Hydraulic Engineering Office (2021))

An elementary school, Dahu elementary school, was chosen as an indoor evacuation shelter (the green house icon in the central area of the map), and then the cost map of Dahu area could be generated, as shown in Figure 3-20 (a). The south and the south-east parts of the Dahu area belong to another watershed, so that those parts were not taken into account. On the other hand, the west, the east and the north parts are

mountainous areas with dense trees and steep slopes where normally no one stands on, especially on rainy days, and hence those parts were also excluded from the cost maps. Given that high-risk areas were the areas to avoid, the cost map could be further improved by increasing the costs at those areas. According to the evacuation map presented in Figure 3-17, the blue shaded areas are flood-prone areas, and the red lines are potential debris flow areas. Besides, the green areas on the north part where two red lines located are a disaster prevention park, Dagouxi Waterfront Park, with a retention pond, where is also a high-risk area during heavy rains. Figure 3-18 shows the illustration of the operation process of the retention pond in the park, which reveals the fact that the whole park may be filled with water during heavy rains. Figure 3-19 is a photo of the retention pond in the park.

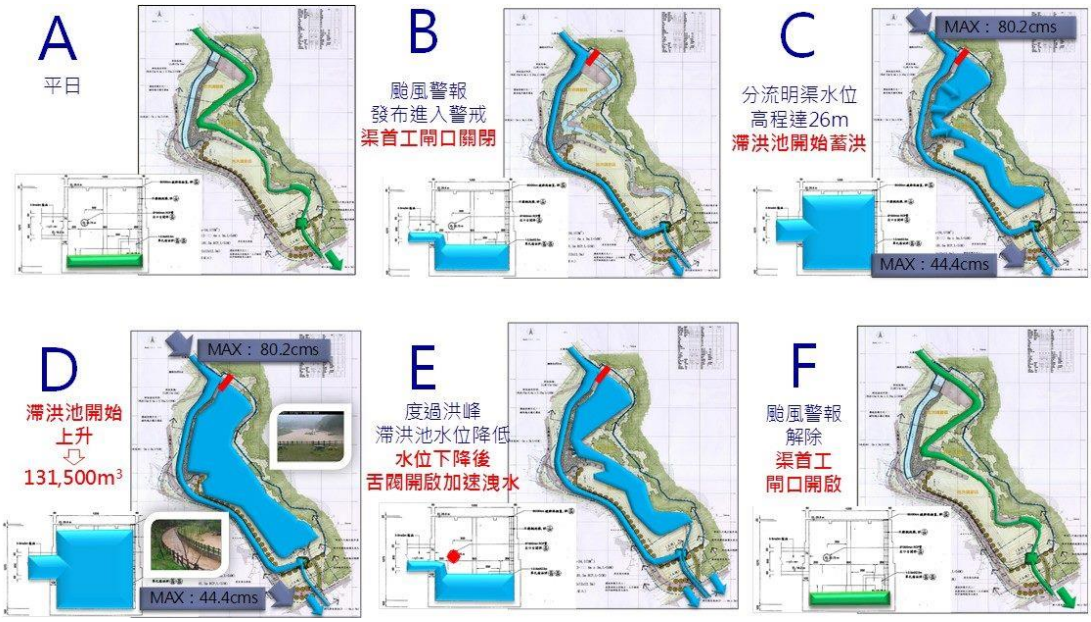

Figure 3-18. The illustration of the operation process of the retention pond in Dagouxi Waterfront Park. (source: Hydraulic Engineering Office (n.d.)) (A) normal situation, (B) when typhoon warning is issued, the channel headwork will be closed, (C) the retention pond will start to store water and its top level is 26 metres, (D) the water level of the retention pond is rising and the total capacity of the pond is 131,500 m^3, (E) after the peak flow, the water level of the retention pond will be decreasing and the gate will be opened to release water, (F) after the typhoon warning is lifted, the channel headwork will be reopened.

Figure 3-19. The retention pond in the Dagouxi Waterfront Park. (source: Center for Weather Climate and Disaster Research (2019))

The improved cost map is shown in Figure 3-20 (b). The two cost maps were utilised for checking the effect of risk maps and flood maps on evacuation routes in the coupled model for the Dahu area.

(a)

(b)

Figure 3-20. (a) The accumulated cost map and (b) the updated accumulated cost map.

3.5 Summary

This chapter introduced agent-based models (ABMs) and elaborated the structures of the models in the study: an evacuation model, a CA 2D overland flow model and an inundation-agent coupled model combining the first two models. ABMs are ideal tools for simulating the actions, reactions and interactions of autonomous individuals and the environment in a complex system, and NetLogo was used to develop the models. The evacuation model in the ABM was designed for agent simulations, whereas the CA 2D overland flow model in the ABM was designed for inundation simulations. Since the former model was for agents and the latter model was for cells, two models could be easily combined together to form a coupled model. The model verification and the possible applications will be described in Chapter 4, Chapter 5 and Chapter 6.

Chapter 4.
Model Verification

Part of this chapter has been submitted for publication.

Chapter 4 Model Verification

The evacuation model and the cellular automata (CA) 2D overland flow model were developed in an agent-based model (ABM). Before applying these models and the coupled model combining the above-mentioned models, model verification is needed to check the models' capability of providing qualified results. For the evacuation model, a historical event in Nice was selected to check whether the model can provide plausible evacuation process, whilst for the CA 2D overland flow model, three benchmark tests and two historical events, one in Nice and one in Taipei, were chosen to investigate whether the model can generate qualified inundation simulations. This chapter will describe the results and the performance of the evacuation model and the CA 2D overland flow model.

4.1 Evacuation Model in the Agent-Based Model

To evaluate the capability of the evacuation model and the performance of the evacuation process, this study used the evacuation model to run agent simulations under different scenarios, S1 – S4 (introduced in Section 3.2.1), for a historical flood event in Magnan area, Nice.

4.1.1 Case Study

A historical flood event in Magnan area in the south part of Nice city, on south-eastern coast of France, was selected for case study. A heavy rainfall hit Nice on the 4 January in 2014, causing scattered flood in Magnan. The rainfall event lasted about 25 hours with two peaks. The hyetograph is shown in Figure 4-1 (a). The Magnan basin covers an area of 17 km^2 and can be divided into two parts: mountainous areas in the upstream with the slope of 5.5% and flat urban areas of 0.21 km^2 in the downstream with the slope of 1.5%. A small river, Magnan River, enters underground sewer systems in the urban areas with an outlet to the Mediterranean Sea at the southeast part of the study area. The study area is a simple residential area, and the size of the area is appropriate for checking the disaster management in detail on a community scale. The 2-metre-resolution digital elevation model (DEM) of the urban area used in the ABM and the hydraulic model is shown in Figure 4-1 (b).

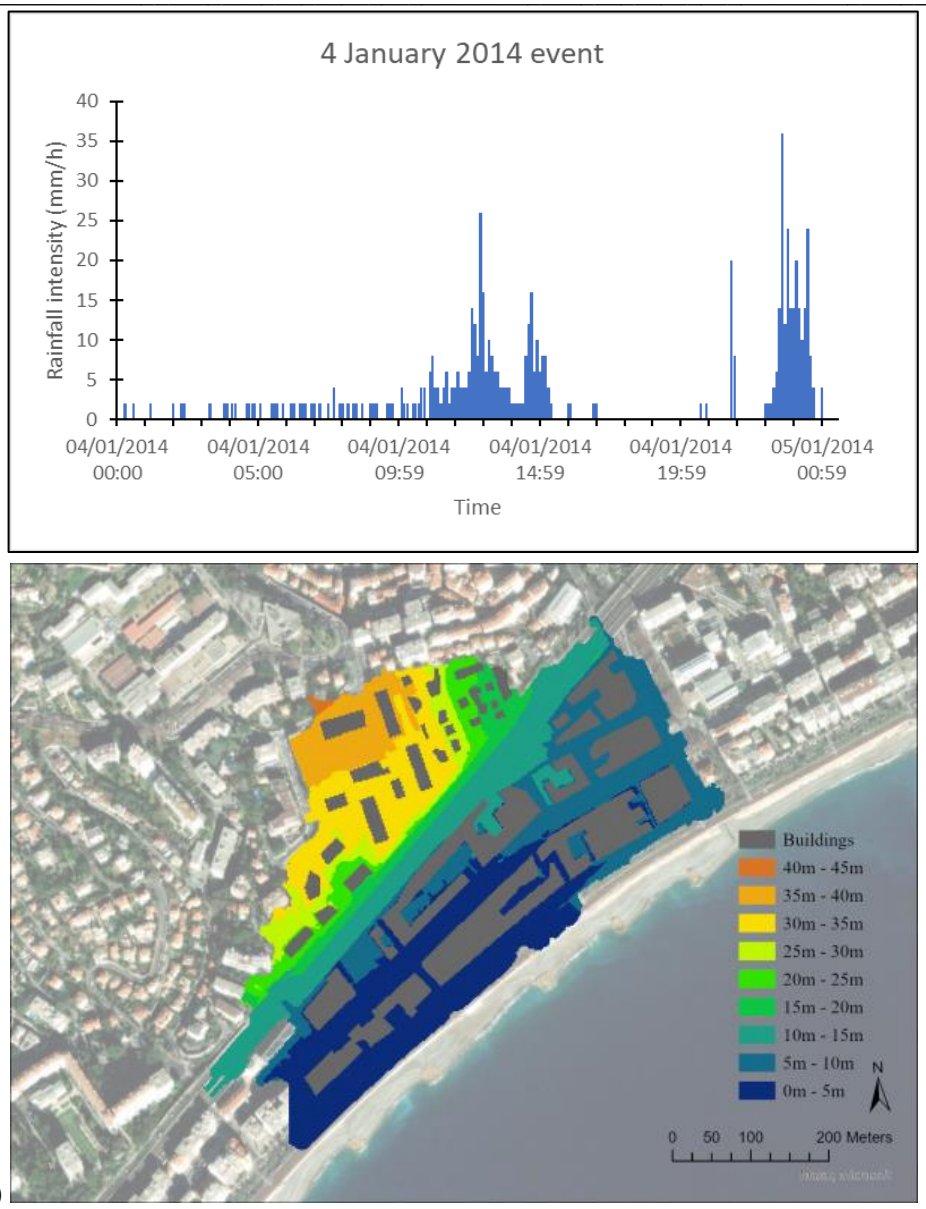

Figure 4-1. (a) The hyetograph of the 4 January 2014 event and (b) the DEM of the study area in Magnan area, Nice, France.

A fire station at the northeast corner of the study site was selected as the shelter, as shown in Figure 3-5. The evacuees of S1 and S3 chose the shortest routes to the shelter, without the consideration of the risk maps and the flood maps. Figure 4-2 shows an example of S1 simulations from t = 46440 s to t = 46475 s. As shown in the figure, the people in the southwest area and south area passed through small flooded lanes between buildings first to the central area and then moved to the shelter. Similarly, the people in the north area went through a narrow flooded passage in the northeast area to reach the shelter. On the contrary, the evacuees of S2 and S4 moved in a safer way with the consideration of the risk maps and the flood maps. Figure 4-3 shows an example of the S2 evacuation simulations from t = 46440 s to t = 46475 s.

The evacuees in the south areas went northeast and turned to the shelter at the most southeast corner, avoiding the flooded lanes. Likewise, the people in the north and northeast areas first made a detour around flooded areas to the central part and then moved towards the shelter.

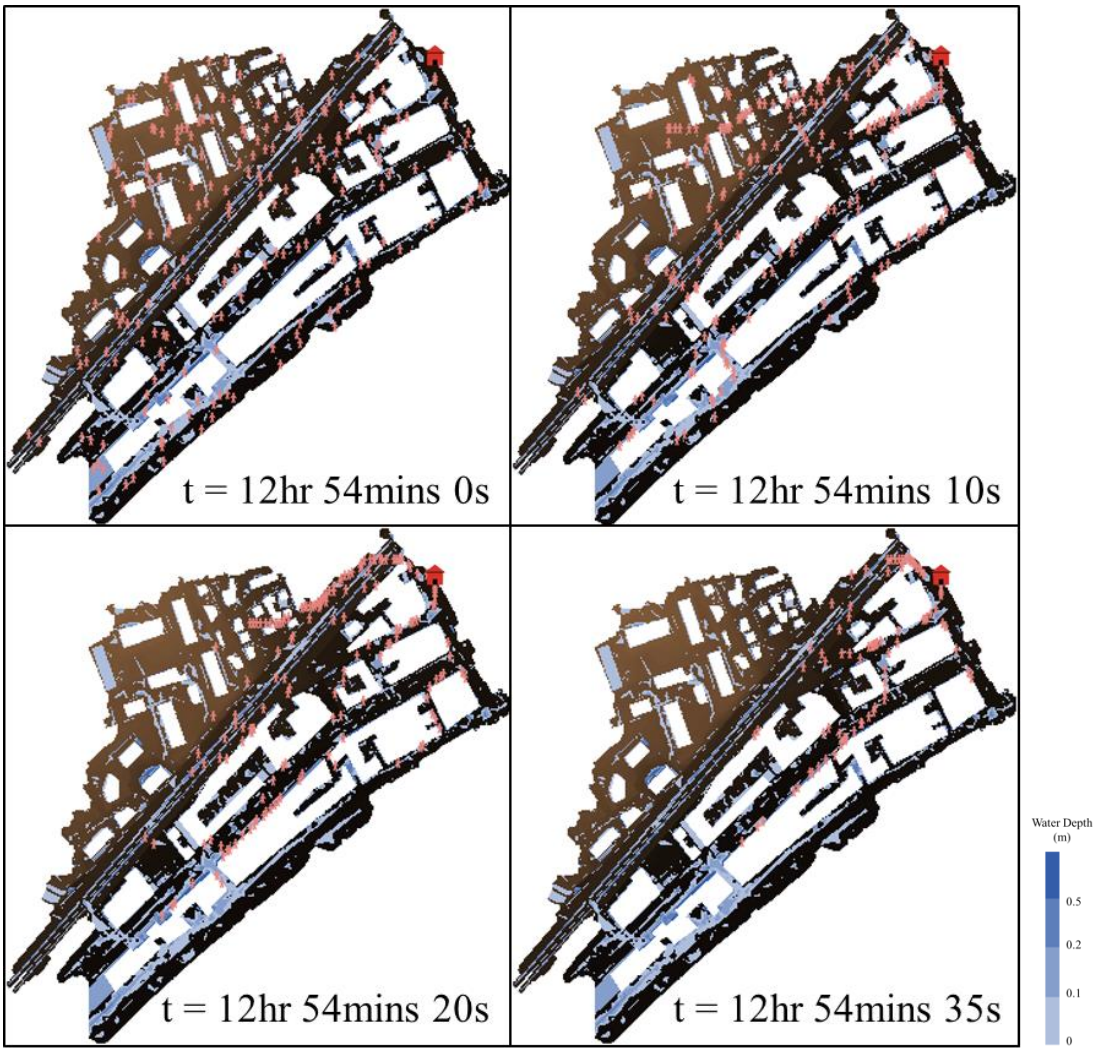

Figure 4-2. An example of S1 simulation.

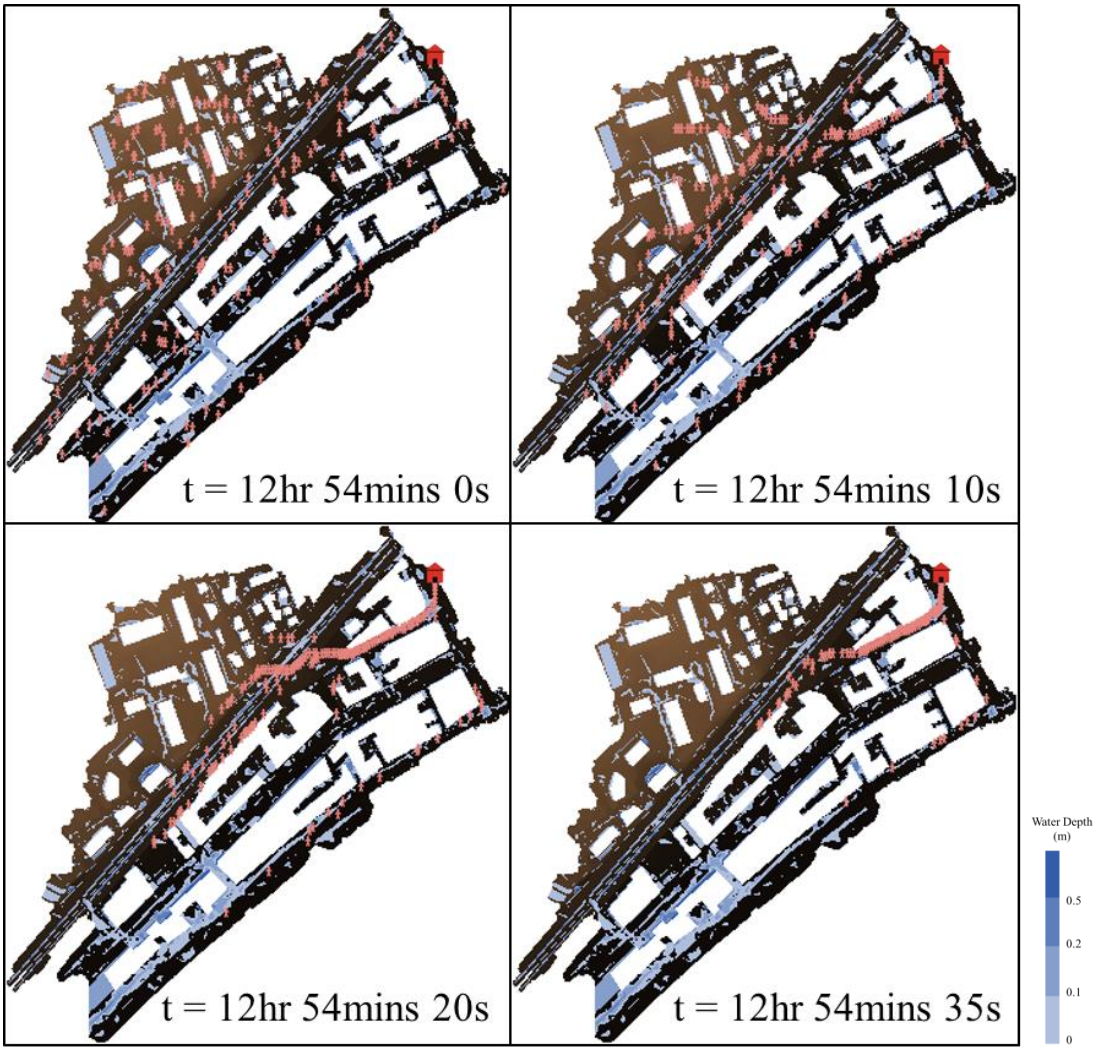

Figure 4-3. An example of S2 simulation.

Figure 4-4 and Figure 4-5 show the average evacuation time and the average evacuation distance of all the successfully evacuated people in each scenario. From Figure 4-5, we can see that the average evacuation distances in S2 and S4, with median values of 458.99 metres and 459.37 metres respectively, are around 8% longer than those in S1 and S3 with median values of 426.59 metres and 422.73 metres, due to the detours the evacuees made in S2 and S4. However, Figure 4-4 tells a consequence of wading into the water whilst evacuating in terms of evacuation time. The average evacuation time in S2 (median = 329.53 s) is longer than those in S1 (median = 315.54 s) in less than 5%, which is not proportionally augmented with the evacuation distances. Moreover, the average evacuation time in S4 and S3 are almost the same with median values of 331.63 s and 331.22 s respectively, even though the average evacuation distances of S4 are longer than that of S3. The evacuees in S3 spent more time, since more evacuees neglecting the flood maps and the risk maps in

S3 waded into water, which slowed their walking speed.

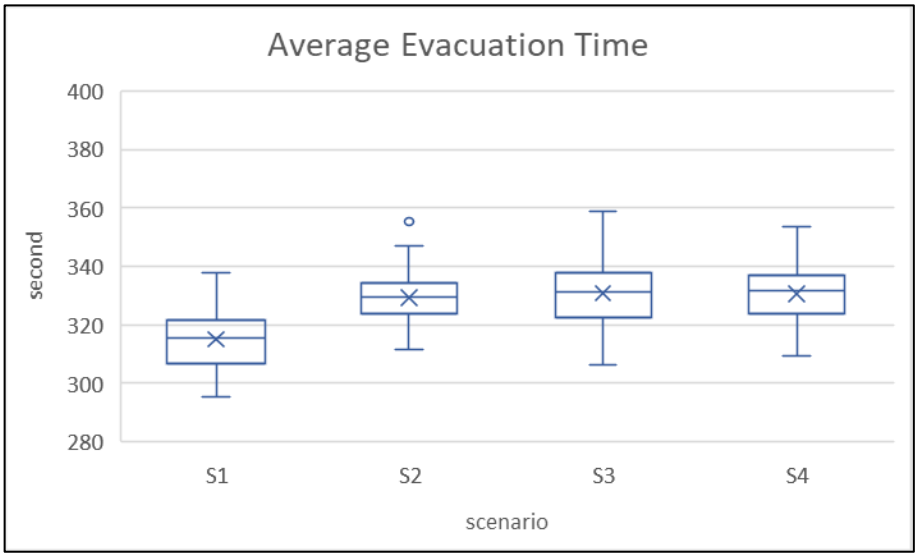

Figure 4-4. The average evacuation time of each scenario.

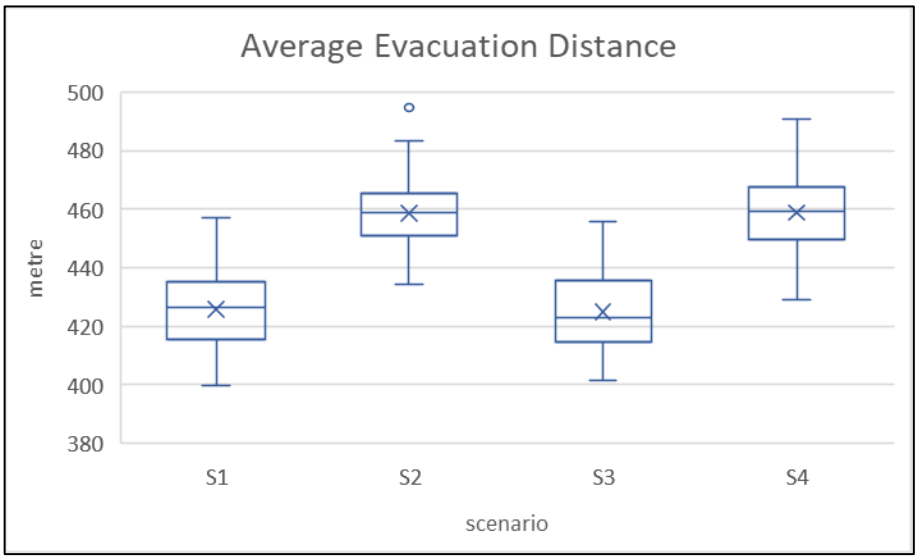

Figure 4-5. The average evacuation distance.

Figure 4-6 compares the general evacuation routes chosen by evacuees without and with the consideration of risk maps and flood maps. The yellow arrows indicate the evacuation directions. It could be seen from the figure that the evacuation distances of S1 and S3 were shorter than those of S2 and S4. However, there were more people in S1 and S3 travelling through flooded areas, especially in southwest areas and small lanes, and even trapped in the water. Figure 4-7 and Figure 4-8 are the boxplots of the percentage of people passing through flooded areas and the percentage of trapped people for each scenario. The boxplots indicate that the consideration of risk maps and flood maps and the evacuation timing substantially affect the performance of the

evacuation process. Many evacuees ever travelled through flood in S1 and in S3, with a median value of 39% and 71%, whilst just few evacuees did in S2 and S4 with a median of 1.5% and 8.5% respectively. Moreover, nearly no one was trapped in S2 (median = 0 and max = 0.5%) and S4 (median = 0.5% and max = 2%), whereas more people in S1 (median = 3%) and S3 (median = 9.5%) were in danger. The people considering the risk maps and flood maps in S2 and S4 would try to keep away from high-risk areas. In contrast, the people in S1 and S3 might move through the flood, which caused more people in danger. Without public crisis awareness and risk culture, some inappropriate behaviour, such as driving through flooded underpasses and rescuing cars in the basement during flood regardless of the high risk, ever happened in reality near the study site in 2015. (Libération, 2015; Radio Télé Luxembourg, 2015) However, since the risk maps and the flood maps could not locate every possible flooded area, some people in S2 and S4 still travelled through the flood. On the other hand, if we expanded the high-risk areas in a conservative way, there would be only few possible routes left for the evacuees, which might cause more problems. Equally, the evacuation timing was also important. If the alarm was sounded late, people would not be able to evacuate in time. Although the people in S2 and S4 would try to keep away from high-risk areas, some were already surrounded by flood before the alarm was sounded. Those people should inevitably pass through flooded areas, let alone the people who evacuated in S1 and S3. From the outputs of the simulations, it was evident that both consideration of the maps and the suitable evacuation timing were crucial, and the former might be more important than the latter in this study.

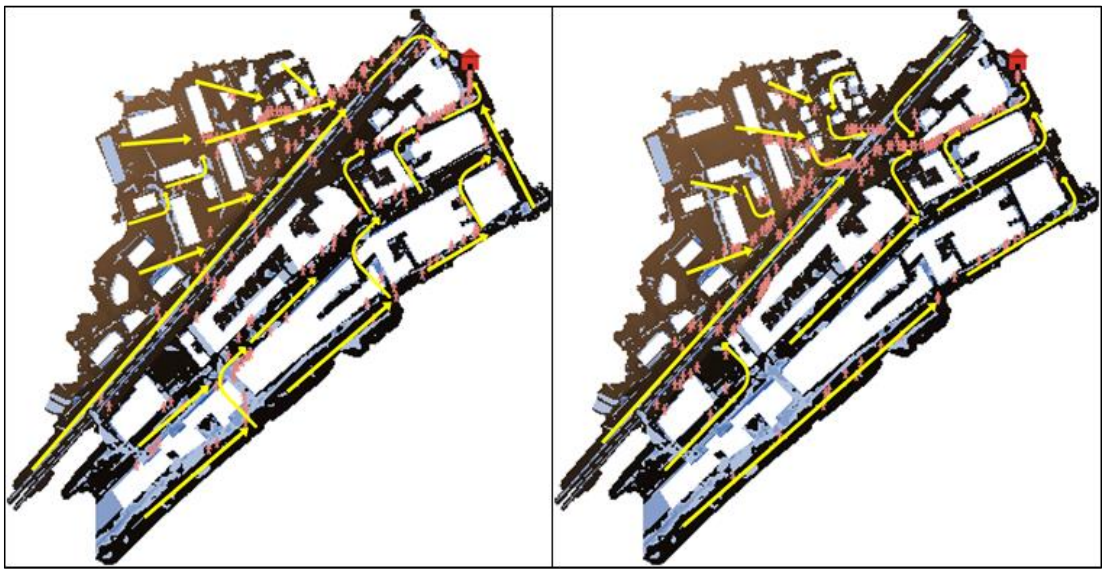

Figure 4-6. The general evacuation routes chosen by evacuees without (left) and with (right) the consideration of risk maps and flood maps.

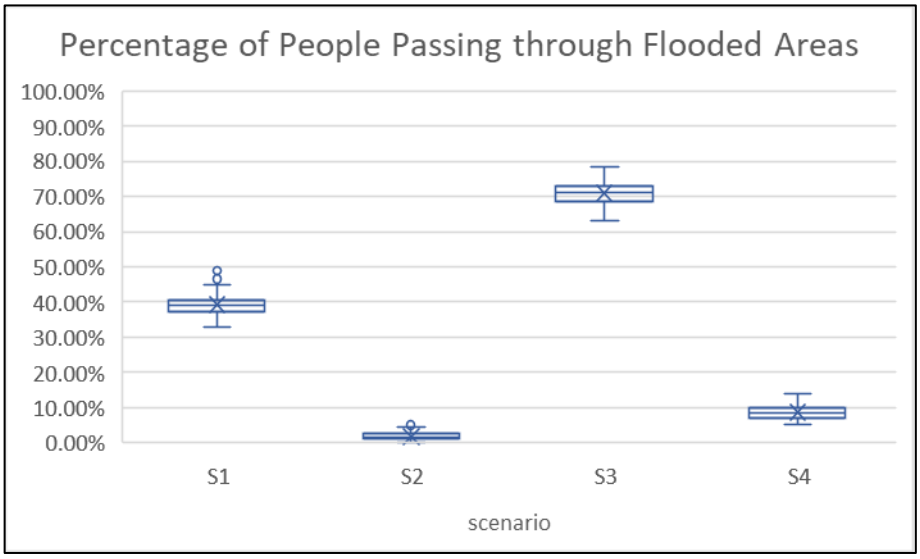

Figure 4-7. The percentages of people passing through flooded areas of each scenario.

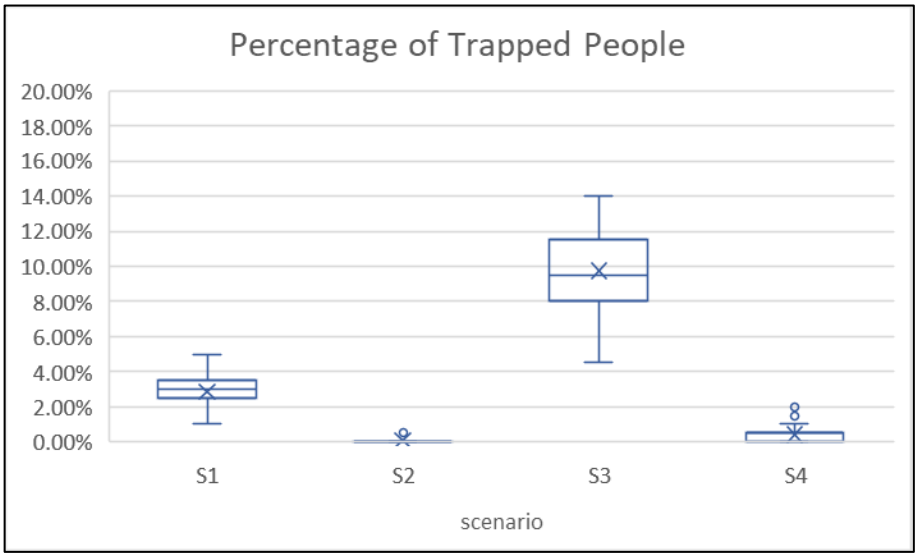

Figure 4-8. The percentages of trapped people of each scenario.

The ABM provided plausible outcome of those non-structural measures: risk maps, flood maps, the warning alarm and evacuation. The percentage of people in danger might be somewhat overestimated in this study. It is because of the simplification of human behaviour designed in the ABM. In this study, only the evacuation process with one shelter was considered in the ABM, and the shelter was assumed to have infinite capacity for all the evacuees. The ABM can be extended in the future to include both evacuation and invacuation (Shelter-in-Place) strategies with multiple shelters with limited capacity. Besides, every evacuee was generated uniformly and was assigned the same parameters. Many other factors including evacuee's age, gender, height, weight, etc., will also affect the evacuation process. Moreover, psychological factors such as panic, bandwagon effect, disobedience, and defiance, also have an impact on evacuation. These factors are worth being improved in the future.

4.1.2 Summary

The evacuation model was developed to investigate possible human behaviours during flood and interaction between evacuees and flood water with different non-structural measures: risk maps, flood maps, the warning alarm and evacuation. The rudimentary model outputs showed the capability of describing plausible outcomes of the non-structural measures. The results showed that the consideration of the maps and the proper warning alarm were vital, and the former might affect the performance of the evacuation process more than the latter in this study. Evacuees with the maps could make a detour around high-risk area, whilst the others would chose the shortest route towards the shelter, potentially putting themselves in danger. The ABM can be further enhanced, extended, and then applied in other regions.

In the study, the prototype of evacuation model was developed, with only basic and simple capability, and the model could be further improved:

- In the study, only one shelter was involved in the model, with infinite capacity for all the evacuees, which could not reflect the reality. The model can include both evacuation and invacuation (Shelter-in-Place) strategies with multiple shelters and with limited capacity. Meanwhile, evacuees may have their own preference for certain shelters and some specific routes.
- Every evacuee was generated uniformly and assigned the same parameters. Many other factors including evacuee's age, gender, height, weight, initial walking speed, etc., will increase the diversity in the ABM.
- Psychological factors such as panic, bandwagon effect, disobedience, and defiance, learning, cooperation, improvisation and so on are worth being included in the ABM and being improved in the future.
- Evacuation drills can be carried out in the study area to check the difference between model prediction and the observation, since there are no observed data so far for model validation.

4.2 CA 2D Overland Flow Model in the Agent-Based Model

To evaluate the performance and capability of the CA inundation model in the ABM, this study compared the model outputs with three UK Environment Agency (EA) benchmark cases (Néelz & Pender, 2013), Test 2, Test 4 and Test 8A, and two historical events, one in Nice, France and one in Taipei, Taiwan.

4.2.1 UK EA Hydraulic Benchmark Tests

The UK EA Hydraulic Benchmark Tests (Néelz & Pender, 2013) were designed to verify whether a hydraulic model is accurate. In this study, three different tests were selected to check the CA model in the ABM: Test2, Test4 and Test 8A. These tests were designed for checking the model outputs of 2D overland flow modelling: Test 2 for an inflow filling 16 depressions areas; Test 4 for the wave propagation of an inflow on a flat area; Test 8A for urban flooding with an inflow and homogeneous rainfall. Brief information about the tests is provided in the following sections, the details of these three tests can be found in (Néelz & Pender, 2013).

4.2.1.1 EA Benchmark Test 2

The Test 2 was designed to check the capability of a hydraulic model to determine flood extent and flood depth. An inflow with a peak flow of 20 m^3/s was applied along a 100 m long line at the northwest corner of the domain (shown as black line in Figure 4-9 (a)). The inflow rose from 0 m^3/s at t = 5 mins up to 20 m^3/s at t = 10 mins and kept constant; then the inflow decreased from 20 m^3/s at t = 86 mins down to 0 m^3/s at t = 91 mins. Linear interpolation was used to interpolate the inflow values, and the inflow information is shown as Figure 4-9 (b). The domain was a 2000 m x 2000 m square with 16 depressions with closed boundaries and resolution of 20 m. The digital elevation model (DEM) of the Test 2 is shown in the Figure 4-9 (a). The initial condition was set as dry bed, and Manning's roughness coefficient was set as 0.03 $s/m^{1/3}$ uniformly on the whole computational domain. The interface of the ABM is shown in the Figure 4-10. The simulation was run until t = 48 hours. The α in Equation (3-17) was set as 0.10. The model prediction of the water levels through time at the centre of each depression and the final flood extent were compared with the other models in (Néelz & Pender, 2013).

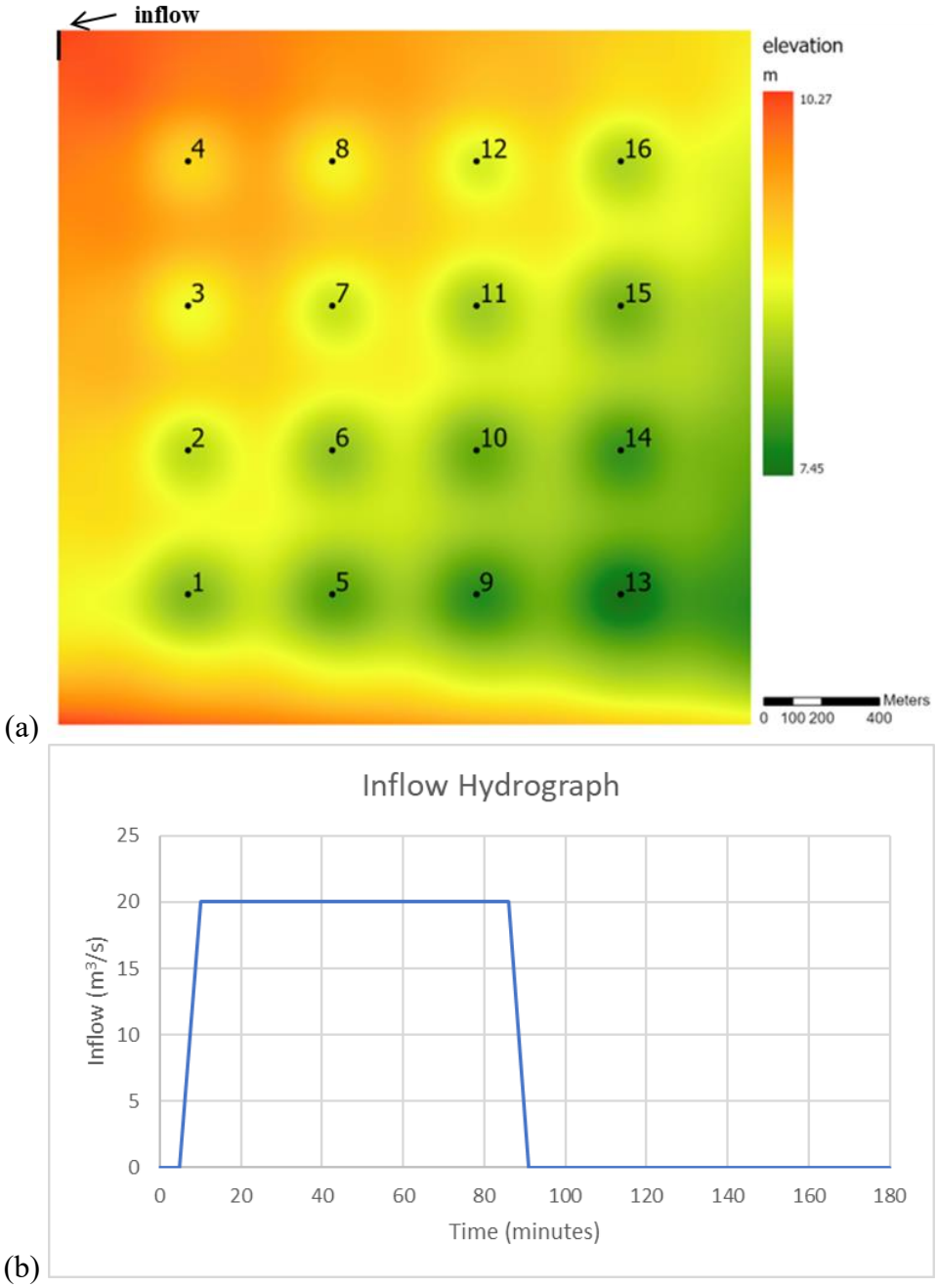

Figure 4-9. (a) The DEM of the Test 2 and (b) the inflow hydrograph of the Test 2.

The simulation results of the CA model were compared with the results of the other models in (Néelz & Pender, 2013). The final inundation predictions shared the same pattern and scale as shown in Figure 4-11. The temporal variation of the water levels at all 16 points predicted by the CA model fell between the upper and lower bound of the other models in Néelz & Pender (2013) with no significant discrepancy. The CA model results at Point 2, 3, 5, 6, 7, 8, 9, 10, 11 and 12 were within the envelope, and the values at Point 9, 13, 14, 15 and 16 were constantly 0 as most models predicted. The peak values of the water levels also occurred at the same timing. However, although the water level at Point 4 was in the envelope, the values were close to the

upper bound. On the contrary, the values of Point 1 were a bit lower than the lower bound. This phenomenon shows that the diffusive-like CA model in the ABM did not propagate the water to the further areas as much as what the other models did whilst ignoring inertial term and only using Manning's equation. The comparisons of water level at each point are shown as Figure 4-12. All the charts in Figure 4-12 on the left hand side are predicted by the models in (Néelz & Pender, 2013) and the charts on the right hand side are predicted by the CA model in the ABM. Since the water levels at the Point 13 – 16 were all dry through the whole simulation, the water levels are not shown here.

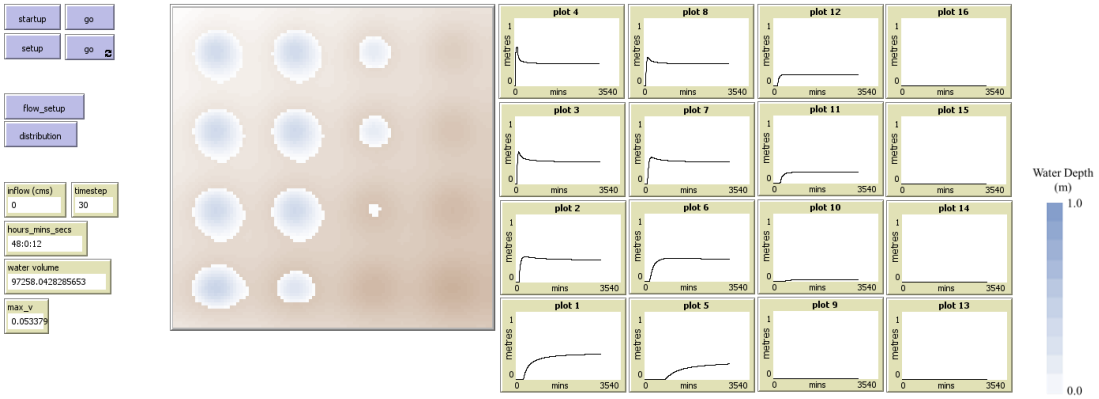

Figure 4-10. The interface of the ABM for the Benchmark Test 2.

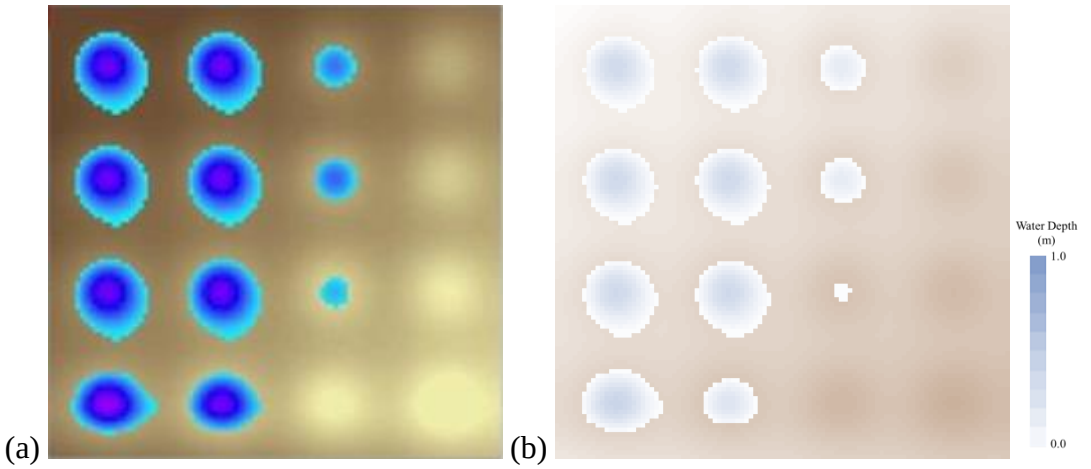

Figure 4-11. (a) The final inundation predicted by most models in (Néelz & Pender, 2013) (source: Néelz & Pender (2013)) and (b) the final inundation predicted by the CA model in the ABM.

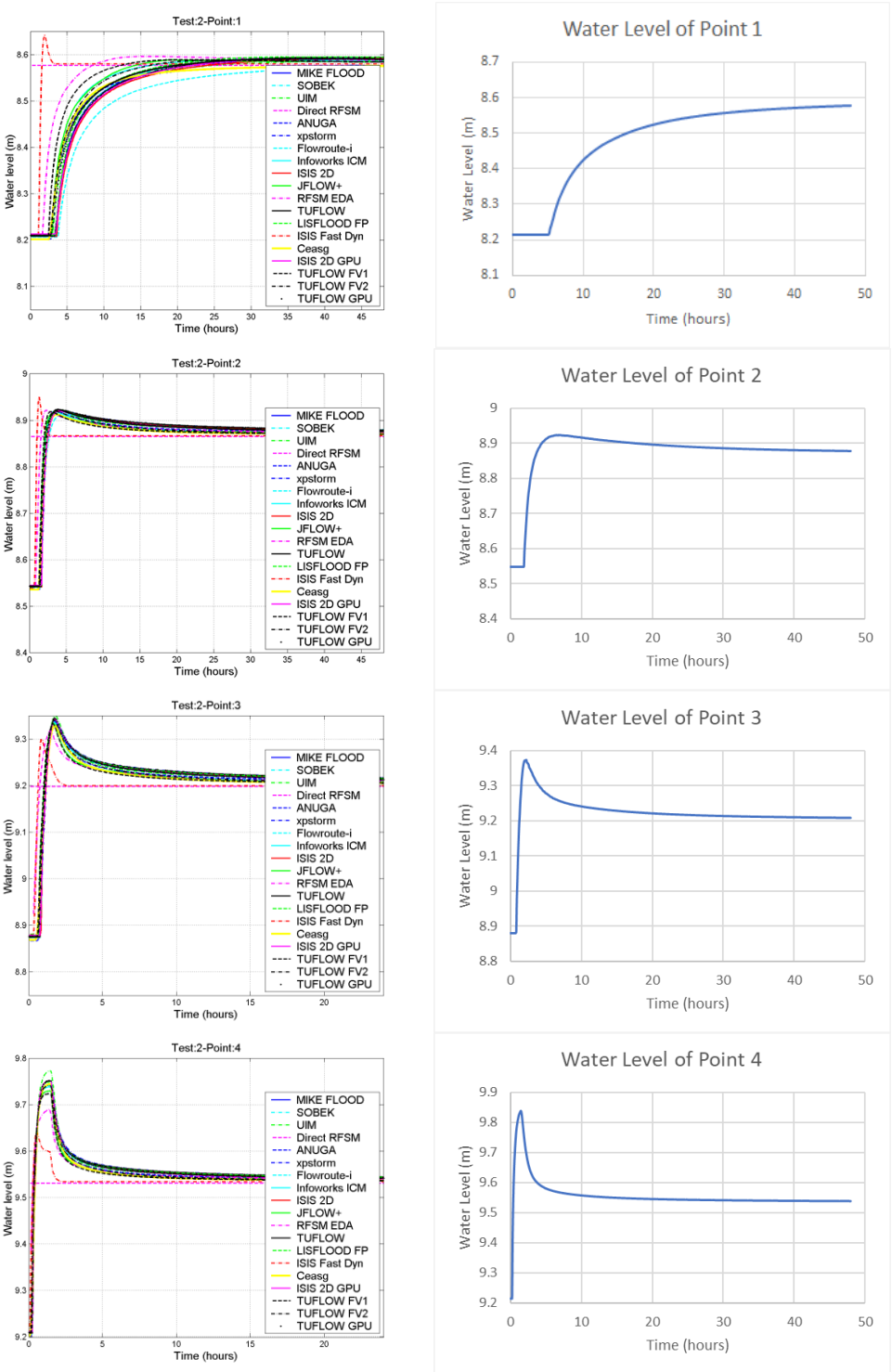

Figure 4-12. The charts on the left hand side: the water levels at the 16 Points predicted by the other models in Néelz & Pender (2013); the charts on the right hand side: the water levels at the 16 Points predicted by the CA model in the ABM.

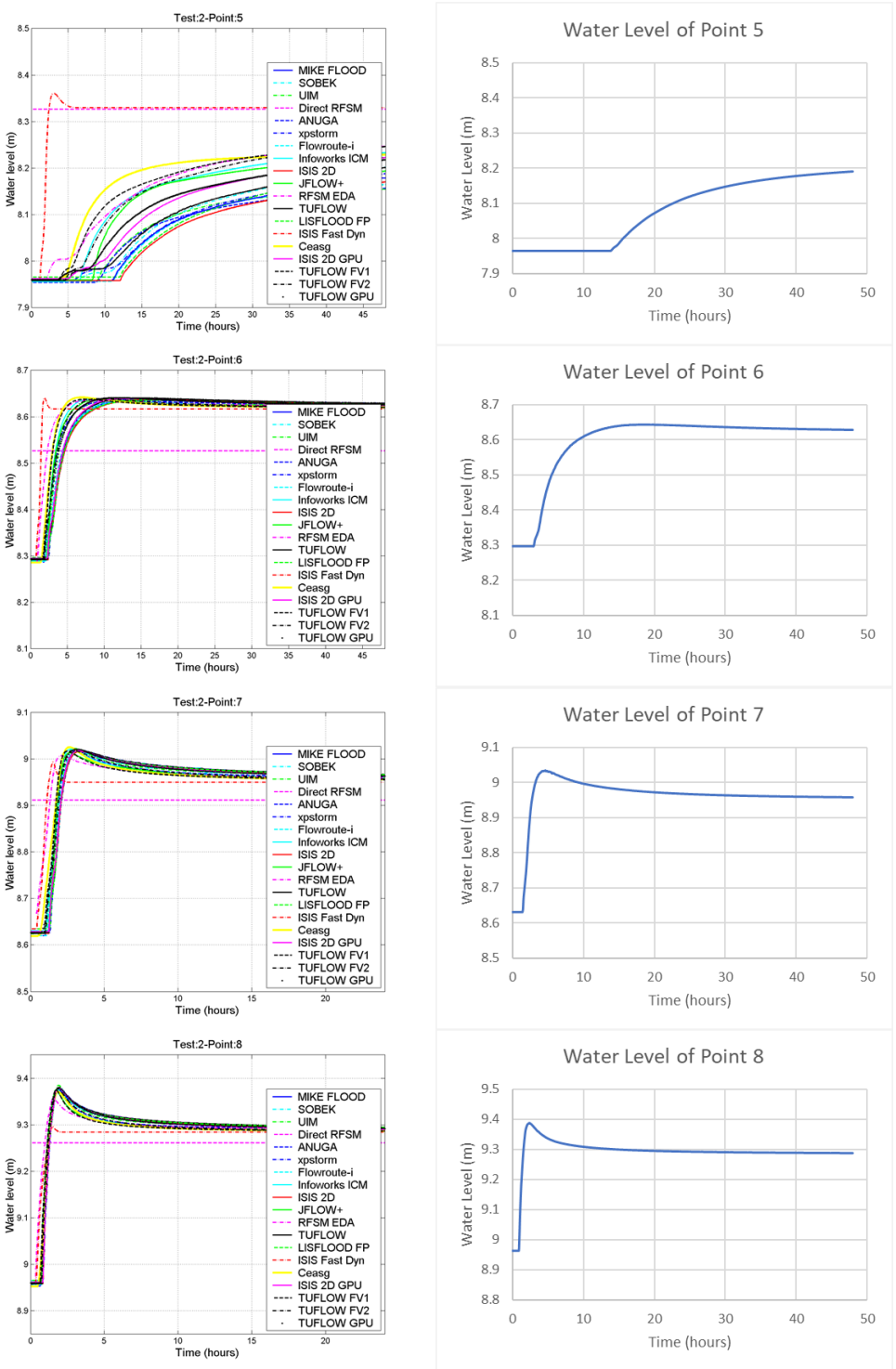

Figure 4-12. (continued) The charts on the left hand side: the water levels at the 16 Points predicted by the other models in Néelz & Pender (2013); the charts on the right hand side: the water levels at the 16 Points predicted by the CA model in the ABM.

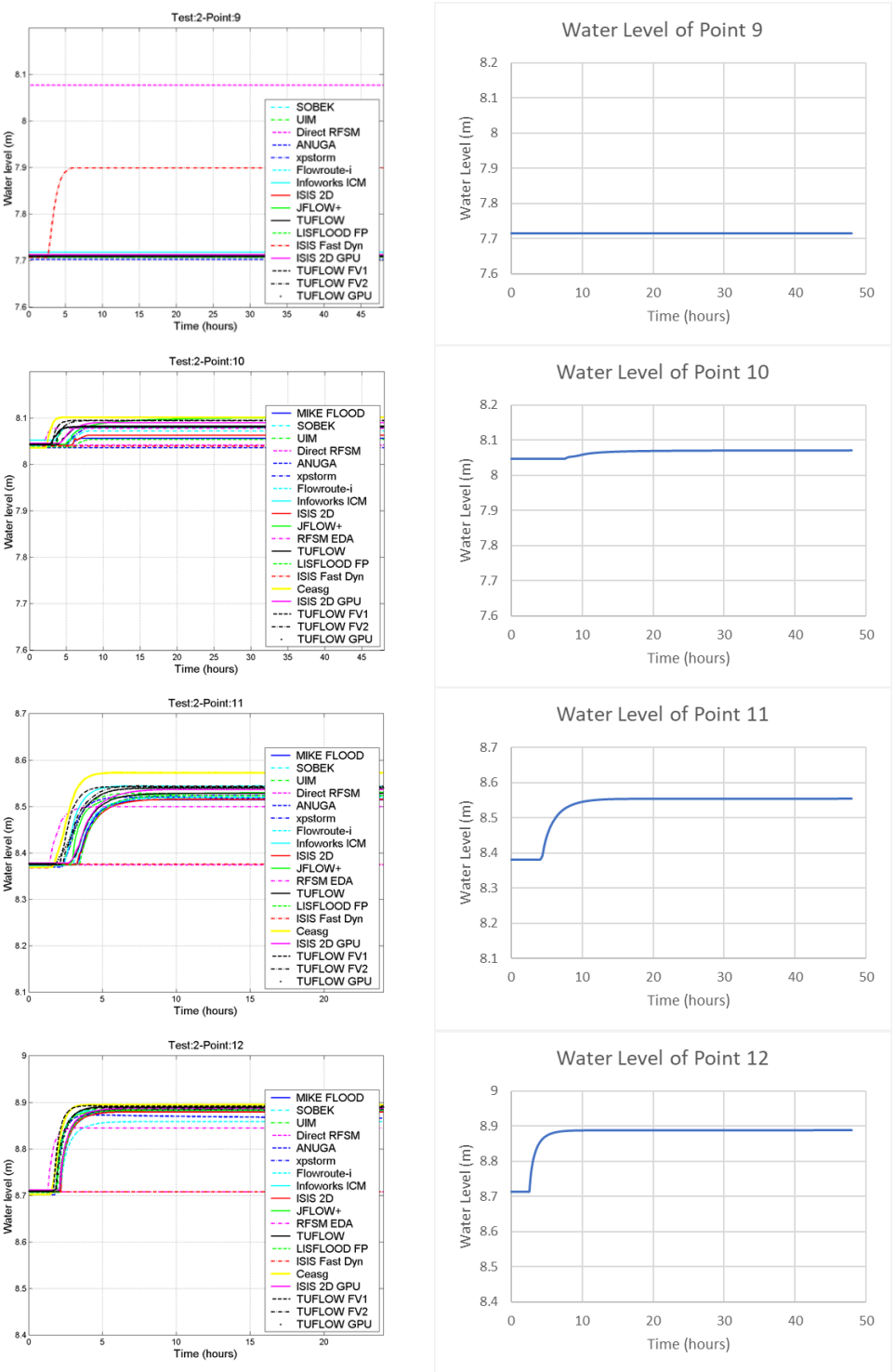

Figure 4-12. (continued) The charts on the left hand side: the water levels at the 16 Points predicted by the other models in Néelz & Pender (2013); the charts on the right hand side: the water levels at the 16 Points predicted by the CA model in the ABM.

Due to the lack of specific benchmark tests or observation data for floodwalls/sandbags or pumps/inlets of sewer systems, this study utilised the Test 2 to check the effects of these structures. For checking the effect of floodwalls/sandbags,

two floodwalls with 400 metres in length and 1 metre in height were placed to protect Depression 4 of the Test 2, shown as the red lines in Figure 4-13 (b). On the other hand, for checking the effect of pumps/inlet, a pump with a flow rate of 1 m^3/s (CMS) was installed to protect Depression 4, shown as the red dot in Figure 4-13 (c). The water depths in the Test 2 simulation at t = 6 h under different scenarios: (a) original, (b) with a pump/inlet (red dot) and (c) with floodwalls/sandbags (red lines) are shown in Figure 4-13. Figure 4-13 (b) shows that water was blocked by the floodwalls and went towards different directions. In contrast, compared with the original one, Figure 4-13 (a), water depth was lowered and flood extent was shrunk by the pump in Figure 4-13 (c). Both important common structural measures for dealing with urban flood can be represented in the CA model in the ABM.

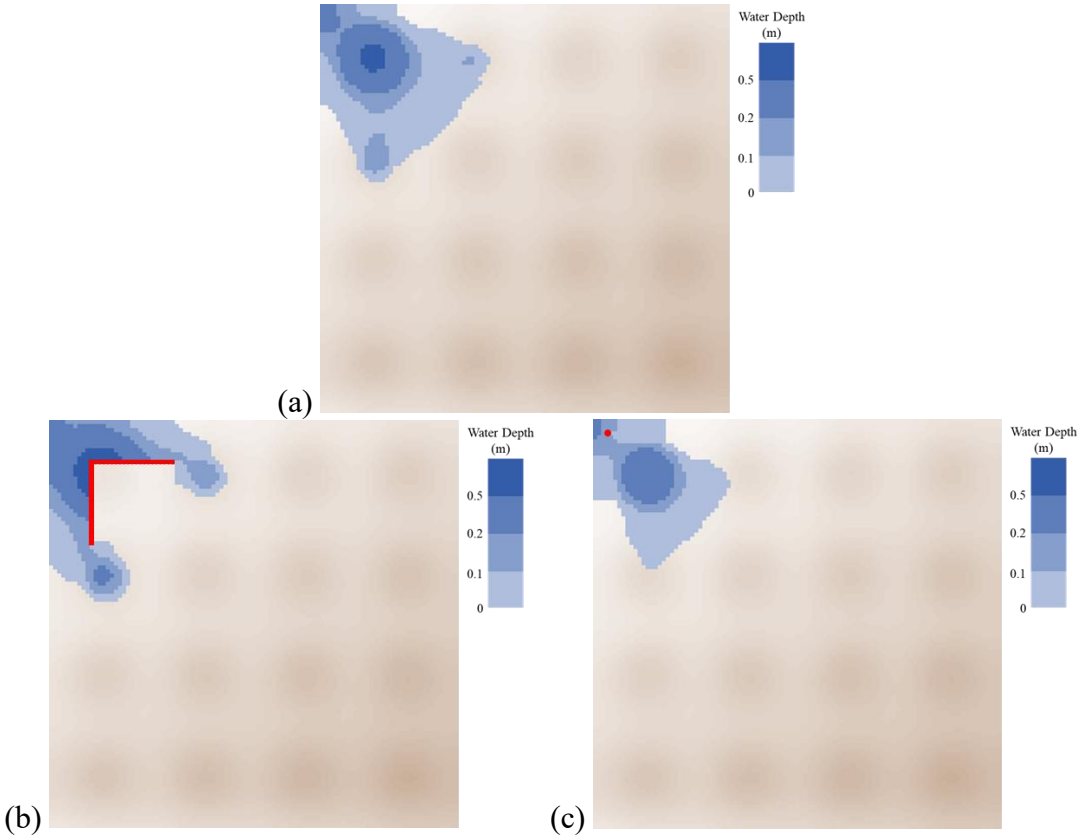

Figure 4-13. Water depth in the Test 2 simulation at t = 6 h under different scenarios: (a) the original simulation, (b) with floodwalls/sandbags (red lines) and (c) with a pump/inlet (red dot).

4.2.1.2 EA Benchmark Test 4

The Test 4 was designed to test the capability of a hydraulic model to simulate the wave propagation and transient velocities and water depth. An inflow with a peak flow of 20 m^3/s was applied along a 20 m long line in the mid-west side of the boundary. The inflow rose from 0 m^3/s at t = 5 min up to 20 m^3/s at t = 60 mins and

kept constant; then the inflow decreased from 20 m^3/s at t = 240 min down to 0 m^3/s at t = 300 min. Linear interpolation was used to interpolate the inflow values, and the inflow information is shown as Figure 4-14 (b). The domain was a 1000 m x 2000 m flat plain with closed boundaries and resolution of 5 m. The domain of the Test 4 is shown in the Figure 4-14 (a). The initial condition was set as dry bed, and Manning's roughness coefficient was set as 0.05 $s/m^{1/3}$ uniformly on the whole computational domain. The simulation was run until t = 5 hours. The α in Equation (3-17) was set as 0.01. The model prediction of water levels and velocities through time at the six points, five of which are on the central line (as shown in Figure 4-14 (a)), and flood extent were compared with the other models in Néelz & Pender (2013).

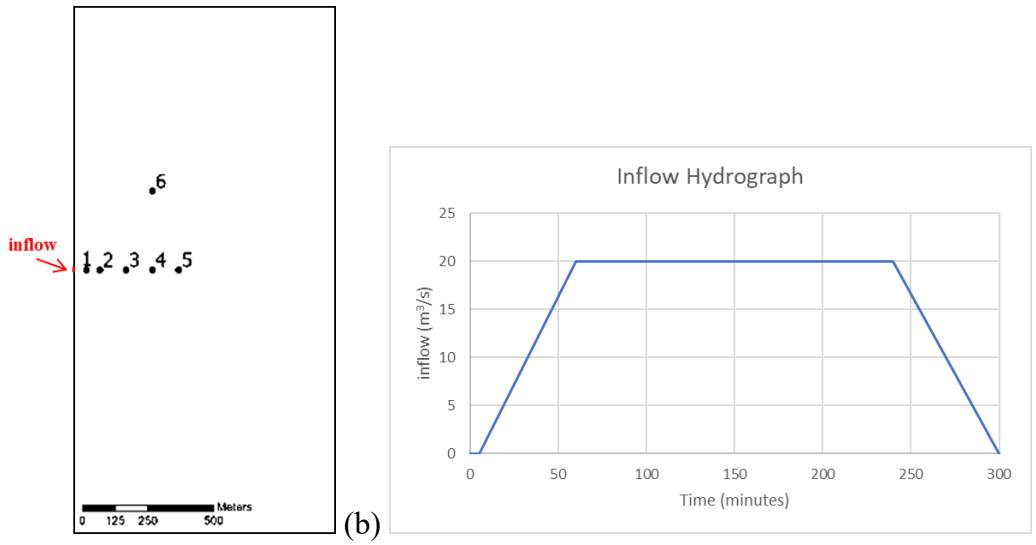

Figure 4-14. (a) The domain of the Test 4 and (b) Inflow Hydrograph of the Test 4.

The simulation results of the CA model were compared with the results of other models in Néelz & Pender (2013). The 0.15 m depth contours at time = 1 hour and at time = 3 hours predicted by the CA model, as shown in Figure 4-16 (b) and (c) (where the black lines are the 0.15 m depth contours), were all in the envelope, as shown in Figure 4-16 (a). The water levels, the velocities, the cross-section of water depths and velocities predicted by the CA model fell between the upper bound and the lower bound of the other models in Néelz & Pender (2013) with no significant discrepancy. The timings of rising and recession stage all occurred at the same time, showing the results of the CA model to be consistent with the other models. The CA model can provide inacceptable results when the time step is not small enough. The diffusive-like CA model needs smaller time step to propagate the wave to the further areas and avoid fluctuation of the values of velocities. Thus, a small value of α was set as 0.01, which was much smaller than that used in the Test 2. The interface of the ABM is shown in the Figure 4-15. The comparison of 0.15 m depth contours at time = 1 hour

and 3 hours is shown as Figure 4-16; the comparisons of water level at each point are shown in Figure 4-17; the comparisons of the velocities at each point are shown as Figure 4-18. The comparisons of cross-section of water levels and velocities along the central line are shown as Figure 4-19. All the charts in Figure 4-17, 4-18 and 4-19 on the left hand side are predicted by the models in Néelz & Pender (2013) and the charts on the right hand side are predicted by the CA model in the ABM.

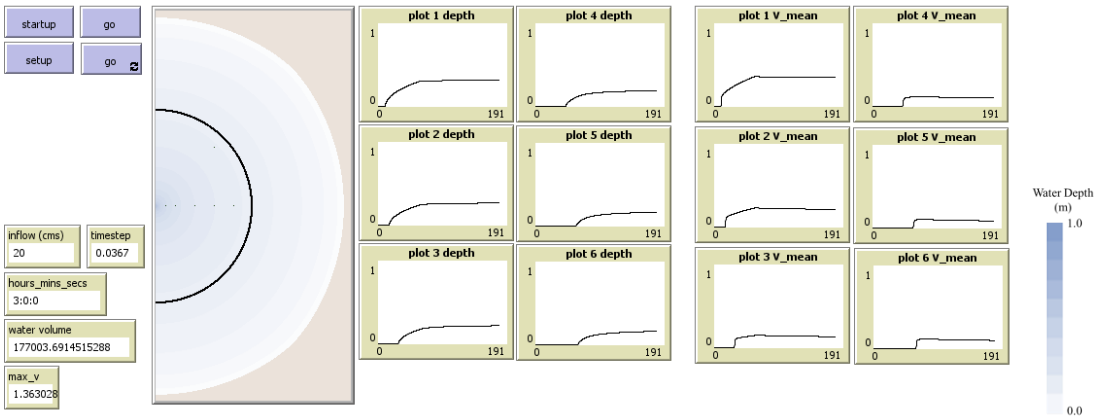

Figure 4-15. The interface of the ABM for the Benchmark Test 4.

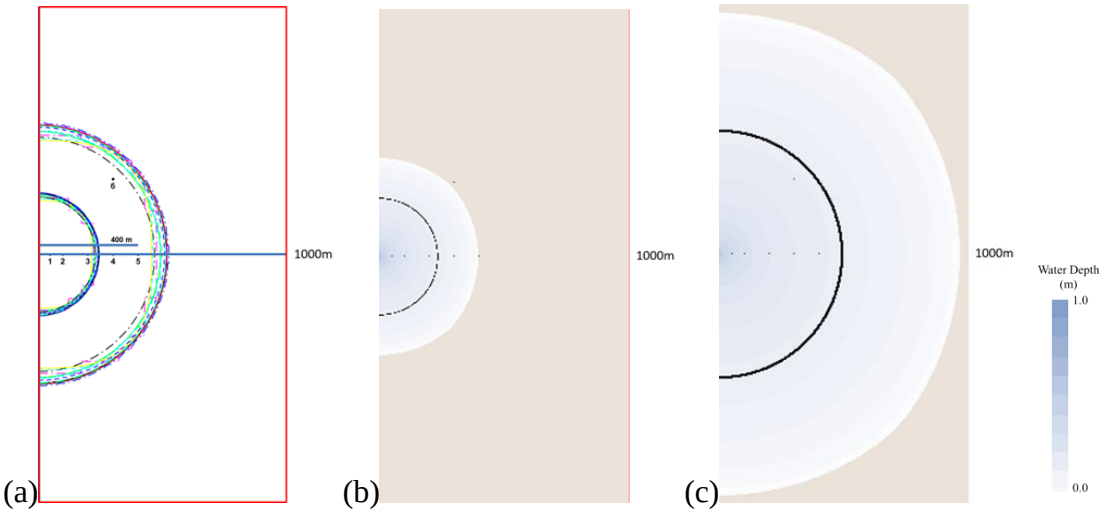

(a) (b) (c)

Figure 4-16. (a) 0.15 m depth contours at time = 1 hour (smaller half circles) and 3 hour (larger half circles) predicted by the other models in the benchmark (Néelz & Pender, 2013) (source: Néelz & Pender (2013)), (b) 0.15 m depth contour at time = 1 hour predicted by the CA model in the ABM, and (c) 0.15 m depth contour at time = 3 hour predicted by the CA model in the ABM.

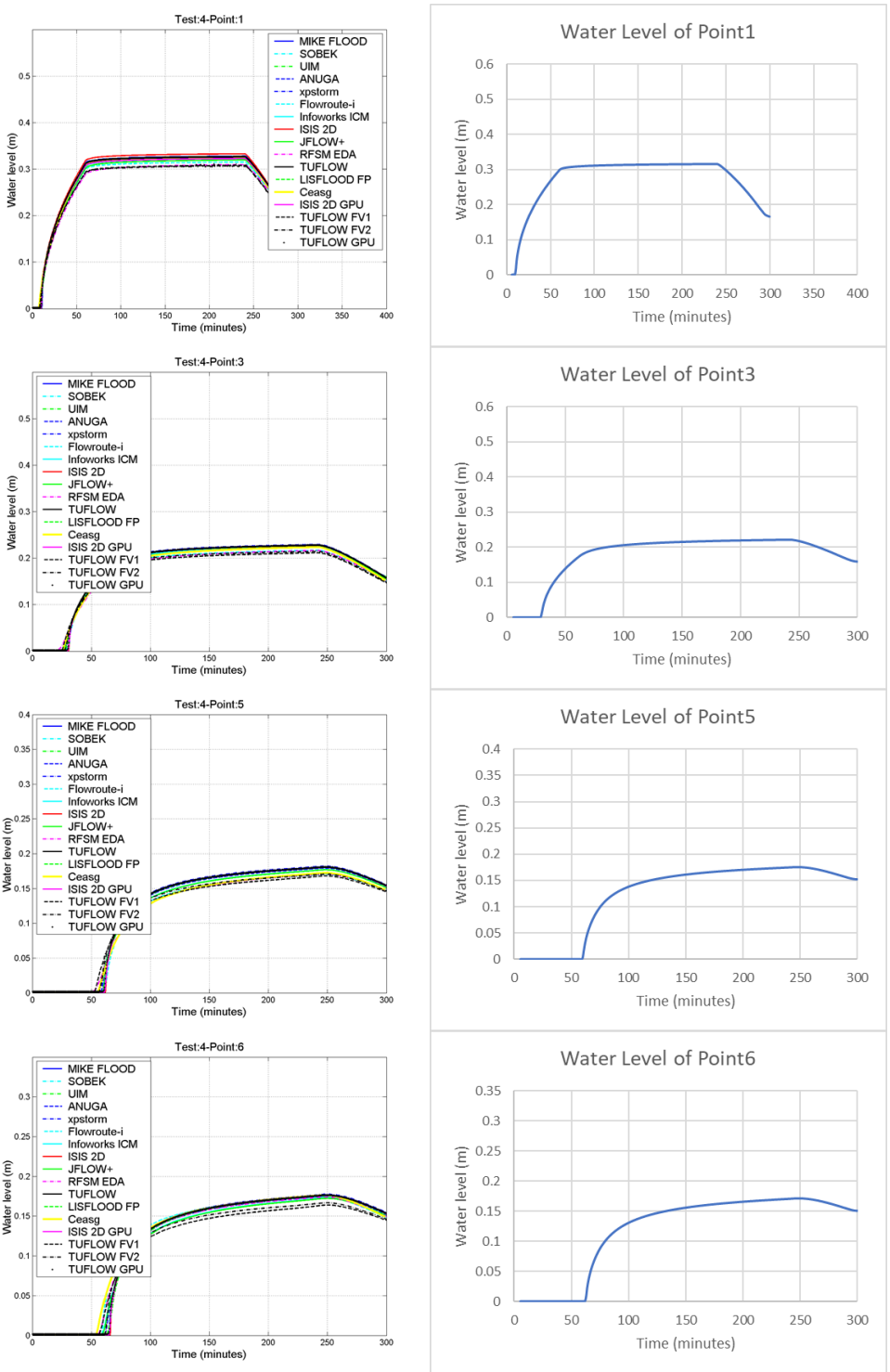

Figure 4-17. The charts on the left hand side: the water levels at the points predicted by the other models in Néelz & Pender (2013) (source: Néelz & Pender (2013)); the charts on the right hand side: the water levels at the points predicted by the CA model in the ABM.

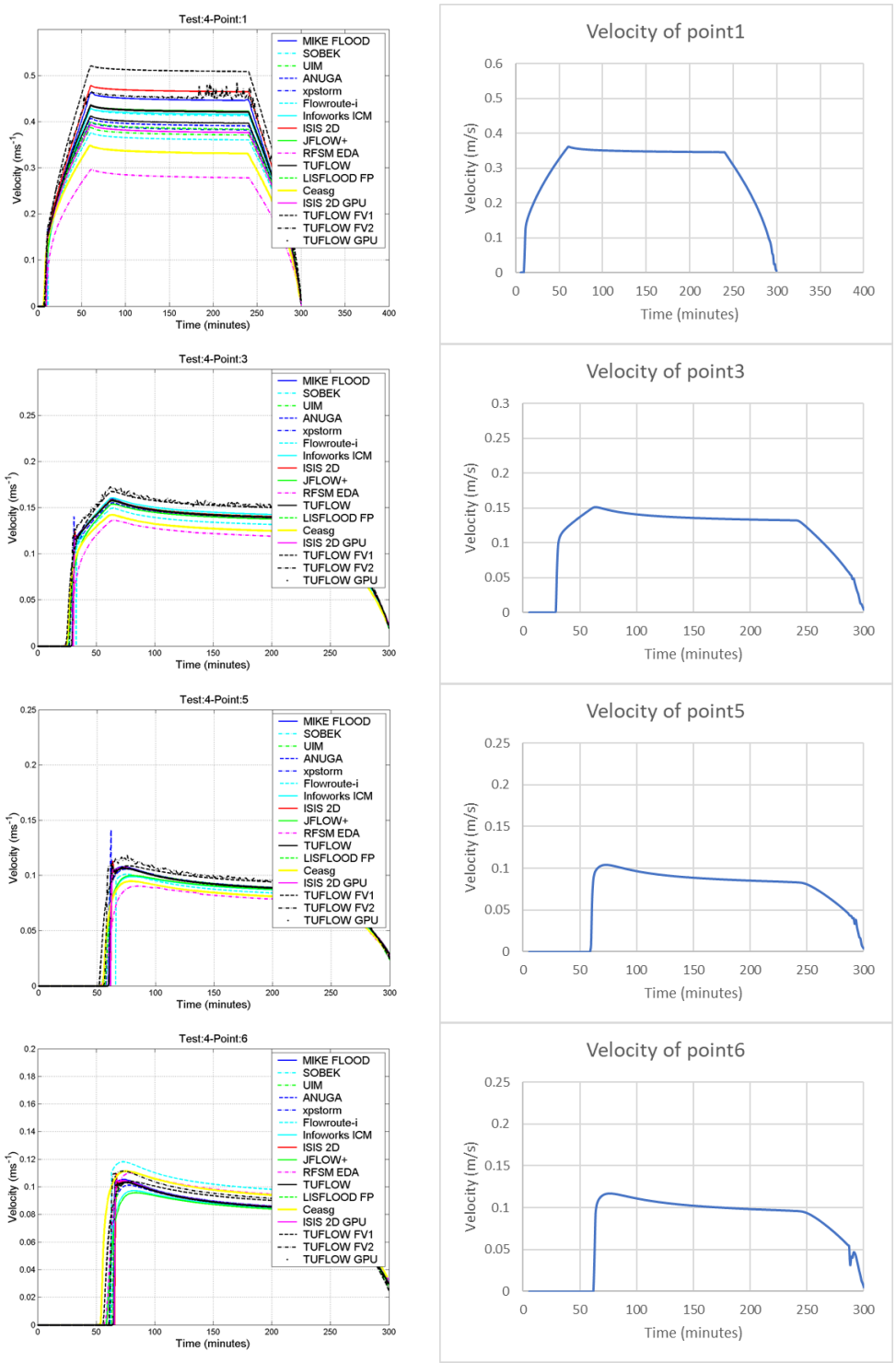

Figure 4-18. The charts on the left hand side: the velocities at the points predicted by the other models in Néelz & Pender (2013) (source: Néelz & Pender (2013)); the charts on the right hand side: the velocities at the points predicted by the CA model in the ABM.

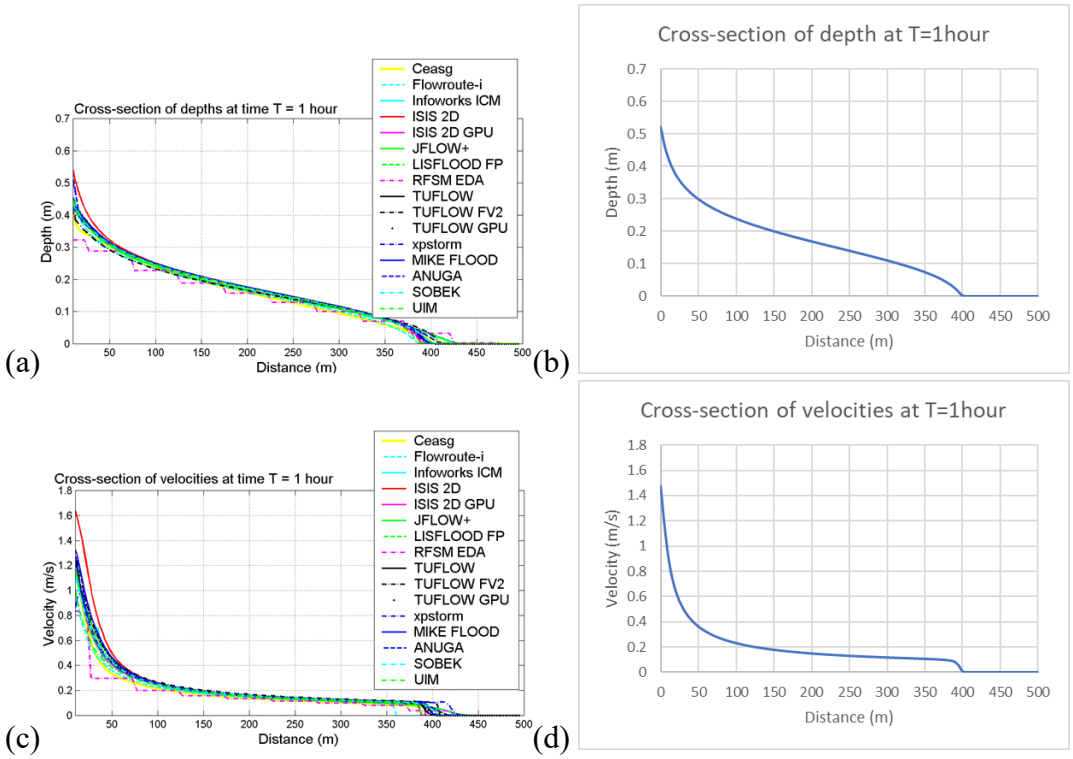

Figure 4-19. (a) The cross-section of depth at time T = 1 hour predicted by the other models in Néelz & Pender (2013), (b) the cross-section of depth at time T = 1 hour predicted by the CA model in the ABM, (c) the cross-section of velocities at time T = 1 hour predicted by the other models in Néelz & Pender (2013), and (d) the cross-section of velocities at time T = 1 hour predicted by the CA model in the ABM.

4.2.1.3 EA Benchmark Test 8A

The Test 8A was designed to evaluate the capability of a hydraulic model to simulate urban flood with relatively complex topography. An extreme rainfall with peak intensity of 400 mm/hour was distributed uniformly on the whole computational domain and a point inflow with a peak flow of 5 m^3/s was applied at the northeast area shown as an X marker in the Figure 4-20 (a). The rainfall intensity sharply rose up to 400 mm/hour from 0 mm/hour at t = 1 min and kept constant; then the rainfall intensity drastically dropped to 0 mm/hour at t = 4 mins. On the other hand, the inflow started entering at t = 20 mins and rose up to 5 m^3/s at t = 37 mins; then the inflow decreased at t = 39 mins down to 0 mm/hour at t = 55 mins. Linear interpolation was used to interpolate the inflow values and rainfall intensity values, and the inflow hydrograph and the hyetograph are shown as Figure 4-20 (b) and 4-20 (c). The domain was a 0.4 km x 0.96 km urban area with closed boundaries and high resolution of 2 m. The DEM of the Test 8A is shown in the Figure 4-20 (a). The initial condition was set as dry bed, and two Manning's coefficient values were used according to the land use: 0.02 $s/m^{1/3}$ for roads and pavements and 0.05 $s/m^{1/3}$ for the else. The α in Equation (3-17) was set as 0.02. The simulation was run until t = 5

hours. The model prediction of water levels and velocities through time and flood extent were compared with the other models in Néelz & Pender (2013).

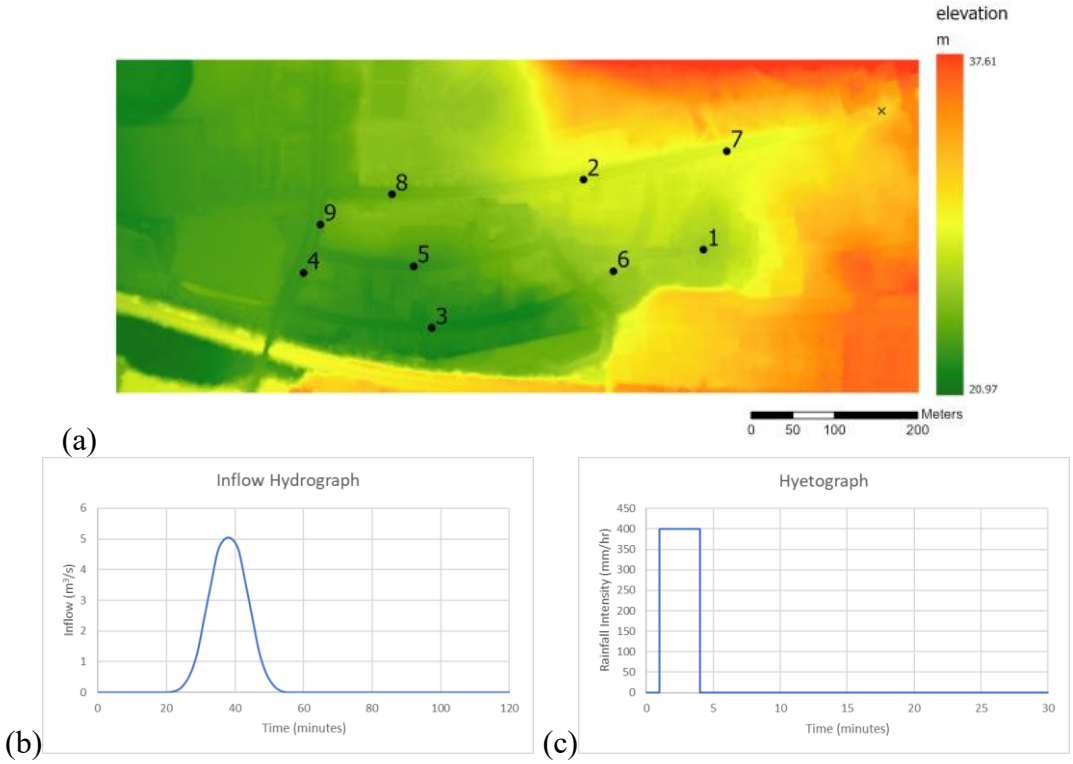

Figure 4-20. (a) The DEM of the Test 8A, (b) inflow Hydrograph of the Test 8A, and (c) hyetograph of the Test 8A.

The simulation results of the CA model were compared with the results of other models in Néelz & Pender (2013). The water levels and the velocities predicted by the CA model fell between the upper bound and the lower bound of the other models in Néelz & Pender (2013) with no significant discrepancy. The timings of rising and recession all occurred at the same time, showing the results of the CA model consistent with the other models. The temporal variations of water level and velocity have 2 rising stages or 2 peaks, due to different timings of the peak inflow and peak rainfall. Despite the consistency of the water levels and the velocities, the flood extent generated by the CA model is a bit smaller than the others, especially those at the intersection in the central area in Figure 4-22, since the wave was not spread well in the CA model neglecting the momentum equation. The diffusive-like CA model needs smaller time step to propagate the wave to the further areas and avoid fluctuation of the values of velocities. The α was set as 0.02, which was much smaller than that used in the Test 2. The interface of the ABM is shown as Figure 4-21. The comparison of the 20 cm contours of peak water depth is shown as Figure 4-22; the comparisons of water level and velocities at each point are shown as Figure 4-23 and 4-24. All the

charts in Figure 4-23 and 4-24 on the left hand side are predicted by the models in Néelz & Pender (2013) and the charts on the right hand side are predicted by the CA model in the ABM.

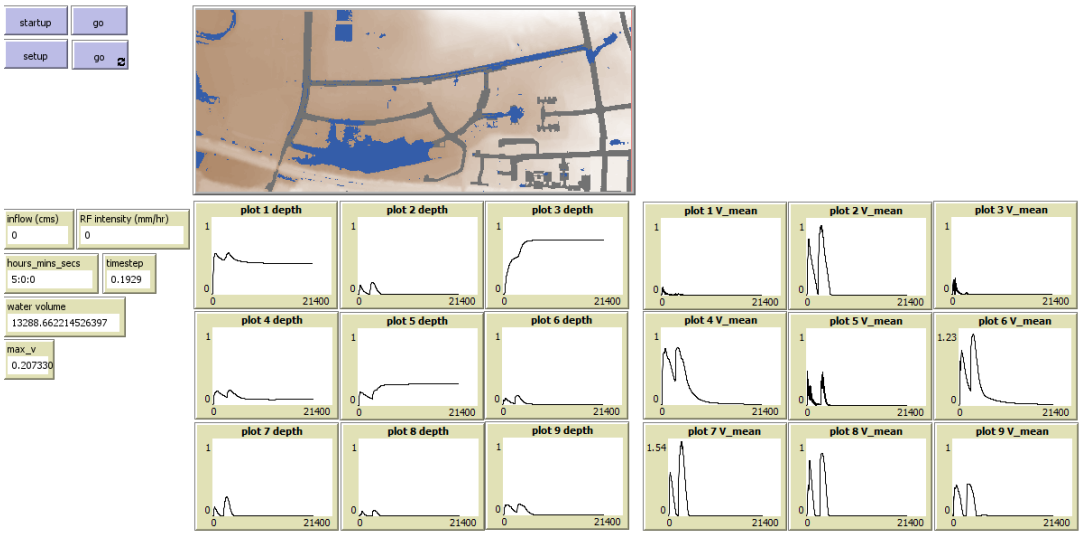

Figure 4-21. The interface of the ABM for the Benchmark Test 8A.

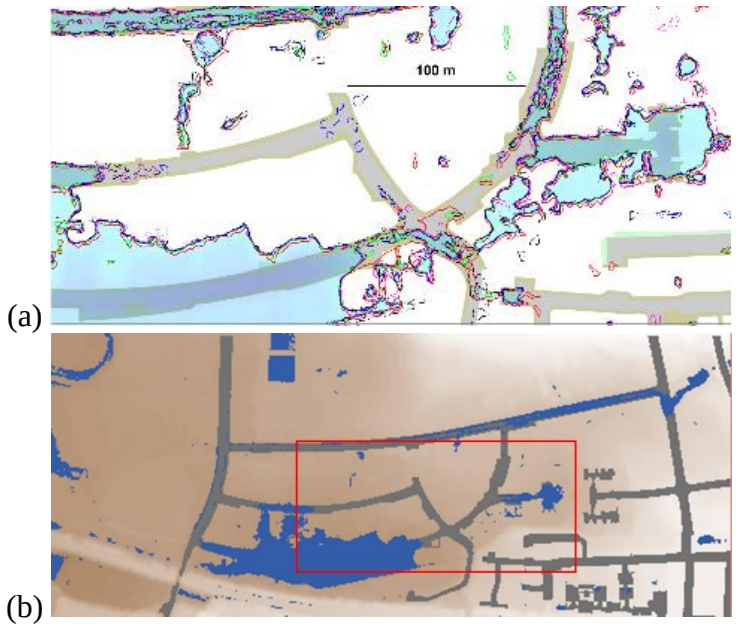

(a)

(b)

Figure 4-22. (a) The 20 cm contours of peak water depth predicted by the other models in the benchmark (Néelz & Pender, 2013) (source: Néelz & Pender (2013)), and (b) the 20 cm contours of peak water depth predicted by the CA model in the ABM; the red rectangle area is the corresponding area.

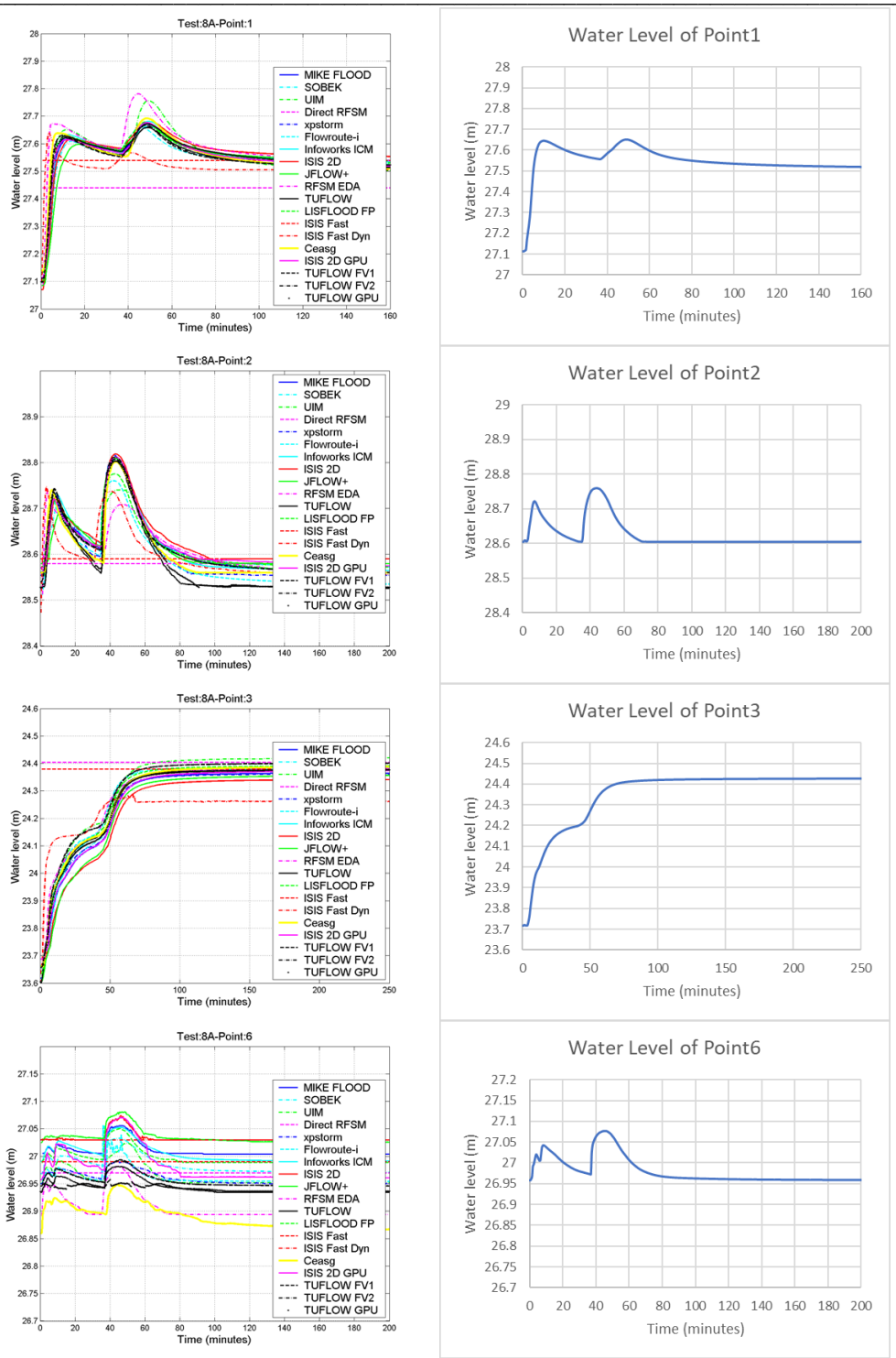

Figure 4-23. The charts on the left hand side: the water levels at the points predicted by the other models in Néelz & Pender (2013); the charts on the right hand side: the water levels at the points predicted by the CA model in the ABM.

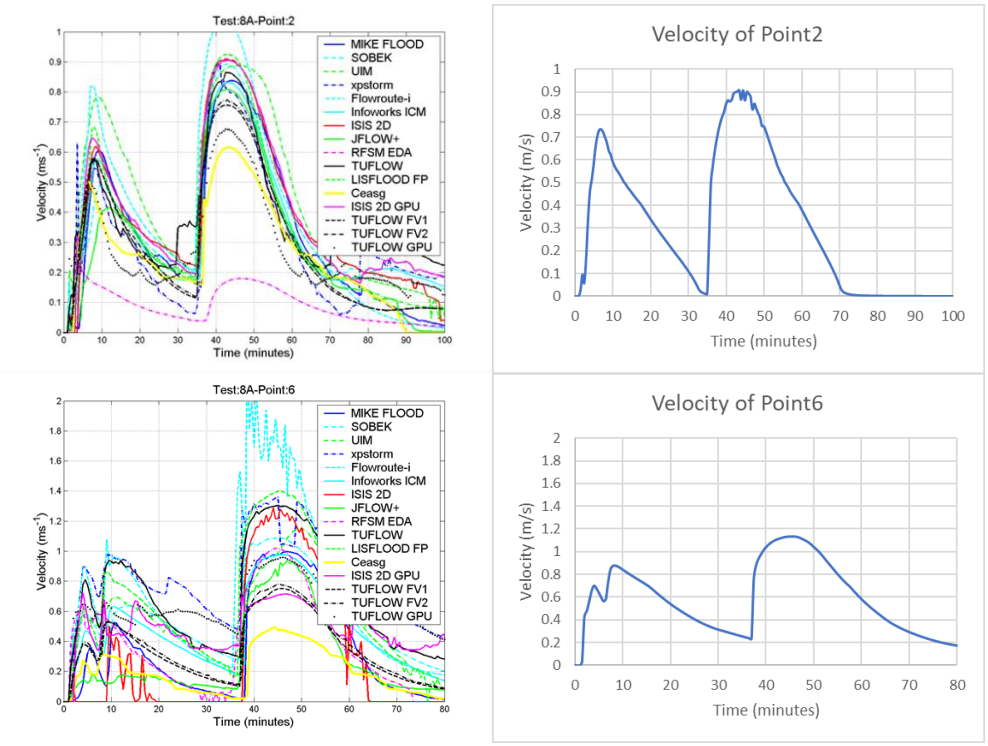

Figure 4-24. The charts on the left hand side: the velocities of the points predicted by the other models in Néelz & Pender (2013); the charts on the right hand side: the velocities at the points predicted by the CA model in the ABM.

4.2.2 Case Study

This study utilised the CA model in the ABM to simulate two historical flood events, one in Magnan area, Nice, France and one in Dahu area, Taipei, Taiwan. Three indices were used to evaluate the model performance: the true positive rate (TPR), the false discovery rate (FDR) and threat score (TS) (Bennet et al., 2013):

$$\text{TPR}\ (\%) = \frac{\text{TP}}{\text{TP} + \text{FN}} \times 100 \tag{4-1}$$

$$\text{FDR}\ (\%) = \frac{\text{FP}}{\text{TP} + \text{FP}} \times 100 \tag{4-2}$$

$$\text{TS}\ (\%) = \frac{\text{TP}}{\text{TP} + \text{FP} + \text{FN}} \times 100 \tag{4-3}$$

where TP is the number of true positives, FN is the number of false negatives, FP is the number of false positives.

4.2.2.1 Magnan, Nice, France

A historical flood event in Magnan area in the south part of Nice, France, was selected

for case study. A heavy rainfall hit Nice on the 4 January in 2014, causing scattered flood in Magnan area. The rainfall event lasted about 25 hours with two peaks. The hyetograph is shown in Figure 4-25 (a). The study area was a simple residential area with a size of 0.21 km^2, and the 2-metre-resolution DEM of the study area used is shown in Figure 4-25 (b). The building areas, grey areas in Figure 4-25 (b), in the hydraulic models were excluded from the computational domain and thus the total precipitation was increased proportionally. Only one Manning's coefficient was used for roads: 0.016 $s/m^{1/3}$. Due to the lack of measured data, the inundation simulation was conducted by both the CA model in the ABM and the MIKE 21 model (Danish Hydraulic Institute, 2016) in this study. The model outputs of the CA model were compared with those of the MIKE 21 model, since the MIKE 21 model is a widely used physics-based model solving full shallow water equations.

The flood maps predicted by the MIKE model and the CA model in the ABM are shown as Figure 4-26. The values of the indices (TPR: 99.34%, FDR: 17.61% and TS: 81.95%) also show the great agreement in the inundation extents between the predictions from the two models. Only subtle differences in the water level can be observed as shown in Figure 4-27 (a), mostly smaller than ± 0.05 m. The big differences in the water levels occurred in some narrow lanes and around building areas, since the wave propagation was not well represented in the CA model neglecting the momentum equation. The waves did not spread well in the CA model when hitting the building areas and entering the narrow lanes, whereas the physics-based model, the MIKE model, could properly transmit the water. In terms of the flood extents, where the maximum water depth was greater than 0.3 metres, two models generated almost the same result showing high agreement. The comparison between the flood maps generated by the MIKE model and the CA model is shown in Figure 4-27 (b). The blue areas in Figure 4-27 (b) are the flood extent predicted by only MIKE model and the red areas, by only the CA model and the green areas, by both models.

(a)

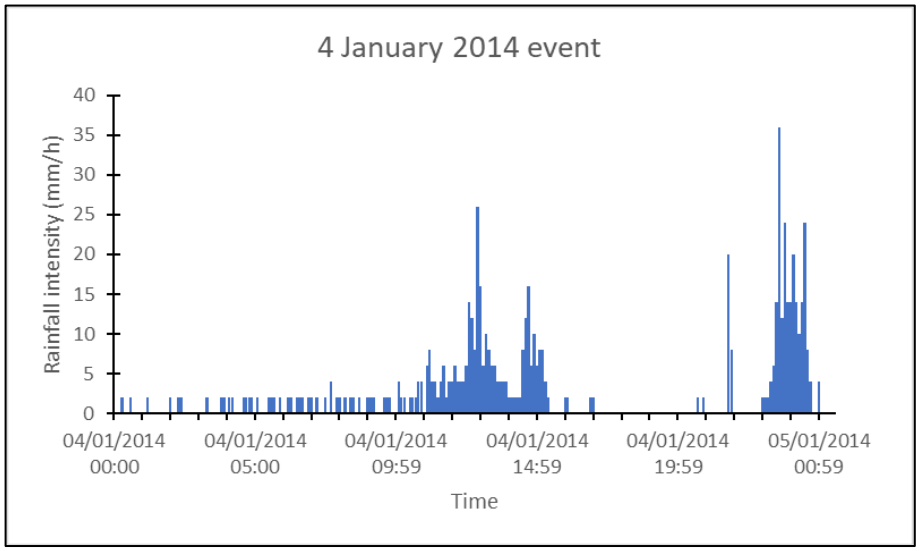

(b)

Figure 4-25. (a) The hyetograph of the 4 January 2014 event, and (b) the DEM of the study area in Magnan area, Nice, France.

(a)

(b)

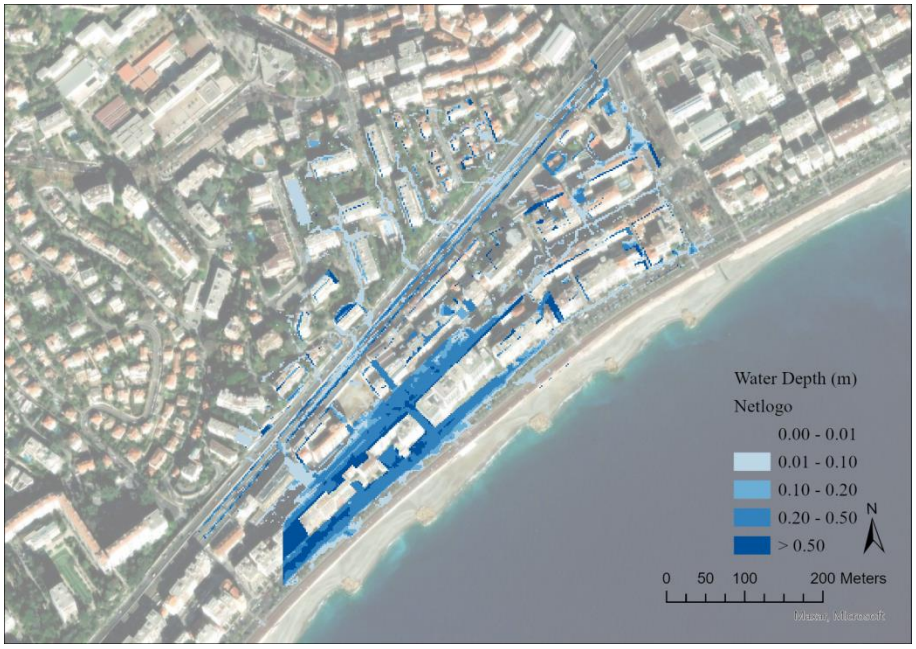

Figure 4-26. (a) The flood map predicted by the MIKE model, and (b) the flood map predicted by the CA model in the ABM.

(a)

(b)

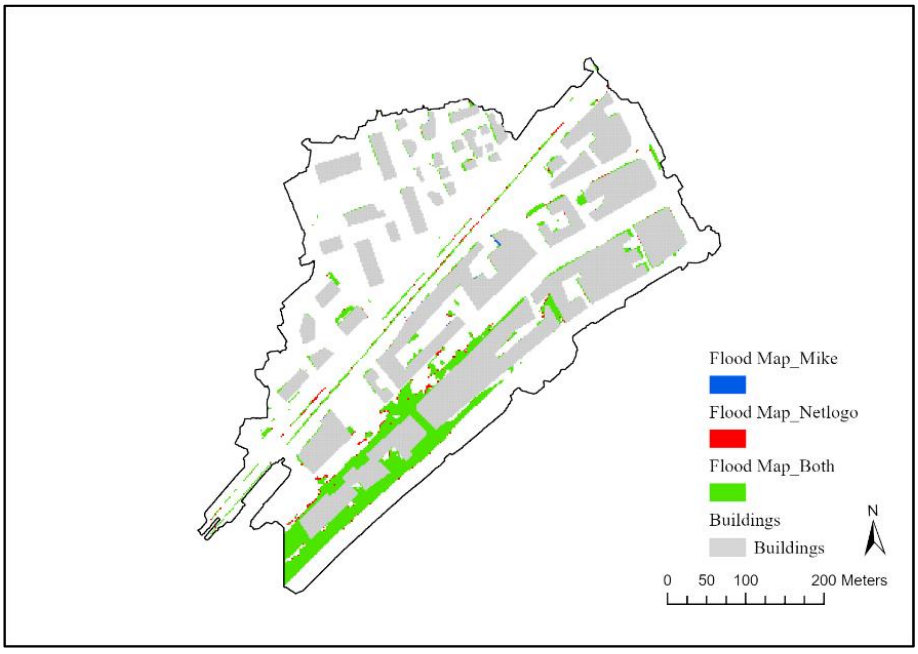

Figure 4-27. (a) The difference of the water depth between the maximum water depths predicted by the MIKE model and the CA model in the ABM (ABM - MIKE), and (b) the comparison between the flood maps generated by the MIKE model and the CA model.

4.2.2.2 Dahu, Taipei, Taiwan

A historical flood event in Dahu area in the north part of Taipei, Taiwan, was selected for case study. A heavy rainfall hit Taipei on 2 June in 2017, causing flood in Dahu area. The duration of the rainfall event was about only 3 hours with peaks of rainfall intensity of more than 100 mm/hour. The hyetograph is shown in Figure 4-28 (a). The Dahu basin covers an area of 4.49 km^2 and can be divided into two parts: mountainous areas in the upstream and flat urban areas of 0.55 km^2 in the downstream. The water from the upstream pours into Dagou Creek and enters a retention pond in Dagouxi Waterfront Park at the north part of the Dahu urban area, as shown as a blue arrow in Figure 4-28 (b). The water in the retention pond and rainfall will go into underground sewer systems in the urban areas and enter to another retention pond in the Dahu Park and then into Keelung River. According to Hydraulic Engineering Office, Public Works Departments, Taipei City Government (n.d.), the maximum capacity of the retention pond in Dagouxi Waterfront Park is 131,500 m^3, the maximum input and the maximum output discharge are 80.2 m^3/s and 44.4 m^3/s respectively. The study area is a simple residential area, and the size of the area is appropriate for checking the disaster management in detail on a community scale. The 5-metre-resolution DEM of the urban area is shown in Figure 4-28 (b), where the building areas (grey areas) were removed from the domain in the hydraulic model and therefore the total amount of rainfall was increased proportionally. Two Manning's coefficient values were used according to the land use: 0.03 $s/m^{1/3}$ for roads and pavements and 0.15 $s/m^{1/3}$ for woods.

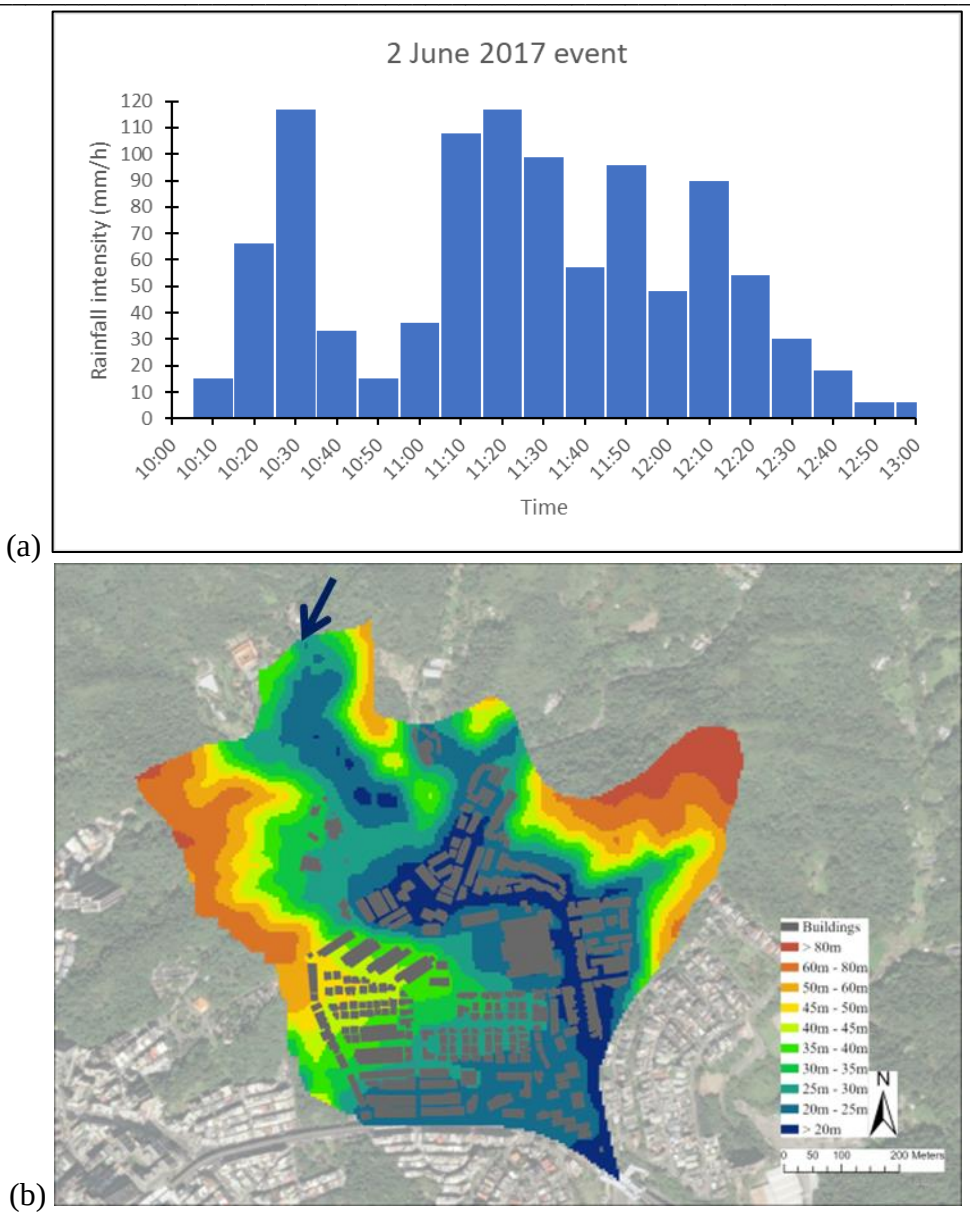

Figure 4-28. (a) The hyetograph of the 2 June 2017 event, and (b) the DEM of the study area in Dahu area, Taipei, Taiwan.

The inundation simulation was conducted by HEC-HMS model (Feldman, 2000) and the CA model in the ABM, and the model outputs were compared with the observations (Taipei City Fire Department, 2017). This study first utilised HEC-HMS model for the upstream part of Dahu areas for calculating the inflow from the upstream, and then the model outputs were used as inputs into the CA model in the ABM. The upstream areas were divided into 6 sub-catchments, as shown in Figure 4-29 (a), where the green shaded area is the urban area used in the ABM. The hydrographs from HEC-HMS were introduced as four point sources into the ABM, as shown in Figure 4-29 (b), where the four blue arrows indicate the location of the inflows from the upstream predicted by HEC-HMS model; the grey areas are the

roads; the red lines are the fences, which act as floodwalls; the red house sign is the shelter inside an elementary school.

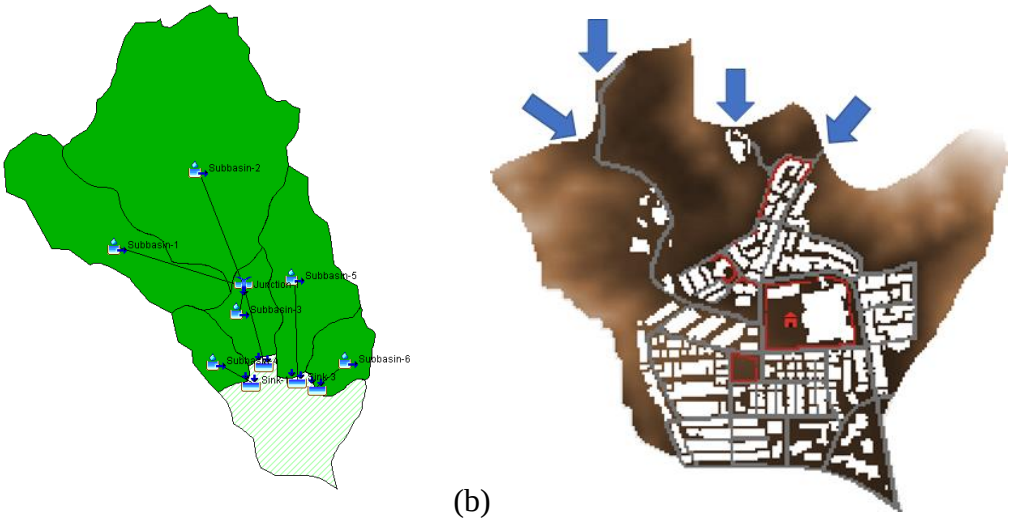

(a) (b)

Figure 4-29. (a) The sub-catchments used in HMS model, and (b) the sub-catchment used in the ABM.

The flood map predicted by the CA model in the ABM is shown as Figure 4-30; where the red areas are the flooded areas delineated by the local authorities. (Taipei City Fire Department, 2017) The flooded areas (water depth ≥ 0.30 m) and the water depths were estimated based on the images from the closed-circuit televisions (CCTVs) at the intersections and based on the addresses and the communities from the disaster reports of the residents. Therefore, addresses and communities were regarded as a single unit when comparing the model results. Furthermore, since the local authorities ignored the flood in retention ponds, parks, hill areas and so on, only the floods on roads and around buildings were compared. The values of the indices defined by Equation 4-1, 4-2 and 4-3 (TPR: 71.62%, FDR: 11.79% and TS: 65.37%) show the satisfactory agreement between the model outputs and the observation in terms of the flooded areas. The biggest difference occurred at the northeast areas, where the CA model did not successfully predict to be inundated as the observation. According to the report (Taipei City Fire Department, 2017), the inundation happened at the areas due to failure of the grate inlets which were covered substantially by fallen leaves and hence the inlets lost the ability to collect water, as shown in Figure 4-31. The three photos on the left hand side were taken from the CCTV showing the inundation through time, and the red dashed circle on the photo indicating the location of blocked inlets. The CA model could not represent this random phenomenon.

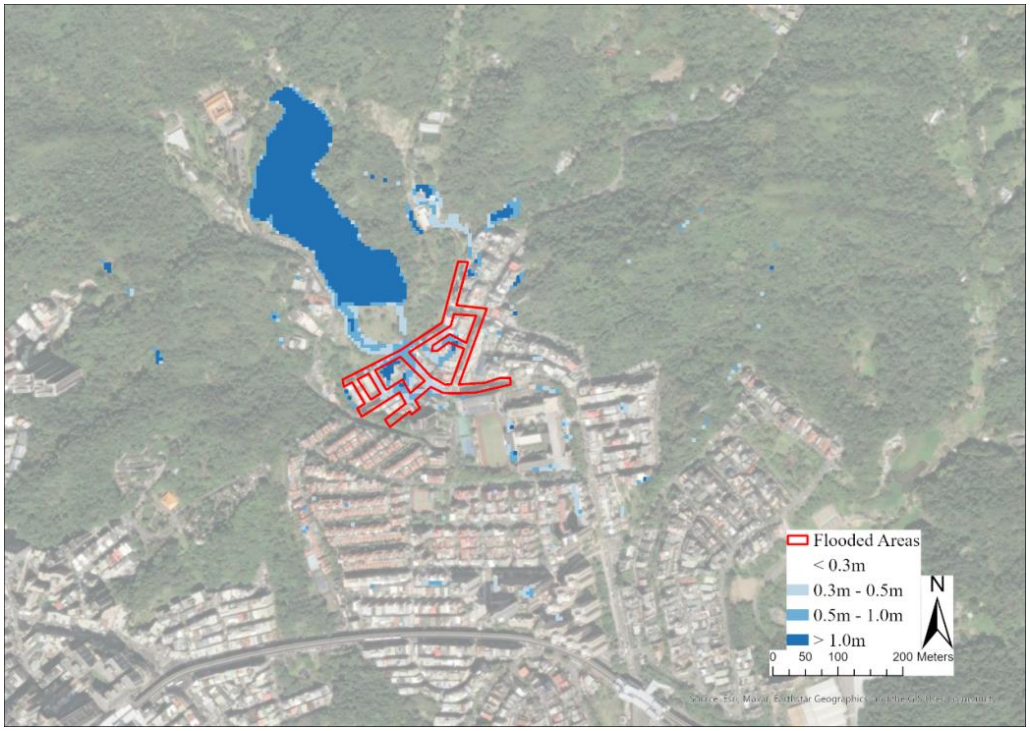

Figure 4-30. The flood map predicted by the CA model in the ABM; the red areas are the flooded areas delineated by the local authorities.

Figure 4-31. The flooded areas (the sky blue areas) and the blocked inlets (the red dashed circle). (source: Taipei City Fire Department (2017a)) The peak accumulated rainfall in an hour recorded by a rain gauge at the upper right corner of the figure was 87.5 mm. According to the videos from the CCTV, the flood started at 11:08 on June 2, with the maximum water depth reaching about 30 centimetres at 12:00, and the flood receded at 12:30.

On the contrary, the maximum observed water depths on the roads were around 30 - 50 cm which were successfully predicted by the CA model. On the other hand, there were discrepancies in the timing of different flood stages. The flood appeared at around 11:00 and reached the peak depths and the maximum flooded extents at round 12:00, and then the inundated areas began to shrink from 12:30. The CA model successfully predicted the onset of the flood at 11:00 but with a lag of about 30 minutes to the largest flooded extent and a 30-minute lag to the recession stage.

4.2.3 Summary

The CA 2D overland flow model in the ABM was developed for inundation simulations, adopting the concept of cellular automata (CA), which redistributed water based on simple rules instead of solving complex physics equations. The CA hydraulic model have been used, verified and validated (Guidolin et al., 2016), but, however, the model has not been built in NetLogo before. Therefore, the model performance of CA 2D inundation simulation of this study was evaluated by comparing the model outputs with UK Environment Agency benchmark cases (Néelz & Pender, 2013) and historical events. Three UK EA benchmark tests (Test 2, Test 4, and Test 8A) and two historical events in Magnan area in Nice (France) and in Dahu area in Taipei (Taiwan) were chosen as case study. The results showed that the model can generate promising model outputs, by comparing the model outputs with the other models' from the benchmark tests and with the observation.

For the UK EA benchmark tests, the inundation predictions of the CA 2D model shared the same pattern with the others', and no meaningful discrepancy in the simulated water levels and velocities occurred.

For the historical event in Magnan area in Nice (France), the flood maps and the water depths predicted by the CA 2D model were almost identical to those predicted by the MIKE model, with only subtle difference. On the contrary, for the historical event in Dahu area in Taipei (Taiwan), the results only showed satisfactory agreement between the model outputs and the observation, since the model did not capture the accidental malfunction of part of the sewer systems. What should be emphasise is that since sewer systems are simplified and not well represented in the CA 2D model, no surcharge flow from inlets will occur, albeit this phenomenon did not happened in the historical events of this study. When applying the CA 2D model in other cases, this shortcoming should be checked.

4.3 Inundation-Agent Coupled Model

To evaluate the capability of the inundation-agent coupled model and the performance of the evacuation process, this study used the coupled model to run coupled simulations for the historical event in Dahu area.

4.3.1 Case Study

This study utilised the inundation-agent coupled model to conduct two coupled simulations under two scenarios in the historical event in Dahu area: evacuation without and with the consideration of risk maps. In each scenario, 200 evacuees were randomly generated on the whole domain except the buildings, the retention pond, the hill areas at the northwest part and the northeast part of the study area. Every agent would move towards the shelter (the red house sign in Figure 4-29 (b) and in Figure 4-32) along the shortest route, regarding the buildings, the retention pond, the hill areas as barriers, at each time step when the warning alarm was sounded at 11:23, (Taipei City Fire Department, 2017) whilst taking risk maps into consideration, the high-risk areas were also regarded as barriers during evacuation process.

The results showed that people were affected by flood water during the evacuation process. When people evacuated without the consideration of the risk map, people might pass through or stay in high-risk areas: 1% of the people trapped and 37% of the people passing through flooded areas in the test simulation. In contrast, if people evacuated with the risk map, people would not step in risky areas and make a detour: no people trapped and 20.5% of the people passing through flooded areas in the test simulation. The examples of the simulations are shown in Figure 4-32. In these preliminary attempts, the coupled model could conduct coupled simulation smoothly without conflict between models and numerical issues.

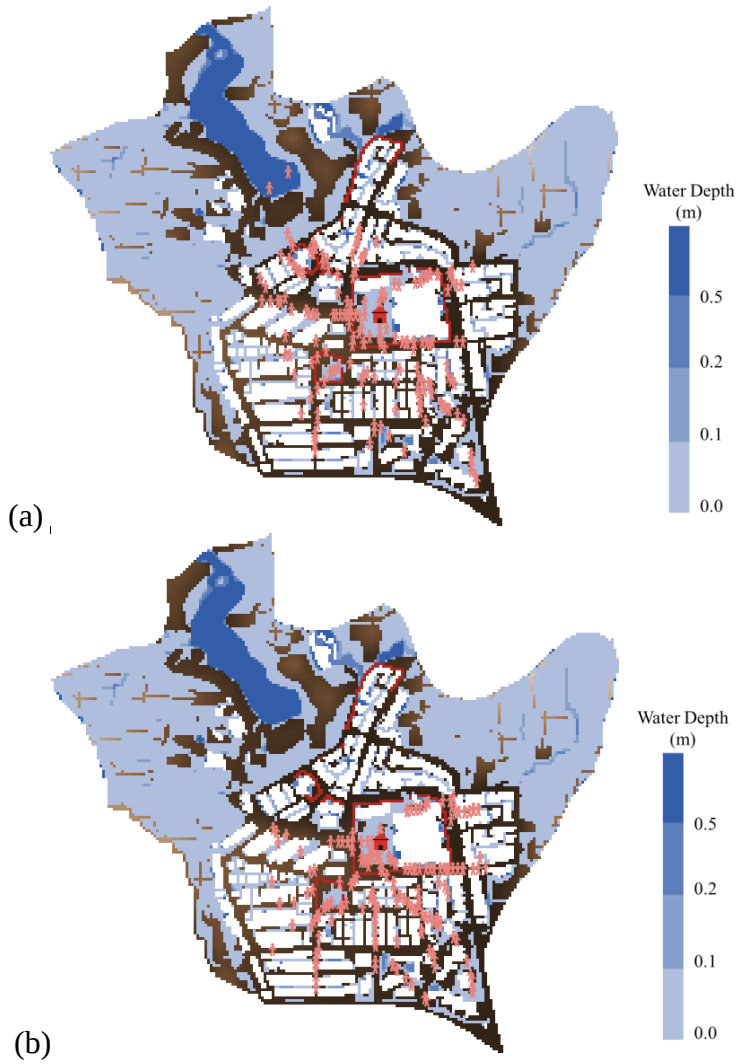

Figure 4-32. Examples of the hydrodynamic-agent coupled model: at 1 minute after the evacuation process (a) without the consideration of the risk map and (b) with the consideration of the risk map; the pink matchstick figures represent the evacuees

4.3.2 Summary

The evacuation model was designed for agent simulations focusing on agents, and the CA 2D overland flow model was designed for inundation simulations focusing on cells. Two models could be easily combined together to form a coupled model for inundation-agent coupled simulation. The results revealed the inundation-agent coupled model capability of conducting inundation simulations and the potential for generating plausible outcomes of the interaction between flood water, response strategies and human behaviour in a complex system during a flood event. Further research should include more factors and details in agent simulation and try to represent both structural and non-structural measures in the coupled model.

Chapter 5.
Applications of
the Coupled Agent-Based Model

Part of this chapter has been published:

Hsu, H. M., & Gourbesville, P. (2023). Introduction of integrated decision support system for flood disaster management. In *IOP Conference Series: Earth and Environmental Science* (Vol. 1136, No. 1, p. 012019). IOP Publishing.

https://doi.org/10.1088/1755-1315/1136/1/012019

Chapter 5 Applications of the Coupled Agent-Based Model

Extreme rainfall events and floods can cause negative impacts on human, property and environment, and thus flood risk management is essential to lower the risk. In addition to the government's work, the public should also learn self-protection and self-rescue. Sufficient education for disaster should be provided to the publics to raise crisis awareness and establish risk culture. Many communities in the Dahu area have participated in relevant trainings since 2019 after the historical events to form their community-based flood risk management. (Center for Weather Climate and Disaster Research, 2019) In order to evaluate the effectiveness of the community-based flood risk management and the proposed strategies from the Taipei city government, the coupled ABM is an ideal tool to analyses the detailed interactions. This chapter will introduce the flood risk management of Dahu area and the applications of the coupled ABM to evaluate the performance of the risk management.

5.1 The Flood Risk Management and Community-Based Flood Risk Management of Dahu Area

After strikes of the historical flood events, Taipei City Government decided to improve the existing flood risk management of Dahu area. According to the report from Taipei City Government (Taipei City Fire Department, 2017a), the government suggested: (1) increasing inlets or ditches to enhance the capability of collecting flood water into sewer systems; (2) informing local communities to respond to incoming heavy rain beforehand and providing information about rainfall and disaster response; (3) enhancing maintenance of the sewer systems; (4) promoting installation of floodwalls and stacking of sandbags; (5) decreasing runoff water from Mifenkeng Creek (as shown in Figure 5-1 (a)) and its tributaries; and (6) diverting runoff water from Mifenkeng Creek and from the creek at north-west part of Dahu. The detailed information about the designs and the application are elaborated in the following paragraphs.

The design standard of the sewer systems in Taipei is 78.8 mm per hour, which may be outdated and insufficient. (Wu & Hetherington, 2021) Therefore, the design standard is planned to improve from 78.8 mm per hour to 88.8 mm per hour. (Liu, 2023; The Merit Times, 2023) Besides, a flood diversion and a retention pond were designed to improve the drainage systems around Mifenkeng Creek by decreasing the runoff toward the urban areas, as shown in Figure 5-1. (Hydraulic Engineering Office, Public Works Departments, Taipei City Government, 2023) Figure 5-1 (a) shows Mifenkeng Creek and the area designed for the retention pond, and the Figure 5-1 (b) shows the location and the shape of the retention pond.

(a) 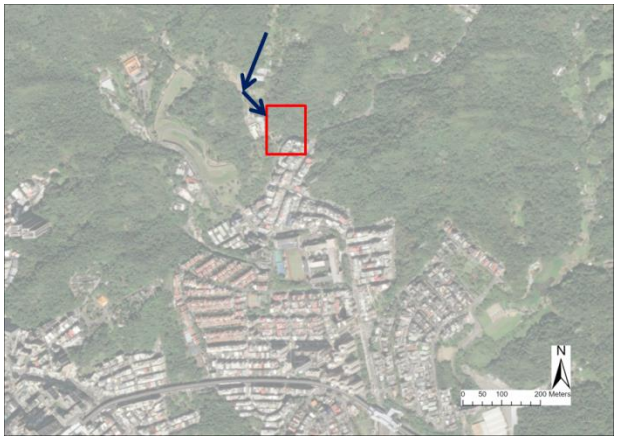 (b) 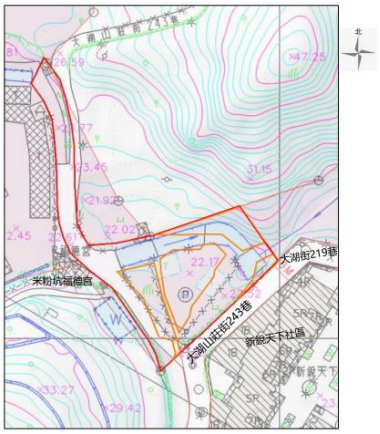

Figure 5-1. (a) The locations of Mifenkeng Creek (blue arrows) and of the drainage improvement project around Mifenkeng Creek (red rectangle). (b) The location of the drainage improvement project around Mifenkeng Creek (Dahushanzhuang Street flood diversion and retention pond B) (the red rectangle of Figure 5-1 (a)). (source: Hydraulic Engineering Office, Public Works Departments, Taipei City Government (2023))

Furthermore, Hydraulic Engineering Office, Public Works Departments, Taipei City Government commissioned and cooperated with Center for Weather Climate and Disaster Research, National Taiwan University and invited local residents of Dahu area to design the community-based flood risk management to form autonomous flood resilient communities to lower the flood risk by lower the vulnerability and increase the capacity, in response to the historical events. For example, local communities improve the evacuation process, and learned how to install and operate floodwalls, to stack and place sandbags, to use portable pumps and to prepare and respond to the crisis, as shown in Figure 5-2.

Figure 5-2. Demonstration and training for (a), (b) installation and operation of floodwalls, (c) stacking and placing sandbags, and (d) operation of portable pumps. (source: Center for Weather Climate and Disaster Research (2019))

After the training, local residents of Dahu area practiced in several typhoon and heavy rain events. For example, people help clean ditches, check the retention pond, place and operate portable pumps before and during the events in 2021, as shown in Figure 5-3, 5-4 and 5-5. More elements were also added to the community-based flood risk management, such as Dahu localised disaster prevention information online platform for local residents, community relief care and localised recovery. Dahu area won a golden medal of autonomous flood resilient communities from Water Resources Agency in 2021, and the communities also helped promote the community-based flood risk management and share their experience to other communities. (Center for Weather Climate and Disaster Research, 2021)

(a)  (b) 

Figure 5-3. Local residents of Dahu area helping (a) check the retention pond in Dagouxi Waterfront Park, and (b) place portable pumps at the area around Mifenkeng Creek for heavy rain on 29 and 30 May 2021. (source: Center for Weather Climate and Disaster Research (2021))

(a)  (b) 

Figure 5-4. Local residents of Dahu area helping (a) clean ditches, and (b) operate floodwalls for a typhoon event on 4 June 2021. (source: Center for Weather Climate and Disaster Research (2021))

 

Figure 5-5. Local residents of Dahu area helping clean ditches and inlets of the sewer systems for a typhoon event on 21 July 2021. (source: Center for Weather Climate and Disaster Research (2021))

5.2 The Applications of the Coupled Agent-Based Model for Flood Risk Management of Dahu Area, Taipei, Taiwan

In order to examine the capability of the inundation-agent coupled ABM and to evaluate the designed risk reduction strategies against the future challenges of flood risk, this study applied the coupled ABM for the flood risk management of Dahu area, focusing on short-duration intense rainfall events, which caused many problems in urban areas and were more difficult to deal with due to short preparation and response time. This study selected the scenario of total accumulated rainfall of 350 mm in 6 hours from the official design rainfalls (Water Resources Agency, n.d.-a) for the applications of the coupled ABM. The official design rainfall is shown as Figure 5-6.

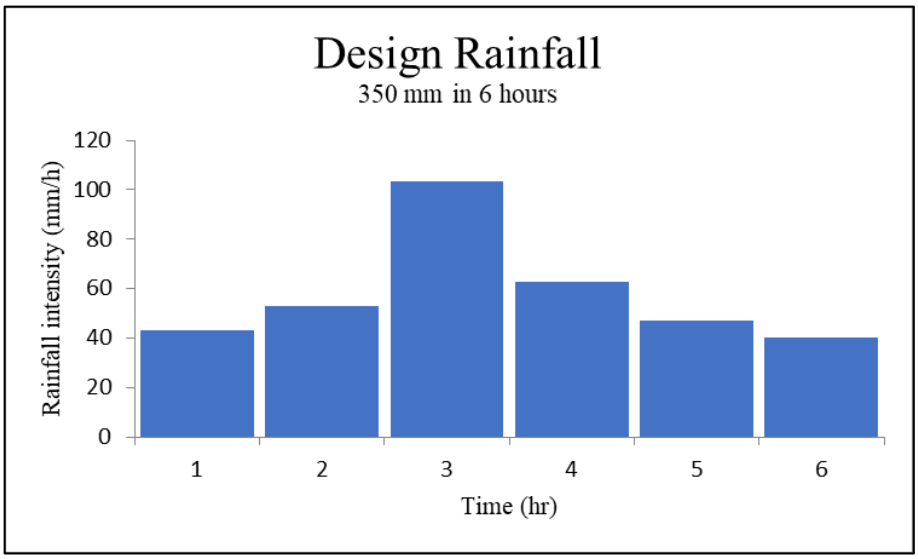

Figure 5-6. The design rainfall for the accumulated rainfall of 350 mm in 6 hours.

Since the duration of the 6-hour scenario is the shortest one of the official flood potential maps (the others' are 12 hours and 24 hours) and the accumulated rainfall and the maximum rainfall intensity of the scenario are close in proportion to those of the historical flood events (the others' are 150 mm and 250 mm, which are smaller than the historical flood events), this scenario is the most appropriate one for analysing the flood risk management of Dahu area. The flood potential map of Taipei under the scenario was presented in Figure 2-21 in Section 2.4.

In the study, five different scenarios are selected, based on the above-mentioned flood risk management in Section 5.1. The five simulation scenarios (S-I – S-V) are listed in Table 5-1.

Table 5-1. The simulation scenarios for the coupled ABM.

	Scenario				
	S-I	S-II	S-III	S-IV	S-V
Risk Map	-	O	O	O	O
Strategies	-	sandbags	ditches and inlets enlarged	inflows diverted and retained	all measures applied in S-II, S-III and S-IV

The structure of the coupled ABM is elaborated in Chapter 3, and the only different parts are the input rainfall data and the additional measures in the next paragraph. For the evacuation timing, according to Hydraulic Engineering Office, Public Works Departments, Taipei City Government (n.d.), the top elevation of the retention pond is 26 m; therefore, the public will start to evacuate towards the shelter when the elevation of the retention pond exceeds the top. The public will evacuate without the consideration of the risk map and the evacuation map in the scenario S-I, whilst in the scenario S-II – S-IV, the maps are taken into account due to the improvement of the evacuation process. All the inlets of the sewer systems will operate properly without any malfunction in all the scenarios, due to regular maintenance by the local residents. The simulation time is 18 hours for the 6 hours events.

In the scenario S-I, no additional measures are applied to the study area, representing the original situation. In the scenario S-II, 1-metre-height sandbags are planned to be placed at the entrance of Dagouxi Waterfront Park for blocking the inflows from the retention pond and from hills at the north and the north-west parts of the study area. Figure 5-7 shows the location of sandbags of the scenario S-II, in which the red line is sandbags and the three dark blue arrows indicate the inflows. The coupled ABM will start to stack the sandbags to 1 metre height preventing the water from entering urban areas when the water level of the retention pond reaches the top at 26 m. In the scenario S-III, in order to represent the suggestion from the government for increasing or enlarging inlets or ditches to enhance the capability of collecting flood water into sewer systems from 78.8 mm per hour to 88.8 mm per hour, the areas of the inlets of the sewer system in the coupled ABM are enlarged proportionally. In the scenario S-IV, in order to represent the suggestion from the government for building a flood diversion and a retention pond and to represent the operation of portable pumps of the community-based flood risk management at the north-east part of the study area, the inflows from the north-east part are taken out. In the scenario S-V, all the three above-mentioned strategies in S-II, S-III and S-IV are applied.

The coupled ABM will run coupled simulations for each scenario, and then the total flooded area (excluding those in the retention pond, the parks and on the hills), the

maximum water depth and the percentage of trapped people and the percentage of people passing through flooded areas will be calculated to evaluate the performance of each scenario.

Figure 5-7. The location of sandbags of the scenario S-II for blocking the inflows from the retention pond and from hills.

5.3 Results and Discussion

Figure 5-8 to Figure 5-12 show the flood map under each scenario, showing the similar flood pattern of the historical event on 2 June 2017 (check Figure 4-30, Section 4.2.2.2). Water from the north and the north-west areas first filled the retention pond and the park and then entered the urban areas. The inflows from the north-east area also caused flood on the streets at the north-east areas, but nearly no water from the inflows could reach the central areas. The main cause of the scattered flood in the urban areas was that the rainfall intensity was much higher than the design standard.

Scenario S-I

Figure 5-8 shows the flood map under the scenario S-I with no additional measures. The total flooded area is 9,850 m^2 which is the largest one amongst the five scenarios. The maximum water depths at the entrance of the park and on the main road in the central area, Dahushanzhuang Street, are 0.87 m and 0.84 m respectively, slowing the walking speed of the evacuees, and there are 48.5% of the evacuees ever passing through flooded areas which are also the worst amongst the scenarios. 10% of the evacuees were trapped inside the park, whilst no one was trapped when taking the risk map into account under the other scenarios.

Figure 5-8. The flood map of the scenario S-I.

Scenario S-II

Figure 5-9 shows the flood map under the scenario S-II with sandbags stacked at the entrance of the park. Since water from the hills was blocked by the sandbags, the maximum water depth at the entrance of the park rose around 23% from 0.87 m to 1.07 m. In contrast, the maximum water depth on the main road was lowered by around 11% from 0.84 m to 0.75 m. The flooded area is 9,650 m^2, just a bit smaller than that of S-I, showing no significant difference. No one was trapped, and 24.5% of evacuees ever passed through flooded areas, around half the number of S-I.

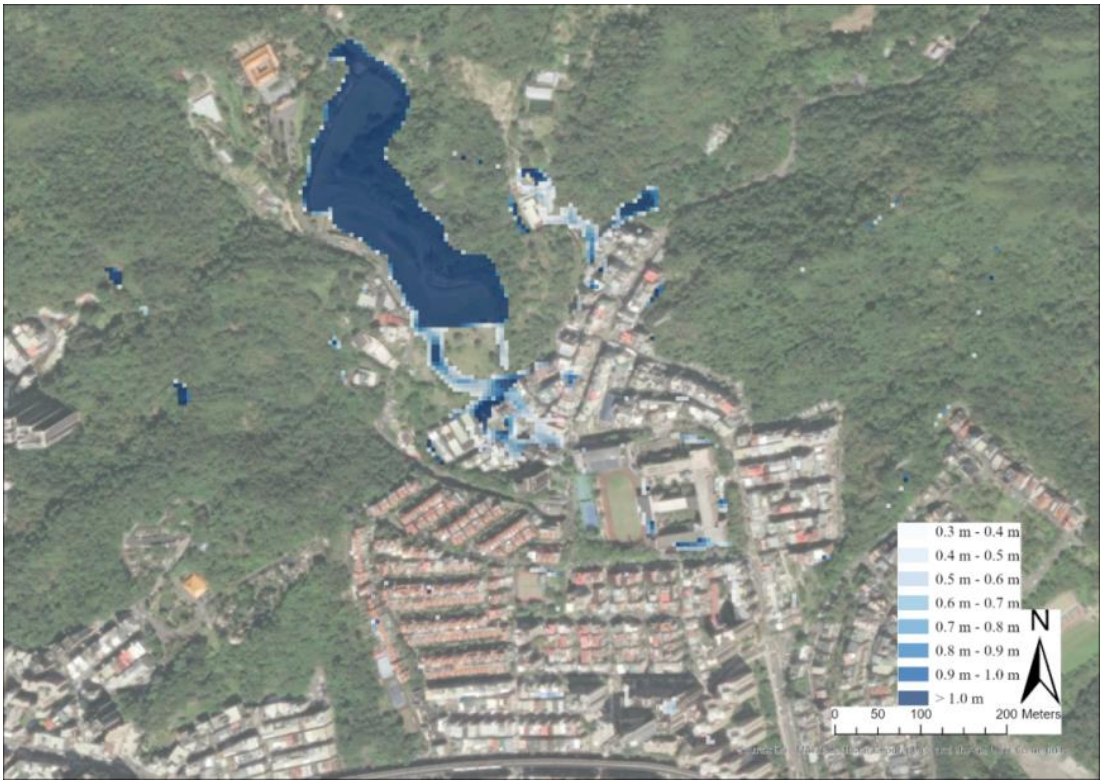

Figure 5-9. The flood map of the scenario S-II.

Scenario S-III

Figure 5-10 shows the flood map under the scenario S-III with improved sewer systems. Since more water went into the sewer systems, the flooded area is decreased by around 9% to 9,000 m^2. The maximum water depths at the entrance of the park and on the main road were also decreased by about 6% and 7% respectively to 0.82 m and 0.78 m. No one was trapped, and 24% of evacuees ever passed through flooded areas, around half the number of S-I.

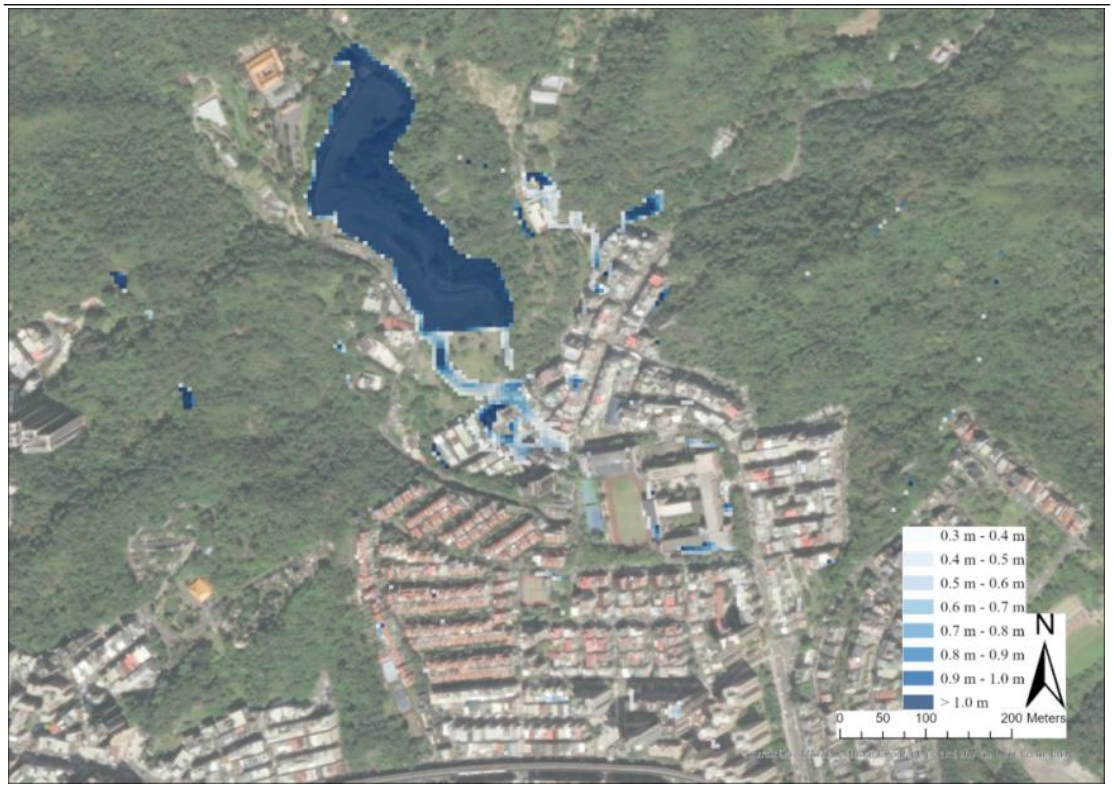

Figure 5-10. The flood map of the scenario S-III.

Scenario S-IV

Figure 5-11 shows the flood map under the scenario S-IV with a flood diversion and a retention pond. Because the inflows from upstream and from the hills at the north-east part of the study area were diverted, drained by portable pumps and retained in the retention pond, the flooded areas at the north-east area is much smaller, and the total flooded area is decreased by around 5% to 9,350 m^2. The maximum water depths at the entrance of the park and on the main road remain the same, 0.87 m and 0.84 m respectively. No one was trapped, and 24% of evacuees ever passed through flooded areas, around half the number of S-I.

Figure 5-11. The flood map of the scenario S-IV.

Scenario S-V

Figure 5-12 shows the flood map under the scenario S-V with all measures applied. The total flooded area is decreased by 18% to 8,075 m^2, which is the smallest one amongst the five scenarios. The water from the hills was blocked by the sandbags, the maximum water depth at the entrance of the park rose around 22% from 0.87 m to 1.06 m. On the contrary, the maximum water depth on the main road was lowered by around 23% from 0.84 m to 0.65 m. No one was trapped, and 24.5% of evacuees ever passed through flooded areas, around half the number of S-I.

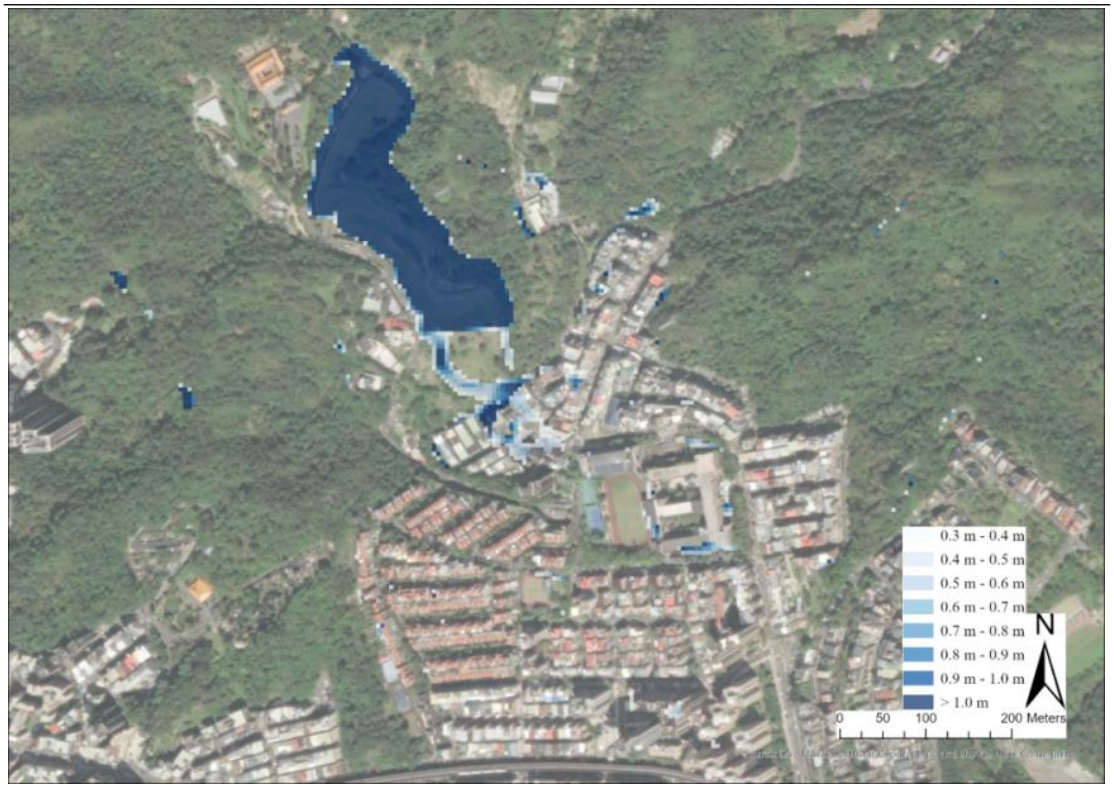

Figure 5-12. The flood map of the scenario S-V.

Table 5-2 lists the total flooded area (excluding those in the retention pond, the parks and on the hills), the maximum water depth and the percentage of trapped people and the percentage of people passing through flooded areas of each scenario.

Table 5-2. The results of each scenario.

	Scenario				
	S-I	S-II	S-III	S-IV	S-V
Flooded Area (m^2)	9,850	9,650	9,000	9,350	8,075
Max Water Depth at the Entrance of the Park (m)	0.87	1.07	0.82	0.87	1.06
Max Water Depth on the Main Road (m)	0.84	0.75	0.78	0.84	0.65
Percentage of Trapped People (%)	10	0	0	0	0
Percentage of People Passing through Flooded Areas (%)	48.5	24.5	24	24	25

Owing to the flood diversion and the additional retention pond at the north-east part of the study area in the scenario S-IV and S-V, the flood at the area were almost eliminated, as the comparison of the maximum water depth at the north-east part of the study area between the scenarios in Figure 5-13. However, in the original situation, the inflows from the north-east part could not reach the central parts and

only caused local flood at the north-east area, and therefore, in order to protect the main flooded areas in the central part, other strategies were needed.

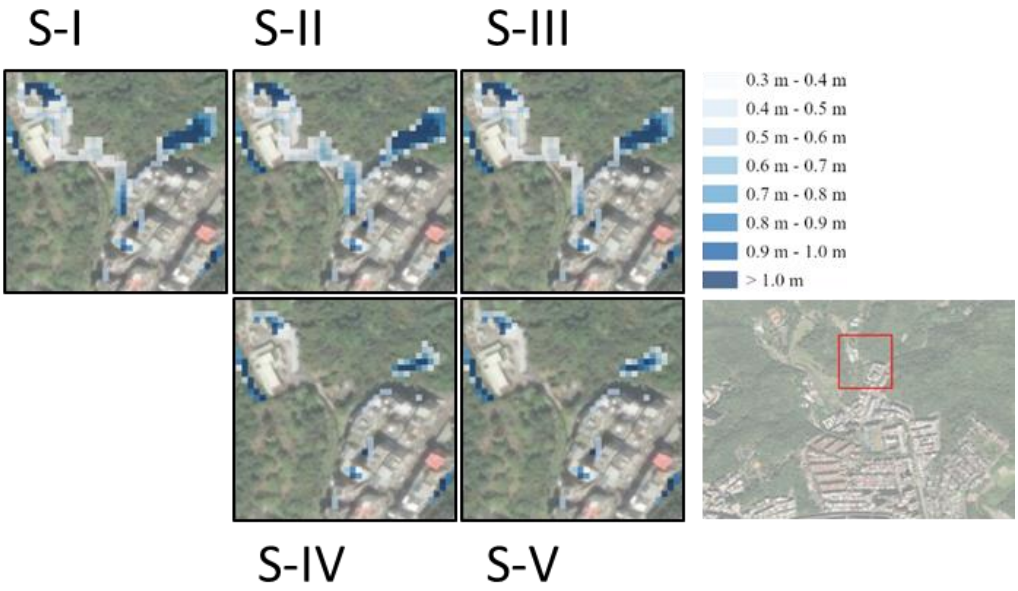

Figure 5-13. The comparison of the maximum water depth at the north-east part of the study area between the scenarios.

Thanks to the sandbags stacked at the entrance of the park in the scenario S-II and S-V, blocking the water from the hills and the retention pond from entering the central part, the maximum water depth at the entrance of the park rose and those on the main road was lowered. The comparison of the maximum water depth around the intersection of the entrance of the park and the main road are shown in Figure 5-14.

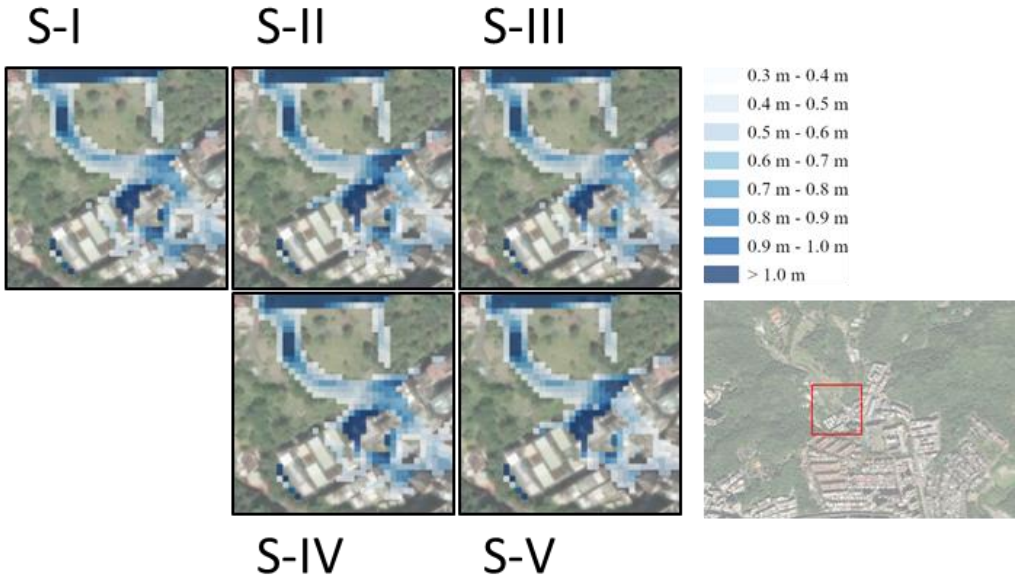

Figure 5-14. The comparison of the maximum water depth around the intersection of the entrance of the park and the main road between the scenarios.

Even though the sandbags and the flood diversion and the additional retention pond in the scenario S-II and S-IV lowered the water depth and decreased the flood area, floods still happened in the urban areas. The floods were only caused by the intense rainfall, and hence other strategies were needed. Enlargement and increase of inlets and ditches could directly enhance the capability of collecting flood water and lower the flood risk extensively in the urban areas. Notably, different strategies could work synergistically. From the result of the scenarios S-V, combining all the strategies could produce a joint effect greater than the sum of the three strategies separately, in terms of the total flooded area and the water depths in the urban areas. Besides, evacuation process could be substantially improved by taking the risk map and evacuation map into consideration. However, other strategies did not create further positive impact on the percentages of trapped people and of people passing through flooded areas of each scenario. Since the flooded areas of all the scenarios were mainly located in the high-risk areas on the risk map (check Figure 3-15), evacuation could proceed without posing a threat to life as long as the evacuees stayed away from high-risk areas. What should be emphasised is that under different scenarios or in the different study sites, the evacuation process may be affected by different risk reduction strategies, showing different results from those of this study.

5.4 Application of the Coupled Agent-Based Model in Disaster Education

Without crisis awareness and risk culture, even with well-designed strategies, people may still have improper behaviours. Many individuals may not be able to understand the importance of self-protection and self-rescue and to prepare for risk of disaster unless they experience the disaster. Previous reports emphasise the importance of disaster prevention education (Groupe URD, 2020) and of self-protection and self-rescue. (Taipei City Fire Department, 2019)

The coupled ABM can be utilised for disaster education, raising public crisis awareness and for establishing community-based flood risk management. Scenarios and strategies can be set up in the coupled ABM with user-friendly interface, and the ABM can be designed as serious games. Figure 5-15 shows some examples of interface elements of the ABM, NetLogo: (a) is button for executing specific commands of the code, such as initialisation and running the simulation; (b) is switch for true/false variables, such as consideration of maps and status of alarm; (c) is slider for setting numbers of specific variables without changing the code, such as the number of sandbags, number of evacuees and the capacity of a shelter; (d) is input for assigning strings or numbers to specific variables, such as names, IDs, simulation duration and output intervals; (e) is chooser for selecting a variable from a list in a drop down menu, such as scenarios and strategies; (f) is plot for drawing specific variables changing with time, such as the number of evacuated people and the number of people in danger; (g) is monitor for displaying specific variables, such as simulation time and time step. Other than these elements, some mouse tools can also be included in the code, and then users can interact with their mouse, such as placing sandbags, placing shelters and deploying pumps. Even users without an engineering or disaster response related background can manipulate the ABM by simply clicking, typing, selecting and sliding the interface elements to conduct simulations and see the result of the world of agents and cells displaying on the interface in real-time, like playing a game.

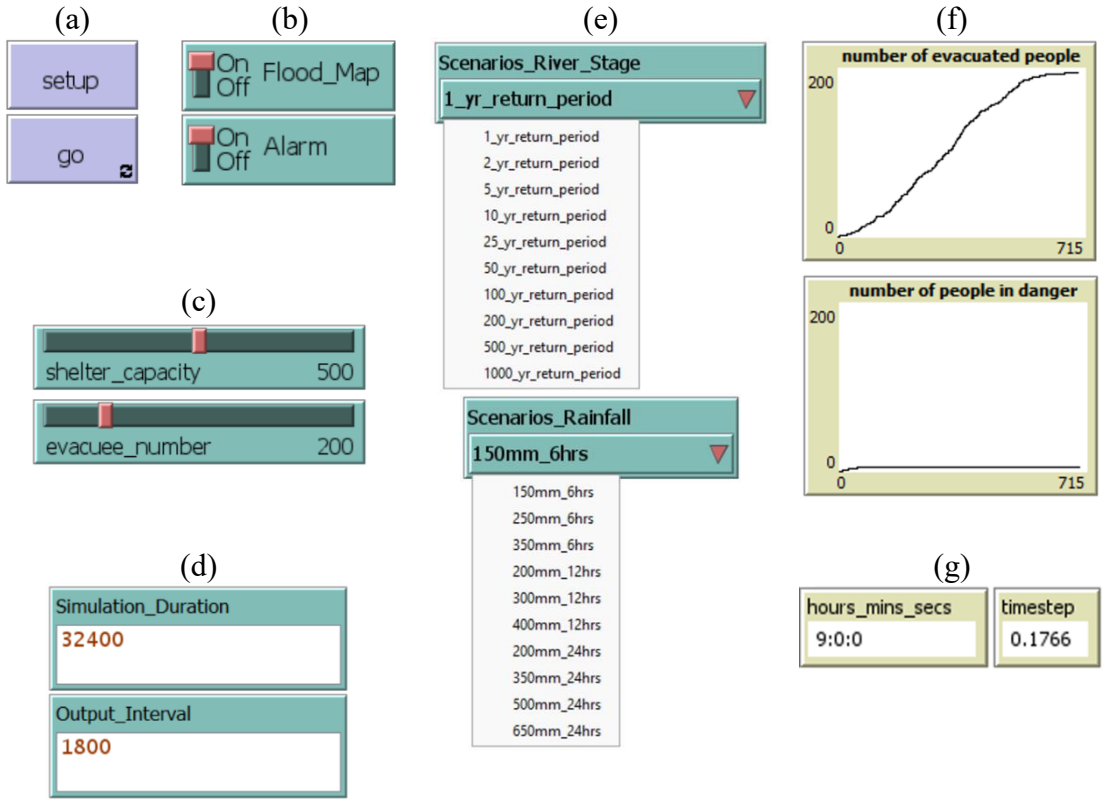

Figure 5-15. Examples of interface elements: (a) buttons, (b) switches, (c) sliders, (d) inputs, (e) choosers, (f) plots and (g) monitors.

Through the ABM, local authorities and responders can receive a plausible result under specific condition they designed for analysing and try to find their way to deal with. On the hand, by playing serious games on the ABM, the public can also learn what may happen, what will be the best way to react and how they can prepare. For example, people may understand a park they usually go for leisure will be full of water in heavy rains, and hence they should avoid entering the park; people can also run a coupled simulation and try to build their defence against flood, and then people can have a basic idea of deployment and use of sandbags and portable pumps. Previous studies show the benefit of serious gaming, (Tsai et al., 2019; Sermet et al., 2020) and, as educational interventions, they can offer positive experience to the users and increase their interest. (Skinner, 2020) Users can experience, learn, and improve those they have learnt.

5.5 Summary

This chapter described the flood risk management, the community-based flood risk management of the study site of Dahu area and the applications of the inundation-agent coupled model to evaluate the performance of different risk reduction strategies. Through the comparison of the results of each scenario, the quality and the effectiveness of the different strategies could be quantified. The coupled ABM was used to evaluate the performance of the flood risk management and the community-based flood risk management of Dahu area. In the study, by comparing the outcomes of the different strategies, the results showed that the combination of all the strategies could synergise and effectively lowered the risk regarding the flood extent and flood depth, but the evacuation processes were mainly affected by the consideration of the maps. Since the flooded areas of all the scenarios were mainly located in the high-risk areas on the risk map, evacuation could proceed without posing a threat to life as long as the evacuees stayed away from high-risk areas. More other scenarios, more strategies and more factors can be also included in the future to further analysing the risk management.

The coupled ABM can be a valuable tool for investigating and improving existing disaster response strategies and for enhancing community-based flood risk management through serious gaming.

Chapter 6.
Integration of the Coupled Agent-Based Model and a Decision Support System

Part of this chapter has been published:

Hsu, H. M., & Gourbesville, P. (2023). Introduction of integrated decision support system for flood disaster management. In *IOP Conference Series: Earth and Environmental Science* (Vol. 1136, No. 1, p. 012019). IOP Publishing.

https://doi.org/10.1088/1755-1315/1136/1/012019

Chapter 6 Integration of the Coupled Agent-Based Model and a Decision Support System

Effective and efficient flood risk management requires on-site information, forecast and appropriate corresponding response strategies and measures. In order to interpret the complex data to responders and decision makers, decision support systems (DSSs) are good tools for providing useful and meaningful information. The coupled ABM can further offer plausible outcomes of complex interaction between human behaviour and environment for decision-making. With the help of the coupled ABM, DSSs can also be utilised for disaster drill, education and demonstration, etc. This chapter will introduce possible applications of the coupled ABM and feasibility of integration of the coupled ABM and DSSs.

6.1 Decision Support Systems

Heavy precipitation events and fluvial flood can cause serious damage to property and fatality, and thus flood disaster management is essential to lower the risk, to prevent and to mitigate the crisis. Effective and efficient flood disaster management requires on-site information, forecast and appropriate corresponding response strategies and measures. Decision support systems (DSSs) can integrate various components, such as monitoring, information transmission, rainfall forecast, inundation simulation, information about historical events and crisis scenarios, and response strategies and measures, by means of information and communication technology (ICT) and internet of things (IoT) and provide relevant information and offer suggestions of action before, during and even after crisis. For instance, Gourbesville et al. (2016; 2018) established a DSS combining several hydrological and hydraulic models and providing real-time assessment and forecasts for water management in south France; Yang et al. (2018; 2020) developed a DSS integrating monitoring sensors, rainfall forecast, model simulation and response strategies against disasters for a science park in central Taiwan. An agent-based decision support tool was also established for community flood evacuation planning in Japan. (Nakanishi et al., 2020) More applications of agent-based modelling for flood problems were reviewed and can be found in Simmonds et al. (2020). With the integration of the coupled ABM (introduced in Chapter 3, 4 and 5), DSSs can further offer plausible outcomes of complex interaction between human behaviour and environment for decision-making and also be utilised for disaster drill, education and demonstration, etc.

This study proposes a concept of integrated DSS structure for flood risk management. The integrated DSS can consist of five main components: hydrological information, database, the coupled ABM, the DSS and its services, as shown in Figure 6-1. The detailed information of each component will be elaborated in the following sections

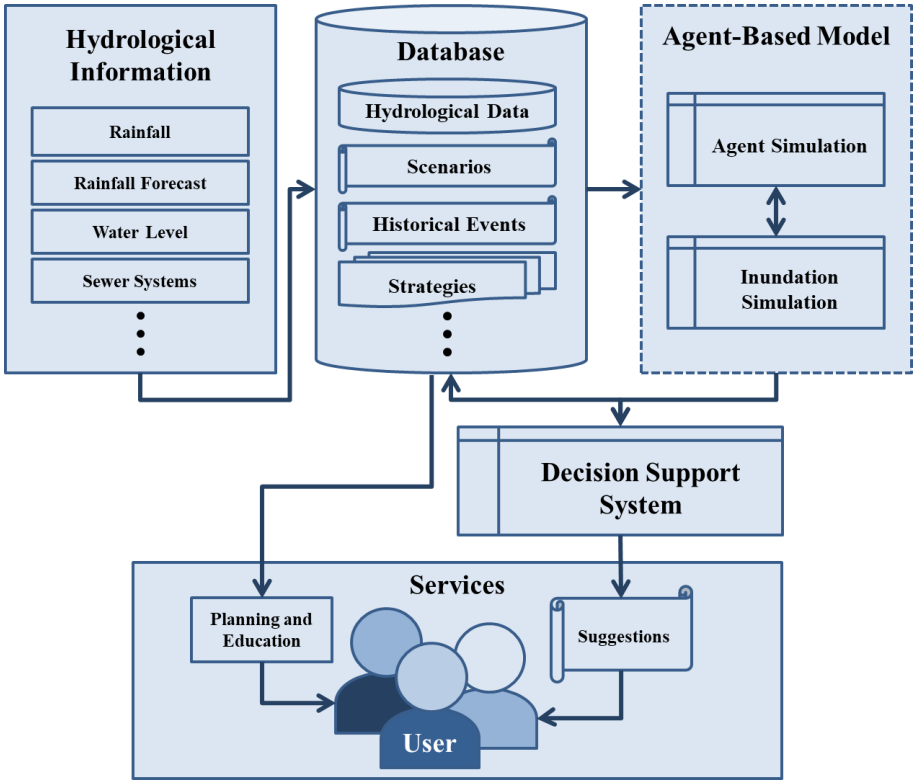

Figure 6-1. The structure of the proposed integrated DSS.

Hydrological Information

Real-time observation and rainfall forecast information are important to flood forecasts. Real-time observation from on-site sensors and monitors, such as rain gauges, water gauges in rivers and in sewer systems, etc. should be stored in the database first, and the information can be imported as initial condition and boundary condition into hydrological and hydraulic models. Then the system should collect rainfall forecast information for hydrological and hydraulic simulation. In this series of process, information and communication technology (ICT) and internet of things (IoT) technology are crucial to data collection and transmission, which should be well-maintained especially during crisis. (Lynggaard-Jensen et al., 2015; Chang et al., 2018; Anzaldi, 2014)

Database

A database is vital for storing and organising the data collected. The data should be well-categorised according to the connection between hydrological data, flood maps, risk maps, risk reduction strategies and so on; therefore, the data can be retrieved accordingly. There are several different kinds of database model, such as hierarchical database, network database and relational database and so on. In this paper, a relational database structure is recommended due to its easy data fetching process and

rapid response. Although a hierarchical structure can be intuitively adopted through the process of risk assessment and strategy development, i.e., scenario-flood-risk maps-strategies, it is not ideal for complex systems in which many factors are interconnected. Database management systems, such as MySQL, Microsoft Access, Oracle database, etc., can be employed to manage the data, enabling users to easily retrieve relevant data, to maintain the database, and to update the database. An example of the database structure is shown in Figure 6-2. The information of the historical events and the simulation output is stored in the Scenarios table and every scenario has a specific ID. Every scenario has one flood map and many risk maps on various aspects, and the relation is connected through the MapID. The outcomes of the scenarios are stored in the Phenomena table, containing the information about the scenarios. Many phenomena may result from the same scenario, and in other words, there are many phenomena having the same scenariosID in the table. Every phenomenon has its corresponding response strategies, and in this case, the same PhenomenaID may appear in different strategies. The related responders are connected with the strategies via ContactID, and therefore, the system can find the contact method of the responders.

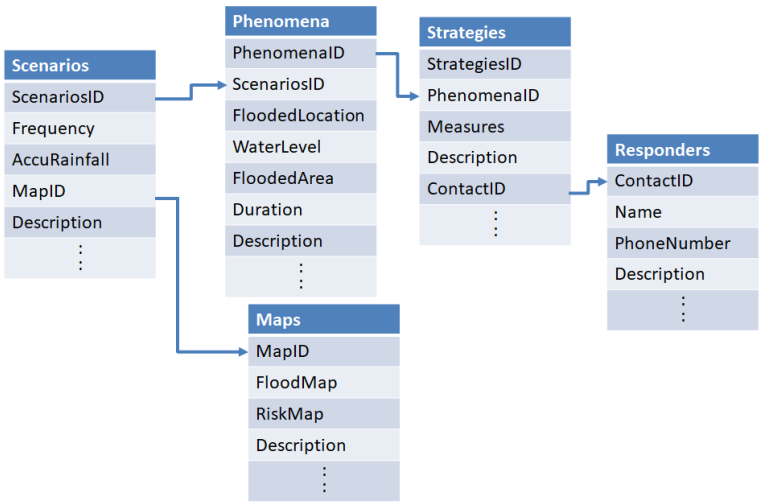

Figure 6-2. An example of the database structure.

The coupled ABM will retrieve relevant data from the database for inundation-agent coupled simulations, and the DSS will also retrieve the most appropriate strategies from the database after analysing the coupled simulation for providing suggestions of actions to users. Possible scenarios should be designed beforehand and then the relevant information can be stored in the database, such as different design return periods rainfall, operation of flood disaster prevention facilities and possible malfunction of the facilities, deployment of disaster prevention devices and personnel, possible compound disaster, possible evacuation routes, etc. Then corresponding risk

reduction strategies and crisis response strategies can be designed accordingly. Furthermore, detailed information of meaningful historical disaster events can also be regarded as designed scenarios.

Risk reduction strategies and crisis response strategies are important components in the database. The strategies can cover all phases of disaster, including disaster preparedness, disaster prevention, disaster mitigation, crisis responses, recovery after disaster. The strategies can include maintenance and operation of structural measures such as sewer systems, sluice gates, deployment and operation of pumps, and non-structural measures such as warning and alarm systems, flood forecast, mobilisation, traffic diversion, evacuation, participation of volunteers (Andjelkovic, 2001), business continuity plan (International Standards Organisation, 2012) and so on. The triggers of the all the strategies should be well-defined, and therefore the connection between the scenarios and the strategies can be utilised for information retrieval in the DSS. Afterwards, the DSS can provide the relevant information and offer suggestions of action before, during and after crisis.

The Coupled Agent-Based Model

The coupled ABM utilises the observation data stored in the database to conduct inundation-agent coupled simulations and then provide plausible outcomes of complex interaction between human behaviour and the environment for decision-making. With the outputs of the coupled simulations, we can delineate high-risk areas and potential inundated areas in detail and generate risk maps and flood maps. The maps can serve as references to evaluate the socio-economic impact, evacuation process and other effect on various aspects apart. All the information of the model output will be collected by the database. The information of the location, the extent and the magnitude of the impacts should all be stored with the help of geographic information system (GIS). For instance, the point shapefile format for storing water level information, locations of historical flood events (damage, water level, discharge), locations of key facilities, and so on; the polyline shapefile format for representing sewer systems, drainage systems, dykes, and so on; the polygon shapefile format for historical flood maps, flood hazard maps, risk maps and so on. Besides, the model outputs of the coupled ABM and the ABM itself can also be stored in the database. The outputs of historical events can serve as reference for future events.

Decision Support System

The decision support system should automatically collect all the relevant information, analyse the information, and then provide useful suggestions of actions. First, the DSS should be designed to automatically collect all the data from the coupled ABM, on-

site information, rainfall forecast and flood forecast and so on. Then the DSS should automatically search from the database and retrieve suggestions of actions from the designed response strategies according to the closet scenarios to the reality and according to the triggers of all the strategies. The suggestions can be displayed on a specific website or provided through mobile applications automatically, and users can also check the information on-line manually. The webpage should update regularly to provide the latest real-time information for end-users. Besides, the contact information of every responder and authority can also be stored in the DSS, and therefore, the DSS can send the suggestions to them directly via mobile applications, email, text messages and so on.

Service

The database and the DSS can serve disaster risk management in all phases. In prevention and mitigation phase, designed scenarios, historical events and detailed risk maps in the database can be utilised for education and demonstration with the help of virtual reality (VR), augmented reality (AR) or Metaverse technology to facilitate the training of emergency personnel and to educate the public. For instance, water level from the risk maps and real-time data can be visualised to perceive the potential dangers through AR (Fuchs-Kittowski et al., 2012; Haynes & Lange, 2016a; 2016b; Haynes et al., 2018; Mirauda et al., 2018; Tomkins & Lange, 2019); VR can also be used to visualise the flood scenarios for educating the public and to survey their behaviour when facing disaster. (Zaalberg & Midden, 2013; Simpson et al., 2022; Fujimi & Fujimura, 2020) In addition, all the scenarios and the response strategies can also be introduced into a virtual world, such as Metaverse environment, for disaster education. Previous studies show the benefit of immerse experience in a virtual environment (Bredl et al., 2012; Lee et al., 2021) for disaster education. Studies shows that virtual environment can help to increase motivation to evacuation and buy flood insurance (Zaalberg & Midden, 2013), to increase investments for disaster prevention (Mol et al., 2022) and to raise people's interest in disaster prevention and to offer information efficiently. (Lai et al., 2011) In disaster preparedness phase, response phase and recovery phase, DSS can automatically provide meaningful suggestions of actions retrieved from the database. Decision makers and responders can act accordingly. Furthermore, the DSS can also be connected with disaster response-related facilities, such as water gates, pumps, traffic lights and so on; then the system can directly operate the facilities, under responders' supervision, during emergency situation. After crisis, DSS can offer recovery strategies. Information of the latest crisis can also be added into the database as new scenarios, and then the risk maps and the strategies can be updated as well after

evaluation of the event.

Potential Added Value

The integrated DSS can help to improve existing risk reduction strategies, response strategies and emergency services. Users can save time and improve performance of reaction to crisis under emergency condition. We can perform detailed simulations to assess the impacts of disaster and then develop corresponding strategies based on the scenarios. Afterwards, we can carry out further simulations to check the strategies and to assess the effect on various aspects, and then refine the strategies through these iterations. At last, all the data should be well-organised and well-categorised into the database, and thus the DSS can automatically provide information and the optimum suggestions of strategies to users according to the real-time situation and flood forecast. The DSS can also be connected with disaster response-related facilities and hence the system can directly operate the facilities during emergency situation. Decision makers and first responders do not need to take a long time to analyse complex data for taking actions.

6.2 Challenges, Constraints and Application in Real-Time

The integrated DSS is designed to provide suggestions of strategies and to be utilised for disaster drill, education and demonstration. Decision makers, first responders and the public can benefit from the system. Despite the advantages in various fields, there are still many gaps inside the structure to be filled. The DSS contains several different components and each one of these has been developed separately over a long period of time. However, these components are not usually well-interconnected. (Anzaldi, 2014) The most important issue about the operation of the DSS is the way of format standardisation, communication and interoperability between the various existing components.

The DSS can also provide real-time observation information and flood forecasts. The system should first collect information from on-site sensors and monitors and then conduct fast flood simulation. For this service, information and communications technology (ICT) and internet of things (IoT) are the main concern. Every sensor and monitor should be well-connected and transmit information stably; however, the transmission commonly has problems during crisis. People should have back-up equipment to maintain the service during crisis. By the same token, we should also consider possibly invalid observation data and adopt substitute algorithm to generate flood forecast and to retrieve relevant responding strategies.

The coupled ABM in the study should be further improved for reflecting the reality. The ABM is a prototype and can only provide some basic phenomena, and more factors of hydraulic simulations and agent simulations should be included. For example, sewer systems are not well represented in hydraulic modelling and no surcharge flow from inlets will occur; complex psychological factors are not considered in agent modelling and agents will not act, react or interact variously, such as herd mentality, disobedience, learning or cooperation. On the other hand, another issue in providing real-time coupled simulation results is the computational efficiency of coupled ABM. All the simulations were conducted by a computer with Processor Intel(R) Core(TM) i7-10700T CPU @ 2.00GHz, 16.0 GB RAM and 64-bit operating system, x64-based processor. Taking the simulations of the study as examples, the coupled simulation of the historical event of Magnan area took 44 hours, 33 minutes and 43 seconds, and the one of Dahu area took 23 hours, 53 minutes and 45 seconds (with coarser cell resolution of 5 metres than that of 2 metres of Magnan area); for the coupled simulations in Section 5.2, the time required to complete the 9-hour simulations ranged from 23 hours, 30 minutes and 3 seconds to 23 hours, 52 minutes and 36 seconds. Coupled simulations may only be acceptable for regular risk analysis, planning, training and education, due to long computational time. Especially for the hydraulic modelling, the CA hydraulic model in NetLogo cannot do any parallel

processing, and thus GPU computing, unlike the WCA2D model written by low-level programming language, C/C++ and OpenCL. (Guidolin et al., 2016) On the contrary, for the agent simulations in Section 3.2 and 4.1, the required time was around 5 minutes, which would be more suitable for emergency response purpose.

6.3 Integration of the Agent-Based Model within Existing Decision Support Systems

Other than establishing the whole above-mentioned integrated DSS, the feasibility of integration of the ABM and an existing DSS should be also considered. This study takes a DSS in Métropole Nice Côte d'Azur, France as example. The DSS, called AquaVar, was established to help deal with the issues of groundwater resources, water supply management and flood risk management. The objective of AquaVar is to provide an overview of the current situation from real-time monitoring and then the forecast from hydrological and hydraulic models. AquaVar integrates several different components as shown in Figure 6-3. (Gourbesville et al., 2018; 2022; 2023) A service bus collects and integrates real-time information including water levels, discharges, water quality, forecasts and data related to different processes. Data are all formalised through Key Performance Indicators (KPIs), alerts and directives. Hydrological and hydraulic models in the predictive systems will simulate based on the data collected by the service bus and then provide the results to the operation centre. Relevant information will then be displayed to users through visualisation.

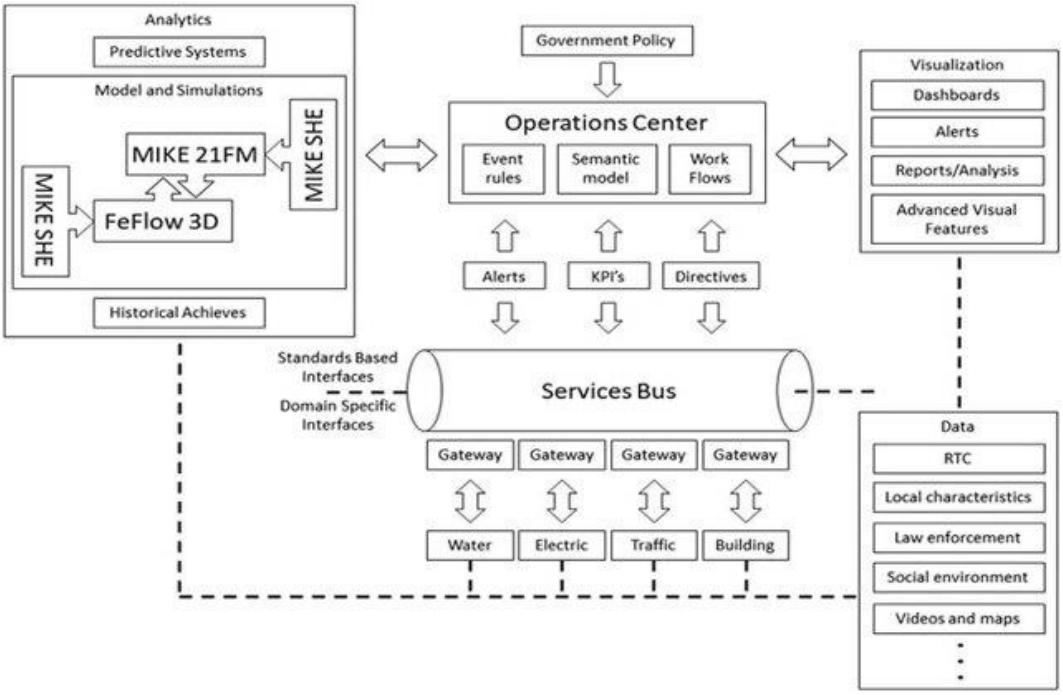

Figure 6-3. The structure of AquaVar. (source: Gourbesville (2023))

In the predictive systems, three models, developed by DHI, are integrated to cover the whole hydrological cycle at the catchment scale: (1) MIKE SHE model, a hydrological model for providing surface flow and groundwater flow as boundary conditions for FeFlow 3D model and MIKE 21 FM model; (2) FeFlow 3D model for 3D simulation of underground aquifer; (3) MIKE 21 FM model for 2D overland flow

simulation. The FeFlow 3D model and MIKE 21 FM model are coupled together for computing the interaction between rivers and groundwater. The models in the predictive systems operate in batch mode, managed by AquaVar orchestrator coordinating the data exchange and transmission.

The software of the coupled ABM, NetLogo, can be controlled by other languages, such as Python, Java and so on, and therefore the model can run simulations in batch mode managed by AquaVar. Here are two ways to integrate the ABM into AquaVar: one is to use the real-time data to run coupled simulations, and the other one is to import the results from predictive systems to run agent simulations.

The real-time information collected by AquaVar is sufficient for conducting inundation simulations in the coupled ABM, as long as the information format is consistent. Thus the coupled ABM can be used directly and model outputs of the coupled ABM can be in comma-separated values (CSV) format, portable network graphics (PNG) format, etc., which can be easily visualised for display after post-processing. However, since the hydrological and hydraulic models in the predictive systems are continually running inundation simulations already, the inundation simulations of the ABM are somehow repetitive and redundant. Theoretically, the physics-based models in the predictive systems can produce better model predictions than the CA 2D overland flow model in the ABM. Importing the better results from the physics-based models and only running agent simulations can save computational time substantially, but nevertheless, only agents will be affected by flood water, but not vice versa. Another problem is about the file formats of the models in the predictive systems. The model outputs from MIKE SHE, MIKE 21 FM and FeFlow 3D are all in specific DHI formats and cannot be used by others, unless with additional services from DHI. Integration of the coupled ABM within AquaVar is feasible, but the above-mentioned trade-offs should be considered.

6.4 Summary

In this chapter, we proposed a concept of a DSS integrating with the coupled ABM for flood risk management. The DSS was designed to provide suggestions of strategies and to be utilised for disaster drill, education and demonstration. Decision makers, first responders and the public could benefit from the system. The coupled ABM could also be integrated within an existing DSS, AquaVar, for example. The aims of the DSS were to improve existing response strategies and emergency services, to enhance the community-based flood risk management, and to raise public crisis awareness. Despite the possible advantages in various fields, there were still many gaps inside the structure to be filled. The most important issue about the operation of the DSS was the way of format standardisation, communication and interoperability between the various existing components.

Chapter 7. Conclusion and Future Perspective

7.1 Conclusions

Floods are the most common natural disasters worldwide. Flood can cause fatality and serious damage to property, and thus, flood risk management is essential to avoid new flood risk, to prevent and to reduce existing impact of floods and to manage residual flood risk.

This study briefly reviewed several historical flood events worldwide, and especially the applications of flood risk treatment of the study areas in France and in Taiwan.

- Different strategies and measures were developed in response to flood disasters, and from flood disasters people also learned lessons to improve existing flood disaster management.
- The concept of flood risk management, community-based flood risk management and risk reduction strategies, both structural measures and non-structural measures, against flood risk were introduced and the applications of the risk management were also described.
- Before crisis, risk maps and flood maps can be useful for deployment and traffic management; the warning and the alert systems delivers important signals for people to follow the instructions for the crisis; suspension of classes and evacuation are effective ways to lower exposure to crisis. During crisis, maintenance of telecommunication, water and power is essential, and volunteers can aid.
- Despite the effectiveness and the importance of flood risk management, without disaster education and risk culture, the risk management may not be able to be performed properly. Therefore, government should provide sufficient disaster education, raise the public's crisis awareness and establish risk culture, and the public should also learn self-protection, self-rescue and participate in community-based flood risk management.

In order to evaluate the effectiveness and outcomes of structural and non-structural measures during a flood event, this study employed an Agent-Based Model (ABM), NetLogo, to analyse the possible actions, reactions and interactions of autonomous individuals and the environment. An evacuation model, a 2D overland flow model and an inundation-agent coupled model combining the first two models were built in the ABM.

- The evacuation model is designed for the agent simulations to investigate possible evacuation process during flood and the effect of risk maps, flood maps and the warning alarm. A historical event in Nice was selected as case study. The rudimentary model outputs showed the capability of generating plausible outcomes of the evacuation process.

- The results showed that the risk/flood maps and the warning alarm timing were important, and the former affect the performance more than the latter in this study. Evacuees with the maps could make a detour around high-risk area, whilst the others would chose the shortest route towards the shelter, potentially putting themselves in danger.
- The 2D overland flow model was designed for inundation simulations, adopting the concept of cellular automata (CA), which redistributed water based on simple rules instead of solving complex physics equations. Three UK EA benchmark tests (Test 2, Test 4, and Test 8A) and two historical events in Magnan area in Nice (France) and in Dahu area in Taipei (Taiwan) were chosen as case study. The results showed that the model can generate promising model outputs, by comparing the model outputs with the other models' from the benchmark tests and with the observation.
- For the UK EA benchmark tests, the inundation predictions of the CA 2D model shared the same pattern with the others', and no meaningful discrepancy in the simulated water levels and velocities occurred.
- For the historical event in Magnan area, the flood maps and the water depths predicted by the CA 2D model were almost identical to those predicted by the MIKE model, with only subtle difference. On the contrary, for the historical event in Dahu area, the results only showed satisfactory agreement between the model outputs and the observation, since the model did not capture the accidental malfunction of part of the sewer systems.
- The evacuation model was designed for agent simulations focusing on agents, and the CA 2D overland flow model was designed for inundation simulations focusing on cells. Two models could be easily combined together to form a coupled model for inundation-agent coupled simulation.
- The results of the inundation-agent coupled model revealed its capability of conducting inundation simulation and the potential for generating plausible outcomes of the interaction between flood water, response strategies and human behaviour in a complex system during a flood event.
- The coupled ABM was also used to evaluate the performance of the flood risk management and the community-based flood risk management of Dahu area. In the study, by comparing the outcomes of the different strategies, the results showed that the combination of all the strategies could synergise and effectively lowered the risk regarding the flood extent and flood depth, but the evacuation processes were mainly affected by the consideration of the maps. Since the flooded areas of all the scenarios were mainly located in the high-risk areas on the risk map, evacuation could proceed without posing a threat to life as long as

the evacuees stayed away from high-risk areas.

- The coupled model can be a valuable tool for investigating and improving existing disaster response strategies and for enhancing community-based flood risk management through serious gaming.
- A concept of a DSS integrating with the coupled ABM for flood risk management is proposed for providing suggestions of strategies. The coupled ABM can also be integrated within an existing DSS. Despite the possible advantages in various fields, there were still many gaps inside the structure to be filled. The most important issue about the operation of the DSS was the way of format standardisation, communication and interoperability between the various existing components.

7.2 Future Perspectives

In the study, the prototype of the coupled ABM was developed, with only basic and simple capability, and the model could be further improved. Furthermore, the integration of the coupled ABM within existing DSSs can be promoted and thus proceed in the future.

For the ABM and the evacuation modelling:

- In the study, only one shelter was involved in the model, with infinite capacity for all the evacuees, which could not reflect the reality. The model can include both evacuation and invacuation (Shelter-in-Place) strategies with multiple shelters and with limited capacity. Meanwhile, evacuees may have their own preference for certain shelters and some specific routes.
- Every evacuee was generated uniformly and assigned the same parameters. Many other factors including evacuee's age, gender, height, weight, initial walking speed, etc., will increase the diversity in the ABM.
- Psychological factors such as panic, bandwagon effect, disobedience, and defiance, learning, cooperation, improvisation and so on are worth being included in the ABM and being improved in the future.
- Evacuation drills can be carried out in the study area to check the difference between model prediction and the observation, since there are no observed data so far for model validation.

For the CA hydraulic model in ABM and the hydraulic modelling:

- In the study, the UK EA benchmark tests were rather ideal and the historical events were comparatively simple. More other cases with complex factors should be included in the future to check the capability and the limitation of the inundation model.
- More factors can be developed in the model, such as 1D hydraulic model for rivers and pipe lines, low impact developments (LIDs), specific standard operating procedures (SOPs) for structural measures (pumps, retention/detention ponds, water gates), etc.

For the coupled ABM and the possible applications:

- More different kinds of agent can be included to represent the reality, such as rescue teams, responders, cars, etc. For example, rescue teams can reach trapped people and save them; responders will actually stack sandbags gradually and meanwhile they can be also trapped by flood water if they cannot finish their job in time; evacuees may move on their feet or by their cars, and meanwhile some people may also walk towards their cars for evacuation.

- NetLogo software cannot perform any parallel processing, and hence computational efficiency should be improved in other ways to meet the needs of crisis response. The improvement can be achieved by applying better algorithms or directly using better hardware.
- Different groups of people can be invited to play the coupled ABM to get feedback from them, including students, local residents, first responders, local authorities, experts from different regions and so on.
- The feasibility of integration of the coupled ABM and existing DSSs was just theoretically evaluated in the study. Further detailed technical information and discussion with the people in charge of the DSS are needed.

Reference

1. 20 minutes. (2020, October 2). Tempête Alex : Les Alpes-Maritimes en vigilance rouge « pluie-inondation », 13 départements en alerte. [Storm Alex: The Alpes-Maritimes in red vigilance "rain-flood", 13 departments on alert]. 20 minutes. Retrieved January 13, 2024, from: https://www.20minutes.fr/societe/2875599-20201002-tempete-alex-alpes-maritimes-places-vigilance-rouge-pluie-inondation-13-departements-alerte
2. Abt, S. R., Wittier, R. J., Taylor, A., & Love, D. J. (1989). Human stability in a high flood hazard zone. *JAWRA Journal of the American Water Resources Association*, 25(4), 881-890. https://doi.org/10.1111/j.1752-1688.1989.tb05404.x
3. Agência de Cooperação Internacional do Japão (2011). Estudo Preparatório para o Projeto de Prevenção e Mitigação de Desastres na Bacia do Rio Itajaí. [Preparatory Study for the Disaster Prevention and Mitigation Project in the Itajaí River Basin]. Santa Catarina: Governo do Estado de Santa Catarina
4. Agencia Estatal de Meteorología (2022). Umbrales y niveles de aviso. [Thresholds and warning levels]. Madrid: Agencia Estatal de Meteorología.
5. Ahimbisibwe, V., Groeneveld, J., Lippe, M., Tumwebaze, S. B., Auch, E., & Berger, U. (2021). Understanding smallholder farmer decision making in forest land restoration using agent-based modeling. *Socio-Environmental Systems Modelling, 3*, 18036-18036. https://doi.org/10.18174/sesmo.2021a18036
6. Akwafuo, S. E., Abah, T., & Oppong, J. R. (2020). Evaluation of the Burden and Intervention Strat-effigies of TB-HIV Co-Infection in West Africa. *J Infect Dis Epidemiol, 6*, 143. https://doi.org/10.23937/2474-3658/1510143
7. Alertablu, Defesa Civil Blumenau (n.d.). AlertaBlu. Prefeitura Municipal de Blumenau. Retrieved January 13, 2024, from: https://alertablu.blumenau.sc.gov.br/c/institucional
8. Ali, A. B. (2018). An assessment of Jeddah's hydraulic protection and management systems of flood. *Open Access Library Journal*, 5(02), 1. http://www.scirp.org/journal/PaperInformation.aspx?PaperID=82777&#abstract
9. Altez, R. (2010). Lo que puede aprenderse de un desastre de muertes masivas: la experiencia de Vargas. [What can be learned from a mass death disaster: Vargas' experience]. *Lecciones Aprendidas del Desastre de Vargas*. Universidad Central de Venezuela.

10. Amadae, S. M., & Watts, C. J. (2023). Red queen and red king effects in cultural agent-based modeling: Hawk dove binary and systemic discrimination. *The Journal of Mathematical Sociology*, 47(4), 283-310. https://doi.org/10.1080/0022250X.2021.2012668
11. An, G., Mi, Q., Dutta-Moscato, J., & Vodovotz, Y. (2009). Agent-based models in translational systems biology. *Wiley Interdisciplinary Reviews: Systems Biology and Medicine*, 1(2), 159-171. https://doi.org/10.1002/wsbm.45
12. Andjelkovic, I. (2001) *Guidelines on non-structural measures in urban flood management*. International Hydrological Programme. Technical Documents in Hydrology, No.50, United Nations Educational, Scientific and Cultural Organization (UNESCO), Paris
13. Ando, K., Ota, H., & Oki, T. (1988). Forecasting the flow of people. *Railway Research Review*, 45(8), 8-14.
14. Anzaldi, G. (2014). A holistic ICT solution to improve matching between supply and demand over the water supply distribution chain. *Journal of Sustainable Development of Energy, Water and Environment Systems*, 2(4), 362-375. https://doi.org/10.13044/j.sdewes.2014.02.0029
15. Basterra, T. (2017, June 4). Las inundaciones de 2010, el peor momento de la historia del hospital. [The 2010 floods, the worst moment in the hospital's history]. El Comercio. Retrieved January 13, 2024, from: https://www.elcomercio.es/asturias/oriente/201706/04/inundaciones-2010-peor-momento-20170604014946-v.html?ref=https%3A%2F%2Fwww.google.com%2F
16. Batica, J. (2015). *Methodology for flood resilience assessment in urban environments and mitigation strategy development* (Doctoral dissertation, Université Nice Sophia Antipolis). https://tel.archives-ouvertes.fr/tel-01159935
17. BBC News (2010, January 3). Brazil landslides 'may close nuclear plants'. BBC News. Retrieve January 13, 2024, from: http://news.bbc.co.uk/2/hi/americas/8438842.stm
18. BBC News. (2022, August 9). South Korea's capital Seoul hit with serious floods. BBC News. Retrieved January 13, 2024, from: https://www.bbc.co.uk/newsround/62479716

19. Bennet, N.D., Croke, B.F.W., Guariso, G., Guillaume, J.H.A., Hamilton, S.H., Jakeman, A.J., Marsili-Libelli, S., Newham, L. T. H., Norton, J. P., Perrin, C., Pierce, S. A., Robson, B., Seppelt, R., Voinov, A. A. Fath, B.D. Andreassian, V. (2013). Characterising performance of environmental models. *Environmental Modelling & Software*. 40(0), 1-20. https://doi.org/10.1016/j.envsoft.2012.09.011
20. Bernardini, G., Quagliarini, E., D'Orazio, M., & Brocchini, M. (2020). Towards the simulation of flood evacuation in urban scenarios: Experiments to estimate human motion speed in floodwaters. *Safety science*, 123, 104563. https://doi.org/10.1016/j.ssci.2019.104563
21. Binacchi, F. (2019, March 13). Inondations mortelles en 2015: La ville de Mandelieu va porter plainte après les propos «irresponsables» d'une association. [Deadly floods in 2015: The city of Mandelieu will file a complaint after the "irresponsible" remarks of an association]. 20minutes. Retrieved January 13, 2024, from: https://www.20minutes.fr/justice/2471483-20190313-inondations-mortelles-2015-ville-mandelieu-va-porter-plainte-apres-propos-irresponsables-association
22. Binacchi, F. (2021a, September 22). Tempête Alex dans les Alpes-Maritimes : un an après, l'enquête est close et les disparus vont être déclarés décédés. [Storm Alex in the Alpes-Maritimes: a year later, the investigation is closed and the missing will be declared dead]. 20minutes. Retrieved January 13, 2024, from: https://www.20minutes.fr/justice/3130531-20210922-tempete-alex-alpes-maritimes-an-apres-enquete-close-disparus-vont-etre-declares-decedes
23. Binacchi, F. (2021b, September 30). Alpes-Maritimes : alors que « la tempête Alex a provoqué des fragilités », la préfecture appelle à la prudence dans les vallées. [Alpes-Maritimes: while "storm Alex caused weaknesses", the prefecture calls for caution in the valleys]. 20minutes. Retrieved January 13, 2024, from: https://www.20minutes.fr/nice/3136411-20210930-alpes-maritimes-alors-tempete-alex-provoque-fragilites-prefecture-appelle-prudence-vallees
24. Bredl, K., Groß, A., Hünniger, J., & Fleischer, J. (2012). The Avatar as a Knowledge Worker? How Immersive 3D Virtual Environments may Foster Knowledge Acquisition. *Electronic Journal of Knowledge Management*, 10(1), pp15-25.

25. C40 Cities Climate Leadership Group. (2015, October). Cities100: Rio De Janeiro - Reservoirs and River Diversion Prevent Flooding. C40 Cities Climate Leadership Group. Retrieved January 13, 2024, from: https://www.c40.org/case-studies/cities100-rio-de-janeiro-reservoirs-and-river-diversion-prevent-flooding/
26. Central Weather Administration. (n.d.). Weather Warning. Central Weather Administration. Retrieved January 13, 2024, from: https://www.cwa.gov.tw/V8/E/P/Warning/FIFOWS.html
27. Center for Weather Climate and Disaster Research, National Taiwan University. (2019). 108 Nián tái běi shì shuǐ zāi zì zhǔ rèn xìng fang zāi shè qū tuī dòng gong zuò qí mò bào gào. [Final report of 2019. Promotion of Autonomous Flood Resilient Communities of Taipei City]. Hydraulic Engineering Office, Public Works Departments, Taipei City Government.
28. Center for Weather Climate and Disaster Research, National Taiwan University. (2021). 110 Nián tái běi shì shuǐ zāi zì zhǔ rèn xìng fang zāi shè qū tuī dòng gong zuò qí mò bào gào. [Final report of 2019. Promotion of Autonomous Flood Resilient Communities of Taipei City]. Hydraulic Engineering Office, Public Works Departments, Taipei City Government.
29. Centre for Research on the Epidemiology of Disasters. (2020). *The Human Cost of Disasters: An overview of the last 20 years 2000-2019*. United Nations Office for Disaster Risk Reduction.
30. Chang, L. C., Chang, F. J., Yang, S. N., Kao, I. F., Ku, Y. Y., Kuo, C. L., & Amin, I. M. Z. B. M. (2018). Building an intelligent hydroinformatics integration platform for regional flood inundation warning systems. *Water*, 11(1), 9. https://doi.org/10.3390/w11010009
31. Chang, T. J., Yu, H. L., Wang, C. H., & Chen, A. S. (2021). Overland-gully-sewer (2D-1D-1D) urban inundation modeling based on cellular automata framework. *Journal of Hydrology*, 603, 127001. https://doi.org/10.1016/j.jhydrol.2021.127001
32. Chanson, H., Brown, R., & McIntosh, D. (2014). Human body stability in floodwaters: the 2011 flood in Brisbane CBD. In *Hydraulic Structures and Society-Engineering Challenges and Extremes: Proceedings of the 5th IAHR International Symposium on Hydraulic Structures (ISHS2014)* (pp. 1-9). The University of Queensland. https://doi.org/10.14264/uql.2014.48

33. Chichorro, F., Correia, L., & Cardoso, P. (2022). Biological traits interact with human threats to drive extinctions: A modelling study. *Ecological Informatics*, 69, 101604. https://doi.org/10.1016/j.ecoinf.2022.101604
34. City of New York. (n.d.-a). The Battery Coastal Resilience. City of New York. Retrieved January 13, 2024, from: https://www.nyc.gov/site/lmcr/progress/battery-coastal-resilience.page
35. City of New York. (n.d.-b). Resiliency and Flood Protection. City of New York. Retrieved January 13, 2024, from: https://www.nyc.gov/site/escr/about/resiliency-and-flood-protection.page
36. City of New York Mayor's Office of Recovery and Resiliency. (2015). Appeal of FEMA's preliminary flood insurance rate maps for New York City. New York: City of New York Mayor's Office of Recovery and Resiliency.
37. Cogoni, F., Bernard, D., Kazhen, R., Valitutti, S., Lobjois, V., & Cussat-Blanc, S. (2023). ISiCell: involving biologists in the design process of agent-based models in cell biology. *bioRxiv*, 2023-06. https://doi.org/10.1101/2023.06.30.547165
38. Communauté de la Riviera Française. (2019, October 23). PLUIE & INONDATION : LES 8 BONS COMPORTEMENTS A ADOPTER [RAIN and FLOOD: THE 8 GOOD BEHAVIORS TO ADOPT]. Communauté de la Riviera Française. Retrieved January 13, 2024, from : https://www.riviera-francaise.fr/les-actualites/item/68-pluie-inondation-les-8-bons-comportements-a-adopter
39. Courtel, F., López, J. L., & Salcedo, A. (2010). El sistema de alerta temprana para Catia La Mar: La experiencia del Proyecto PREDERES. [The early warning system for Catia La Mar: The experience of the PREDERES Project]. *Lecciones Aprendidas del Desastre de Vargas*. Universidad Central de Venezuela.
40. Crouse, K. N., Desai, N. P., Cassidy, K. A., Stahler, E. E., Lehman, C. L., & Wilson, M. L. (2022). Larger territories reduce mortality risk for chimpanzees, wolves, and agents: Multiple lines of evidence in a model validation framework. *Ecological Modelling, 471*, 110063. https://doi.org/10.1016/j.ecolmodel.2022.110063

41. Cuellar, B. (2020, February 15) A cinco años del 15-F: memoria de la tragedia en Sierras Chicas. [Five years after 15-F: memory of the tragedy in Sierras Chicas]. La Voz. Retrieved January 13, 2024, from: https://www.lavoz.com.ar/ciudadanos/a-cinco-anos-del-15-f-memoria-de-tragedia-en-sierras-chicas/
42. Cyril Bottollier-Lemallaz. (2023, October 23). Bus emportés par la tempête Aline près de Nice : "Une erreur humaine" [Buses swept away by storm Aline near Nice: “A human error”]. actu Nice. Retrieved January 13, 2024, from: https://actu.fr/provence-alpes-cote-d-azur/saint-martin-vesubie_06127/bus-emportes-par-la-tempete-aline-pres-de-nice-une-erreur-humaine_60242434.html
43. Daghriri, T., & Ozmen, O. (2021). Quantifying the Effects of Social Distancing on the Spread of COVID-19. *International journal of environmental research and public health, 18*(11), 5566. https://doi.org/10.3390/ijerph18115566
44. Damien Allemand. (2023a, October 10). Alerte rouge: les impressionnantes images des bus de la Métropole de Nice pris au piège par la montée des eaux [Red alert: impressive images of Nice Metropolis buses trapped by rising waters]. Nice Matin. Retrieved January 13, 2024, from: https://www.nicematin.com/faits-divers/alerte-rouge-les-impressionnantes-images-des-bus-de-la-metropole-de-nice-pris-au-piege-par-la-montee-des-eaux-880483?utm_content=link&utm_term=Page.NiceMatin&utm_campaign=facebook&utm_source=nonli&utm_medium=Social%20media
45. Damien Allemand. (2023b, November 2). Tempête Ciaran: au moins deux morts et 16 blessés, 820.000 foyers toujours dans le noir... suivez notre direct [Storm Ciaran: at least two dead and 16 injured, 820,000 homes still in the dark... follow our live stream]. Nice Matin. Retrieved January 13, 2024, from : https://www.nicematin.com/meteo/tempete-ciaran-12-million-de-foyers-prives-delectricite-au-moins-un-mort-le-var-et-les-alpes-maritimes-en-alerte-orange-notre-direct-882978?utm_content=photo&utm_term=Page.NiceMatin&utm_campaign=facebook&utm_source=nonli&utm_medium=Social%20media

46. Damien Allemand. (2023c, November 2). Tempête Ciaran: la ville de Nice annonce la fermeture des plages ce jeudi à 14h [Storm Ciaran: the city of Nice announces the closure of the beaches this Thursday at 2 p.m.]. Nice Matin. Retrieved January 13, 2024, from: https://www.nicematin.com/meteo/tempete-ciaran-la-ville-de-nice-annonce-la-fermeture-des-plages-ce-jeudi-a-14h-882997?utm_content=link&utm_term=Page.NiceMatin&utm_campaign=facebook&utm_source=nonli&utm_medium=Social%20media
47. Danish Hydraulic Institute (DHI). (2014) MIKE URBAN Collection System User Guide
48. Danish Hydraulic Institute (DHI). (2016a) MIKE FLOOD 1D-2D Modelling - User Manual
49. Danish Hydraulic Institute (DHI). (2016b). MIKE 21 Flow Model & MIKE 21 Flood Screening Tool – Hydrodynamic Module
50. Dano, U. L. (2020). Flash flood impact assessment in Jeddah City: An analytic hierarchy process approach. *Hydrology*, 7(1), 10. https://doi.org/10.3390/hydrology7010010
51. Davies, R. (2015, February 16) 320 Mm of Rain in 12 Hours – 6 Killed in Floods in Córdoba, Argentina. Floodlist. Retrieved January 13, 2024, from: https://floodlist.com/america/320-mm-rain-6-killed-floods-cordoba-argentina
52. Dawson, R. J., Peppe, R., & Wang, M. (2011). An agent-based model for risk-based flood incident management. *Natural hazards, 59*(1), 167-189. https://doi.org/10.1007/s11069-011-9745-4
53. de Oliveira Simoyama, F., Sarti, F. M., & Battisti, M. C. G. (2022). Effects of disclosing inspection scores of health facilities. *Socio-Economic Planning Sciences, 81*, 101183. https://doi.org/10.1016/j.seps.2021.101183
54. Département des Alpes-Maritimes. (2021). Tempête Alex : 1 an après le drame. [Storm Alex: 1 year after the tragedy]. Retrieved January 13, 2024, from: https://www.departement06.fr/actualites-24/tempete-alex-1-an-apres-le-drame-45753.html?cHash=67c5bff13d47e7c237166282162b451f
55. Dias, C., Abd Rahman, N., & Zaiter, A. (2021). Evacuation under flooded conditions: Experimental investigation of the influence of water depth on walking behaviors. *International Journal of Disaster Risk Reduction*, 58, 102192. https://doi.org/10.1016/j.ijdrr.2021.102192

56. Direction de la Prévention et de la Gestion des Risques. (2017). *Document d'information communal sur les risques majeurs*. [Municipal information document on major risks] Nice: Ville de Nice
57. Dorgigné, Y., Abily, M., Salvan, L., & Gourbesville, P. (2018). Creation and Life of an Operational Crisis Management Centre in Nice Metropolis: Consolidation of Flood Events Handling Using Feedbacks Following the 3rd October Flood Event. In *Advances in Hydroinformatics: SimHydro 2017-Choosing the Right Model in Applied Hydraulics* (pp. 483-496). Springer Singapore. https://doi.org/10.1007/978-981-10-7218-5_34
58. Drager, K. H., Lovas, G. G., Wiklund, J. O., & Soma, H. (1993). Objectives of Modelling Evacuation from Buildings during Accidents: Some Path-model Scenarios. *Journal of Contingencies and Crisis Management*, 1(4), 207-214. https://doi.org/10.1111/j.1468-5973.1993.tb00112.x
59. Dressler, G., Müller, B., Frank, K., & Kuhlicke, C. (2016). Towards thresholds of disaster management performance under demographic change: exploring functional relationships using agent-based modeling. *Natural Hazards and Earth System Sciences, 16*(10), 2287-2301. https://doi.org/10.5194/nhess-16-2287-2016
60. Emilie Moulin. (2023, November 2). Le boulevard Maréchal Juin submergé par les vagues à Antibes [Boulevard Maréchal Juin submerged by waves in Antibes]. Nice Matin. Retrieved January 13, 2024, from : https://www.nicematin.com/meteo/tempete-ciaran-le-boulevard-marechal-juin-submerge-par-les-vagues-a-antibes-883032?utm_content=link&utm_term=Page.NiceMatin&utm_campaign=facebook&utm_source=nonli&utm_medium=Social%20media
61. European Commission's Directorate-General for European Civil Protection and Humanitarian Aid Operations (2022, October 28). Nigeria | Floods – DG ECHO Daily Map | 28/10/2022. European Commission's Directorate-General for European Civil Protection and Humanitarian Aid Operations. Retrieved January 13, 2024, from: https://reliefweb.int/map/nigeria/nigeria-floods-dg-echo-daily-map-28102022

62. Facultad de Ingenieria, Universidad Nacional de La Plata (2013). Estudio sobre la inundación ocurrida los días 2 y 3 de abril de 2013 en las ciudades de La Plata, Berisso y Ensenada. [Study on the flood that occurred on April 2 and 3, 2013 in the cities of La Plata, Berisso and Ensenada]. La Plata: Universidad Nacional de La Plata http://sedici.unlp.edu.ar/handle/10915/27334
63. Flache, A., Mäs, M., & Keijzer, M. A. (2022). Computational approaches in rigorous sociology: agent-based computational modeling and computational social science. *Handbook of Sociological Science*, 57-72.
64. Folha de S.Paulo (2010, April 9). Bombeiros confirmam 184 mortes em decorrência das chuvas no Rio. [Firefighters confirm 184 deaths due to rain in Rio]. Folha de S.Paulo. Retrieved January 13, 2024, from: https://www1.folha.uol.com.br/cotidiano/2010/04/718546-bombeiros-confirmam-184-mortes-em-decorrencia-das-chuvas-no-rio.shtml
65. French Government. (2020). Les conséquences de la tempête Alex dans les Alpes-Maritimes. [The consequences of storm Alex in the Alpes-Maritimes]. Retrieved December 15, 2023, from: https://www.gouvernement.fr/conseil-des-ministres/2020-10-07/les-consequences-de-la-tempete-alex-dans-les-alpes-maritimes
66. Fuchs-Kittowski, F., Simroth, S., Himberger, S., Fischer, F., & Schley, M. (2012). A Content Platform for Smartphone-based Mobile Augmented Reality. *EnviroInfo* (pp. 403-411). Dessau, Germany
67. Fujimi, T., & Fujimura, K. (2020). Testing public interventions for flash flood evacuation through environmental and social cues: The merit of virtual reality experiments. *International Journal of Disaster Risk Reduction*, 50, 101690. https://doi.org/10.1016/j.ijdrr.2020.101690
68. Ghimire, B., Chen, A. S., Guidolin, M., Keedwell, E. C., Djordjević, S., & Savić, D. A. (2013). Formulation of a fast 2D urban pluvial flood model using a cellular automata approach. *Journal of Hydroinformatics*, 15(3), 676-686. https://doi.org/10.1016/j.mex.2023.102202
69. Gourbesville, P., Du, M., Zavattero, E., & Ma, Q. (2016). DSS architecture for water uses management. *Procedia engineering*, 154, 928-935. https://doi.org/10.1016/j.proeng.2016.07.512

70. Gourbesville, P., Du, M., Zavattero, E., Ma, Q., & Gaetano, M. (2018). Decision support system architecture for real-time water management. *Advances in Hydroinformatics* (pp. 259-272). Springer, Singapore. https://doi.org/10.1007/978-981-10-7218-5_17
71. Gourbesville, P., Gaetano, M., & Ma, Q. (2018). AquaVar: real time models for underground and surface waters management at catchment scale. *EPiC Ser Eng*, 3, 836-843.
72. Gourbesville, P., Tallé, H. A., & Ghulami, M. (2022). AquaVar: High Performance Computing for Real Time Water Management. *Proceedings of the 39th IAHR World Congress* https://doi.org/10.3850/IAHR-39WC2521711920221397
73. Gourbesville, P. (2023). Added value of deterministic models in Decision Support Systems. In *IOP Conference Series: Earth and Environmental Science* (Vol. 1136, No. 1, p. 012011). IOP Publishing. https://doi.org/10.1088/1755-1315/1136/1/012011
74. Gouvernement, [@gouvernementFR]. (2016, June 2). [X]. X. Retrieved January 13, 2024, from: https://twitter.com/gouvernementFR/status/738276915715440640
75. Grases, J. Amundaray, J, Malaver, A., Feliziani, P., Franceschi, L., and Rodríguez, J. (2000). Efectos de las lluvias caídas en Venezuela en Diciembre de 1999. [Effects of the rains that fell in Venezuela in December 1999]. Informe Comisión. OCHA-PNUD-CAF.
76. Grimm, V., & Railsback, S. F. (2005). *Individual-based modeling and ecology*. Princeton university press.
77. Grimm, V., Berger, U., Bastiansen, F., Eliassen, S., Ginot, V., Giske, J., ... & DeAngelis, D. L. (2006). A standard protocol for describing individual-based and agent-based models. *Ecological modelling*, *198*(1-2), 115-126. https://doi.org/10.1016/j.ecolmodel.2006.04.023
78. Grimm, V., Berger, U., DeAngelis, D. L., Polhill, J. G., Giske, J., & Railsback, S. F. (2010). The ODD protocol: a review and first update. *Ecological modelling*, *221*(23), 2760-2768. https://doi.org/10.1016/j.ecolmodel.2010.08.019
79. Grimm, V., Railsback, S. F., Vincenot, C. E., Berger, U., Gallagher, C., DeAngelis, D. L., ... & Ayllón, D. (2020). The ODD protocol for describing agent-based and other simulation models: A second update to improve clarity, replication, and structural realism. *Journal of Artificial Societies and Social Simulation*, *23*(2). http://dx.doi.org/10.18564/jasss.4259

80. Groupe URD. (2020). Évaluation en temps réel de la réponse à la tempête Alex dans les Alpes-Maritimes - 15 et 16 octobre 2020. [Real-time assessment of the response to storm Alex in the Alpes-Maritimes - October 15 and 16, 2020]. Retrieved January 13, 2024, from: https://en.calameo.com/read/00368008687178aa8fdc5
81. Groupe URD. (2021a). Évaluation en temps réel de la réponse aux inondations du 4 octobre 2020 dans les Alpes-Maritimes - mission n°2 - du 2 au 6 décembre 2020. [Real-time evaluation of the response to the floods of October 4, 2020 in the Alpes-Maritimes - mission n°2 - from December 2 to 6, 2020]. Retrieved January 13, 2024, from: https://www.urd.org/wp-content/uploads/2021/02/Rapport-ETR2_Roya_-2021_FINAL.pdf
82. Groupe URD. (2021b). Réponses solidaires : le « laboratoire » de la Roya. [Solidarity responses: the "laboratory" of the Roya]. Retrieved January 13, 2024, from: https://www.urd.org/fr/revue_humanitaires/reponses-solidaires-le-laboratoire-de-la-roya/
83. Guidolin, M., Chen, A. S., Ghimire, B., Keedwell, E. C., Djordjević, S., & Savić, D. A. (2016). A weighted cellular automata 2D inundation model for rapid flood analysis. *Environmental Modelling & Software*, 84, 378-394. https://doi.org/10.1016/j.envsoft.2016.07.008
84. Haynes, P. S., & Lange, E. (2016a). In-situ flood visualisation using mobile AR. *2016 IEEE Symposium on 3D User Interfaces (3DUI)* (pp. 243-244). IEEE. https://doi.org/10.1109/3DUI.2016.7460061
85. Haynes, P., & Lange, E. (2016b). Mobile augmented reality for flood visualisation in urban riverside landscapes. *JoDLA–Journal of Digital Landscape Architecture*, 1, 254-262. http://dx.doi.org/10.14627/537612029
86. Haynes, P., Hehl-Lange, S., & Lange, E. (2018). Mobile augmented reality for flood visualisation. *Environmental modelling & software*, 109, 380-389. https://doi.org/10.1016/j.envsoft.2018.05.012
87. Hinch, R., Probert, W. J., Nurtay, A., Kendall, M., Wymant, C., Hall, M., ... & Fraser, C. (2021). OpenABM-Covid19—An agent-based model for non-pharmaceutical interventions against COVID-19 including contact tracing. *PLOS Computational Biology*, 17(7), e1009146. https://doi.org/10.1371/journal.pcbi.1009146

88. Hirabayashi, Y., Mahendran, R., Koirala, S. et al. (2013). Global flood risk under climate change. *Nature Climate Change* 3, 816–821 https://doi.org/10.1038/nclimate1911
89. Hsu, M. H., Chen, S. H., & Chang, T. J. (2000). Inundation simulation for urban drainage basin with storm sewer system. *Journal of hydrology*, 234(1-2), 21-37. https://doi.org/10.1016/S0022-1694(00)00237-7
90. Hsu, H. M., & Gourbesville, P. (2022). Applications of non-structural measures and self-protection against flood in urban areas in Taiwan and in France. In *Proc. 39th IAHR World Congress* (pp. 19-24). https://doi.org/10.3850/IAHR-39WC2521711920221389
91. Hsu, H. M., & Gourbesville, P. (2023). Introduction of integrated decision support system for flood disaster management. In *IOP Conference Series: Earth and Environmental Science* (Vol. 1136, No. 1, p. 012019). IOP Publishing. https://doi.org/10.1088/1755-1315/1136/1/012019
92. Hydraulic Engineering Office, Public Works Departments, Taipei City Government. (2021). tái běi shì nèi hú qū dà hú lǐ jiǎn yì shuǐ zāi shū sàn bì nàn lù xiàn dì tú. [The Simple Flood Evacuation Route Map of Dahu Village, Neihu District, Taipei City]. Water Resources Agency. Retrieved January 13, 2024, from: https://wrafpc.tw/web/community/2021/08/12/%E8%87%BA%E5%8C%97%E5%B8%82%E5%85%A7%E6%B9%96%E5%8D%80%E5%A4%A7%E6%B9%96%E9%87%8C/
93. Hydraulic Engineering Office, Public Works Departments, Taipei City Government. (2022). pái shuǐ fáng hóng shè shī. [Drainage and flood control facilities]. Taipei City Government. Retrieved January 13, 2024, from: https://heo.gov.taipei/cp.aspx?n=74868ADCB1ECC932

94. Hydraulic Engineering Office, Public Works Departments, Taipei City Government. (2023). gōng mín cān yù huì yì zī xùn: xīng bàn běn fǔ 112 nián dù `mǐ fěn kēng xī zhōu biān pái shuǐ gǎi shàn gong chéng (dà hú shān zhuāng jiē tiáo hóng chén shā chí B chí)' dì 2 cì gōng tīng huì. [Citizen Participation Meeting Information: The second public hearing on the "Drainage Improvement Project around Mifenkeng Creek (Dahushanzhuang Street Flood Diversion and Retention Pond B)" was held in 2023.]. Taipei City Government. Retrieved January 13, 2024, from: https://heo.gov.taipei/News_Content.aspx?n=1C35353E4DE6D317&sms=59AD6E6606F6002F&s=9A610A102706BBB7
95. Hydraulic Engineering Office, Public Works Departments, Taipei City Government. (n.d.). dà gōu xī sheng tài zhì shuǐ yuan qū [Dagouxi Ecological Waterfront Park]. Taipei City Government. Retrieved January 13, 2024, from: https://heo.gov.taipei/cp.aspx?n=DCE0CC34F327F43A
96. International Federation of Red Cross and Red Crescent Societies (2022). Emergency Plan of Action (EPoA) Nigeria: Floods Anticipation. International Federation of Red Cross and Red Crescent Societies. Retrieved January 13, 2024, from: https://reliefweb.int/report/nigeria/nigeria-floods-anticipation-emergency-plan-action-dref-operation-ndeg-mdrng034
97. International Standards Organisation. (2012). Societal security—business continuity management systems – Requirements. ISO 22301:2012, London, British Standards Institution
98. International Organization for Standardization. (2018). Risk management–Principles and guidelines. *International Organization for Standardization, Geneva, Switzerland.*
99. Ishigaki, T., Kawanaka, R., Onishi, Y., Shimada, H., Toda, K., Baba, Y. (2009). Assessment of Safety on Evacuating Route During Underground Flooding. In: *Advances in Water Resources and Hydraulic Engineering*. Springer, Berlin, Heidelberg. https://doi.org/10.1007/978-3-540-89465-0_27
100. Jocteur Monrozier, A. (2021, September 30). Il y a un an, la tempête Alex ravageait les vallées de la Vésubie et de la Roya. [A year ago, storm Alex ravaged the Vésubie and Roya valleys]. France Bleu. Retrieved January 13, 2024, from: https://www.francebleu.fr/infos/meteo/il-y-a-un-la-tempete-alex-ravageait-les-vallees-de-la-vesubie-et-de-la-roya-1632912585

101. Jonkman, S. N., & Penning-Rowsell, E. (2008). Human instability in flood flows 1. *JAWRA Journal of the American Water Resources Association*, 44(5), 1208-1218. https://doi.org/10.1111/j.1752-1688.2008.00217.x
102. Kang, J. G. (2017, July 24). 1 sigan pog-ue 2345 chae chimsu…'3 dae dosi' incheon ssugdaebat. [2,345 houses flooded in one hour of heavy rain... 'three major cities' Incheon wilderness]. Yonhap News. Retrieved January 13, 2024, from: https://www.hankyung.com/society/article/201707248032Y
103. Karvonen, R.A., A. Hepojoki, H.K. Huhta, and A. Louhio (2000) *The Use of Physical Models in Dam-Break Analysis. RESCDAM Final Report.* Helsinki University of Technology, Helsinki, Finland.
104. Kerr, C. C., Stuart, R. M., Mistry, D., Abeysuriya, R. G., Rosenfeld, K., Hart, G. R., ... & Klein, D. J. (2021). Covasim: an agent-based model of COVID-19 dynamics and interventions. *PLOS Computational Biology*, 17(7), e1009149. https://doi.org/10.1371/journal.pcbi.1009149
105. Kim, Y. B. (2021, September 28). incheonsi, chimsu daeeung wihae seumateu hasudo guchug naseo. [Incheon City builds a smart sewer system to deal with floods]. Incheonin. Retrieved January 13, 2024, from: https://www.incheonin.com/news/articleView.html?idxno=82757
106. Kitchin, R. (2014). The real-time city? Big data and smart urbanism. *GeoJournal*, 79, 1-14. https://doi.org/10.1007/s10708-013-9516-8
107. Lagrange, B. (2020). Tempête Alex dans les Alpes-Maritimes : bilan d'une mobilisation hors norme. [Storm Alex in the Alpes-Maritimes: assessment of an exceptional mobilisation]. Croix-Rouge Française. Retrieved January 13, 2024, from: https://www.croix-rouge.fr/Actualite/Tempete-Alex/Tempete-Alex-dans-les-Alpes-Maritimes-bilan-d-une-mobilisation-hors-norme-2445
108. Lai, J. S., Chang, W. Y., Chan, Y. C., Kang, S. C., & Tan, Y. C. (2011). Development of a 3D virtual environment for improving public participation: Case study–The Yuansantze Flood Diversion Works Project. *Advanced Engineering Informatics*, 25(2), 208-223. https://doi.org/10.1016/j.aei.2010.05.008

109. La Nueva España. (2010, June 17). Asturias sufre la mayor inundación de su historia tras desbordarse el Nalón y el Sella. [Asturias suffers the biggest flood in its history after the Nalón and Sella overflow]. La Nueva España. Retrieved January 13, 2024, from: https://www.lne.es/asturias/2010/06/17/asturias-sufre-mayor-inundacion-historia-21319897.html
110. La Política Online (2018, March 31). En La Plata encaran la etapa final de las obras hidráulicas para evitar inundaciones. [In La Plata they face the final stage of hydraulic works to avoid flooding]. La Política Online. Retrieved January 13, 2024, from: https://www.lapoliticaonline.com/nota/112101-en-la-plata-encaran-la-etapa-final-de-las-obras-hidraulicas-para-evitar-inundaciones/
111. Lee, H. S. (2018, March 28). seoulsi, jibjunghou daebi 6300yeo gague chimsubangjisiseol seolchi musang jiwon. [Seoul City provides free support for the installation of flood prevention facilities to over 6,300 households in preparation for heavy rains]. Medical Today. Retrieved January 13, 2024, from: https://mdtoday.co.kr/news/view/179523386659148
112. Lee, S., Ha, G., Kim, H., & Kim, S. (2021). A collaborative Serious Game for fire disaster evacuation drill in Metaverse. *Journal of Platform Technology*, 9(3), 70-77.
113. Lee, H. K., Hong, W. H., & Lee, Y. H. (2019). Experimental study on the influence of water depth on the evacuation speed of elderly people in flood conditions. *International journal of disaster risk reduction*, 39, 101198. https://doi.org/10.1016/j.ijdrr.2019.101198
114. Le Figaro. (2023, November 3). Tempête Aline : l'état de catastrophe naturelle reconnu pour 10 communes des Alpes-Maritimes [Storm Aline: a state of natural disaster recognised for 10 municipalities in the Alpes-Maritimes]. Le Figaro. Retrieved January 13, 2024, from : https://www.lefigaro.fr/nice/tempete-aline-l-etat-de-catastrophe-naturelle-reconnu-pour-10-communes-des-alpes-maritimes-20231103
115. Libération. (2015, October 4). Dix-sept morts lors de violentes inondations sur la Côte d'Azur. [Seventeen dead in violent floods on the Côte d'Azur]. Libération. Retrieved January 13, 2024, from: https://www.liberation.fr/france/2015/10/04/treize-morts-lors-de-violentes-inondations-sur-la-cote-d-azur_1396768/

116. Lim, Y. H. (2021, August 24). namdong-gu, guwol 3 dong chimsupihae yebang wihan usujeolyusiseol seolchi chagsu. [Namdong-gu begins installation of rainwater retention facility to prevent flood damage in Guwol 3-dong]. Gyeongin Maeil. Retrieved January 13, 2024, from: https://www.kmaeil.com/news/articleView.html?idxno=300114
117. Liu, Y. X. (2023, July 26). jí duān qì hòu bào yǔ pín fán běi shì shí yǔ liàng chāo guò 78.8 háo mǐ néng dǎng ma? [Frequent heavy rains under extreme climate. Can Taipei City stand the rainfall exceeding 78.8 mm per hour?]. TVBS News. Retrieved January 13, 2024, from: https://news.tvbs.com.tw/life/2190540
118. López, J. L., Pérez-Hernández, D., & Courtel, F. (2010). Monitoreo y evaluación del comportamiento de las presas de retención de sedimentos en el estado Vargas. [Monitoring and evaluation of the behaviour of sediment retention dams in Vargas state]. *Lecciones Aprendidas del Desastre de Vargas*. Universidad Central de Venezuela.
119. Lovas, G. G. (1994, June). Performance Measurements of Evacuation Systems. In *Fire safety science-Proceedings of the fourth international symposium* (pp. 589-600).
120. Lynggaard-Jensen, A., Mark, O., & Gourbesville, P. (2015). ICT for urban water infrastructure. *Water for Development – Charting a Water Wise Path*, Chapter: 5, 28.
121. Mas, E., Suppasri, A., Imamura, F., & Koshimura, S. (2012). Agent-based simulation of the 2011 great east Japan earthquake/tsunami evacuation: An integrated model of tsunami inundation and evacuation. *Journal of Natural Disaster Science*, 34(1), 41-57. https://doi.org/10.2328/jnds.34.41
122. Mathilde Frénois. (2023, October 20). Après les dégâts de la tempête Aline dans les Alpes-Maritimes : «C'est comme au jeu de l'oie, on retourne à la case départ» [After the damage from storm Aline in the Alpes-Maritimes: "It's like a game of goose, we're going back to square one"]. Libération. Retrieved January 13, 2024, from : https://www.liberation.fr/societe/ville/tempete-aline-a-nice-les-secours-sur-le-pied-de-guerre-au-petit-matin-20231020_VRE7IK2X35DI7PUPJ3KR66SLRY/

123. Mérou, N. (2020, October 2). Tempête Alex : les Alpes-Maritimes en vigilance rouge, plusieurs personnes portées disparues. [Storm Alex: the Alpes-Maritimes on red alert, several people missing]. France Bleu. Retrieved January 13, 2024, from: https://www.francebleu.fr/infos/meteo/les-alpes-maritimes-passe-en-vigilance-rouge-ce-vendredi-2-octobre-2020-a-partir-de-midi-1601613490
124. Météo-France. (2015). 3 octobre 2015 Catastrophe sur la Côte d'Azur. [October 3, 2015 Disaster on the Côte d'Azur]. Retrieved January 13, 2024, from: http://pluiesextremes.meteo.fr/france-metropole/Catastrophe-sur-la-Cote-d-Azur.html
125. Météo-France. (2020a). Tempête Alex : pluies diluviennes exceptionnelles dans les Alpes-Maritimes. [Storm Alex: exceptional torrential rains in the Alpes-Maritimes]. Retrieved December 15, 2023, from: https://meteofrance.com/actualites-et-dossiers/actualites/tempete-alex-pluies-diluviennes-exceptionnelles-dans-les-alpes
126. Météo-France. (2020b). 2020: une année d'extrêmes. [2020: a year of extremes] Retrieved January 13, 2024, from: https://meteofrance.com/actualites-et-dossiers/actualites/climat/une-annee-2020-mouvementee
127. Météo-Paris. (2020, October 3). Tempête Alex : inondations catastrophiques dans les Alpes-Maritimes [Storm Alex: catastrophic flooding in the Alpes-Maritimes]. Meteo-Paris. Retrieved January 13, 2024, from : https://www.meteo-paris.com/actualites/tempete-alex-inondations-catastrophiques-dans-les-alpes-maritimes
128. Ministère de l'Intérieur. (2015). Les intempéries dans les Alpes-Maritimes et le Var. [Bad weather in the Alpes-Maritimes and the Var]. Retrieved January 13, 2024, from: https://mobile.interieur.gouv.fr/Archives/Archives-des-actualites/2015-Actualites/Les-intemperies-dans-les-Alpes-Maritimes-et-le-Var
129. Ministerio de Agricultura Alimentación y Medio Ambiente: Confederación Hidrográfica del Cantábrico (2014). Demarcación hidrográfica del cantábrico occidental memoria resumen de los mapas de peligrosidad y riesgo de inundación. [Hydrographic demarcation of the western cantábrian summary report of flood hazard and risk maps]. Ministerio de Agricultura Alimentación y Medio Ambiente: Madrid : Ministerio de Agricultura Alimentación y Medio Ambiente.

130. Mirauda, D., Erra, U., Agatiello, R., & Cerverizzo, M. (2018). Mobile augmented reality for flood events management. *Water Studies*, 47, 418-424. https://doi.org/10.2495/SDP-V13-N3-418-424
131. Mizutori, M., & Guha-Sapir, D. (2017). Economic losses, poverty and disasters 1998–2017. *United Nations office for disaster risk reduction*, 4, 9-15.
132. Mol, J. M., Botzen, W. J. W., & Blasch, J. E. (2022). After the virtual flood: Risk perceptions and flood preparedness after virtual reality risk communication. *Judgment and Decision Making*, 17(1), 189. https://doi.org/10.1017/S1930297500009074
133. Município de Itajaí (n.d.). [historical flood maps]. Município de Itajaí. Retrieved January 13, 2024, from: https://geoitajai.github.io/sie/dcitajai.html
134. Nakanishi, H., Black, J., & Suenaga, Y. (2019). Investigating the flood evacuation behaviour of older people: A case study of a rural town in Japan. *Research in Transportation Business & Management*, 30, 100376. https://doi.org/10.1016/j.rtbm.2019.100376
135. National Science and Technology Center for Disaster Reduction. (n.d.). Zāi hài qián shì dì tú [Disaster Potential Map]. National Science and Technology Center for Disaster Reduction. Retrieved January 13, 2024, from: https://dmap.ncdr.nat.gov.tw/1109/map/
136. National Science and Technology Center for Disaster Reduction. (n.d.). Guó jiā zāi hài fáng jiù kē jì zhōng xīn LINE guān fāng zhàng hào [National Science and Technology Center for Disaster Reduction Line official account]. National Science and Technology Center for Disaster Reduction. Retrieved January 13, 2024, from: https://datahub.ncdr.nat.gov.tw/incorporation
137. National Science and Technology Center for Disaster Reduction. (2021). qì hòu biàn qiān zāi hài fēng xiǎn tú [climate change disaster risk map]. Retrieved January 13, 2024, from: https://dra.ncdr.nat.gov.tw/Frontend/AdvanceTool/TotalRisk
138. National Taiwan University. (2012). *Produce, integration and application of the vulnerability and risk maps of Taiwan (1/2)*. Taipei: Water Resources Agency.
139. Néelz, S., & Pender, G. (2013). Benchmarking the latest generation of 2D hydraulic modelling packages. *Environment Agency: Bristol, UK.*

140. Nice Matin. (2023a, November 3). Tempête et intempéries: on fait le point sur l'état des routes ce vendredi dans les Alpes-Maritimes [Storm and bad weather: we take stock of the state of the roads this Friday in the Alpes-Maritimes]. Nice Matin. Retrieved January 13, 2024, from : https://www.nicematin.com/info-trafic/tempete-et-intemperies-on-fait-le-point-sur-letat-des-routes-ce-vendredi-dans-les-alpes-maritimes-883182?utm_content=link&utm_term=Page.NiceMatin&utm_campaign=facebook&utm_source=nonli&utm_medium=Social%20media
141. Nice Matin. (2023b, November 3). Un accès au tunnel Liautaud à Nice fermé à la circulation ce vendredi en raison d'une forte houle [Access to the Liautaud tunnel in Nice closed to traffic this Friday due to heavy swell]. Nice Main. Retrieved January 13, 2024, from : https://www.nicematin.com/info-trafic/un-des-acces-au-tunnel-liautaud-a-nice-ferme-a-la-circulation-ce-vendredi-en-raison-dune-forte-houle-883178?utm_content=link&utm_term=Page.NiceMatin&utm_campaign=facebook&utm_source=nonli&utm_medium=Social%20media
142. Nice Matin (2023c, November 2). Tempête Ciaran: la circulation des trains entre Nice et Vintimille a repris après des chutes de pierres sur la voie [Storm Ciaran: train traffic between Nice and Ventimiglia resumed after rock falls on the track]. Nice Matin. Retrieved January 13, 2024, from : https://www.nicematin.com/faits-divers/tempete-ciaran-la-circulation-des-trains-a-larret-entre-nice-et-vintimille-apres-des-chutes-de-pierres-sur-la-voie-883087?utm_content=link&utm_term=Page.NiceMatin&utm_campaign=facebook&utm_source=nonli&utm_medium=Social%20media
143. Nakanishi, H., Wise, S., Suenaga, Y., & Manley, E. (2020). Simulating emergencies with transport outcomes Sim (SETOSim): Application of an agent-based decision support tool to community evacuation planning. *International journal of disaster risk reduction*, 49, 101657. https://doi.org/10.1016/j.ijdrr.2020.101657
144. Oh, W. S., Yu, D. J., & Muneepeerakul, R. (2021). Efficiency-fairness trade-offs in evacuation management of urban floods: The effects of the shelter capacity and zone prioritization. *Plos one*, 16(6), e0253395. https://doi.org/10.1371/journal.pone.0253395
145. O'Shea, T., Bates, P., & Neal, J. (2020). Testing the impact of direct and indirect flood warnings on population behaviour using an agent-based model. *Natural Hazards and Earth System Sciences*, 20(8), 2281-2305. https://doi.org/10.5194/nhess-20-2281-2020

146. Pan American Health Organization (PAHO), (1999). Epidemiological Bulletin / PAHO, Vol. 20, No. 4, pp 1-2. Retrieved November 25, 2022, from: https://www.paho.org/english/sha/be994venez.htm
147. Pérez, M. (2020, February 15) A 60 meses del desastre: recordar para transformar las Sierras Chicas. [60 months after the disaster: remembering to transform the Sierras Chicas]. Milenio. Retireved January 13, 2024, from: https://elmilenio.info/2020/02/15/a-60-meses-del-desastre-recordar-para-transformar-las-sierras-chicas/
148. Petry, B. (2002). Keynote lecture: Coping with floods: Complementarity of structural and non-structural measures. *Flood defence, 1*. https://www.iahr.org/library/infor?pid=16214
149. Pinto, J., & de Castro, B. S. (2022). Os desastres climáticos e a coordenação de políticas públicas municipais, o caso do Centro de Operações Rio–Rio de Janeiro-Brasil. [Catastrophes climatiques et coordination des politiques publiques municipales, le cas du Centre d'Opérations Rio-Rio de Janeiro-Brésil]. *Territorium*, (29 (II)), 111-121. https://doi.org/10.14195/1647-7723_29-2_9
150. Préfet des Alpes-Maritimes. (2016). Inondations des 3 et 4 octobre 2015 dans les Alpes-Maritimes - retour d'experience - rapport final. [Floods of October 3 and 4, 2015 in the Alpes-Maritimes - feedback from the past experience - final report]. Nice: Préfet des Alpes-Maritimes.
151. Radio Télé Luxembourg. (2015, October 4). Inondations dans les Alpes-Maritimes : des habitants sont morts, pris au piège dans le parking de leur résidence. [Floods in the Alpes-Maritimes: residents died, trapped in the parking lot of their residence]. Radio Télé Luxembourg. Retrieved January 13, 2024, from: https://www.rtl.fr/actu/debats-societe/inondations-dans-les-alpes-maritimes-des-habitants-sont-morts-pris-au-piege-dans-le-parking-de-leur-residence-7779971092
152. Redacción Clarín (2019, March 7). Antes y ahora: el arroyo El Gato desde un dron. [Then and now: El Gato stream from a drone]. Clarín. Retrieved January 13, 2024, from: https://www.clarin.com/politica/ahora-arroyo-gato-dron_0_8MGGhBnRJ.html

153. Rédaction Nice. (2021, October 4). Alpes-Maritimes. Les établissements scolaires fermés dès midi, les parents invités à récupérer leurs enfants. [Alpes-Maritimes. Schools closed at noon; parents invited to pick up their children]. Actu.fr. Retrieved January 13, 2024, from: https://actu.fr/provence-alpes-cote-d-azur/nice_06088/alpes-maritimes-les-etablissements-scolaires-fermes-des-midi-les-parents-invites-a-recuperer-leurs-enfants_45384788.html
154. Rentschler, J., Salhab, M., & Jafino, B. A. (2022). Flood exposure and poverty in 188 countries. *Nature communications*, 13(1), 3527.
155. Renn, O. (2013). A Generic Model for Risk Governance: Concept and Application to Technological Installations. *Risk Governance of Offshore Oil and Gas Operations*, Cambridge University Press. 9-33.
156. Rentschler, J., Salhab, M., & Jafino, B. A. (2022). Flood exposure and poverty in 188 countries. *Nature communications*, 13(1), 3527. https://doi.org/10.1038/s41467-022-30727-4
157. Rodríguez, L., Dávila, A., Hernández, J., Amaya, B., & Prado, J. (2010). Programa PREDERES: Programa de prevención de desastres y reconstrucción social en el Estado Vargas. [PREDERES Program: Disaster prevention and social reconstruction programme in Vargas State]. *Lecciones Aprendidas del Desastre de Vargas*. Universidad Central de Venezuela.
158. Roh, J. (2022, August 10). Torrential rain lessens in S.Korean capital amid heavy flood damage. Reuters. Retrieved January 13, 2024, from: https://www.reuters.com/world/asia-pacific/torrential-rain-lessens-skorean-capital-amid-heavy-flood-damage-2022-08-10/
159. Rosenzweig, C., & Solecki, W. (2014). Hurricane Sandy and adaptation pathways in New York: Lessons from a first-responder city. *Global Environmental Change*, 28, 395-408. https://doi.org/10.1016/j.gloenvcha.2014.05.003
160. Salvan, L. (2017*). Knowledge base and modelling for urban stormwater management: application to Nice, France* (Doctoral dissertation, Université Côte d'Azur). https://tel.archives-ouvertes.fr/tel-01737020
161. Filipuzzi, S. (2021, April 2). La Plata: las fotos de la trágica inundación ocurrida hace 8 años. [La Plata: photos of the tragic flood that occurred 8 years ago]. La Nación. Retrieved January 13, 2024, from: https://www.lanacion.com.ar/sociedad/la-plata-las-fotos-de-la-tragica-inundacion-ocurrida-hace-8-anos-nid02042021/

162. Sermet, Y., Demir, I., & Muste, M. (2020). A serious gaming framework for decision support on hydrological hazards. *Science of The Total Environment*, 728, 138895. https://doi.org/10.1016/j.scitotenv.2020.138895
163. Severo, D.L., Cordero, A., Tachini, M. & dos Santos Silva, H. (2011). Análise Hidrometeorológica do Evento de 2008, no Vale do Itajaí - Santa Catarina. [Hydrometeorological Analysis of the 2008 Event, in the Itajaí Valley - Santa Catarina]. XIX SBRH - Simpósio Brasileiro de Recursos Hídricos
164. Simmonds, J., Gómez, J. A., & Ledezma, A. (2020). The role of agent-based modeling and multi-agent systems in flood-based hydrological problems: a brief review. *Journal of Water and Climate Change*, 11(4), 1580-1602. https://doi.org/10.2166/wcc.2019.108
165. Simpson, M., Padilla, L., Keller, K., & Klippel, A. (2022). Immersive storm surge flooding: Scale and risk perception in virtual reality. *Journal of Environmental Psychology*, 101764, https://doi.org/10.1016/j.jenvp.2022.101764
166. Skinner, C. (2020). Flash Flood!: a SeriousGeoGames activity combining science festivals, video games, and virtual reality with research data for communicating flood risk and geomorphology, *Geoscience Communication*, 3, 1–17, https://doi.org/10.5194/gc-3-1-2020
167. SNCF TER SUD Provence-Alpes-Côte d'Azur, [@TERSUD_SNCF]. (2023, November 2). [X]. X. Retrieved January 13, 2024, from: https://twitter.com/TERSUD_SNCF/status/1720100173962211711?ref_src=twsrc%5Etfw%7Ctwcamp%5Etweetembed%7Ctwterm%5E1720160406117765189%7Ctwgr%5Efc309df9eff7232b312a568921d3aeda76349b90%7Ctwcon%5Es3_&ref_url=https%3A%2F%2Fwww.nicematin.com%2Ffaits-divers%2Ftempete-ciaran-la-circulation-des-trains-a-larret-entre-nice-et-vintimille-apres-des-chutes-de-pierres-sur-la-voie-883087
168. Suetsugi, K. (1996, November). Control of floodwater and improvements of evacuation system for floodplain management. In *Floodplain risk management, Proceedings of an international workshop*. Hiroshima (pp. 11-13).
169. Tabari, H. (2020). Climate change impact on flood and extreme precipitation increases with water availability. *Scientific reports, 10*(1), 13768. https://doi.org/10.1038/s41598-020-70816-2

170. Taipei City Fire Department. (2015a). tái běi shì zhèng fǔ sū dí lè (Sourdelor) fēng zāi zāi hài fáng jiù chǔ lǐ bào gào. [Taipei City Government's report on typhoon disaster prevention and rescue for typhoon Soudelor]. Taipei: Taipei City Government
171. Taipei City Fire Department. (2015b). tái běi shì zhèng fǔ dù juān (Dujuan) fēng zāi zāi hài fang jiù chǔ lǐ bào gào. [Taipei City Government's report on typhoon disaster prevention and rescue for typhoon Dujuan]. Taipei: Taipei City Government
172. Taipei City Fire Department. (2016a). tái běi shì zhèng fǔ yīn yìng ní bó tè (Nepartak) tái fēng yìng biàn chǔ zhì zuò wéi jì zhī yuán tái dōng xiàn jiù zāi jí fù yuán chóng jiàn gōng zuò bào gào [Taipei City Government's report on typhoon disaster emergency response report and report of support for rescue and recovery for Taitung County for typhoon Nepartak]. Taipei: Taipei City Government
173. Taipei City Fire Department. (2016b). tái běi shì zhèng fǔ yīn yìng méi jī jì mǎ lè kǎ tái fēng yìng biàn chǔ zhì zuò wéi jì fù yuan chóng jiàn gōng zuò bào gào. [Taipei City Government's report on typhoon disaster emergency response and recovery report for typhoon Megi and Malakas]. Taipei: Taipei City Government
174. Taipei City Fire Department. (2017a). tái běi shì zhèng fǔ yīn yìng 0602 shuǐ zāi zāi hài yìng biàn chù zhì zuò wéi jì fù jiù jiǎn tǎo gōng zuò zǒng jié bào gào. [Taipei City Government's report on flood disaster emergency response and recovery report for flood event on 02 June]. Taipei: Taipei City Government
175. Taipei City Fire Department. (2017b). tái běi shì zhèng fǔ yīn yìng ní suō (Nesat) tái fēng yìng biàn chǔ zhì zuò wéi jì fù jiù gōng zuò jiǎn tǎo bào gào. [Taipei City Government's report on typhoon disaster emergency response and recovery report for typhoon Nesat]. Taipei: Taipei City Government
176. Taipei City Fire Department. (2018a). tái běi shì zhèng fǔ yīn yìng mǎ lì yà (Maria) tái fēng yìng biàn chǔ zhì zuò wéi jì fù jiù gōng zuò jiǎn tǎo bào gào. [Taipei City Government's report on typhoon disaster emergency response and post-disaster review report for typhoon Maria]. Taipei: Taipei City Government
177. Taipei City Fire Department. (2018b). 0823 rè dài dī yā shuǐ zāi zāi hài yìng biàn chǔ zhì zuò wéi jì zāi hòu jiǎn tǎo bào gào. [Report on flood disaster emergency response and post-disaster review report for tropical depression on 23 August]. Taipei: Taipei City Government

178. Taipei City Fire Department. (2018c). 0908 tái běi shì shuǐ zāi zāi hài yìng biàn chǔ zhì zuò wéi jì zāi hòu jiǎn tǎo bào gào. [Taipei City Government's report on flood disaster emergency response and post-disaster review for flood event on 08 September]. Taipei: Taipei City Government
179. Taipei City Fire Department. (2019a). tái běi shì 0722 shuǐ zāi zāi hài yìng biàn chǔ zhì zuò wéi jì zāi hòu jiǎn tǎo bào gào. [Taipei City Government's report on flood disaster emergency response and post-disaster review report for flood event on 22 July]. Taipei: Taipei City Government
180. Taipei City Fire Department. (2019b). tái běi shì zhèng fǔ lì qí mǎ (Lekima) tái fēng yìng biàn chǔ zhì zuò wéi jì zāi hòu jiǎn tǎo bào gào. [Taipei City Government's report on typhoon disaster emergency response and post-disaster review report for typhoon Lekima]. Taipei: Taipei City Government
181. Taipei City Fire Department. (2019c). tái běi shì zhèng fǔ mǐ tǎ (Mitag) tái fēng yìng biàn chǔ zhì zuò wéi jì zāi hòu jiǎn tǎo bào gào. [Taipei City Government's report on typhoon disaster emergency response and post-disaster review report for typhoon Mitag]. Taipei: Taipei City Government
182. Taipei City Emergency Operations Center. (n.d.). Taipei City Disaster Prevention Info Website. Taipei City Government. Retrieved January 13, 2024, from: https://www.eocmap.gov.taipei/eocmap
183. The Merit Times. (2023, September 5). běi shì páis huǐ biāo zhǔn nǐ tí gāo zhì 88.8 há omǐ [The drainage standard of Taipei City is planned to be raised to 88.8 mm per hour]. The Merit Times. Retrieved January 13, 2024, from: https://www.merit-times.com/NewsPage.aspx?unid=857550
184. Thompson, P. A., & Marchant, E. W. (1995a). A computer model for the evacuation of large building populations. *Fire safety journal*, 24(2), 131-148. https://doi.org/10.1016/0379-7112(95)00019-P
185. Thompson, P. A., & Marchant, E. W. (1995b). Computer and fluid modelling of evacuation. *Safety Science*, 18(4), 277-289. https://doi.org/10.1016/0925-7535(94)00036-3
186. Tisue, S., & Wilensky, U. (2004, October). NetLogo: Design and implementation of a multi-agent modeling environment. In *Proceedings of agent* (Vol. 2004, pp. 7-9).

187. Tomkins, A., & Lange, E. (2019). Interactive Landscape Design and Flood Visualisation in Augmented Reality. *Multimodal Technologies and Interaction*, 3(2), 43. https://doi.org/10.3390/mti3020043
188. Tsai, M.-H., Chang, Y.-L., Shiau, S., & Wang, S.-M. (2019). Exploring the effects of a serious game-based learning package for disaster prevention education: The case of Battle of Flooding Protection. *International Journal of Disaster Risk Reduction*, 43(January 2019), 101393, https://doi.org/10.1016/J.IJDRR.2019.101393.
189. TUBS. (2011). *Taipei City in Taiwan*. [Scalable Vector Graphics]. Wikimedia Commons. Retrieved May 26, 2024, from: https://commons.wikimedia.org/wiki/File:Taipei_City_in_Taiwan.svg
190. TUBS. (2015). *Département 06 in France 2016*. [Scalable Vector Graphics]. Wikimedia Commons. Retrieved May 26, 2024, from: https://commons.wikimedia.org/wiki/File:D%C3%A9partement_06_in_France_2016.svg
191. Universidad Nacional de La Plata (2017). Las inundaciones en La Plata, Berisso y Ensenada: análisis de riesgo, estrategias de intervención. Hacia la construcción de un observatorio ambiental. [Floods in La Plata, Berisso and Ensenada: risk analysis, intervention strategies. Towards the construction of an environmental observatory]. La Plata: Universidad Nacional de La Plata http://sedici.unlp.edu.ar/handle/10915/59633
192. United Nations International Children's Emergency Fund (2022). Nigeria Emergency Flood Response. United Nations International Children's Emergency Fund. Retrieved January 13, 2024, from: https://www.unicef.org/nigeria/reports/nigeria-emergency-flood-response
193. United National Office for Disaster Risk Reduction. (2017). *Words into Action Guidelines. National Disaster Risk Assessment. Governance System, Methodologies and Use of Results.* United National Office for Disaster Risk Reduction.
194. United National Office for Disaster Risk Reduction. (n.d.). Structural and non-structural measures. United National Office for Disaster Risk Reduction. Retrieved January 13, 2024, from: https://www.undrr.org/terminology/structural-and-non-structural-measures

195. United Nations Office for the Coordination of Humanitarian Affairs (2022). United Nations releases US$10.5 million for Nigeria floods response. United Nations Office for the Coordination of Humanitarian Affairs. Retrieved January 13, 2024, from: https://reliefweb.int/report/nigeria/united-nations-releases-us105-million-nigeria-floods-response
196. Ville de Cannes. (n.d.). Tsunami [Tsunami]. Ville de Cannes. Retrieved January 13, 2024, from: https://www.cannes.com/fr/cadre-de-vie/prevention-des-risques-majeurs-securite/prevention-des-risques-majeurs-1/les-risques-naturels/tsunami.html
197. Ville de Nice. (n.d. -a). L'information préventive [Preventive information]. Ville de Nice. Retrieved January 13, 2024, from : https://www.nice.fr/fr/gestion-des-risques/l-information-preventive
198. Ville de Nice. (n.d. -b). Tempêtes, séismes, attentats : Soyez alerté par SMS en temps réel [Storms, earthquakes, attacks: Be alerted by SMS in real time]. Ville de Nice. Retrieved January 13, 2024, from : https://www.nice.fr/fr/actualites/tempetes-seismes-attentats-soyez-alerte-par-sms-en-temps-reel?type=articles
199. Ville de Nice. (2010). Le Plan Familial de mise en Sureté (PFMS) [The Family Safety Plan (PFMS)]. Ville de Nice. Retrieved January 13, 2024, from : https://www.nice.fr/fr/gestion-des-risques/l-information-preventive
200. Ville de Nice. (2012). Le Plan d'Organisation de Mise en Sûreté d'un Etablissement (POMSE) [The Security Organization Plan for an Establishment (POMSE)]. Ville de Nice. Retrieved January 13, 2024, from : https://www.nice.fr/fr/gestion-des-risques/l-information-preventive
201. Ville de Nice. (2017). Le Document d'Information Communal sur les Risques Majeurs DICRIM [The Municipal Information Document on Major Risks]. Ville de Nice. Retrieved January 13, 2024, from : https://www.nice.fr/fr/gestion-des-risques/l-information-preventive
202. Wang, C. H., Wang, J. Y., Yu, H. L., Tseng, C. Y., Lin, C. F., & Chang, T. J. (2021). An Integrated Pluvial Flood Analysis with Dual Drainage Modeling (Cellular Automata Overland Flow-Street Gully Inlet-Stormwater Sewer Networks): The Development of Real-time Flood Inundation Forecasting Platform in Taipei City. *Journal of Taiwan Agricultural Engineering, 66(2).* https://doi.org/10.29974/JTAE.202109_67(3).0001

203. Wang, H., Mostafizi, A., Cramer, L. A., Cox, D., & Park, H. (2016). An agent-based model of a multimodal near-field tsunami evacuation: Decision-making and life safety. *Transportation Research Part C: Emerging Technologies, 64*, 86-100. https://doi.org/10.1016/j.trc.2015.11.010
204. Wang, Z., & Jia, G. (2021). A novel agent-based model for tsunami evacuation simulation and risk assessment. *Natural hazards, 105*, 2045-2071. https://doi.org/10.1007/s11069-020-04389-8
205. Water Resources Agency. (n.d.-a). Disaster Prevention Information Service Network: file download. Water Resources Agency, MOEA. Retrieved January 13, 2024, from: https://fhy.wra.gov.tw/fhyv2/disaster/downloads
206. Water Resources Agency. (n.d.-b). Warning Information. Water Resources Agency, MOEA. Retrieved January 13, 2024, from: https://fhy.wra.gov.tw/fhyv2/alert/warn/en
207. Wijaya, O. T., Yang, T. H., Hsu, H. M., & Gourbesville, P. (2023). A rapid flood inundation model for urban flood analyses. *MethodsX*, 10, 102202. https://doi.org/10.1016/j.mex.2023.102202
208. Wilensky, U. (1999). NetLogo. http://ccl.northwestern.edu/NetLogo/. Center for Connected Learning and Computer-Based Modeling, Northwestern University, Evanston, IL.
209. Wirth, E., & Szabó, G. (2018). Overlap-avoiding Tickmodel: an agent-and GIS-based method for evacuation simulations. *Periodica Polytechnica Civil Engineering*, 62(1), 72-79. https://doi.org/10.3311/PPci.10823
210. Wu, S. W. & Hetherington, W. (2021, July 23). Cities' rain drainage outdated: report. Taipei Times. Retrieved January 13, 2024, from: https://www.taipeitimes.com/News/taiwan/archives/2021/07/25/2003761429
211. Yang, T. H., Yang, S. C., Kao, H. M., Wu, M. C., & Hsu, H. M. (2018). Cyber-physical-system-based smart water system to prevent flood hazards. *Smart Water*, 3, 1-13. https://doi.org/10.1186/s40713-018-0008-3

212. Yang, T. H., Hsu, H. M., & Kao, H. M. (2020). Integrations of an Early Warning System and Business Continuity Plan for Disaster Management in a Science Park. In *Advances in Hydroinformatics: SimHydro 2019-Models for Extreme Situations and Crisis Management* (pp. 171-179). Springer Singapore. https://doi.org/10.1007/978-981-15-5436-0_14
213. Yoo, C. M. (2022, August 11). Seoul to build deep underground rainwater tunnels in 6 flood-prone areas. Yonhap News. Retrieved January 13, 2024, from: https://en.yna.co.kr/view/AEN20220811004500315
214. Yoon, T. H. (2017, July 23). incheon 110mm 'pog-u'…samang 1myeong·jutaeg deung 547gos chimsu (jonghab2bo). [Incheon 110mm 'heavy rain'… 1 death, 547 houses flooded, etc. (Comprehensive report 2)]. Yonhap News. Retrieved January 13, 2024, from: https://www.yna.co.kr/view/AKR20170723028052065
215. Youssef, A. M., Pradhan, B., & Sefry, S. A. (2016). Flash flood susceptibility assessment in Jeddah city (Kingdom of Saudi Arabia) using bivariate and multivariate statistical models. *Environmental Earth Sciences*, 75(1), 12. https://doi.org/10.1007/s12665-015-4830-8
216. Zaalberg, R., & Midden, C. J. (2013). Living behind dikes: mimicking flooding experiences. *Risk Analysis*, 33(5), 866-876. https://doi.org/10.1111/j.1539-6924.2012.01868.x